41st Annual Meeting
The Korean Society of Developmental Biology

2022 Post COVID-19, the Organ to Single Cell

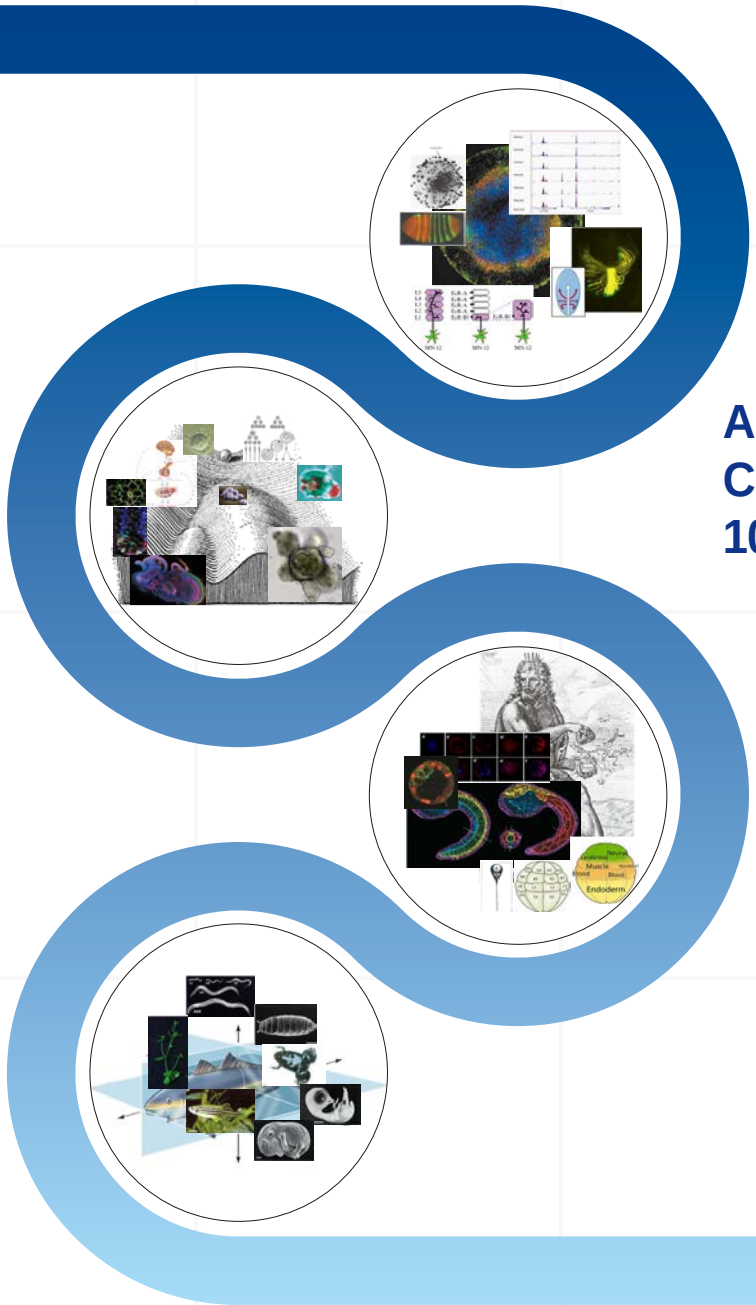

AUG 19-20, 2022
Chung-Ang University Seoul Campus, 100th Anniversary Memorial Hall

주 최 : (사)한국발생생물학회

후 원 : 머크, 한국과학기술정보연구원, SC pharma, 한국애보트, 엘지화학, 자이스코리아, 애티스랩, 아름사이언스, 유비코리아, 영사이언스, 넥셀, 에피바이오텍, 티앤알바이오팹, 특허법인SRB, 아이젠파마코리아, 엘케이바이오사이언스, 스페바이오, 브렉소젠, 바오밥헬스케어, 엔아이, 에이비엠랩스, T.L.S, 골드퍼시픽, 자연과학, 한화제약, 써모피셔사이언티픽, 서울의과학연구소

듀파스톤®정 경구투여는 편리하고 효과적인
Luteal Phase Support 요법입니다.[1,2]

ORAL.

Duphaston®
Dydrogesterone

Experienced in **>113 Million** Patients[3]	Experienced in **>20 Million** Pregnancies[3,4]	Available in over **100 Countries**[4]

References)

1. Abbott laboratories Company Core Data Sheet Dydrogesterone, 10th May 2019. **2.** Ozer G, Yuksel B, Yucel Cicek OS, Kahraman S. Oral dydrogesterone vs. micronized vaginal progesterone gel for luteal phase support in frozen-thawed single blastocyst transfer in good prognosis patients. J Gynecol Obstet Hum Reprod. 2021;50(5):102030. doi: 10.1016/j.jogoh.2020.102030. **3.** Tournaye H, Sukhikh GT, Kahler E, et al. A Phase III randomized controlled trial comparing the efficacy, safety and tolerability of oral dydrogesterone versus micronized vaginal progesterone for luteal support in in vitro fertilization Hum Reprod. 2017;32(5):1019-1027
4. Podzolkova N, Tatarchuk T, Doshchanova A, et al. Dydrogesterone treatment for menstrual-cycle regularization in routine clinical practice: a multicentre observational study. *Gynecol Endocrinol.* 2016;32(3):246–249

Prescribing Information

전문의약품

듀파스톤정(디드로게스테론)

Abbott

Duphaston®
Dydrogesterone

KOR2210816

ZEISS LSM 980 NIR

기술이 발전하며 새로운 발견에 대한 기준이 높아지고 있습니다.
더 나은 이미징 퀄리티와 속도, 퍼포먼스를 내기 위해서는 새로운 장비가 필요할 때도 있죠.
그 변화를 위한 최고의 컨포컬 현미경, ZEISS LSM 9 Series를 지금 바로 확인해보세요.

더 쉽고 빠르고 정확한 이미징, ZEISS LSM 9 Series 와 함께하세요.

- 빠른 스캔 속도와 훌륭한 이미지 퀄리티
- Super-resolution 전용 Hardware system
- 자동으로 샘플을 찾는 AI Sample Finder
- 더욱 다양한 모듈을 사용할 수 있는 ZEN blue

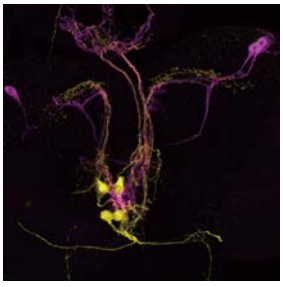

Hugin neurons in the *Drosophila* larval brain

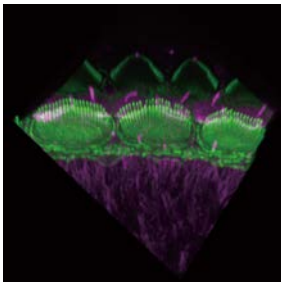

Mouse cochlear hair cell (3D)

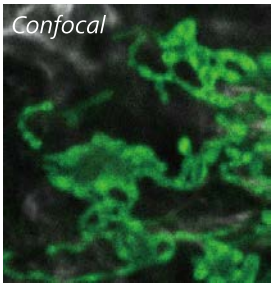

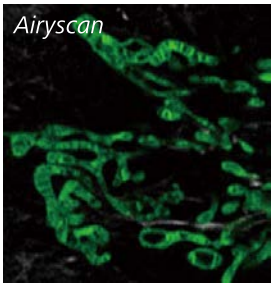

Mitochondria Live COS7 cells

NIR Detection 역량을 더해 다중형광염색에 더 강력해진 자이스 컨포컬

자이스의 가장 강력한 컨포컬, ZEISS LSM 980 NIR 와 함께 900nm까지 간섭 없는 다중형광염색을 경험해 보세요.

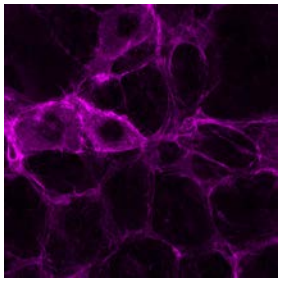

Cos 7 Cells Channel mode, Alexa 488 NIR

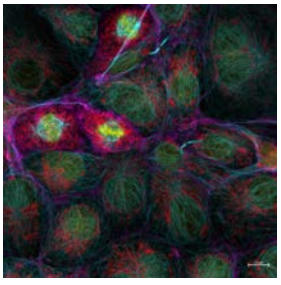

Cos 7 Cells Channel mode, 750 700 488 405 merge Scalebar NIR

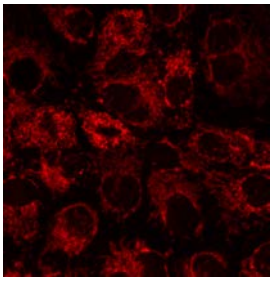

Cos 7 Cells Channel mode, Alexa 750 NIR

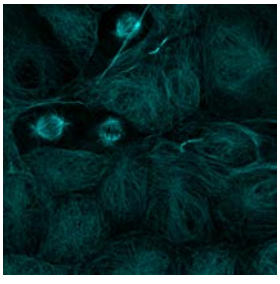

Cos 7 Cells Channel mode, Alexa 700 NIR

자이스 코리아 현미경 솔루션 사업부
서울시 송파구 법원로 135 소노타워 13층

Homepage: https://www.zeiss.co.kr/microscopy
Email: microscopy.kr@zeiss.com
Phone: 02-1661-3140

ZEISS

Seeing beyond

에피바이오텍
대한민국 #1 모낭 연구소

비임상 CRO

에피바이오텍은 15년 이상의 오랜 줄기세포, 탈모 연구 경험과 전문성을 기반으로 탈모 전문 플랫폼 기술을 보유하고 있습니다. 제약 및 바이오 산업계의 요구에 맞춘 최적의 발모 효능 검증 서비스를 제공합니다.

발모효능시험

다양한 모낭 세포를 확보하고 있으며 모발 조직 배양 및 다양한 동물 실험을 통해 제품 검토 및 개발 단계에서 기대하는 효능 검증 및 투여 용량에 대한 적절성을 검증해 드립니다.

다양한 모낭 세포 확보
In vitro
Cell scale research

세포 수준에서의 효능 평가

보유 모낭 구성 세포주

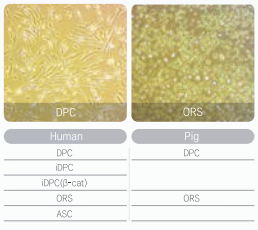

Hair 조직배양
Ex vivo
Organ scale research

쥐의 콧수염 모낭
돼지의 피부 모낭

쥐의 콧수염 모낭을 이용한 organ culture

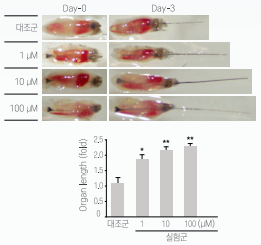

다양한 동물 실험
In vivo
Organism scale research

① 발모 촉진 동물 모델
② 탈모 유도 동물 모델

발모촉진 실험

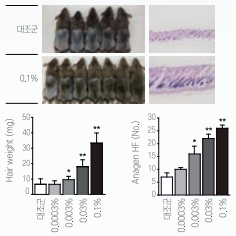

발모 관련 기전 연구

In vitro/In vivo
표적유전자 발굴
단백질 저해제 이용 연구
Paracrine 효과 평가
발모 관련 성장인자 평가

성장인자 및 주요기전 유전자 발현 평가

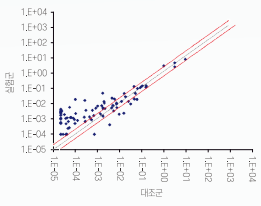

CMO 서비스

우수한 세포 분리 및 배양, 분화기술을 보유하고 있으며 임상시료 및 세포치료제 위탁 생산에 더해 품질 분석과 문서화 작업까지 동반하는 고객 맞춤형 CMO 서비스를 제공합니다.

차세대 세포 & 유전자 치료제 시설

Crispr-Cas9을 이용한 **gene knock-in** 또는 **knock-out system** 구축

차세대 유전자 가위 기반 기술 **(Base and Prime editing)** 확보

최신 GMP 기준 적용된 시설

외부 오염과 교차 오염에 대한 가능성 원천 차단


입구 통로


세포은행보관실


배양실1


배양실2


분리실


배양


멸균


공기조화실

epibiotech

[본사/송도연구실] 인천광역시 연수구 송도과학로 32, M동 1903호
[세포치료제 생산센터] 인천광역시 연수구 송도과학로 32, M동 15층
[판교연구실] 경기도 성남시 분당구 판교역로 240, A동 510-3호
[Tel] 070-4209-0556 [팩스] 032-209-8239
[이메일] info@epibiotech.com [홈페이지] http://epibiotech.com

Thermo Fisher Scientific Pipette Calibration Center

전브랜드 모델_교정 / 점검 / 수리

서비스 신청하기

PCC Open

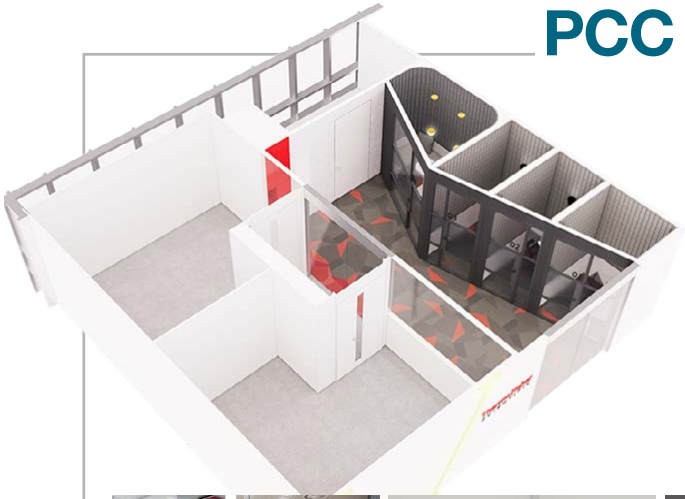

Pipette Calibration Center

써모 피셔 사이언티픽 코리아 파이펫 캘리브레이션 센터

써모 피셔 사이언티픽 코리아의 캘리브레이션 센터는 고객 파이펫에 대한 정기적인 교정 및 유지보수 서비스를 제공하여 고객의 실험의 정확도와 정밀도를 향상시킬 수 있습니다.

또한 다양한 고객 맞춤형 프로그램 및 수준 높은 서비스를 통해 샘플 핸들링의 솔루션을 제공 드립니다.

써모 피셔 사이언티픽 캘리브레이션 센터에 많은 관심 가져 주시고 여러분의 솔직한 의견과 제안도 기꺼이 보내주시기 바랍니다.

Contact : KR-LPD- PCC@thermofisher.onmicrosoft.com

- 고객의 실험실에서 진행하는 출장 교정
- ISO8655 기준에 따른 반입 교정
- 제조사 구분 없이 모든 브랜드 Pipette 교정
- 오염물 제거 등의 유지보수 서비스 제공

thermofisher.com
Thermo Fisher Scientific 써모 피셔 사이언티픽 솔루션스 유한회사
서울시 강남구 광평로 281 수서 오피스빌딩 12층, 06349 | 대표번호 : 02-2023-0600

ThermoFisher SCIENTIFIC

특허법인 IP & LAW FIRM SRB는

최고의 IP 법률 서비스를 제공하고 있습니다.

특허법인 SRB는 제약/바이오, 화학/소재, 전기/전자/통신/반도체, 기계, 상표 및 디자인 분야의
변리사들로 이루어진 국내 최고의 지식재산 전문가 그룹입니다.
고객들의 지적재산권 보호를 위해 항상 **최고의 IP 법률 서비스**를 제공하고 있습니다.

서비스 소개

특허, 실용신안, 상표 및 디자인 출원 및 등록
- 출원서 제출을 비롯한 특허청 관련 업무 대리
- 거절이유 통지 대응 및 등록 절차 대리 등

선행기술조사 및 출원 전 등록가능성 검토
- 등록가능성 검토 및 IP 확보 방향성 제시

특허 동향 조사 및 분석 사업
- 고객 Needs에 부합하는 특허 분석 사업
- 상장 심사를 위한 사전 특허 분석 작업

지식재산권 분쟁, 소송 및 계약 업무
- 각종 지식재산권 관련 분쟁, 소송 업무 대리
- 각종 국문/영문 계약서 작성 및 리뷰

기술 수요기업 발굴 및 기술이전 절차 수행
- 기술 수요자-공급자 발굴 및 연결 지원
- 각종 국문/영문 계약서 작성 및 리뷰

지식 재산권 관리, 자문 및 교육
- IP 관련 다양한 주제에 맞춰 방문 교육 및 강연
- IP 팀 보유가 어려운 기업의 관리 및 자문 업무

담당 변리사 소개

윤대웅 변리사 (대표)

건국대학교 동물생명공학과 (학사)
고려대학교 기술경영학과 (석사)
변리사 46기 (2009)

최용기 변리사

아주대학교 화학공학과 (학사)
변리사 47기 (2010)

박종문 변리사

홍익대학교 전자전기공학부 (학사)
변리사 47기 (2010)

이종성 변리사

고려대학교 생명과학과 (학사)
변리사 50기 (2013)

최종윤 변리사

서울대학교 응용생물학과 (학사)
변리사 54기 (2017)

김승준 변리사

서울대학교 응용생물화학과 (학사)
변리사 57기 (2020)

박소영 변리사

건국대학교 응용생물과학과 (학사)
변리사 58기 (2021)

11월 중 개소 예정

Sagacious. Righteous. Beneficial.

윤대웅 변리사
010-9704-0627
dwyoon@ipnlaw.com

제41회 한국발생생물학회
정기학술대회

2022 Post COVID-19,
the Organ to Single Cell

2022년 8월 19일(금) ~ 8월 20일(토)
중앙대학교 서울캠퍼스
100주년 기념관(지하 5층)

주 최: (사)한국발생생물학회
후 원: 머크, 한국과학기술정보연구원, SC pharma,
한국애보트, 엘지화학, 자이스코리아, 애티스랩,
아름사이언스, 유비코리아, 영사이언스, 넥셀,
에피바이오텍, 티앤알바이오팹, 특허법인SRB,
아이젠파마코리아, 엘케이바이오사이언스, 스페바이오,
브렉소젠, 바오밥헬스케어, 엔아이, 에이비엠랩스,
T.L.S, 골드퍼시픽, 자연과학, 한화제약,
써모피셔사이언티픽, 서울의과학연구소

환 영 사

2022년도 제41회 정기학술대회를 아름다운 도심 경치를 배경으로 한 중앙대학교에서 8월 19일과 20일(금/토) 양일간 개최합니다. 지난 3년간 COVID-19 대유행으로 국내 · 외적으로 어려운 상황을 겪고 있습니다. 다행히, 우리나라는 세계적으로 COVID-19 문제를 잘 극복하고 있는 환경을 조성하였다고 생각합니다. 이에 이번 학회를 대면으로 개최하게 되었습니다.

발생생물학은 생명과학에서 가장 근간이 되는 학문입니다. 따라서 지속적인 연구자의 수적 증가 및 연구내용의 확장과 교류가 절실합니다.

제41회 정기학술대회는 2022년을 맞아 코로나 대유행을 이겨내고, 새로운 기운을 모아 더욱 발전하자는 의미로 “2022 Post COVID-19, the Organ to Single Cell”을 주제로 하였습니다. 이를 통해 발생생물학의 발전을 염원하고, 우리 학회가 세계적으로 약진하는 소망을 함께 하고자 합니다.

이번 학술대회에서는 각 분과에서 훌륭한 업적을 이루고 계신 기조 강연 연사분들과 최근 학문 성과가 우수한 연구자분들의 강의와 학문 후속세대(젊은/신진과학자)의 학술발표를 통해 우리 분야의 발전을 예견해 볼 수 있는 시간을 마련하고자 합니다.

25대 회장단에서는 사단법인 한국발생생물학회에 애정을 가지고 계신 모든 회원님들께서 편안하고 즐거운 마음으로 학술교류의 장이 될 수 있도록 노력하였으며, 마지막으로 제41회 정기학술대회가 원만히 진행될 수 있도록 힘을 모아주신 임원분들께 감사드립니다.

많은 성원과 격려 부탁드립니다.

감사합니다.

(사)한국발생생물학회 회장 류범용

제41회 한국발생생물학회 정기학술대회 학술 프로그램

2022 Post COVID-19, the Organ to Single Cell

주최: (사)한국발생생물학회
장소: 중앙대학교 서울캠퍼스 100주년 기념관(지하 5층)
일자: 2022년 8월 19일(금)~8월 20일(토)

8월 19일 (금) 오후 13:00~18:00			좌장
13:00 – 13:30	등록		
13:30 – 13:40	**개회식 (회장 환영 인사, 중앙대학교 총장 축사)**		(사회) 학술위원장
13:40 – 14:20	기조강연 I	발생공학과 미니돼지모델의 현황 및 미래 **김선욱 센터장**(생명공학연구원 미래형동물자원센터)	최영석 교수
14:20 – 15:00	기조강연 II	The present and future of environmental DNA **곽인실 교수**(전남대학교)	김길중 교수
15:00 – 15:10	**Coffee Break**		
15:10 – 17:10	심포지엄 I	Development of biomarkers and identification of signalling pathways related to reproductive toxicity of pesticides **권우성 교수**(경북대학교)	전용필 교수 손영창 교수
		해양오염 유해인자 영향평가 연구 **정지현 박사**(한국해양과학기술원)	
		Drug-induced renal injury and regeneration in zebrafish as an animal model **강영선 교수**(고려대학교)	
		영장류 및 인간화 마우스를 이용한 조혈계 질병 기전 연구 **유경록 교수**(서울대학교)	
17:10 – 18:00	**포스터 세션**		
17:20 – 18:00	**이사회**		(사회) 총무위원장
18:00	**리셉션**		(사회) 학술위원장

8월 20일 (토) 오전 9:00~17:30			좌장
09:00 – 10:00	심포지엄 II (젊은과학자)	Convergent differentiation of multiciliated cells **채신혁 박사과정**(UNIST)	권우성 교수
		Establishment of a male fertility prediction model with sperm RNA markers in pigs as a translational animal model **방원기 박사과정**(중앙대학교)	
		Energy pathways involved in the maturation of the Pacific oyster, *Crassostrea gigas* **박수진 박사과정**(부경대학교)	
10:00 – 11:00	심포지엄 III (신진과학자)	Effects of environmental stressors in antioxidant response of scallops **송진아 박사**(한국해양과학기술원)	정한성 교수
		Zebrafish as a model system to investigate human liver diseases **Azra Memon 박사**(원광대학교)	
		Exploring the mechanism of trehalose: dual functions of PI3K/Akt and VPS34/mTOR pathways in porcine oocytes and cumulus cells **채련 박사**(충북대학교)	
11:00 – 11:10	**Coffee Break & Booth Tour**		
11:10 – 11:50	기조강연 III	행동을 조절하는 신경회로의 발생과 진화 **이준호 교수**(서울대학교)	이현식 교수
11:50 – 13:00	Luncheon Seminar: “Application of 3D bioprinting for the world’s welfare” **강동구 박사**(바오밥헬스케어(주)) 공동협찬: (주)아름사이언스, (주)Total Lab Service		
13:00 – 15:00	심포지엄 IV	Metabolic restructuring and cell fate conversion through controlling cellular organelles **이만렬 교수**(순천향대학교)	현상환 교수 최태영 교수
		Single-cell lineage recording unravels epigenetic priming of cell fates in early embryo development **김익수 교수**(가천대학교)	
		Effect of nanoplastics on the behavioral and nutritional characteristics of aquatic organisms **채유은 박사**(안전성평가연구소 생태위해성평가센터)	
		Chemokine regulates eye morphogenesis in *Xenopus* **정호성 교수**(연세대학교)	
15:00 – 15:10	**Coffee Break & Booth Tour**		

15:10 – 17:10	심포지엄 V	지속 가능한 미래 생물자원 확보를 위한 남극 어류 연구 **김진형 박사**(한국해양과학기술원 극지연구소)	권준영 교수 장훈 교수
		Enhanced hepatic functionality in long-term cultured 3D spheroids of zebrafish liver cells **김용준 단장**(한국과학기술연구원 환경안정성연구단)	
		Tumor-host interaction regulates cancer anorexia **염은별 교수**(경북대학교)	
		Cardiotoxicity evaluation of drugs using human PSC-derived cardiomyocytes **문성환 교수**(상지대학교)	
17:20	**시상 및 폐회**		(사회) 학술위원장
17:30	**총회**		(사회) 총무위원장
8월 20일 (토) 오후 14:00~17:00 의학 심포지엄: 착상(Implantation)의 심층분석			**좌장**
14:00 – 14:05	**개회사(한국발생생물학회 류범용 회장)**		(사회) 김슬기 (서울대학교 의과대학)
Session 1: 불응성 자궁내막 및 아셔만 증후군의 치료			
14:05 – 14:20	약물치료_PRP 포함 **채수진 원장**(아이오라여성의원)		김석현 (대한생식 의학회장)
14:20 – 14:35	수술 치료 및 재발방지 **권혁찬 원장**(미래와희망산부인과)		
14:35 – 14:50	줄기세포 **조정현 원장**(사랑아이여성의원)		
14:50 – 15:20	패널토의 **김광례 과장**(서울여성병원), **황경주 교수**(아주대학교병원), **이희선 원장**(라헬여성의원), **윤지성 원장**(아가온여성의원)		
15:20 – 15:40	**Coffee Break & Booth Tour**		
Session 2: 최신 치료법들의 임신 성적			
15:40 – 15:55	AI time 랩스 **정미경 연구소장**(서울라헬여성의원 난임의학연구소)		이정호 (대한보조 생식학회장)
15:55 – 16:10	ERA, CD138 등 자궁내막검사 **김자연 원장**(감자와눈사람여성의원)		
16:10 – 16:25	자연주기 요법 등 새로운 프로토콜 **박경의 원장**(디온여성의원)		
16:25 – 17:00	패널토의 **백은찬 원장**(분당제일여성병원), **박찬우 원장**(서울아이앤여성의원), **김정훈 원장**(엠여성의원), **정구성 원장**(드림아이여성의원)		

제41회 한국발생생물학회
정기학술대회 초록

목 차

기조강연

심포지엄 I

심포지엄II: 한국발생생물학회 젊은과학자

심포지엄Ⅲ: 한국발생생물학회 신진과학자

심포지엄Ⅳ

심포지엄Ⅴ

의학 심포지엄 Session 1: 불응성 자궁내막 및 아셔만 증후군의 치료

의학 심포지엄 Session 2: 최신 치료법들의 임신 성적

발표자 초록

포스터 초록

기조강연

Dev. Reprod. Vol 26, 2022 (Suppl. 1). pp 3

기조강연 I

발생공학과 미니돼지모델의 현황 및 미래

김선욱

생명공학연구원 미래형동물자원센터

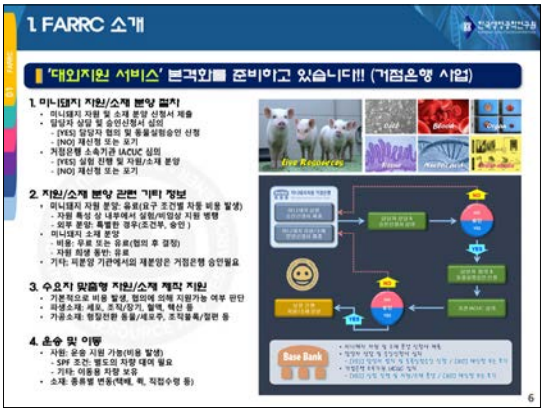


2. 미니돼지모델 개발 필요성
4차 산업혁명 : 인공지능 → '디지털 뉴딜' 추진
Industrial Revolution 4.0
1.0
Mechanical
2.0
Electrical
3.0
Internet
4.0
Digital
1784
1870
1969
Today
Digital 시대
data
Harvard Business Review
BIG DATA
Digital 뉴딜
7


2. 미니돼지모델 개발 필요성
4차 산업혁명 : 바이오 → '디지털 바이오' 부각
BIO
data
DATA SCIENCE
BIO Digital
디지털 헬스케어
K바이오 디지털 뉴딜
Analysis
바이오 data
바이오 Digital 뉴딜
8


2. 미니돼지모델 개발 필요성
디지털化 : 생명연구자원 → 모델동물
모델동물
9


2. 미니돼지모델 개발 필요성
생명연구자원 → "공유" 중요성 부상 → 공유자원
10


2. 미니돼지모델 개발 필요성
from RESOURCES to DIGIT
RESOURCES
정책/제도
Policy
DIGIT
과학기술
산업경제
11

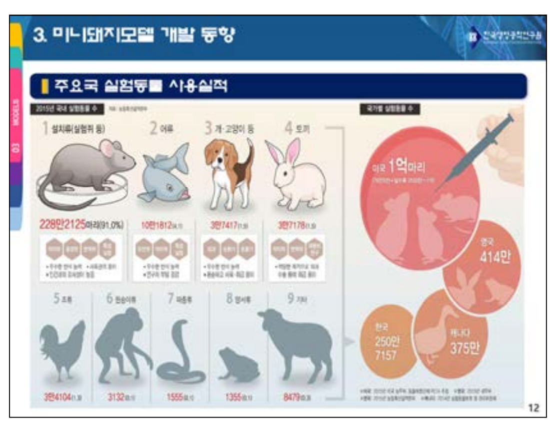
3. 미니돼지모델 개발 동향
주요국 실험동물 사용실적
12


3. 미니돼지모델 개발 동향
실험동물 사용실적
최근 8년간 국내 연간 실험동물 사용 수(단위: 만 마리)
??
자료: 농림축산검역본부
183.4
196.7
241.2
250.7
287.8
308.2
372.7
371.2
연평균증가율 14.6%
2012년
2013년
2014년
2015년
2016년
2017년
2018년
2019년
13


3. 미니돼지모델 개발 동향
모델동물 선택
■ 소동물
Mouse
Rat
1. 유전학적 특성이 다른 많은 계통 유지 가능
→다양한 연구목적에 사용가능
2. 생활주기, 수명이 짧아 세대교대를 빨리 진행한다.
3. 번식능력이 높고 사육관리가 용이하다.
4. 다수의 동물을 일시 사용 가능하다.
→통계적 결론 도달 용이
5. 가격이 싸다.
6. 체중이 적어 시험물질에 소요되는 비용이 저렴하다.
7. 부피가 적어 취급이 용이하다.
Ethical concern
High costs
Long life-span
■ 중대동물
High similarity to human in anatomy, physiology, etc
Goats
Sheep
Mini-pig
Dog
Monkey
14


3. 미니돼지모델 개발 동향
중대동물모델 선택
■ 소동물모델
Mouse
Rat
1. 유전학적 특성이 다른 많은 계통 유지 가능
→다양한 연구목적에 사용가능
2. 생활주기, 수명이 짧아 세대교대를 빨리 진행한다.
3. 번식능력이 높고 사육관리가 용이하다.
4. 다수의 동물을 일시 사용 가능하다.
→통계적 결론 도달 용이
5. 가격이 싸다.
6. 체중이 적어 시험물질에 소요되는 비용이 저렴하다.
7. 부피가 적어 취급이 용이하다.
Ethical concern
High costs
Long life-span
■ 중대동물모델
High similarity to human in anatomy, physiology, etc
Tg Easy!!
Low transgenesis
Goats
Sheep
Mini-pig
Dog
Monkey
15


3. 미니돼지모델 개발 동향
미니돼지모델 기반 비임상 platform 중요
Drug R&D
Clinical Trial
Target ID & Validation
Hit Generation
Lead Gen & Optimization
Pre Clinical Animal Studies
Phase 1 Safety
Phase 2 Efficacy Safety
Phase 3 Efficacy Safety
FDA Review & Approval
비임상 평가 (미니돼지 활용 필요)
Ready to Preclinical Trials
미니돼지모델 활용을 통한 "임상시험 성공률 제고", "적용증 확대" 등 기대
16


3. 미니돼지모델 개발 동향
미니돼지 기본 정보
미니돼지 정의 및 현황
Representative mini-pigs
Reproduction
Göttingen
Ohmini
Lee Song
NIH
Hanford
Hormel
Pitman-moore
Mexican hairless
Yucatan
17


3. 미니돼지모델 개발 동향
인간-(미니)돼지 유사성
Anatomy & physiology
Brain, Liver, Small intestine
Heart
Pigs
Humans
18


3. 미니돼지모델 개발 동향
미니돼지 활용 분야
미니돼지 활용 주요 연구분야
19


3. 미니돼지모델 개발 동향
발생공학 기술 혁신
The Story of Dolly
발생공학
: 포유동물의 생식세포(난자, 정자) 및 수정란을
이용한 실험적 조작에 관한 학문
1996년 7월 5일
Stuffed Dolly
Clone the sheep "Dolly"
연관분야/기술
1. 불임클리닉: 인공수정/시험관아기 시술
2. 진화/고고: 멸종(위기)동물 복원(매머드)
3. 환경/생태: 종 보존기술
4. 바이오의학: 형질전환 모델동물 제작 기술
Scottish Blackface
(Egg Donor)
Finn-Dorset
(Nuclear Donor)
Egg Cell
Mammary Cell
Enucleation
Combine Cells
Blastocyst
Surrogate Ewe
Dolly
20


3. 미니돼지모델 개발 동향
체세포핵치환/복제 기법 이용 형질전환 미니돼지 제작
체세포핵치환 (somatic cell nuclear transfer; SCNT)
유전자 결손 체세포주 구축
Somatic cells
Tg vector /system
Tg cell line
체세포 핵치환
Mii oocyte
Enucleation
Donor cells
Injection
Fusion
체외배양, 수정란이식, 산자생산
2-cell
8-cell
Blastocyst
Embryo transfer
Tg pig
21


3. 미니돼지모델 개발 동향
Stage 1
형질전환/복제
22


3. 미니돼지모델 개발 동향
1세대 바이오인공장기
2016
2009
2001
2001
1993
1992
1984
1969
1964
1963-1964
1920
1875
1838
1667
Xenotransplantation in China: Present status
Tibetan macaques
Rhesus monkeys
Liver
Kidney
Corneal
Skin
GTKO
GTKO/CD46
WZS pig
hCTLA4Ig
Ai Xin Tang
GGTA1β-/GalNT2/CMAH
Neonatal pig islets (NPIs)
BMVs
NPIs
23

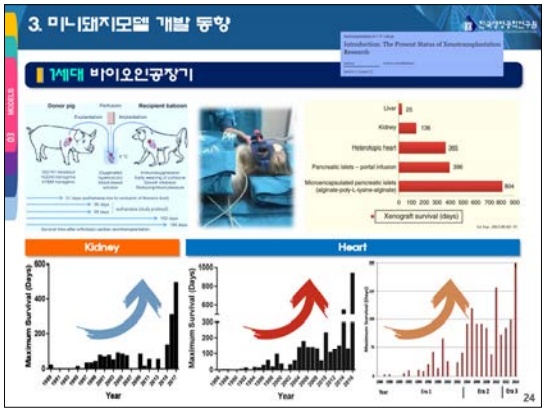
3. 미니돼지모델 개발 동향
1세대 바이오인공장기
Donor pig
Recipient baboon
Liver
Kidney
Heterotopic heart
Pancreatic islets – portal infusion
Microencapsulated pancreatic islets (alginate-poly-L-lysine-alginate)
Xenograft survival (days)
Kidney
Heart
Maximum Survival (Days)
Year
24

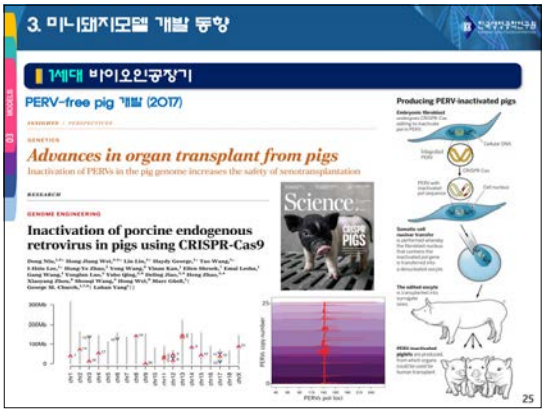
3. 미니돼지모델 개발 동향
1세대 바이오인공장기
PERV-free pig 개발 (2017)
Advances in organ transplant from pigs
Inactivation of PERVs in the pig genome increases the safety of xenotransplantation
Science
Inactivation of porcine endogenous retrovirus in pigs using CRISPR-Cas9
Producing PERV-inactivated pigs
25


3. 미니돼지모델 개발 동향
2세대 바이오인공장기
Chimeric organ (blastocyst complementation)
Pancreas
Thymus
Kidney
Pancreas / POC
Human-pig chimera
1. Generation of autologous iPSCs
2. Interspecies blastocyst complementation
3. Removal of pancreata and isolation of islets
4. Transplantation of islets into diabetic mice
26


3. 미니돼지모델 개발 동향
1세대 바이오인공장기
The JoongAng
61일 만에 멈춘 몸 속 돼지 심장, 시한부 환자 에겐 '희망'
돼지 심장 이식 과정
❶ 유전자 교정
유전자 가위로 면역 거부 반응 일어나지 않도록 유전자 4개 차단, 6개 추가
❷ 복제
유전자 10개를 교정한 돼지 배아를 복제, 대리모에 착상시켜 출산
❸ 심장 이식
유전자 변형 돼지 심장을 환자에 이식, 면역 억제 신약도 투여
27


3. 미니돼지모델 개발 동향
Stage 1
Stage 2
바이오장기
형질전환/복제
28

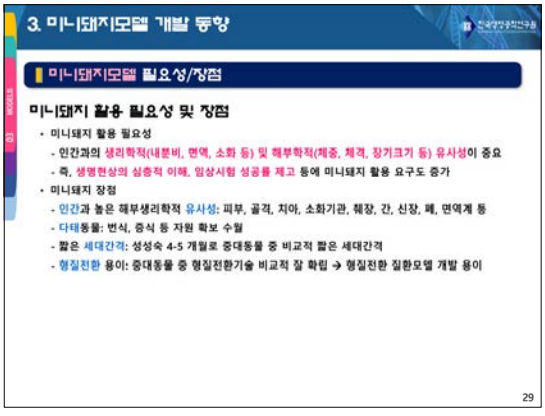
3. 미니돼지모델 개발 동향
미니돼지모델 필요성/장점
미니돼지 활용 필요성 및 장점
• 미니돼지 활용 필요성
- 인간과의 생리학적(내분비, 면역, 소화 등) 및 해부학적(체중, 체격, 장기크기 등) 유사성이 중요
- 즉, 생명현상의 심층적 이해, 임상시험 성공률 제고 등에 미니돼지 활용 요구도 증가
• 미니돼지 장점
- 인간과 놀은 해부생리학적 유사성: 피부, 골격, 치아, 소화기관, 췌장, 간, 신장, 폐, 면역계 등
- 다태동물: 번식, 증식 등 자원 확보 수월
- 짧은 세대간격: 성성숙 4-5 개월로 중대동물 중 비교적 짧은 세대간격
- 형질전환 용이: 중대동물 중 형질전환기술 비교적 잘 확립 → 형질전환 질환모델 개발 용이
29

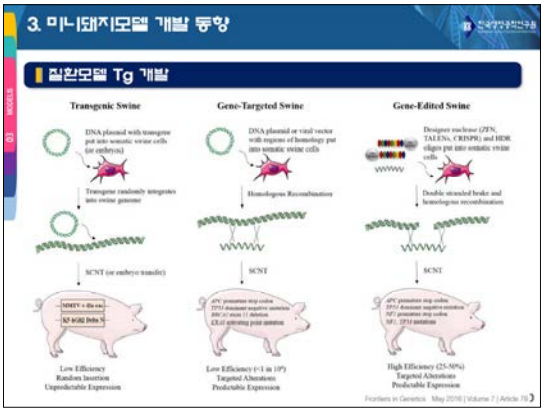
3. 미니돼지모델 개발 동향
질환모델 Tg 개발
Transgenic Swine
Gene-Targeted Swine
Gene-Edited Swine
SCNT (or embryo transfer)
Low Efficiency
Random Insertion
Unpredictable Expression
Low Efficiency (~1 in 10⁹)
Targeted Alterations
Predictable Expression
High Efficiency (25-50%)
Targeted Alterations
Predictable Expression

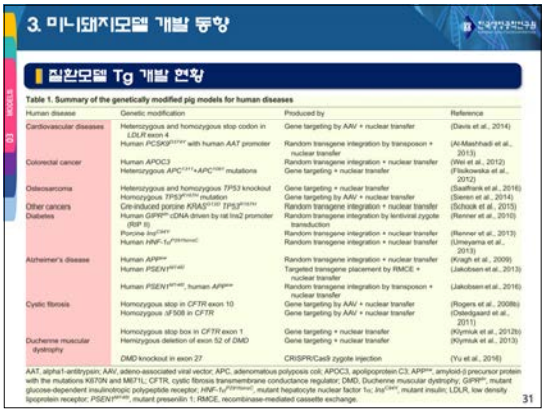
3. 미니돼지모델 개발 동향
질환모델 Tg 개발 현황
Table 1. Summary of the genetically modified pig models for human diseases
31


3. 미니돼지모델 개발 동향
Stage 1
Stage 2
Stage 3
질환모델
바이오장기
형질전환/복제
32


4. FARRC 미니돼지모델 개발 현황
유발 모델등록 개발 현황
33

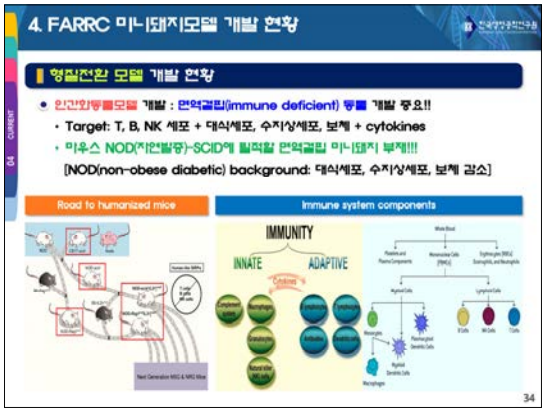
4. FARRC 미니돼지모델 개발 현황
형질전환 모델 개발 현황
Target: T, B, NK 세포 + 대식세포, 수지상세포, 보체 + cytokines
Road to humanized mice
Immune system components
IMMUNITY
INNATE
ADAPTIVE
34


4. FARRC 미니돼지모델 개발 현황
형질전환 모델 개발 현황
원인유전자: IL2rg, ADA, IL-7, RAG1/2, Artemis 등의 돌연변이
SCID 원인유전자
SCID 유전자 결손 임상증상(표현형)
Table 1
SCID classification
35


4. FARRC 미니돼지모델 개발 현황
형질전환 모델 개발 현황
SCID 돼지 모델: IL2rg, Artemis(자연발생), RAG1, RAG2, double mutant 등
– 다양한 유전자 조작 방법 이용 생산 및 표현형 관찰
Development of Severe Combined Immunodeficient (SCID) Pig Models for Translational Cancer Modeling: Future Insights on How Humanized SCID Pigs Can Improve Preclinical Cancer Research
TABLE 1 | Previously described SCID-pig models.
36

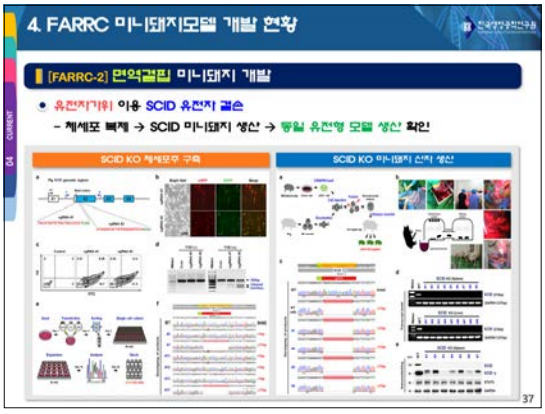
4. FARRC 미니돼지모델 개발 현황
[FARRC-2] 면역결핍 미니돼지 개발
유전자가위 이용 SCID 유전자 결손
- 체세포 복제 → SCID 미니돼지 생산 → 동일 유전형 모델 생산 확인
SCID KO 체세포주 구축
SCID KO 미니돼지 신규 생산
37


4. FARRC 미니돼지모델 개발 현황
형질전환 모델 개발 현황
돼지로 인간의 피 생산... 헌혈 필요없는 세상 가까워졌다
CRISPR
이종간 수혈?
신규 헌혈 방법?
새로운 혈액?
38


4. FARRC 미니돼지모델 개발 현황
형질전환 모델 개발 현황
실험동물 크기 & 활용성 : 미니돼지 (활용) 기치제고
• 육종/유지관리 에너지 감소 : 고전 육종 대비 시간/비용 최소화, 유지관리 용이성 제고
• 신약 개발 비용 절감 : 비임상 약물 TEST 비용 최소화
기축
(More food)
실험동물
(More efficient)
39


4. FARRC 미니돼지모델 개발 현황
형질전환 모델 개발 현황
왜소증 환자 치료 최적 실험동물 모델 부재
• 기존 모델의 표현형 한계: 크기 감소, no 연관 표현형 (인간 유사성 낮음)
마우스 GHR KO 모델
마우스 GHRH KO 모델
돼지 GHR KO 모델
40


4. FARRC 미니돼지모델 개발 현황
형질전환 모델 개발 현황
Dwarf KO 미니돼지 제작
- 유전자가위, 체세포 핵치환 기법 이용
Dwarf KO 미니돼지 신규 제작
표현형 (성장저하, 복부비만, 골 발달 이상)
41


4. FARRC 미니돼지모델 개발 현황
형질전환 모델 개발 현황
Drug R&D
Clinical Trial
Target ID & Validation
Hit Generation
Lead Gen & Optimization
Pre Clinical Animal Studies
Phase 1 Safety
Phase 2 Efficacy Safety
Phase 3 Efficacy Safety
FDA Review & Approval
비임상 평가 (소형 미니돼지 활용 필요)
Ready to Preclinical Trials
"연구개발 비용 최소화", "신산업 육성" → "미니돼지 활용 활성화" 기대
42


5. FARRC 미니돼지모델 미래
Design your animals!!
data
43


5. FARRC 미니돼지모델 미래
Ctrl-C/V → "Ctrl-X/V"
Ctrl + C
Ctrl + V
COPY
PASTE
WHAT is NEXT?
Creation of new area
CTRL + V
44


5. FARRC 미니돼지모델 미래
Design your animals!!
Stage 1
Stage 2
Stage 3
Stage 4
???
질환모델
바이오장기
형질전환/복제
45


5. FARRC 미니돼지모델 미래
Elevate the value!!
돼지고기 1근
만원입니다
형질전환 미니돼지
생명연구자원
가치제고
미래 질지리 창출
바이오의학 산업생태계 혁신
국민 삶의 질 향상
JOBS
46


감사합니다
미래형동물자원센터 FARRC

:

Dev. Reprod. Vol 26, 2022 (Suppl. 1). pp 11

기조강연II

eDNA의 현재: 수생태계의 정밀화

곽인실

전남대학교

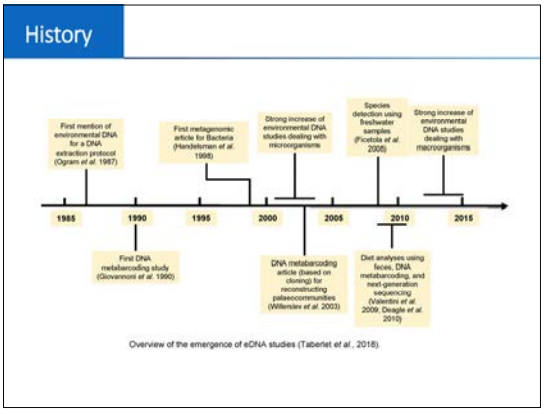

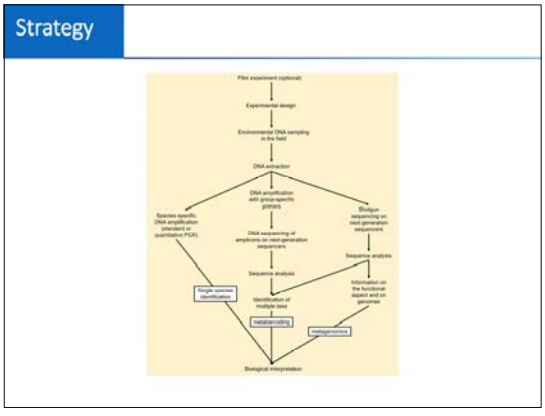

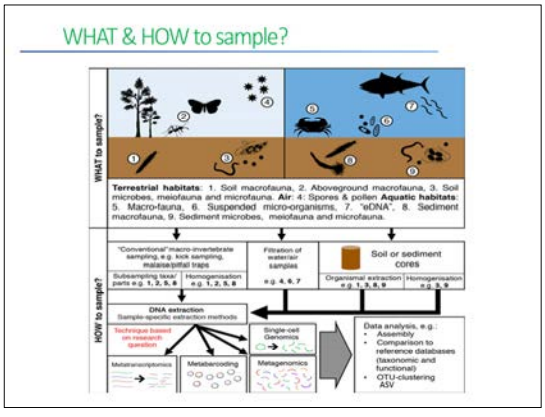

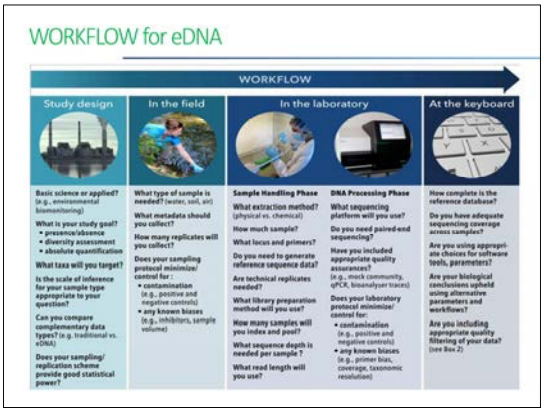

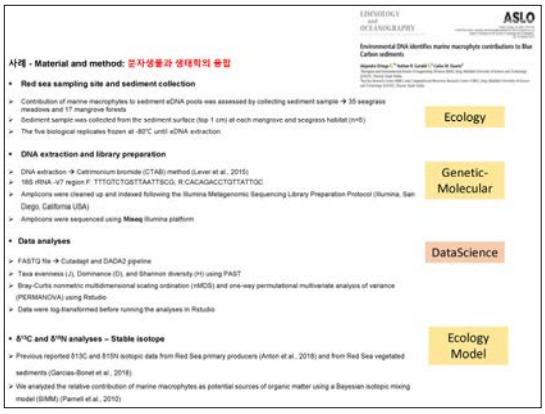
ASLO
Environmental DNA identifies marine macrophyte contributions to Blue Carbon sediments
사례 - Material and method: 분자생물과 생태학의 융합
Red sea sampling site and sediment collection
Ecology
DNA extraction and library preparation
Genetic-Molecular
Data analyses
DataScience
δ13C and δ15N analyses – Stable isotope
Ecology Model

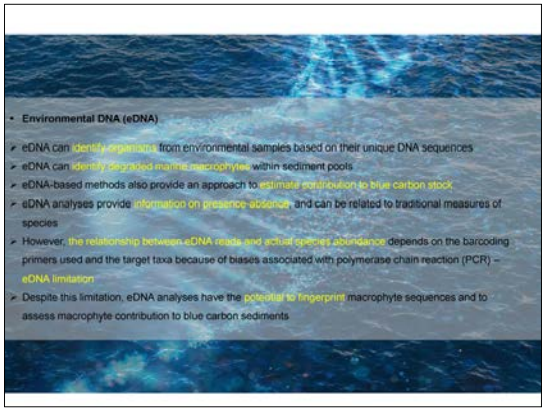
Environmental DNA (eDNA)
eDNA can identify organisms from environmental samples based on their unique DNA sequences
eDNA can identify degraded marine macrophytes within sediment pools
eDNA-based methods also provide an approach to estimate contribution to blue carbon stock
eDNA analyses provide information on presence-absence, and can be related to traditional measures of species
However, the relationship between eDNA reads and actual species abundance depends on the barcoding primers used and the target taxa because of biases associated with polymerase chain reaction (PCR) – eDNA limitation
Despite this limitation, eDNA analyses have the potential to fingerprint macrophyte sequences and to assess macrophyte contribution to blue carbon sediments


국제 현황: NCBI db에 등록된 주요 eDNA Seq. No.
In K.Lab. 2021.12.

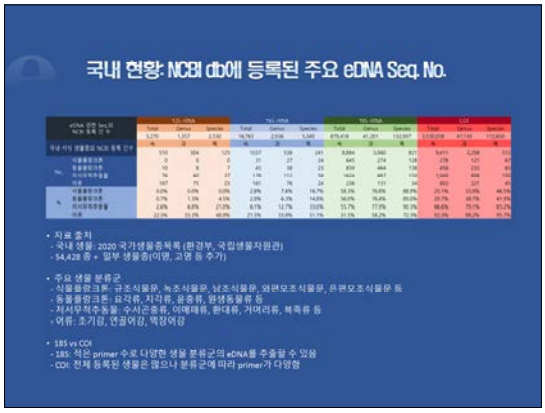
국내 현황: NCBI db에 등록된 주요 eDNA Seq. No.
• 지료 출처
- 국내 생물: 2020 국가생물종목록 (환경부, 국립생물자원관)
- 54,428 종 + 일부 생물종(이명, 고명 등 추가)
• 주요 생물 분류군
- 식물플랑크톤: 규조식물문, 녹조식물문, 남조식물문, 와편모조식물문, 은편모조식물문 등
- 동물플랑크톤: 요각류, 지각류, 윤충류, 원생동물류 등
- 저서무척추동물: 수서곤충류, 이매패류, 환대류, 거머리류, 복족류 등
- 어류: 초기갑, 연골어강, 맥점어강
• 18S vs COI
- 18S: 적은 primer 수로 다양한 생물 분류군의 eDNA를 추출할 수 있음
- COI: 전체 등록된 생물은 많으나 분류군에 따라 primer가 다양함


eDNA 분석 결과에 대한 주요 네거티브
ASV 또는 OTU Frequency와 Field 생물 밀도와의 관계
환경에 있지 않는 생물에 대한 eDNA 검출
- 담수 생물에 해양 어류가 검출됨
- 국내 미출현종이 검출됨

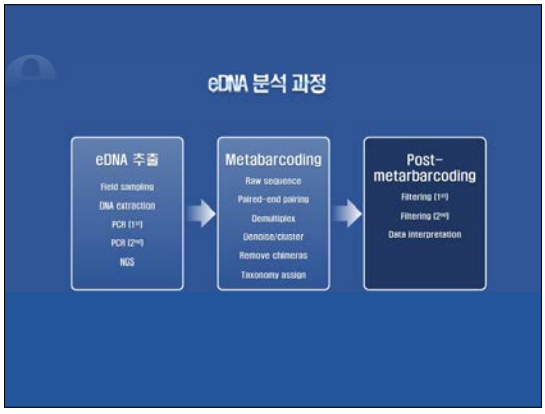
eDNA 분석 과정
eDNA 추출
Field sampling
DNA extraction
PCR [1st]
PCR [2nd]
NGS
Metabarcoding
Raw sequence
Paired-end pairing
Demultiplex
Denoise/cluster
Remove chimeras
Taxonomy assign
Post-metarbarcoding
Filtering [1st]
Filtering [2nd]
Data interpretation

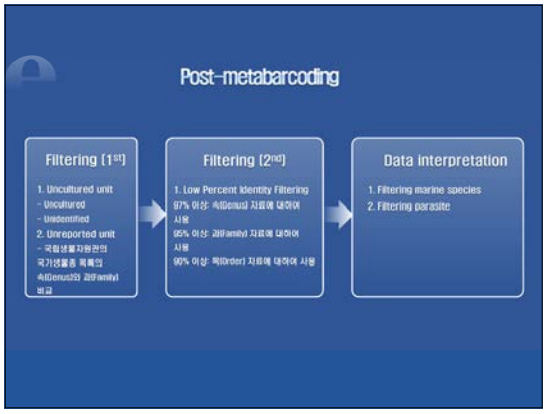

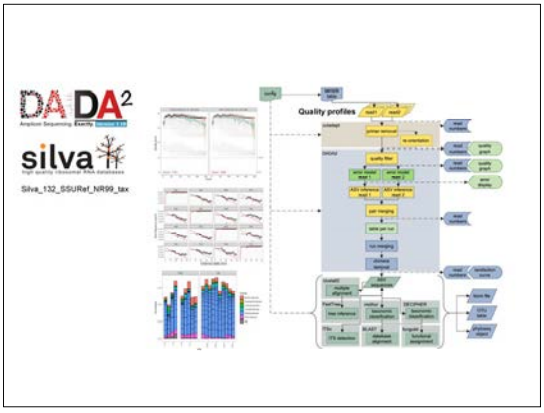

Contents

5 Pelagic biodiversity and biotic interaction assessment

I. 조사 지점 및 채집 방법

1) 섬진강 하구-광양만 8개 지점
2) 2019년 5월, 2020년 9월
3) 원수 채집
4) 기초 수질 항목 측정

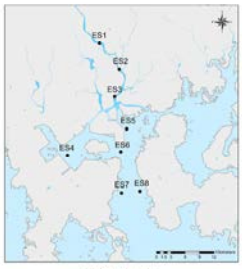

Fig. 1. Sampling map.

5 Pelagic biodiversity and biotic interaction assessment

II. DNA 추출 및 증폭

1) DNA Isolation Kit를 이용하여 genomic DNA 추출
2) 프라이머를 이용하여 18S rRNA 증폭 (1380F_EU, 1510R_EU)
3) MiSeqTM NGS platform을 이용하여 library 구축
4) Read trimming, chimera removing, paired-end merging 등의 염기서열 preprocessing 진행
5) OTU에 기반하여 서열을 구분하여, BLASTn을 이용하여 계통학적인 분류

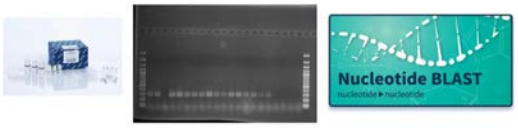

5 Pelagic biodiversity and biotic interaction assessment

III. 분석 방법

1) 생물종 군집화: Algae, Fungi, Protozoa, Inv-meta
2) 진핵생물 군집 차이 분석
   - Bray-Curtis dissimilarity에 기반한 비차원척도법
   - 조사 시기와 정점에 따른 차이분석을 위한 ANOSIM 분석
3) 상호작용 평가
   - Mantel test를 이용하여 생물 그룹간, 환경변수와의 상호작용 평가
   - 주요 환경변수: 수온, 확산(지리적 요인)
4) OTU-OTU 네트워크 분석
   - Spearman correlation에 기반한 co-occurrence 분석

5 Pelagic biodiversity and biotic interaction assessment

Ⅳ. 분석 결과 – 메타바코딩 결과 요약

1) 식물플랑크톤: Chlorophyta, Bacillariophyta
2) 균류: Ascomycota, Chytridiomycota
3) 원생생물: Ciliophora
4) 무척추동물: Arthropoda
5) 어류: Cypriniformes

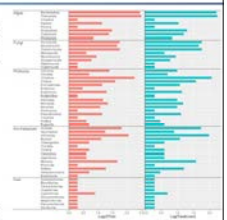

Fig. 2. Sequencing information and distribution of most abundant taxonomic and function linages.

Community	Reads	OTUs	Phylum	Class	Order	Family	Genus	Species
Algae	497,919	1,264	8	37	106	176	321	544
Fungi	30,559	252	8	26	44	73	95	114
Protozoa	82,831	717	16	39	106	169	269	359
Inv-metazoa	106,510	294	14	22	64	167	205	235
Fishes	4,959	15	1	1	9	10	12	12

5 Pelagic biodiversity and biotic interaction assessment

Ⅳ. 분석 결과 – NMDS 분석: 시공간적 차이에 따른 군집 변화

1) 군집 구조는 시간적 차이는 유의하였으나, 공간적 차이는 유의하지 않음

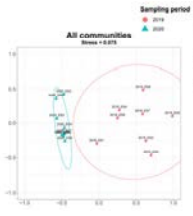

Grouping	Algae	Protozoa	Inv-metazoan
Temporal	0.966 (0.001)	0.606 (0.001)	0.856 (0.001)
Spatial	0.137 (0.120)	0.578 (0.001)	0.235 (0.026)

Fig. 3. NMDS analysis for communities based on community composition across regions and seasons.

5 Pelagic biodiversity and biotic interaction assessment

Ⅳ. 분석 결과 – 상호작용 및 네트워크 분석

1) Pairwise biointeraction: 무척추동물과 물고기 간에 상호작용이 강함
2) Network analysis: 네트워크의 중심 sequence는 해양성 규조류로 나타남

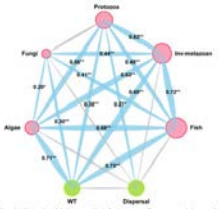

Fig. 4. Pairwise biointeraction between all communities and impacts of water temperature and dispersal on community composition.

Fig. 5. Network analysis of biotic and abiotic interactions.

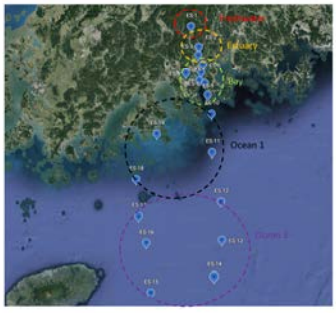

1. Survey location
Freshwater: ES-1 (St 1)

Estuary: ES-2 (St 2)
ES-3 (St 3)

Bay: ES-4 (St 4)
ES-5 (St 5)
ES-6 (St 6)
ES-7 (St 7)
ES-8 (St 8)
ES-9 (St 9)

Ocean 1: ES-10 (St 10)
ES-19 (St 11)
ES-11 (St 12)
ES-18 (St 13)

Ocean 2: ES-12 (St 14)
ES-17 (St 15)
ES-13 (St 16)
ES-16 (St 17)
ES-14 (St 18)
ES-15 (St 19)

Flowchart (0.1% cutoff) _ 18S rRNA V9

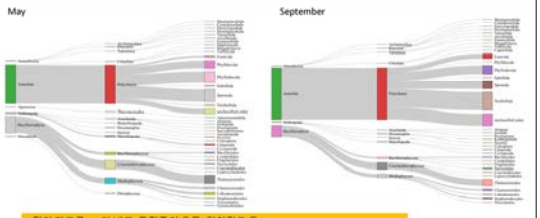

5월의 다모류MSI와 비교, 특정종의 유무, 일치정도 등
9월의 다모류MSI와 비교
전체적인 5월과 9월의 우점종의 동일여부, 차이여부

Flowchart _ Real-data

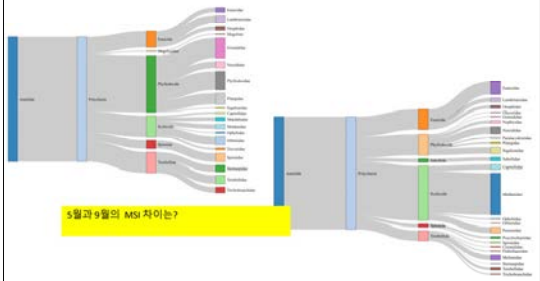

5월과 9월의 MSI 차이는?

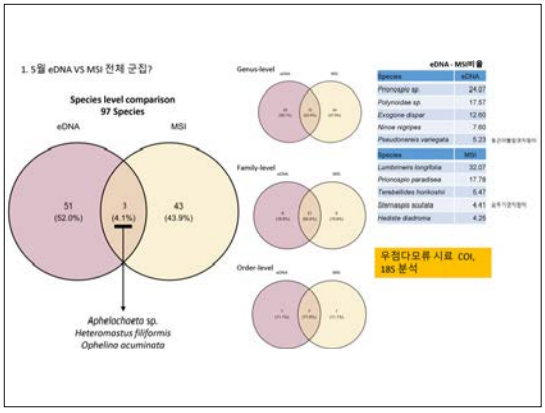

1 삼지창무늬깔따구(*Polypedilum scalaenum*) 위 내용물 분석

I. 조사 지점 및 채집 방법
1) 한강, 금강, 영산강, 낙동강 5개 보 지점
2) 2019년 3월 ~ 7월 (매월)
3) Surber net, dredge, Ekman grab, Ponar grab 등을 이용하여 *Polypedilum scalaenum* 채집

II. 먹이원 분석 방법
1) 소화기관(위, 장) 적출
2) 광학현미경 하 식물플랑크톤과 동물플랑크톤을 검경 및 동정

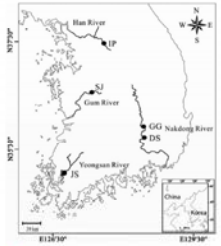

Fig. 1. Map showing the sampling sites in the Han River (IP: Ipsoh Weir), Gum River (SJ: Sejong Weir), Yeongsan River (JS: Juksan Weir), and Nakdong River (GG: Gangjeong Goryeong Weir, DS: Dalseong Weir).

1 삼지창무늬깔따구 위 내용물 분석

III. *P. scalaenum*의 소화기관 내 먹이원 조성
1) 규조류, 녹조류, 동물성 플랑크톤, 식물체, 식물 씨앗, 식물뿌리, 화분 등
2) 지점별로 식물플랑크톤 조성이 다름
3) 달성보와 강정고령보에서 식물플랑크톤의 다양성이 높았음

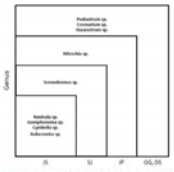

Fig. 4. Comparison of differences and similarities after microscopic examination of the contents of the stomach and intestine of the *Polypedilum scalaenum* by sites. IP: Ipsoh Weir, SJ: Sejong Weir, JS: Juksan Weir, and GG: Gangjeong Goryeong Weir, DS: Dalseong Weir.

Fig. 5. Comparison of Similarities and Differences of Phytoplankton among the sites, IP: Ipsoh Weir, SJ: Sejong Weir, JS: Juksan Weir, and GG: Gangjeong Goryeong Weir, DS: Dalseong Weir (Precise Monitoring of the Phytoplankton in Weir Area, 2018).

2 Gut contents analysis of 4th Instar Midge Larvae

I. 조사 지점 및 채집 방법
1) 금강, 영산강, 낙동강 4개 보 지점
2) 2019년 6월 ~ 7월 (매월)
3) Surber net, dredge, Ekman grab, ponar grab 등을 이용하여 *Polypedilum scalaenum* 채집

II. 먹이원 분석 방법
1) 소화기관(위, 장) 적출
2) 18S rRNA gene의 V9 region 서열 분석하여 종을 확인

Figure 3. Map of the study sites in the Gum River (SJ: Sejong Weir), Yeongsan River (JS: Juksan Weir), and Nakdong River (GG: Gangjeong Goryeong Weir, DS: Dalseong Weir).

2 Gut contents analysis of 4th Instar Midge Larvae

III. DNA 추출 및 증폭
1) DNeasy Blood & Tissue Kit를 이용하여 Genomic DNA 추출
2) 프라이머를 이용하여 18S rRNA 증폭
3) MiSeqTM NGS platfor을 이용하여 library 구축
4) Read trimming, chimera removing, paired-end merging 등의 염기서열 preprocessing 진행
5) OUT/ASV에 기반하여 서열을 구분
6) BLASTn을 이용하여 계통학적인 분류 수행

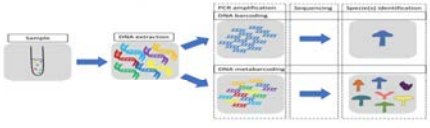

2 Gut contents analysis of 4th Instar Midge Larvae

IV. 분석 결과 – 위 내 출현 종 목록
1) 총 1,019,526 paired-end reads 추출
2) 16목 17과 확인
3) 우점한 OTU에 해당하는 종
: *Paractinolaimus* sp. (Nematoda)
4) 식물플랑크톤이 대부분을 차지함
(Tetrahymena sp., Pseudopediastrum sp.)

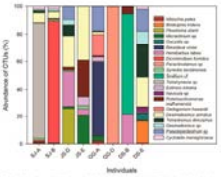

Figure 2. Abundance of OTUs among the individuals in the gut contents of Chironomidae based on the species or genus identification level (18S V9 region; IS-A-9: Sejong Weir, IS-F-8: Juksan Weir, GG-A-D: Gangjeong Goryeong Weir, and DS-B-E: Dalseong Weir).

Table 1. List of the Operational Taxonomic Unit (OTU) in the gut contents of Chironomidae based on the 18SV9 region (IS-A-9: Sejong Weir, IS-F-8: Juksan Weir, GG-A-D: Gangjeong Goryeong Weir, and DS-B-E: Dalseong Weir).

2 Gut contents analysis of 4th Instar Midge Larvae

Ⅳ. 분석 결과 – 생태적 특성

1) Selectivity index (E') 산출, planktonic prey를 선호하는 것으로 나타남
2) *D. armatus, E. minima, T. dimorphus*를 선호하는 것으로 나타남
3) 먹이원이 되는 각 종은 특정 수질 환경과 관계를 가짐

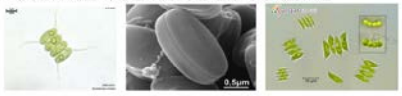

Table 2. Relative abundances and selectivity indexes (E') of phytoplankton species present in the gut content of Chironomidae in the water from where Chironomidae was obtained.

Taxa	Relative Abundance of Prey		Selectivity Index (E')
	Gut Contents (RG)	In the Water (PI)	
Cyclotella meneghiniana	8.85	73.53	−0.79
Desmodesmus armatus	49.32	3.98	0.85
Eolimna minima	4.77	0.53	0.80
Navicula sp.	3.20	1.38	0.40
Nitzschia palea	3.09	10.61	−0.55
Oscyotis sp.	4.62	7.16	−0.22
Tetradesmus dimorphus	26.14	2.81	0.81

제주 강정정수장 32

필터지(100um) 진핵생물 (18S rRNA) 분석

처리명	조사지	조사시기
St-1	고근산배수지	2020년 10월 31일
St-2	동홍배수지	
St-3	도순천	
St-4	제2강정교	
St-5	제2강정교하류	
St-6	제2강정교상류	
St-7	강정취수장	
St-8	강정취수장 침전지	
St-9	강정취수장 침전지 유	
JK-1	취수장 표층	2020년 10월 28일
JK-4	강정 여과지	

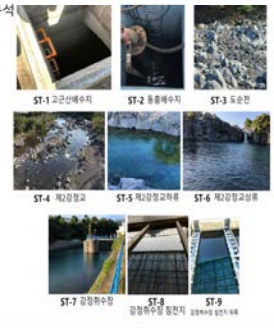

- 채수기 및 비커를 이용하여 2L를 채수
- 진핵생물 전체 유무 판단 분석

전남대학교

4대강 보 유충의 중장 해부 및 위내용물 분석 33

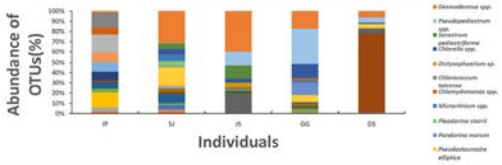

전남대학교

마이크로바이옴 분석 34

야외 채집 C. flaviplumus (노랑털깔따구)

Firmicutes (Clostridiales, 7.94%) / *G. tokunagai*: 0.66%

-The Clostridia are a highly polyphyletic class of Firmicutes, including Clostridium and other similar genera. They are distinguished from the Bacilli by lacking aerobic respiration. They are obligate anaerobes and oxygen is toxic to them. Species of the class Clostridia are often but not always Gram-positive (see Halanaerobium hydrogenoformans) and have the ability to form spores.[3] Studies show they are not a monophyletic group, and their relationships are not entirely certain. Currently, most are placed in a single order called Clostridiales, but this is not a natural group and is likely to be redefined in the future.

Most species of the genus Clostridium are saprophytic organisms that ferment plant polysaccharides [2] and are found in many places in the environment, most notably the soil. However, the genus does contain some human pathogens (outlined below). The toxins produced by certain members of the genus Clostridium are among the most dangerous known. Examples are tetanus toxin (known as tetanospasmin) produced by C. tetani and botulinum toxin produced by C. botulinum. Some species have been isolated from women with bacterial vaginosis.[3]

=> 파상풍독소, 세균성염증, 결대염기성

Fusobacteria (Fusobacteriales, 6.25%) / *G. tokunagai*: 0.01%

-Fusobacteria contribute to several diseases, including periodontal diseases, Lemierre's syndrome, and tropical skin ulcers.

=> 치주염, 세균감염성 인후통 합병증, 피부궤양

전남대학교

3 Gut contents analysis of silver croaker

Ⅰ. 조사 지점 및 채집 방법

1) 광양만 연안 4개 정점
2) 2018년 6월 말 ~ 7월 초
3) 보구치 위 내용물과 해수 표층수 채집

Ⅱ. 먹이원 분석 방법

1) 소화기관(위, 장) 적출
2) 보구치 위: COI-specific primers
   표층수: 18S V9 primers

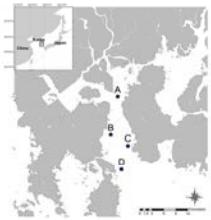

Fig. 1. Map of the study region of Gwangyang Bay in South Korea. Four sites were named as A, B, C, and D.

3 Gut contents analysis of silver croaker

Ⅲ. DNA 추출 및 증폭

1) DNeasy Blood & Tissue Kit를 이용하여 Genomic DNA 추출
2) 프라이머를 이용하여 18S rRNA 증폭
3) MiSeqTM NGS platfor을 이용하여 library 구축
4) Read trimming, chimera removing, paired-end merging 등의 염기서열 preprocessing 진행
5) OTU에 기반하여 서열을 구분
6) BLASTn을 이용하여 계통학적인 분류 수행

Process	Program	Result
Assembly -MiSeq PE	FLASH	Assembled reads (SE, fastq)
Pre-processing (denoising)	CD-HIT-OTU / rDnaTools	Removed noise data
Clustering	CD-HIT-OTU / rDnaTools	OTU cluster

3 Gut contents analysis of silver croaker

Ⅳ. 분석 방법

1) 메타바코딩 결과 확인: heatmap 분석
2) 형태적 분류와 메타바코딩 결과 비교
3) 보구치 위에서 확인된 진핵생물 군집 분석
   - Bray-Curtis dissimilarity에 기반한 비차원척도법
   - 조사 정점에 따른 차이, 어류 크기에 따른 차이
4) 먹이 선택성 Selectivity index (E') 분석
   - 생물상 조사와 메타바코딩 분석을 통해 파악된 전체 생물상 자료 구축
   - 먹이 선택성 지수 계산

3 Gut contents analysis of silver croaker

Ⅴ. 분석 결과 – 메타바코딩 결과

1) 보구치 위와 수표층 내의 생물 종 출현이 매우 다르게 나타남.
   -> 보구치는 저서성 어류로 서식처가 퇴적물에 근접

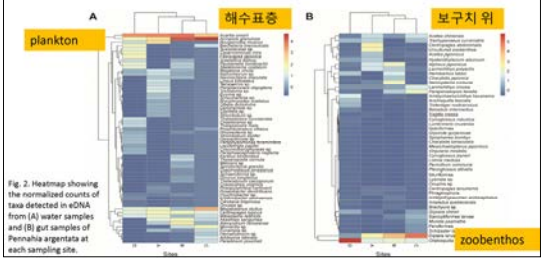

Fig. 2. Heatmap showing the normalized counts of taxa detected in eDNA from (A) water samples and (B) gut samples of Pennahia argentata at each sampling site.

3 Gut contents analysis of silver croaker

Ⅴ. 분석 결과 – 형태적 분류와 메타바코딩 결과 비교

1) 생물 군집에 따라 확인되는 정도가 다르게 나타남
2) 각 Primer에 기반한 결과와 육안 분석에 따라 확인된 속이 매우 다르게 나타남.

Fig. 3. Venn diagram of (A) fish, (B) macrozoobenthos, and (C) zooplankton genera detected using morphological assessments (top) and environmental DNA from water samples (left) and gut samples (right).

3 Gut contents analysis of silver croaker

Ⅴ. 분석 결과 – 보구치 gut 내 진핵생물 군집 분석

1) 공간적으로는 유의한 차이-종조성과 WT, TC가 차이
2) 체장별로는 차이가 유의하지 않았음.
   small (<79mm), medium(79mm< < 141mm), large(141mm <)

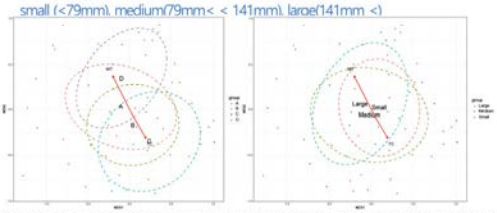

Fig. 4. Non-metric multidimensional scaling ordination of the prey items of silver croaker and the significant environmental variables at P < .05 (red lines with arrows). 54 individuals grouped by (A) sampling sites and (B) their body length. The abbreviated environmental variables are WT, water temperature and TC, total carbon concentration.

3 Gut contents analysis of silver croaker

Ⅴ. 분석 결과 – 먹이 선택성 분석

1) 보구치는 specialist feeding strategy를 가짐-> 갯가재, 파리목을 선호
2) 조사 정점별 선택성 차이가 나타남

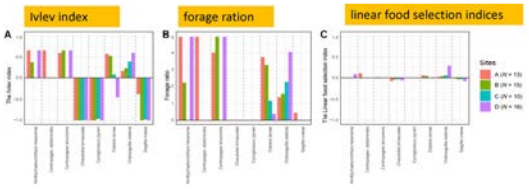

Fig. 5. Selectivity indices calculated for the common species in the *Pennahia argentata* diet and environment. Histograms indicate (A) the Ivlev index, (B) the forage ration, and (C) linear food selection indices of each model, and *N* refers to the number of individuals.

4 Comparison of water sampling

Ⅰ. 조사 지점 및 채집 방법

1) 섬진강 하구-광양만 15개 지점
2) 2018년 6월, 9월
3) 원수, 동물플랑크톤 채집
4) 기초 수질 항목 측정(수온, 염도, 총인, 총질소, 총탄소, 클로로필 a 농도)

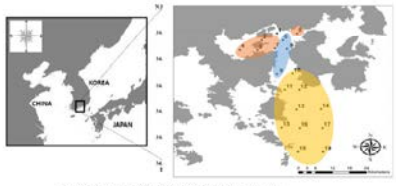

Figure 1. Map of the study sites (black closed circles) in Gwangyang Bay.

4 Comparison of water sampling

II. DNA 추출 및 증폭

1) PowerSoil DNA Isolation Kit를 이용하여 Genomic DNA 추출
2) 프라이머를 이용하여 18S rRNA 증폭
3) MiSeqTM NGS platform을 이용하여 library 구축
4) Read trimming, chimera removing, paired-end merging 등의 염기서열 preprocessing 진행
5) OTU에 기반하여 서열을 구분하여, BLASTn을 이용하여 계통학적인 분류

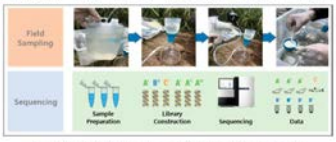

Figure 2. Analytical procedure of environmental DNA (eDNA) extraction and metagenomic sequencing.

4 Comparison of water sampling

III. 분석 방법

1) The self-organizing map (SOM)
   - 33개의 변수 간의 관계분석 및 클러스터 구분
2) 군집 다양도 분석
   - richness, diversity 계산

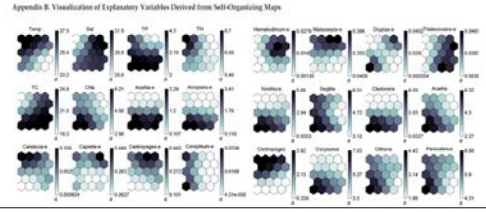

4 Comparison of water sampling

IV. 분석 결과 – Plankton group의 조사 방법 간 결과 비교

1) eDNA metabarcoding 결과
   - diatom이 우점
   - 동물플랑크톤 중에서는 calanoid copepods가 우점
2) 현미경 검경 결과
   - 주요 동물플랑크톤은 Cladocera와 Copepoda
3) Richness와 diversity의 경우 두 방법 간에 결과가 유사함

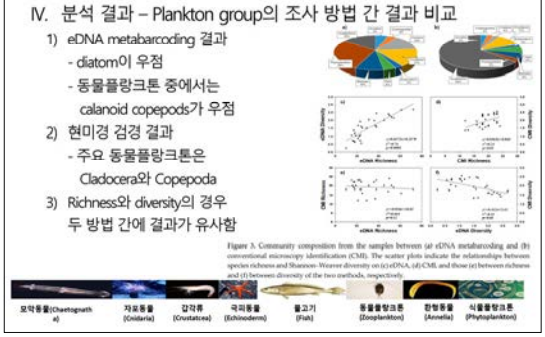

Figure 3. Community composition from the samples between (a) eDNA metabarcoding and (b) conventional microscopy identification (CMI). The scatter plots indicate the relationships between species richness and Shannon–Weaver diversity on (c) eDNA, (d) CMI, and those (e) between richness and (f) between diversity of the two methods, respectively.

4 Comparison of water sampling

IV. 분석 결과 – 생지화학적 특징

1) 조사 결과는 조사 시기와 정점에 따라 구분; June, September, S1-6, S7-9, S10-15 차이
2) 연안 플랑크톤 군집의 출현 패턴을 시공간적 특성으로 추출 구분

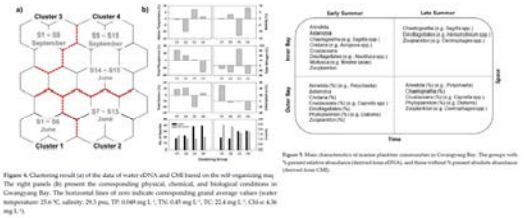

Figure 4. Clustering result (a) of the data of water eDNA and CMI based on the self-organizing map. The right panels (b) present the corresponding physical, chemical, and biological conditions in Gwangyang Bay. The horizontal lines of zero indicate corresponding grand average values (water temperature: 25.6 °C, salinity: 29.3 psu, TP: 0.049 mg L^{-1}, TN: 0.45 mg L^{-1}, TC: 22.4 mg L^{-1}, Chl-a: 4.36 mg L^{-1}).

감사합니다.

Dev. Reprod. Vol 26, 2022 (Suppl. 1). pp 19

기조강연Ⅲ

행동을 조절하는 신경회로의 발생과 진화

이준호
서울대학교
(elegans@sun.ac.kr)

심포지엄 Ⅰ

Dev. Reprod. Vol 26, 2022 (Suppl. 1). pp 23

Development of biomarkers and identification of signalling pathways related to reproductive toxicity of pesticides

권우성

경북대학교

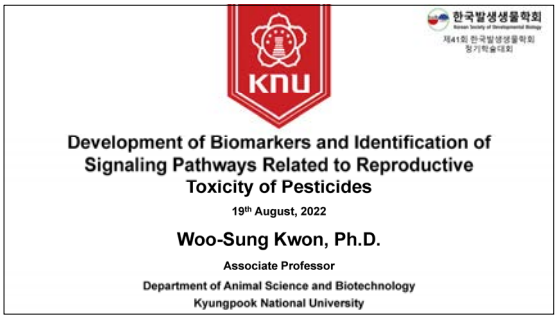

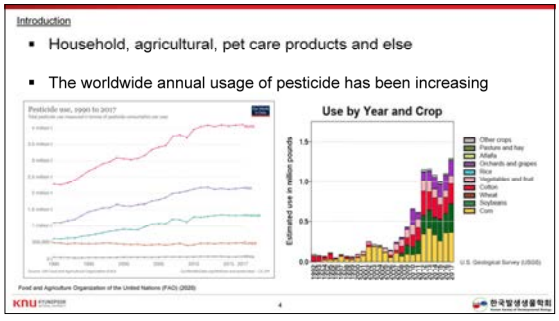

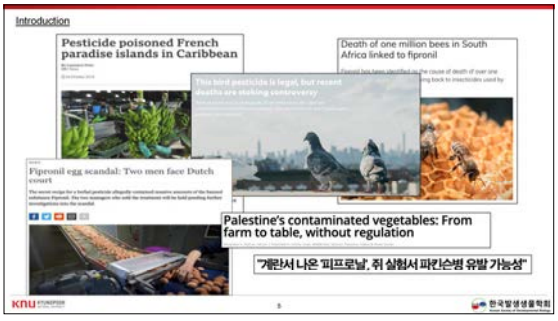

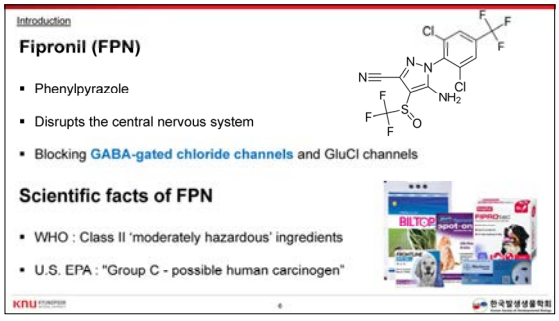

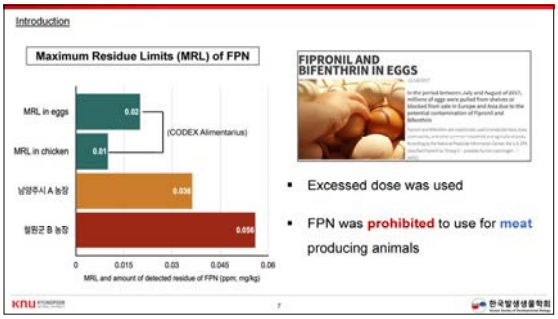
Introduction
Maximum Residue Limits (MRL) of FPN
MRL in eggs
MRL in chicken
남양주시 A 농장
철원군 B 농장
0.02
0.01
0.038
0.056
(CODEX Alimentarius)
0
0.015
0.03
0.045
0.06
MRL and amount of detected residue of FPN (ppm; mg/kg)
FIPRONIL AND BIFENTHRIN IN EGGS
Excessed dose was used
FPN was prohibited to use for meat producing animals


Introduction
Widespread of FPN in global environment via streams and ground water
FPN are ubiquitous in U.S. and Dutch waste and surface water
REGIONAL TRANSPORT
DRY DEPOSITION
PRECIPITATION
EVAPORATION SPRAY DRIFT WIND EROSION
RUNOFF
RECHARGE
GROUND WATER DISCHARGE TO STREAMS
RECHARGE FROM STREAMS
ENTRY THROUGH WELLS
(Majewski and Capel et al.1995.)
(Henk A Tennekes,2018.)
Pesticides in Groundwater
U.S. Geological Survey (USGS)

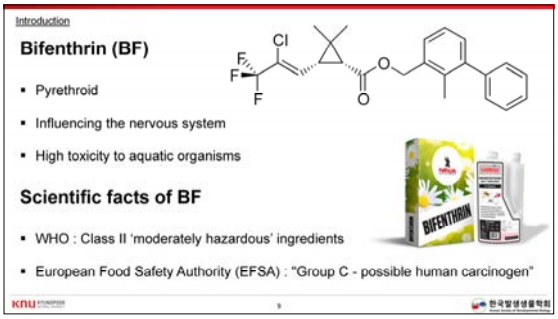
Introduction
Bifenthrin (BF)
Pyrethroid
Influencing the nervous system
High toxicity to aquatic organisms
Cl
F
F
F
O
O
BIFENTHRIN
Scientific facts of BF
WHO : Class II 'moderately hazardous' ingredients
European Food Safety Authority (EFSA) : "Group C - possible human carcinogen"

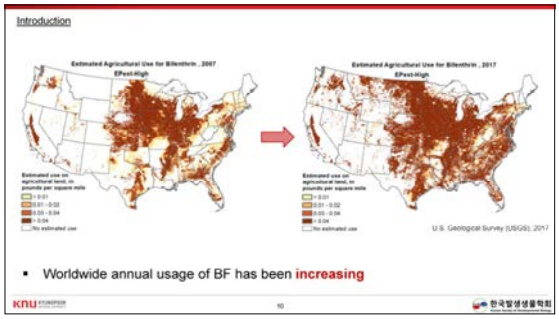
Introduction
Estimated Agricultural Use for Bifenthrin , 2007
EPest-High
Estimated Agricultural Use for Bifenthrin , 2017
EPest-High
U.S. Geological Survey (USGS), 2017
Worldwide annual usage of BF has been increasing

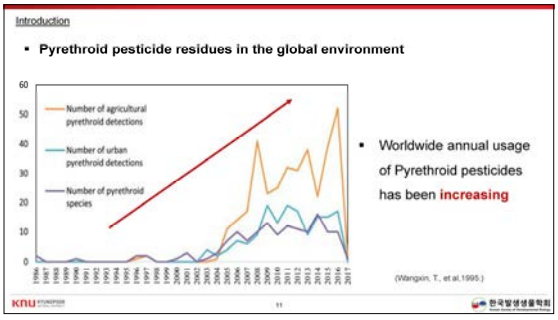
Introduction
Pyrethroid pesticide residues in the global environment
Number of agricultural pyrethroid detections
Number of urban pyrethroid detections
Number of pyrethroid species
60
50
40
30
20
10
0
(Wangxin, T., et al.1995.)
Worldwide annual usage of Pyrethroid pesticides has been increasing

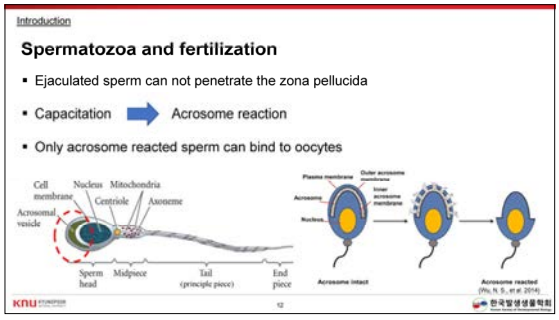
Introduction
Spermatozoa and fertilization
Ejaculated sperm can not penetrate the zona pellucida
Capacitation
Acrosome reaction
Only acrosome reacted sperm can bind to oocytes
Cell membrane
Nucleus
Mitochondria
Centriole
Axoneme
Acrosomal vesicle
Sperm head
Midpiece
Tail (principle piece)
End piece
Plasma membrane
Outer acrosome membrane
Inner acrosome membrane
Acrosome
Nucleus
Acrosome intact
Acrosome reacted

Introduction

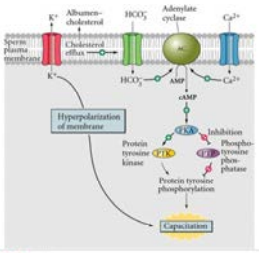

Capacitation

- Final stage of sperm maturation
- Occurs in the female reproductive duct
- PKA and tyrosine phosphorylation
- Flagellum beats more rapidly (hyperactivated)

Objectives

- Despite the adverse effects of pesticide, there has been limited rese arch on those effects on sperm function and mechanism
- Hence, the present study was designed to evaluate the effects of **pe sticides** on **male fertility** in terms of **sperm functions** and **mechan ism**

Materials & Methods

- **Animals**

  8- to 12-week-old, matured ICR Mouse

- **Preparation of the spermatozoa**

  Cauda epididymis

  Incubated to induce the capacitation

  (for 90 min under 5% CO_2 in air at 37 °C)

- **Concentration of pesticides**

  FPN: 0.1, 1, 10, 100, and 300 μM; **BF:** 0.1, 1, 10, and 100 μM

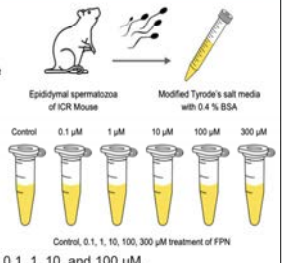

Materials & Methods

- **Computer assisted sperm analyzer (CASA)**

  Sperm Motility (Rapid,%; Slow,%; Medium,%; Progressive,%)

  Motion kinematics (VCL, μm/s; VSL, μm/s; VAP, μm/s; BCF, Hz; ALH, μm)

- **Hoechst 33258/chlortetracycline Fluorescence (H33258/CTC)**

  Live non-capacitated pattern (F pattern)

  Live capacitated pattern (B pattern)

  Live acrosome-reacted pattern (AR pattern)

  Dead pattern (D pattern)

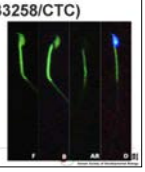

Materials & Methods

- **Intracellular ATP level, Cell cytotoxicity and viability**

  ATP Assay Kit (Abcam, Cambridge, UK)

  Cell Cytotoxicity Assay Kit (Abcam, Cambridge, UK)

- **Western blot**

  phospho-PKA substrate activity

  tyrosine phosphorylation

  α-tubulin (endogenous loading control)

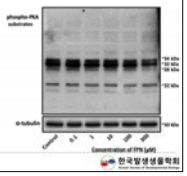

Materials & Methods

- **In vitro fertilization (IVF)**

  Eight to twelve years old female ICR male mice

  super-ovulation was induced using PMSG and hCG

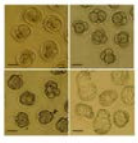

- **Statistical analysis**

  One-way ANOVA using the SPSS software (Version 25.0, IBM, Armonk, NY, USA)

  Tukey's multiple comparison test

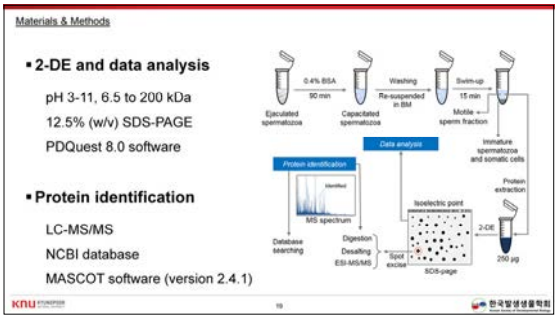
Materials & Methods
▪ 2-DE and data analysis
pH 3-11, 6.5 to 200 kDa
12.5% (w/v) SDS-PAGE
PDQuest 8.0 software
▪ Protein identification
LC-MS/MS
NCBI database
MASCOT software (version 2.4.1)
0.4% BSA
90 min
Washing
Re-suspended in BM
Swim-up
15 min
Ejaculated spermatozoa
Capacitated spermatozoa
Motile sperm fraction
Immature spermatozoa and somatic cells
Data analysis
Protein identification
Protein extraction
MS spectrum
Isoelectric point
2-DE
250 μg
Database searching
Digestion Desalting ESI-MS/MS
Spot excise
SDS-page

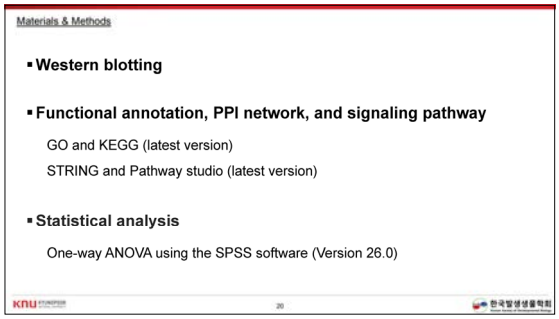
Materials & Methods
▪ Western blotting
▪ Functional annotation, PPI network, and signaling pathway
GO and KEGG (latest version)
STRING and Pathway studio (latest version)
▪ Statistical analysis
One-way ANOVA using the SPSS software (Version 26.0)

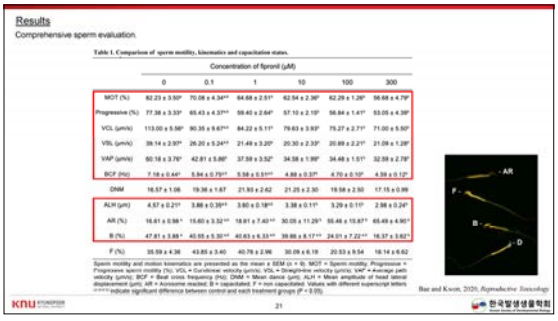
Results
Comprehensive sperm evaluation.
AR
B
D

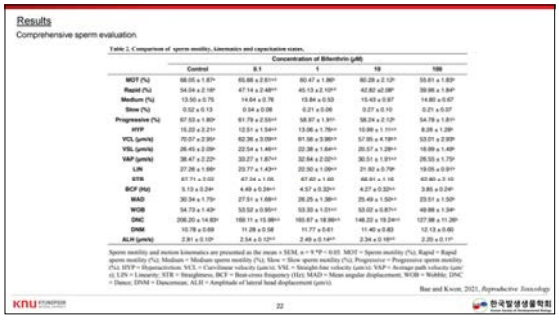
Results
Comprehensive sperm evaluation.

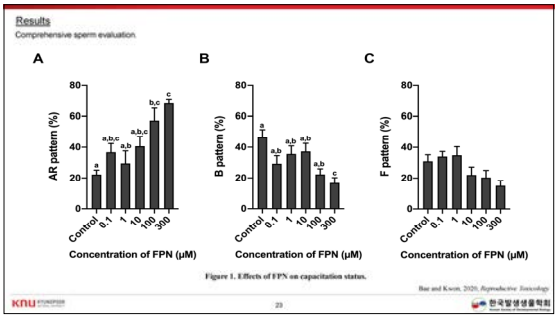
Results
Comprehensive sperm evaluation.
A
B
C
AR pattern (%)
B pattern (%)
F pattern (%)
Control
0.1
1
10
100
300
Concentration of FPN (μM)
Figure 1. Effects of FPN on capacitation status.

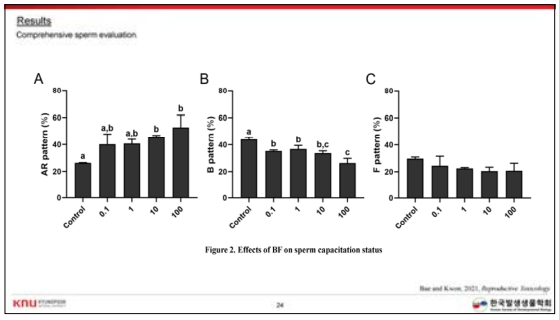
Results
Comprehensive sperm evaluation.
A
B
C
AR pattern (%)
B pattern (%)
F pattern (%)
Control
0.1
1
10
100
Figure 2. Effects of BF on sperm capacitation status

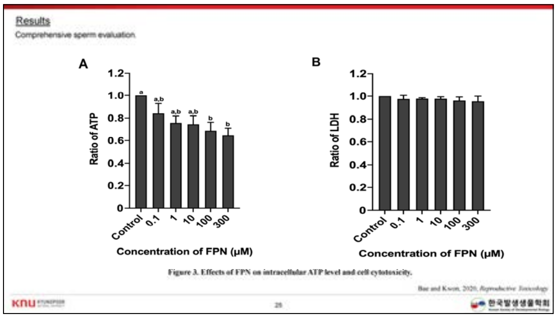
Results
Comprehensive sperm evaluation
A
Ratio of ATP
Concentration of FPN (μM)
B
Ratio of LDH
Concentration of FPN (μM)
Figure 3. Effects of FPN on intracellular ATP level and cell cytotoxicity.
Bae and Kwon, 2020, Reproductive Toxicology
25

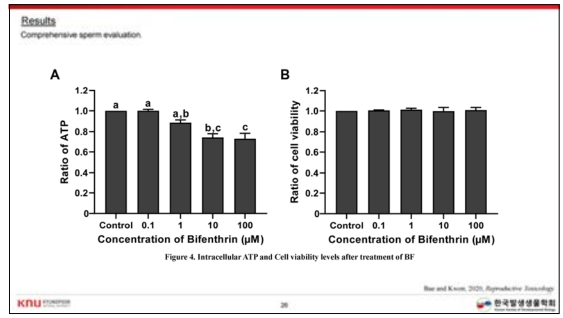
Results
Comprehensive sperm evaluation
A
Ratio of ATP
Concentration of Bifenthrin (μM)
B
Ratio of cell viability
Concentration of Bifenthrin (μM)
Figure 4. Intracellular ATP and Cell viability levels after treatment of BF
Bae and Kwon, 2020, Reproductive Toxicology
26

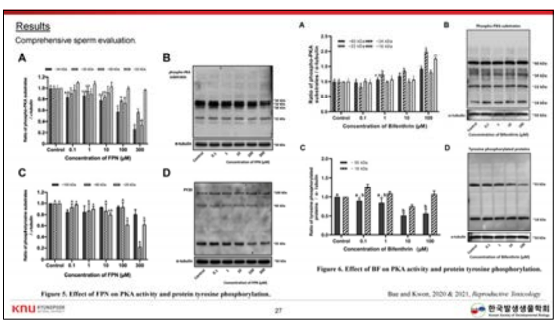
Results
Comprehensive sperm evaluation
Figure 5. Effect of FPN on PKA activity and protein tyrosine phosphorylation.
Figure 6. Effect of BF on PKA activity and protein tyrosine phosphorylation.
Bae and Kwon, 2020 & 2021, Reproductive Toxicology
27

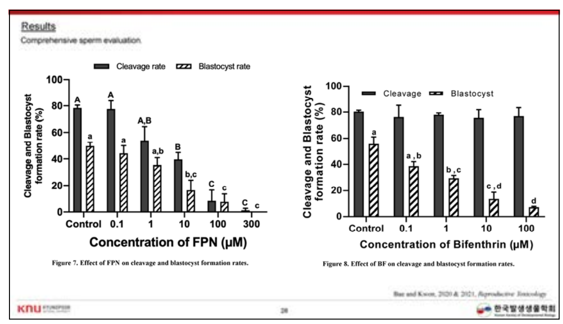
Results
Comprehensive sperm evaluation
Cleavage rate
Blastocyst rate
Cleavage and Blastocyst formation rate (%)
Concentration of FPN (μM)
Cleavage
Blastocyst
Concentration of Bifenthrin (μM)
Figure 7. Effect of FPN on cleavage and blastocyst formation rates.
Figure 8. Effect of BF on cleavage and blastocyst formation rates.
Bae and Kwon, 2020 & 2021, Reproductive Toxicology
28

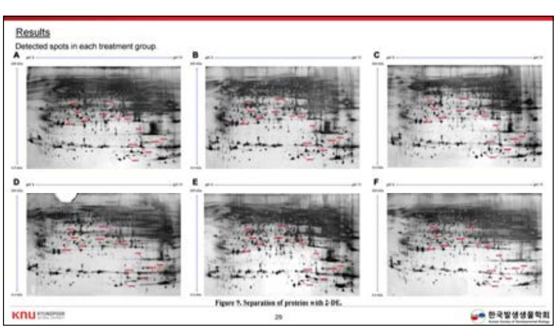
Results
Detected spots in each treatment group
Figure 9. Separation of proteins with 2-DE.
29


Results
Identification of differentially expressed proteins (DEPs)
Table 3. Differentially expressed proteins (> 3-fold) identified by LC-MS/MS (FPN).
Table 4. Differentially expressed proteins (> 3-fold) identified by LC-MS/MS (BF).
30

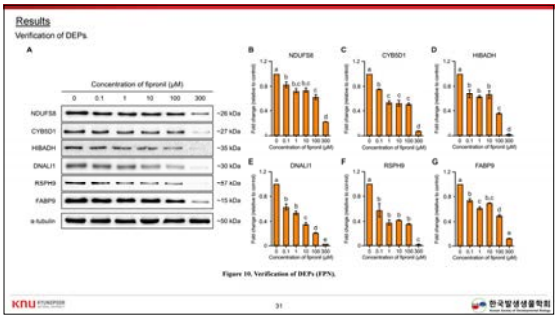
Results
Verification of DEPs.
Figure 10. Verification of DEPs (FPN).

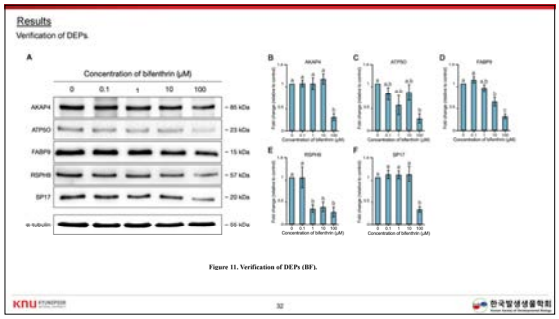
Results
Verification of DEPs.
Figure 11. Verification of DEPs (BF).

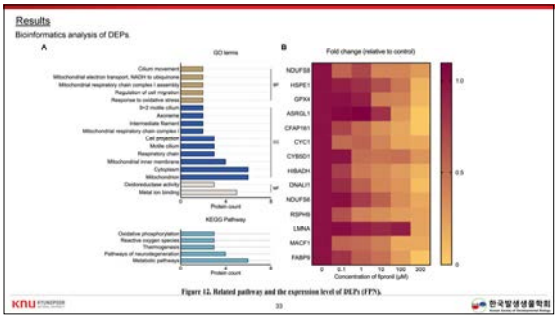
Results
Bioinformatics analysis of DEPs.
Figure 12. Related pathway and the expression level of DEPs (FPN).

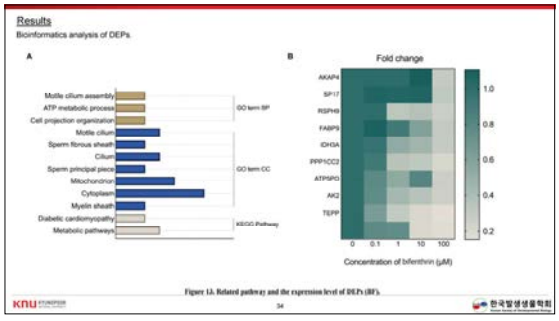
Results
Bioinformatics analysis of DEPs.
Figure 13. Related pathway and the expression level of DEPs (BF).

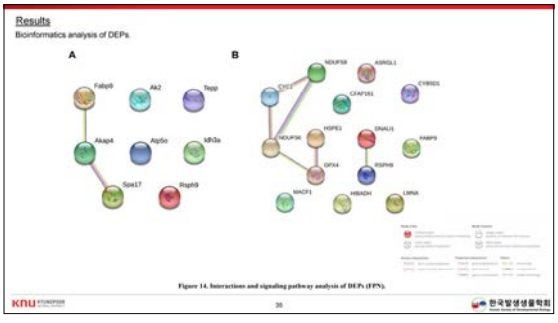
Results
Bioinformatics analysis of DEPs.
Figure 14. Interactions and signaling pathway analysis of DEPs (FPN).

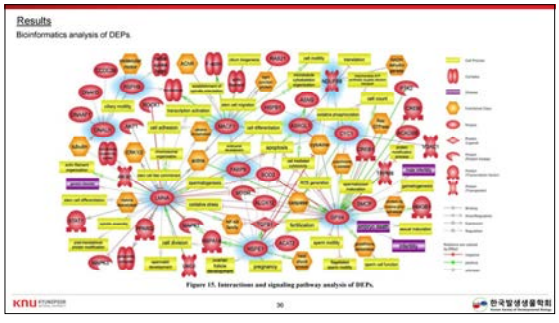
Results
Bioinformatics analysis of DEPs.
Figure 15. Interactions and signaling pathway analysis of DEPs.

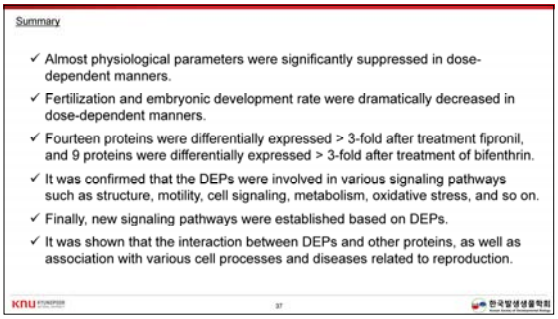
Summary
✓ Almost physiological parameters were significantly suppressed in dose-dependent manners.
✓ Fertilization and embryonic development rate were dramatically decreased in dose-dependent manners.
✓ Fourteen proteins were differentially expressed > 3-fold after treatment fipronil, and 9 proteins were differentially expressed > 3-fold after treatment of bifenthrin.
✓ It was confirmed that the DEPs were involved in various signaling pathways such as structure, motility, cell signaling, metabolism, oxidative stress, and so on.
✓ Finally, new signaling pathways were established based on DEPs.
✓ It was shown that the interaction between DEPs and other proteins, as well as association with various cell processes and diseases related to reproduction.

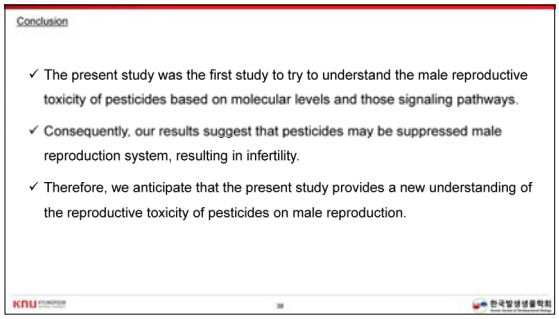
Conclusion
✓ The present study was the first study to try to understand the male reproductive toxicity of pesticides based on molecular levels and those signaling pathways.
✓ Consequently, our results suggest that pesticides may be suppressed male reproduction system, resulting in infertility.
✓ Therefore, we anticipate that the present study provides a new understanding of the reproductive toxicity of pesticides on male reproduction.

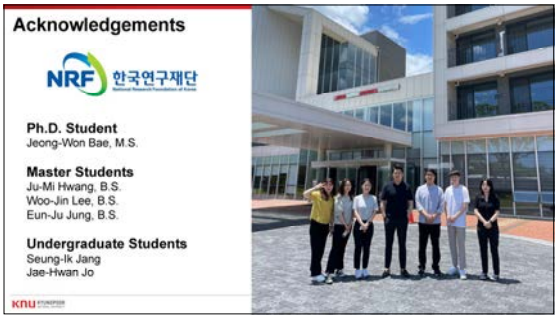
Acknowledgements
NRF 한국연구재단
Ph.D. Student
Jeong-Won Bae, M.S.
Master Students
Ju-Mi Hwang, B.S.
Woo-Jin Lee, B.S.
Eun-Ju Jung, B.S.
Undergraduate Students
Seung-Ik Jang
Jae-Hwan Jo

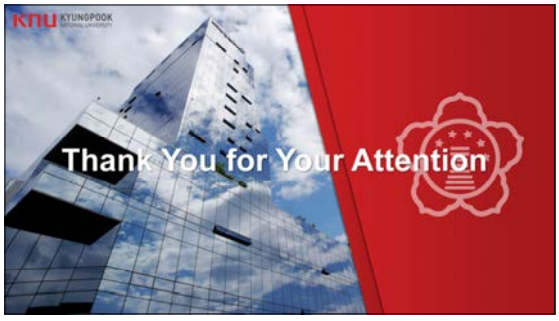
KYUNGPOOK
Thank You for Your Attention

Dev. Reprod. Vol 26, 2022 (Suppl. 1). pp 30

해양오염 유해인자 영향평가 및 사례연구

정지현

한국해양과학기술원

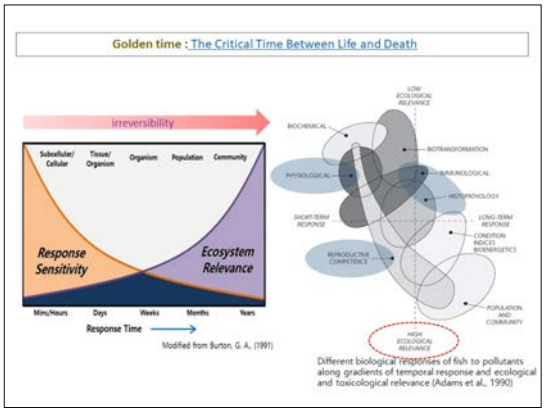

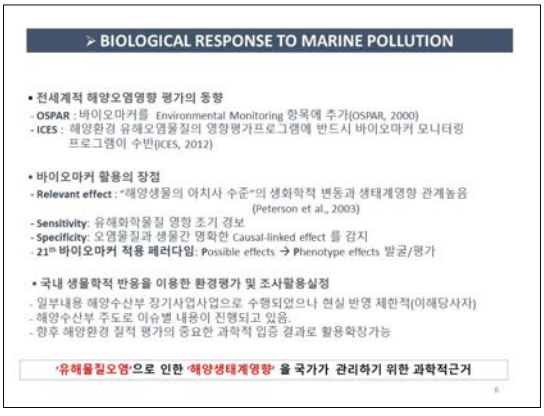


연구사례 1.
● 사례1. 해양사고 영향 규명 연구 사례
'유류오염 환경영향평가 및 환경복원연구(2009~2018)' 종료


The Hebei sprit oil spill
✓ 2007년 12월 7일
✓ 3종 중동산 원유 12,547 kL (10,900 M/T; 78,918 barrels) 유출
✓ 서해안 전역이 유출된 기름에 의해 오염됨
HEBEI SPIRIT Oil Spill Pollution

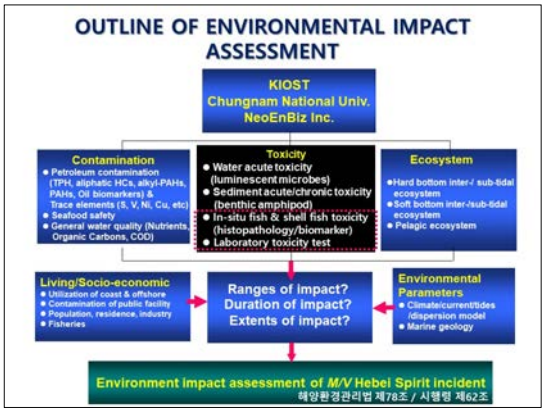
OUTLINE OF ENVIRONMENTAL IMPACT ASSESSMENT
KIOST
Chungnam National Univ.
NeoEnBiz Inc.
Contamination
● Petroleum contamination (TPH, aliphatic HCs, alkyl-PAHs, PAHs, Oil biomarkers) & Trace elements (S, V, Ni, Cu, etc)
● Seafood safety
● General water quality (Nutrients, Organic Carbons, COD)
Toxicity
● Water acute toxicity (luminescent microbes)
● Sediment acute/chronic toxicity (benthic amphipod)
● In-situ fish & shell fish toxicity (histopathology/biomarker)
● Laboratory toxicity test
Ecosystem
●Hard bottom inter-/ sub-tidal ecosystem
●Soft bottom inter-/sub-tidal ecosystem
● Pelagic ecosystem
Living/Socio-economic
● Utilization of coast & offshore
● Contamination of public facility
● Population, residence, industry
● Fisheries
Ranges of impact?
Duration of impact?
Extents of impact?
Environmental Parameters
● Climate/current/tides /dispersion model
● Marine geology
Environment impact assessment of M/V Hebei Spirit incident
해양환경관리법 제78조 / 시행령 제62조

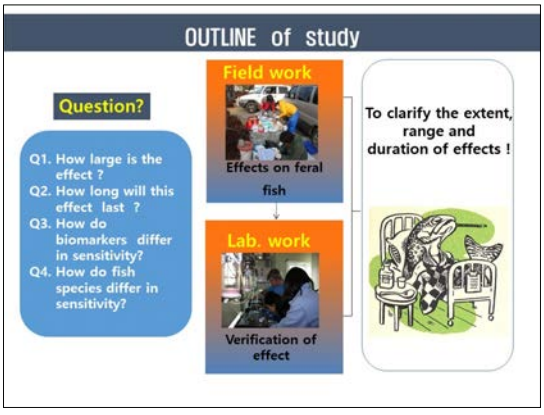
OUTLINE of study
Question?
Q1. How large is the effect ?
Q2. How long will this effect last ?
Q3. How do biomarkers differ in sensitivity?
Q4. How do fish species differ in sensitivity?
Field work
Effects on feral fish
Lab. work
Verification of effect
To clarify the extent, range and duration of effects !


2007년 12월~2017년 12월

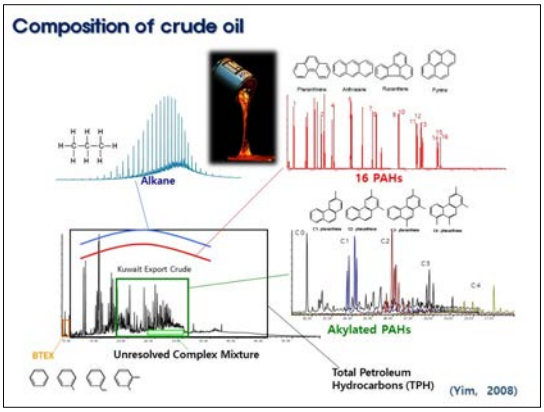
Composition of crude oil
Alkane
16 PAHs
Kuwait Export Crude
Akylated PAHs
BTEX
Unresolved Complex Mixture
Total Petroleum Hydrocarbons (TPH)
(Yim, 2008)

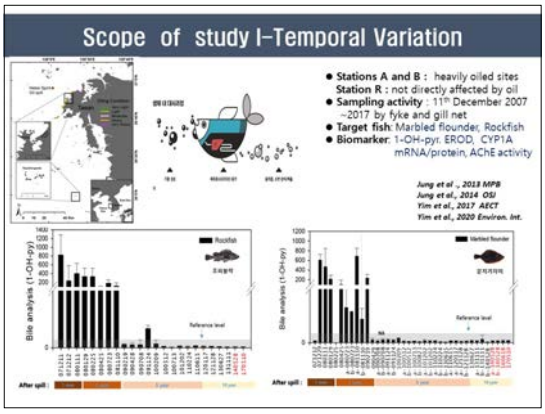
Scope of study I-Temporal Variation
Stations A and B : heavily oiled sites
Station R : not directly affected by oil
Sampling activity : 11th December 2007 ~2017 by fyke and gill net
Target fish: Marbled flounder, Rockfish
Biomarker: 1-OH-pyr. EROD, CYP1A mRNA/protein, AChE activity
Jung et al., 2013 MPB
Jung et al., 2014 OSJ
Yim et al., 2017 AECT
Yim et al., 2020 Environ. Int.
Bile analysis (1-OH-pyr)
Rockfish
Marbled flounder
Reference level
After spill

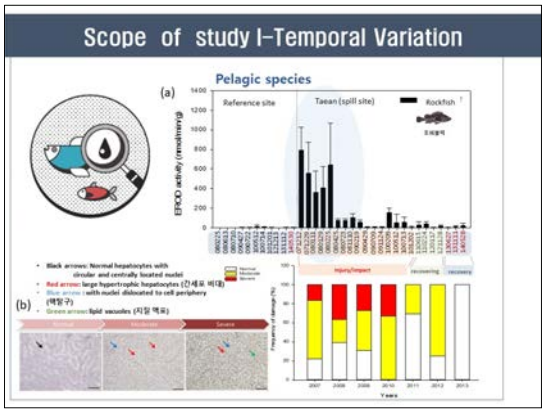
Scope of study I-Temporal Variation
Pelagic species
(a)
Reference site
Taean (spill site)
Rockfish
EROD activity (nmol/min/mg)
(b)
Injury/impact
recovering
recovery
Years

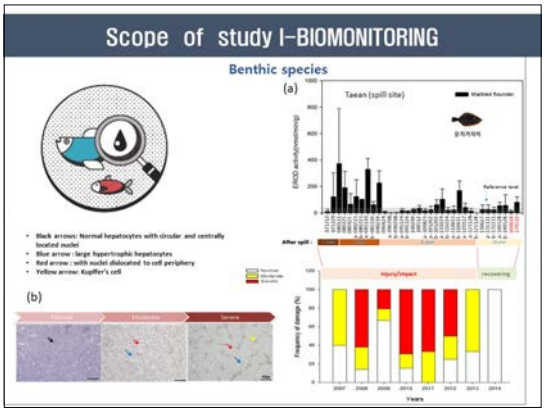
Scope of study I-BIOMONITORING
Benthic species
(a)
Taean (spill site)
Marbled flounder
Reference level
After spill
Injury/impact
recovering
(b)
Years

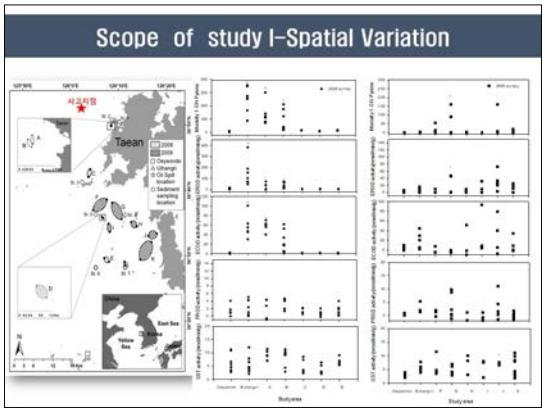
Scope of study I-Spatial Variation
사고지점
Taean
East Sea
Yellow Sea

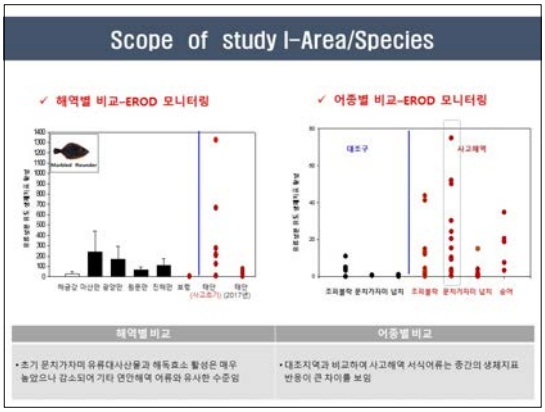
Scope of study I-Area/Species
✓ 해역별 비교-EROD 모니터링
✓ 어종별 비교-EROD 모니터링
Marbled flounder
대조구
사고해역
해역별 비교
어종별 비교
•초기 문치가자미 유류대사산물과 해독효소 활성은 매우 높았으나 감소되어 기타 연안해역 어류와 유사한 수준임
•대조지역과 비교하여 사고해역 서식어류는 종간의 생체지표 반응이 큰 차이를 보임

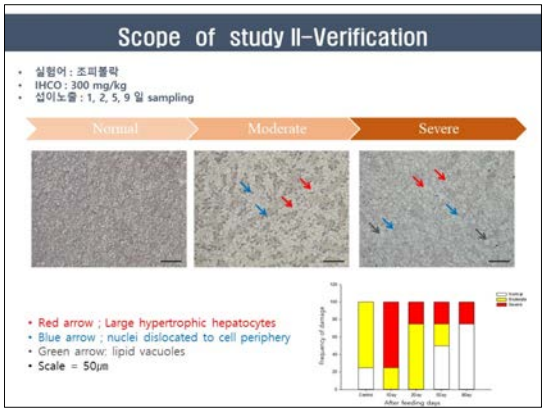
Scope of study II-Verification
실험어 : 조피볼락
IHCO : 300 mg/kg
섭이노출 : 1, 2, 5, 9 일 sampling
Normal
Moderate
Severe
Red arrow ; Large hypertrophic hepatocytes
Blue arrow ; nuclei dislocated to cell periphery
Green arrow: lipid vacuoles
Scale = 50μm
Frequency of damage
After feeding days

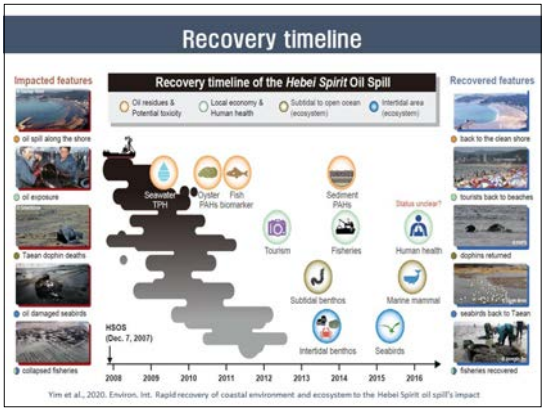
Recovery timeline
Recovery timeline of the Hebei Spirit Oil Spill
Impacted features
Recovered features
Seawater TPH
Oyster PAHs biomarker
Fish PAHs biomarker
Sediment PAHs
Tourism
Fisheries
Human health
Subtidal benthos
Marine mammal
Intertidal benthos
Seabirds
HSOS (Dec. 7, 2007)
2008 2009 2010 2011 2012 2013 2014 2015 2016
Yim et al., 2020. Environ. Int. Rapid recovery of coastal environment and ecosystem to the Hebei Spirit oil spill's impact

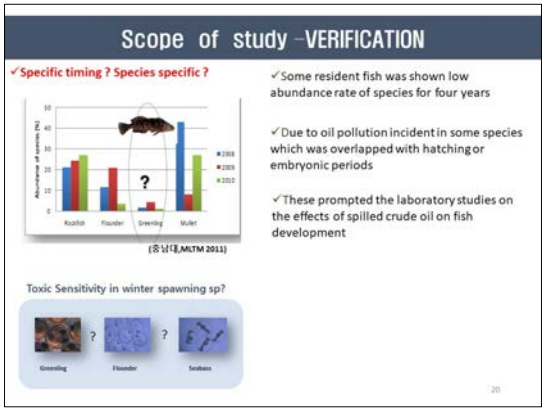
Scope of study –VERIFICATION
✓Specific timing ? Species specific ?
✓Some resident fish was shown low abundance rate of species for four years
✓Due to oil pollution incident in some species which was overlapped with hatching or embryonic periods
✓These prompted the laboratory studies on the effects of spilled crude oil on fish development
Toxic Sensitivity in winter spawning sp?
Greening
Flounder
Seabass

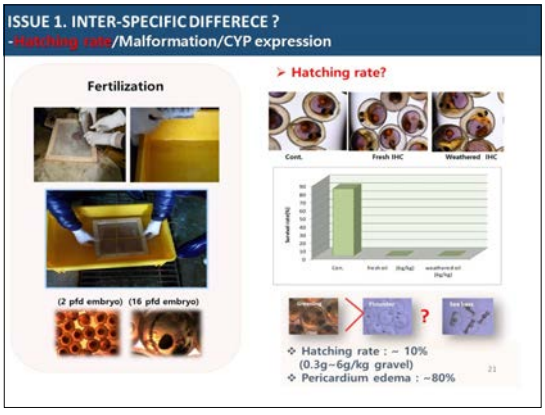
ISSUE 1. INTER-SPECIFIC DIFFERECE ?
-Hatching rate/Malformation/CYP expression
Fertilization
(2 pfd embryo) (16 pfd embryo)
➢ Hatching rate?
Cont.
Fresh IHC
Weathered IHC
✧ Hatching rate : ~ 10% (0.3g~6g/kg gravel)
✧ Pericardium edema : ~80%

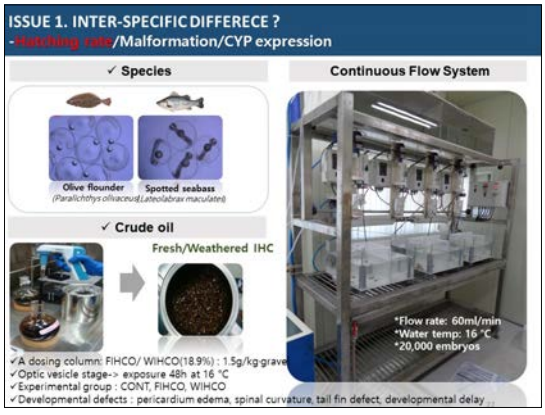
ISSUE 1. INTER-SPECIFIC DIFFERECE ?
-Hatching rate/Malformation/CYP expression
✓ Species
Olive flounder
Spotted seabass
(Parallichthys olivaceus)(Lateolabrax maculatus)
✓ Crude oil
Fresh/Weathered IHC
Continuous Flow System
*Flow rate: 60ml/min
*Water temp: 16 ℃
*20,000 embryos
✓A dosing column: FIHCO/ WIHCO(18.9%) : 1.5g/kg·grave
✓Optic vesicle stage-> exposure 48h at 16 ℃
✓Experimental group : CONT, FIHCO, WIHCO
✓Developmental defects : pericardium edema, spinal curvature, tail fin defect, developmental delay

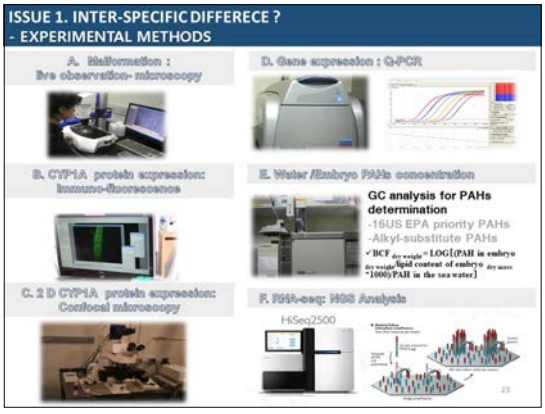
ISSUE 1. INTER-SPECIFIC DIFFERECE ?
- EXPERIMENTAL METHODS
A. Malformation : live observation- microscopy
B. CYP1A protein expression: Immuno-fluorescence
C. 2 D CYP1A protein expression: Confocal microscopy
D. Gene expression : Q-PCR
E. Water /Embryo PAHs concentration
GC analysis for PAHs determination
-16US EPA priority PAHs
-Alkyl-substitute PAHs
F. RNA-seq: NGS Analysis
HiSeq2500

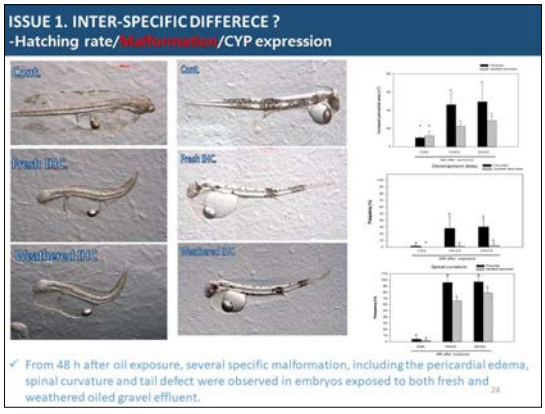
ISSUE 1. INTER-SPECIFIC DIFFERECE ?
-Hatching rate/Malformation/CYP expression
Cont.
Fresh IHC
Weathered IHC
✓ From 48 h after oil exposure, several specific malformation, including the pericardial edema, spinal curvature and tail defect were observed in embryos exposed to both fresh and weathered oiled gravel effluent.

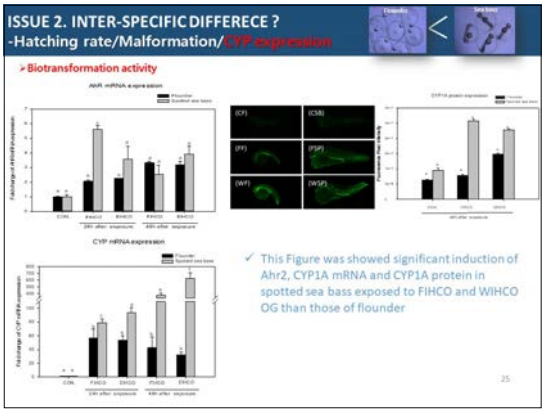
ISSUE 2. INTER-SPECIFIC DIFFERECE ?
-Hatching rate/Malformation/CYP expression
Biotransformation activity
This Figure was showed significant induction of Ahr2, CYP1A mRNA and CYP1A protein in spotted sea bass exposed to FIHCO and WIHCO OG than those of flounder

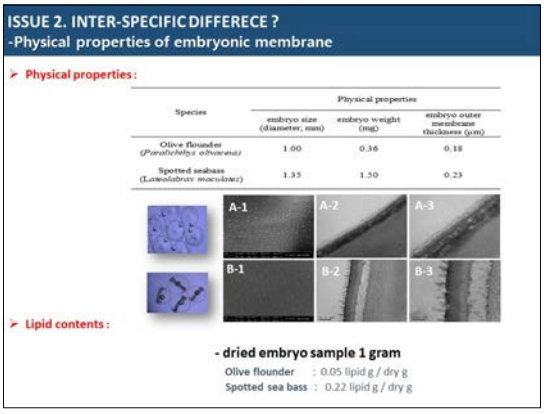
ISSUE 2. INTER-SPECIFIC DIFFERECE ?
-Physical properties of embryonic membrane
Physical properties :
Species
Physical properties
embryo size (diameter, mm)
embryo weight (mg)
embryo outer membrane thickness (μm)
Olive flounder (Paralichthys olivaceus) 1.00 0.36 0.18
Spotted seabass (Lateolabrax maculatus) 1.35 1.50 0.23
A-1
A-2
A-3
B-1
B-2
B-3
Lipid contents :
- dried embryo sample 1 gram
Olive flounder : 0.05 lipid g / dry g
Spotted sea bass : 0.22 lipid g / dry g

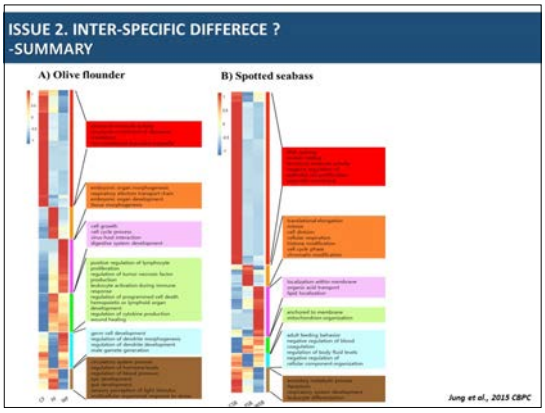
ISSUE 2. INTER-SPECIFIC DIFFERECE ?
-SUMMARY
A) Olive flounder
B) Spotted seabass
Jung et al., 2015 CBPC

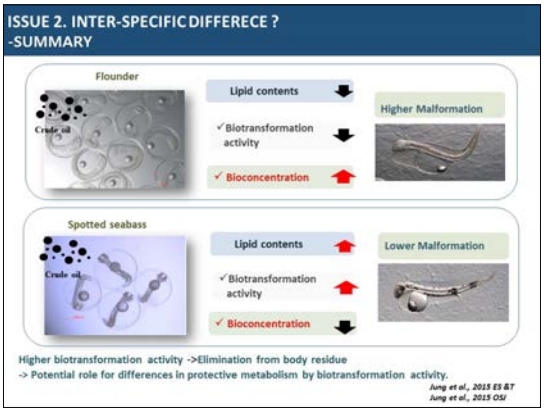
ISSUE 2. INTER-SPECIFIC DIFFERECE ?
-SUMMARY
Flounder
Crude oil
Lipid contents
Biotransformation activity
Bioconcentration
Higher Malformation
Spotted seabass
Crude oil
Lipid contents
Biotransformation activity
Bioconcentration
Lower Malformation
Higher biotransformation activity ->Elimination from body residue
-> Potential role for differences in protective metabolism by biotransformation activity.
Jung et al., 2015 ES&T
Jung et al., 2015 OSI


연구사례 2
사례2. 정책결정기반연구 사례
'해양환경 유해물질의 평가 및 관리기술개발(2014~2021)'
'선체부착생물 관리기술개발(2021~2025)'

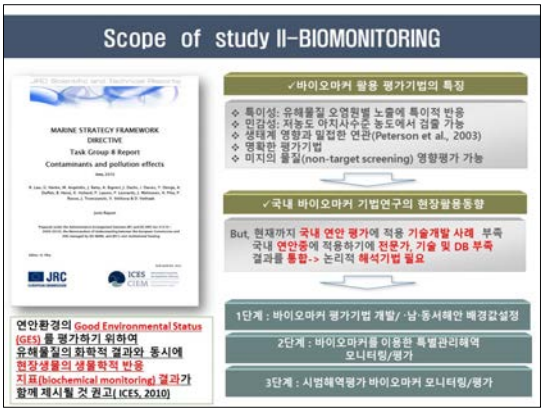
Scope of study II-BIOMONITORING
MARINE STRATEGY FRAMEWORK DIRECTIVE
Task Group 8 Report
Contaminants and pollution effects
JRC
ICES
✓바이오마커 활용 평가기법의 특징
✧ 특이성: 유해물질 오염원별 노출에 특이적 반응
✧ 민감성: 저농도 아지사수준 농도에서 검출 가능
✧ 생태계 영향과 밀접한 연관(Peterson et al., 2003)
✧ 명확한 평가기법
✧ 미지의 물질(non-target screening) 영향평가 가능
✓국내 바이오마커 기법연구의 현장활용동향
But, 현재까지 국내 연안 평가에 적용 기술개발 사례 부족
국내 연안중에 적용하기에 전문가, 기술 및 DB 부족
결과를 통합-> 논리적 해석기법 필요
연안환경의 Good Environmental Status (GES) 를 평가하기 위하여
유해물질의 화학적 결과와 동시에
현장생물의 생물학적 반응
지표(biochemical monitoring) 결과가
함께 제시될 것 권고(ICES, 2010)
1단계 : 바이오마커 평가기법 개발/ ·남·동서해안 배경값설정
2단계 : 바이오마커를 이용한 특별관리해역 모니터링/평가
3단계 : 시범해역평가 바이오마커 모니터링/평가

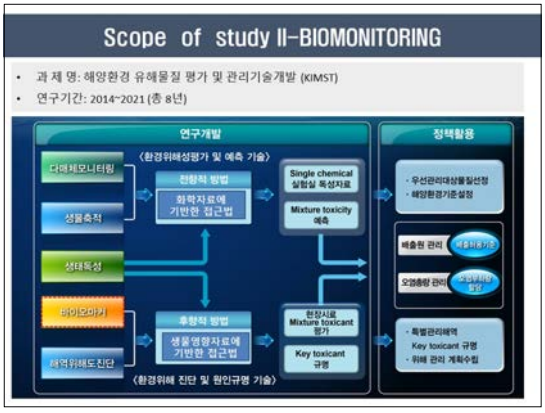
Scope of study II-BIOMONITORING
• 과 제 명: 해양환경 유해물질 평가 및 관리기술개발 (KIMST)
• 연구기간: 2014~2021 (총 8년)
연구개발
정책활용
다매체모니터링
생물축적
생태독성
바이오마커
해역위해도진단
〈환경위해성평가 및 예측 기술〉
전향적 방법
화학자료에 기반한 접근법
후향적 방법
생물영향자료에 기반한 접근법
Single chemical 실험실 독성자료
Mixture toxicity 예측
현장시료 Mixture toxicant 평가
Key toxicant 규명
〈환경위해 진단 및 원인규명 기술〉
• 우선관리대상물질선정
• 해양환경기준설정
배출원 관리
오염총량 관리
• 특별관리해역
Key toxicant 규명
• 위해 관리 계획수립

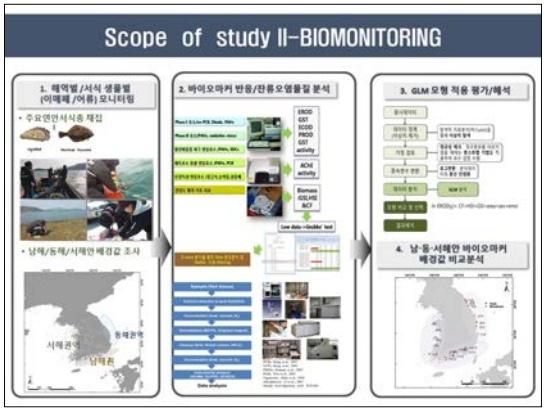
Scope of study II-BIOMONITORING
1. 해역별/서식 생물별 (어매패 /어류) 모니터링
• 주요연안서식종 채집
• 남해/동해/서해안 배경값 조사
서해권
동해권
남해권
2. 바이오마커 반응/잔류오염물질 분석
EROD
GST
ECOD
PROD
GST activity
AChE activity
Biomass (GSI,HSI) ACF
3. GLM 모형 적용 평가/해석
4. 남·동·서해안 바이오마커 배경값 비교분석

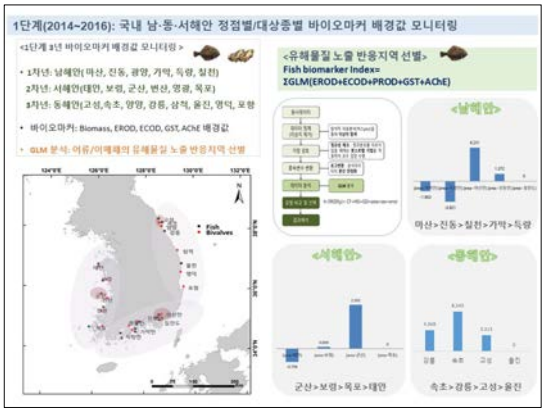
1단계(2014~2016): 국내 남·동·서해안 정점별/대상종별 바이오마커 배경값 모니터링
<1단계 3년 바이오마커 배경값 모니터링 >
• 1차년: 남해안(마산, 진동, 광양, 가막, 득량, 칠천)
2차년: 서해안(태안, 보령, 군산, 변산, 영광, 목포)
3차년: 동해안(고성,속초, 양양, 강릉, 삼척, 울진, 영덕, 포항
• 바이오마커: Biomass, EROD, ECOD, GST, AChE 배경값
• GLM 분석: 어류/어매패의 유해물질 노출 반응지역 선별
<유해물질 노출 반응지역 선별>
Fish biomarker Index=
IGLM(EROD+ECOD+PROD+GST+AChE)
Fish
Bivalves
<남해안>
마산>진동>칠천>가막>득량
<서해안>
군산>보령>목포>태안
<동해안>
속초>강릉>고성>울진

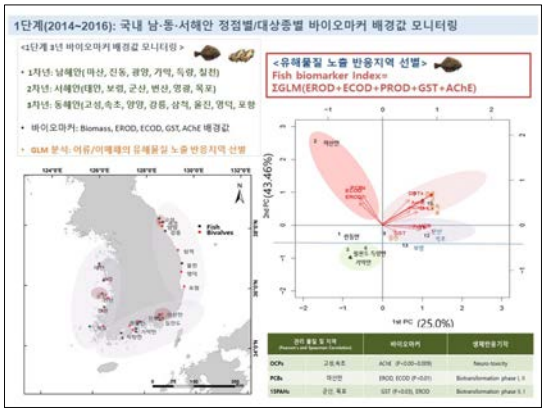
1단계(2014~2016): 국내 남·동·서해안 정점별/대상종별 바이오마커 배경값 모니터링
<1단계 3년 바이오마커 배경값 모니터링 >
• 1차년: 남해안(마산, 진동, 광양, 가막, 득량, 칠천)
2차년: 서해안(태안, 보령, 군산, 변산, 영광, 목포)
3차년: 동해안(고성,속초, 양양, 강릉, 삼척, 울진, 영덕, 포항
• 바이오마커: Biomass, EROD, ECOD, GST, AChE 배경값
• GLM 분석: 어류/어매패의 유해물질 노출 반응지역 선별
<유해물질 노출 반응지역 선별>
Fish biomarker Index=
IGLM(EROD+ECOD+PROD+GST+AChE)
Fish
Bivalves
2nd PC (43.46%)
1st PC (25.0%)

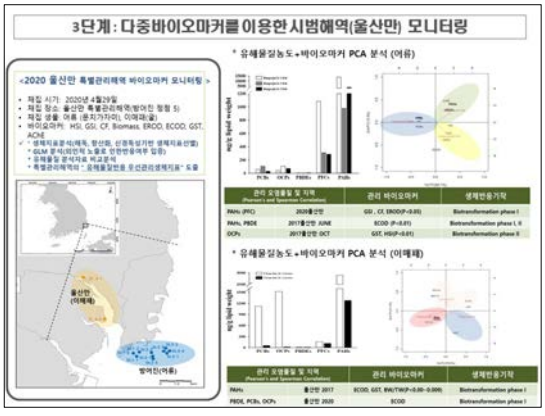
3단계 : 다중바이오마커를 이용한 시범해역(울산만) 모니터링
<2020 울산만 특별관리해역 바이오마커 모니터링 >
• 채집 시기: 2020년 4월29일
• 채집 장소: 울산만 특별관리해역(방어진 정점 5)
• 채집 생물: 어류 (문치가자미), 이매패(굴)
• 바이오마커: HSI, GSI, CF, Biomass, EROD, ECOD, GST, AChE
✓ * 생체지표분석(해독, 항산화, 신경독성기반 생체지표선별)
* GLM 분석(선정된 노출로 인한반응여부 입증)
* 유해물질 분석자료 비교분석
* 특별관리해역의 " 유해물질반응 우선관리생체지표" 도출
* 유해물질농도+바이오마커 PCA 분석 (어류)
관리 오염물질 및 지역
관리 바이오마커
생체반응기작
PAHs (PFC)
2020울산만
GSI , CF, EROD(P<0.05)
Biotransformation phase I
PAHs, PBDE
2017울산만 JUNE
ECOD (P<0.01)
Biotransformation phase I, II
OCPs
2017울산만 OCT
GST, HSI(P<0.01)
Biotransformation phase II
* 유해물질농도+바이오마커 PCA 분석 (이매패)
울산만 (이매패)
방어진(어류)
PAHs
울산만 2017
ECOD, GST, BW/THSI(P<0.05~0.009)
Biotransformation phase I
PBDE, PCBs, OCPs
울산만 2020
ECOD
Biotransformation phase I

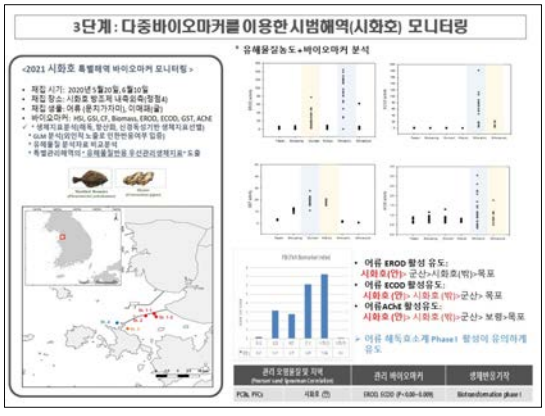
3단계 : 다중바이오마커를 이용한 시범해역(시화호) 모니터링
<2021 시화호 특별해역 바이오마커 모니터링 >
• 채집 시기: 2020년5월20일,6월10일
• 채집 장소: 시화호 방조제 내측공측(정점4)
• 채집 생물: 어류(문치가자미), 이매패(굴)
• 바이오마커: HSI, GSI, CF, Biomass, EROD, ECOD, GST, AChE
✓ * 생체지표분석(해독, 항산화, 신경독성기반 생체지표선별)
* GLM 분석(선정된 노출로 인한반응여부 입증)
* 유해물질 분석자료 비교분석
* 특별관리해역의 " 유해물질반응 우선관리생체지표" 도출
* 유해물질농도+바이오마커 분석
• 어류 EROD 활성 유도:
시화호(간)> 군산>시화호(벅)>목포
• 어류 ECOD 활성유도:
시화호 (간)> 시화호 (벅)>군산> 목포
• 어류AChE 활성유도:
시화호 (간)> 시화호 (벅)>군산> 보령>목포
➢ 어류 해독효소계 Phase I 활성이 유의하게 유도
관리 오염물질 및 지역
관리 바이오마커
생체반응기작
PCBs, PFC
시화호 (간)
EROD, ECOD (P<0.05~0.009)
Biotransformation phase I

SUMMARY

- 연안환경 유해물질오염 및 영향을 모니터링할 수 있는 현장 생물의 생체지표 발굴 및 구축
- 어류/이매패류 생체지표 -동·서남 배경값농도 구축
- 생체지표 결과의 GLM 모형적용시도
  - 지역간의 차이를 지수화/객관화에 용이-> 연안관리에 활용가능
- 3단계 특별관리해역 모니터링 분석결과 :
- **울산만**: 관리유해화학물질: PAHs 류, OCPs류
  관리 생체지표 : EROD, ECOD
- **시화호(안)**: 관리유해화학물질 : PCBs류, PFCs
  관리 생체지표: EROD, ECOD, AChE

연구사례 2

사례2. 정책결정기반연구 사례

'해양환경 유해물질의 평가 및 관리기술개발(2014~2021)' 종료

'선체부착생물 관리기술개발(2021~2025)' 진행중

BIOFOULING

- **The biological settlement of vessels :** adverse effects such as speed reduction, economic loss(up to 40%), increase periodical dry-docking operations, and, consequently contamination of toxic wastes (Kotrikla, 2009; Champ 2000).

Figure 3. Envirocart being operated by a diver (above). (Below) Half-cleaned tug photographed during testing for the Western Australia Department of Fisheries. Photos from Franmarine, http://www.gagecroadsdiving.com.au/projects/envirocart/.

Hull Cleaning Wastewater?

[현재 선체 수중 청소 → 미래 선체 수중 청소]

- 현재 수중다이버들이 선체 부착생물을 제거 과정 중 해저바닥에 떨어져, 항만 고유 생태계의 심각한 오염을 야기함.
- 본 과제에서는 **선체부착생물제거 로봇플랫폼개발**로 **선체부착생물 제거 및 포집**(제1과제)하는 과정에서 **생태계 위해성 평가 및 관리하여, IMO 선체 대응 및 국내 관련 법률정비 제도화**(제2과제)하는 것임.

국제동향-Hull Cleaning Wastewater?

국제 기구의 관심: Biofouling 지침서 채택 및 프로젝트 수행_1

IMO instruments on biofouling

- *Guidelines for the control and management of ships' biofouling to minimize the transfer of invasive aquatic species* (2011 Biofouling Guidelines).
- *Guidance for minimizing the transfer of invasive aquatic species as biofouling (hull fouling) for recreational craft* (MEPC.1/Circ.792).

12 Lead Partnering Countries (LPCs)

7 Recipients

GloBallast Project (2000-2004,2007-2017)
-BWMConvention 채택(2004)
-R&D Forum & GlobalTestNet (2010~)
-BWMC 발효 (2017.9.8)
-BWMS 형식승인정보 (2008~)

Funding

GEF grant USD 6.9 M

co-financing USD ~41 M

Project duration

5 years

Start: Dec-2018

연구의 최종목표

연구개발 최종목표

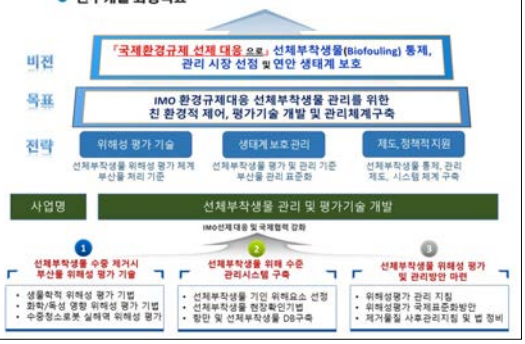


Hull Cleaning Wastewater?
화학/독성 영향 위해성평가기법 개발_B:독성영향분야
주관연구기관: KIOST
공동, 위탁연구기관 : 순천향대학교, ㈜네오엔비즈, 경상대학교(위탁), 인천대학교
01
02
03
04
05
연구 목표
연구수행 계획
주요 연구 내용

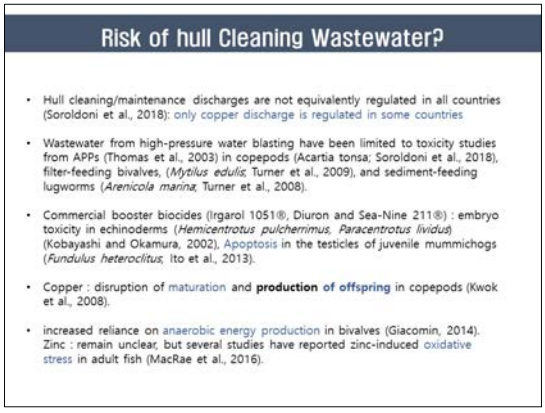
Risk of hull Cleaning Wastewater?
Hull cleaning/maintenance discharges are not equivalently regulated in all countries (Soroldoni et al., 2018): only copper discharge is regulated in some countries
Wastewater from high-pressure water blasting have been limited to toxicity studies from APPs (Thomas et al., 2003) in copepods (Acartia tonsa; Soroldoni et al., 2018), filter-feeding bivalves, (Mytilus edulis; Turner et al., 2009), and sediment-feeding lugworms (Arenicola marina; Turner et al., 2008).
Commercial booster biocides (Irgarol 1051®, Diuron and Sea-Nine 211®) : embryo toxicity in echinoderms (Hemicentrotus pulcherrimus, Paracentrotus lividus) (Kobayashi and Okamura, 2002). Apoptosis in the testicles of juvenile mummichogs (Fundulus heteroclitus; Ito et al., 2013).
Copper : disruption of maturation and production of offspring in copepods (Kwok et al., 2008).
increased reliance on anaerobic energy production in bivalves (Giacomin, 2014). Zinc : remain unclear, but several studies have reported zinc-induced oxidative stress in adult fish (MacRae et al., 2016).


Risk of hull Cleaning Wastewater?
2-1. 선체부착생물을 수중제거시 발생하는 부산물(?) 의 독성발현 요소
In water cleaning
Robot 처리장치
Toxicity ?
수중제거파생물
입자+용존
필터후-수중제거
용존
화학적 유해요인:
(AFS /입자/용존)


Risk of hull Cleaning Wastewater?
2-1. 선체부착생물을 수중제거시 발생하는 부산물(?) 의 독성발현 요인
<수중청소배출물>
입자
X 3500 (paint + 조류+ 플랑크톤)
X 3,000
X 8,500배
X 6,500배

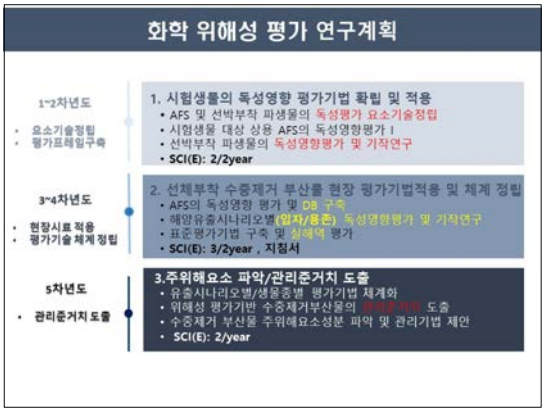
화학 위해성 평가 연구계획
1~2차년도
요소기술정립
평가프레임구축
1. 시험생물의 독성영향 평가기법 확립 및 적용
AFS 및 선박부착 파생물의 독성평가 요소기술정립
시험생물 대상 상용 AFS의 독성영향평가 I
선박부착 파생물의 독성영향평가 및 기작연구
SCI(E): 2/2year
3~4차년도
현장시료 적용
평가기술 체계 정립
2. 선체부착 수중제거 부산물 현장 평가기법적용 및 체계 정립
AFS의 독성영향 평가 및 DB 구축
해양유출시나리오별 (입자/용존) 독성영향평가 및 기작연구
표준평가기법 구축 및 실해역 평가
SCI(E): 3/2year , 지침서
5차년도
관리준거치 도출
3.주위해요소 파악/관리준거치 도출
유출시나리오별/생물종별 평가기법 체계화
위해성 평가기반 수중제거부산물의 관리준거치 도출
수중제거 부산물 주위해요소성분 파악 및 관리기법 제안
SCI(E): 2/year


연구범위-평가대상/범위
AFS Target BIOCIDE
AFS 2종씩
생물 6종
어류
갑각류
극피
동물플랑크톤
식물플랑크톤(4)
대상 시료
AFS: 2종씩
청소 배출물: 선체청소배출물
생물종별 독성평가/기법 구축
수상용AFS 독성 평가/기법구축
선체청소배출물 독성평가/기법 구축
생물종별 독성파라메터 도출
독성자료생산 (생물 6종)
생체유해성 및 독성기작규명
Omics를 이용한 독성기작규명
수중 제거작업
배출물(처리전/후)

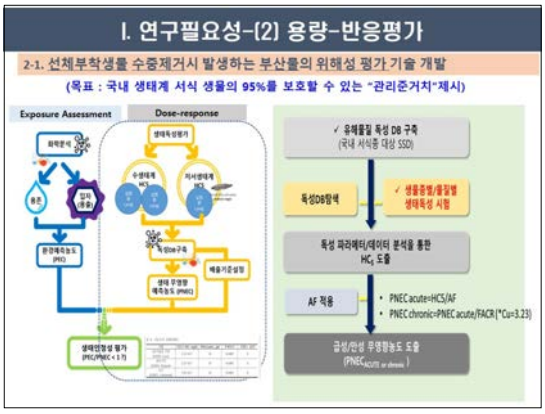
I. 연구필요성-(2) 용량-반응평가
2-1. 선체부착생물을 수중제거시 발생하는 부산물의 위해성 평가 기술 개발
(목표 : 국내 생태계 서식 생물의 95%를 보호할 수 있는 "관리준거치"제시)
Exposure Assessment
Dose-response
✓ 유해물질 독성 DB 구축
(국내 서식종 대상 SSD)
독성DB함약
✓ 생물종별/물질별 생태독성 시험
독성 파라메터/데이터 분석을 통한 HC5 도출
AF 적용
• PNEC acute=HC5/AF
• PNEC chronic=PNEC acute/FACR(*Cu=3.23)
급성/만성 무영향농도 도출


연구범위-평가대상/범위
Current guidelines concerning the use of fish within OECD include acute toxicity to juvenile fish (OECD 203) (OECD, 1992a), fish short-term toxicity to embryo and sac fry (OECD 212)
Antifouling System
Exposure to embryonic Olive flounder & Rockfish
[웅존 + 입자]
[입자]
LC50/EC50
Paralichthys olivaceus
Sebastes schlegelii
Morphogenesis
Transcriptome analysis
Mortality (LC50)
Pericardial edema
Spinal curvature
Tailfin defect (EC50)
•시험생물별 독성파라메터
•아치사독성기전연구

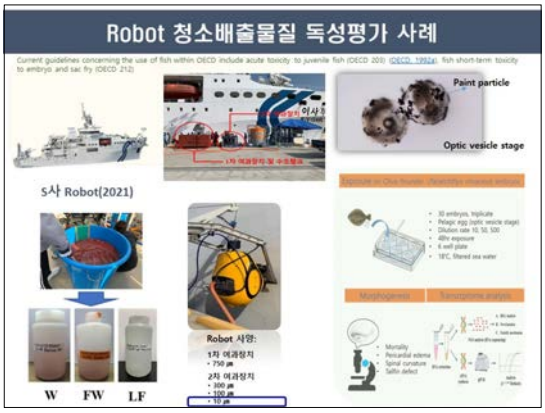
Robot 청소배출물질 독성평가 사례
Paint particle
Optic vesicle stage
S사 Robot(2021)
Robot 사양:
1차 여과장치
• 750 ㎛
2차 여과장치
• 300 ㎛
• 100 ㎛
• 10 ㎛
W
FW
LF

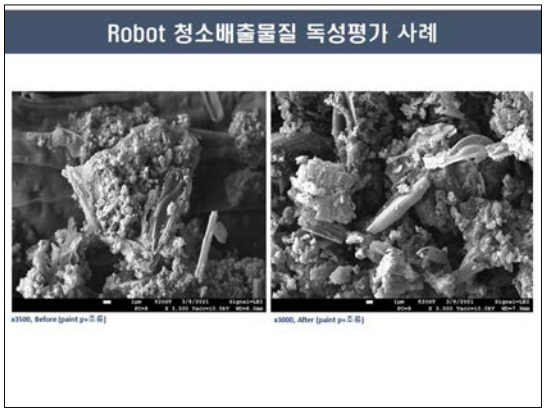
Robot 청소배출물질 독성평가 사례
x3500, Before (paint p+조류)
x3000, After (paint p+조류)

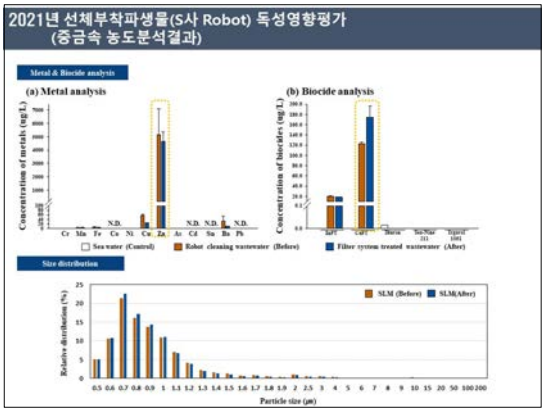
2021년 선체부착생물(S사 Robot) 독성영향평가
(중금속 농도분석결과)
Metal & Biocide analysis
(a) Metal analysis
(b) Biocide analysis
Concentration of metals (ng/L)
Concentration of biocides (ng/L)
Cr Mn Fe Co Ni Cu Zn As Cd Sn Sb Pb
N.D.
Sea-water (Control)
Robot cleaning wastewater (Before)
Filter system treated wastewater (After)
Size distribution
SLM (Before)
SLM(After)
Relative distribution (%)
Particle size (㎛)

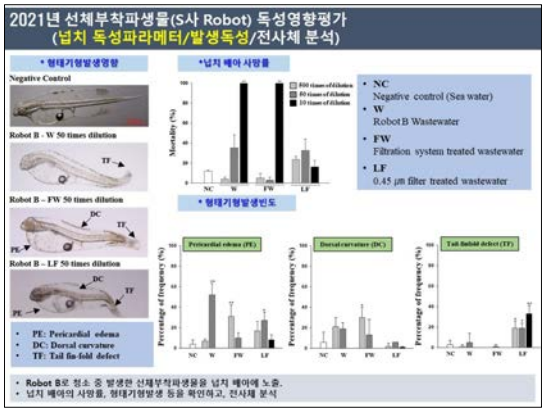
2021년 선체부착생물(S사 Robot) 독성영향평가
(넙치 독성파라메터/발생독성/전사체 분석)
• 형태기형발생영향
•넙치 배아 사망률
Negative Control
Robot B - W 50 times dilution
Robot B – FW 50 times dilution
Robot B – LF 50 times dilution
PE
DC
TF
Mortality (%)
• NC
Negative control (Sea water)
• W
Robot B Wastewater
• FW
Filtration system treated wastewater
• LF
0.45 ㎛ filter treated wastewater
• 형태기형발생빈도
Pericardial edema (PE)
Dorsal curvature (DC)
Tail fin fold defect (TF)
Percentage of frequency (%)
• PE: Pericardial edema
• DC: Dorsal curvature
• TF: Tail fin-fold defect
• Robot B로 청소 중 발생한 선체부착생물을 넙치 배아에 노출,
• 넙치 배아의 사망률, 형태기형발생 등을 확인하고, 전사체 분석

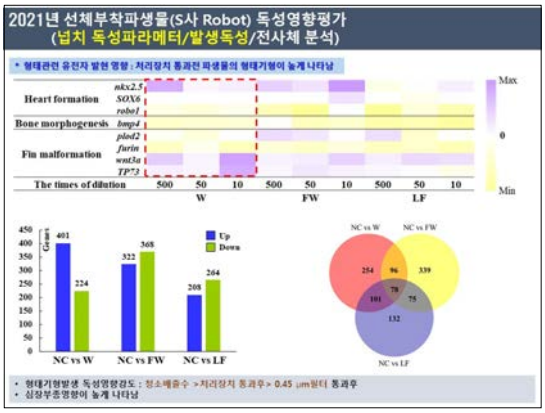
2021년 선체부착파생률(S사 Robot) 독성영향평가
(넙치 독성파라메터/발생독성/전사체 분석)
• 형태관련 유전자 발현 영향 : 처리장치 통과전 파생물의 형태기형이 높게 나타남
Heart formation
mkx2.5
SOX6
robo1
Bone morphogenesis
bmp4
Fin malformation
plod2
furin
wnt3a
TP73
The times of dilution
500 50 10 500 50 10 500 50 10
W FW LF
Max
0
Min
Genes
Up
Down
NC vs W
NC vs FW
NC vs LF
• 형태기형발생 독성영향강도 : 청소배출수 >처리장치 통과후> 0.45 μm필터 통과후
• 심장부종영향이 높게 나타남

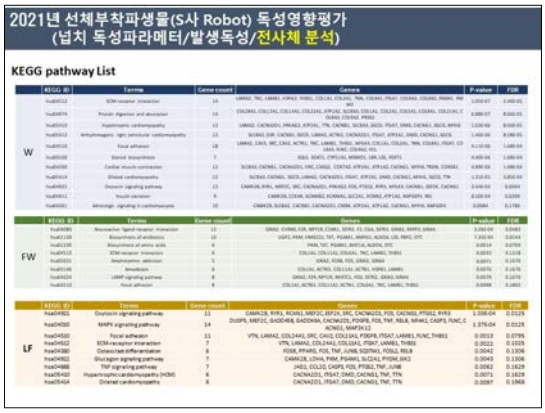
2021년 선체부착파생률(S사 Robot) 독성영향평가
(넙치 독성파라메터/발생독성/전사체 분석)
KEGG pathway List
W
FW
LF

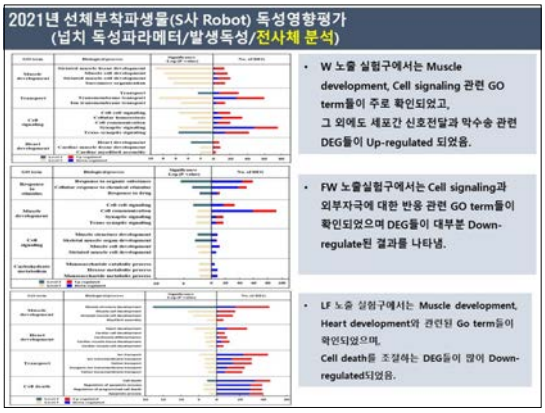
2021년 선체부착파생률(S사 Robot) 독성영향평가
(넙치 독성파라메터/발생독성/전사체 분석)
• W 노출 실험구에서는 Muscle development, Cell signaling 관련 GO term들이 주로 확인되었고,
그 외에도 세포간 신호전달과 막수송 관련 DEG들이 Up-regulated 되었음.
• FW 노출실험구에서는 Cell signaling과 외부자극에 대한 반응 관련 GO term들이 확인되었으며 DEG들이 대부분 Down-regulate된 결과를 나타냄.
• LF 노출 실험구에서는 Muscle development, Heart development와 관련된 Go term들이 확인되었으며,
Cell death를 조절하는 DEG들이 많이 Down-regulated되었음.

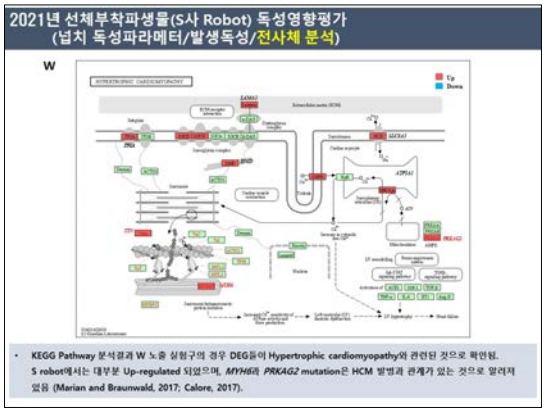
2021년 선체부착파생률(S사 Robot) 독성영향평가
(넙치 독성파라메터/발생독성/전사체 분석)
W
Up
Down
• KEGG Pathway 분석결과 W 노출 실험구의 경우 DEG들이 Hypertrophic cardiomyopathy와 관련된 것으로 확인됨.
S robot에서는 대부분 Up-regulated 되었으며, MYH6와 PRKAG2 mutation은 HCM 발병과 관계가 있는 것으로 알려져 있음 (Marian and Braunwald, 2017; Calore, 2017).

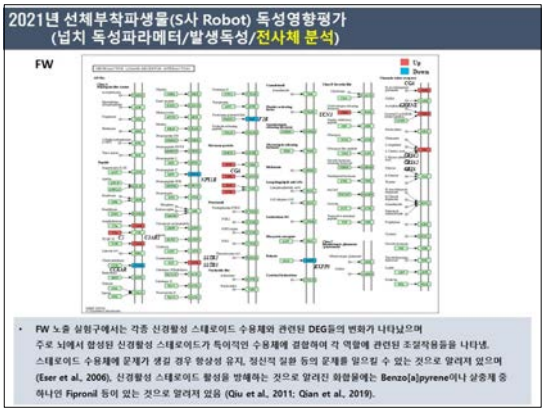
2021년 선체부착파생률(S사 Robot) 독성영향평가
(넙치 독성파라메터/발생독성/전사체 분석)
FW
Up
Down
• FW 노출 실험구에서는 각종 신경활성 스테로이드 수용체와 관련된 DEG들의 변화가 나타났으며
주로 뇌에서 합성된 신경활성 스테로이드가 특이적인 수용체에 결합하여 각 역할에 관련된 조절작용들을 나타냄.
스테로이드 수용체에 문제가 생길 경우 항상성 유지, 정신적 질환 등의 문제를 일으킬 수 있는 것으로 알려져 있으며
(Eser et al., 2006), 신경활성 스테로이드 활성을 방해하는 것으로 알려진 화합물에는 Benzo[a]pyrene이나 살충제 중 하나인 Fipronil 등이 있는 것으로 알려져 있음 (Qiu et al., 2011; Qian et al., 2019).

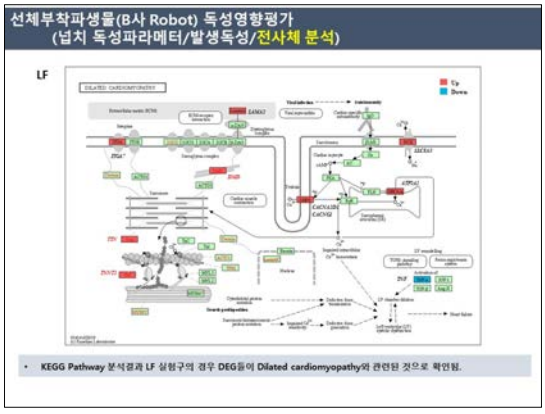
선체부착파생률(B사 Robot) 독성영향평가
(넙치 독성파라메터/발생독성/전사체 분석)
LF
Up
Down
• KEGG Pathway 분석결과 LF 실험구의 경우 DEG들이 Dilated cardiomyopathy와 관련된 것으로 확인됨.

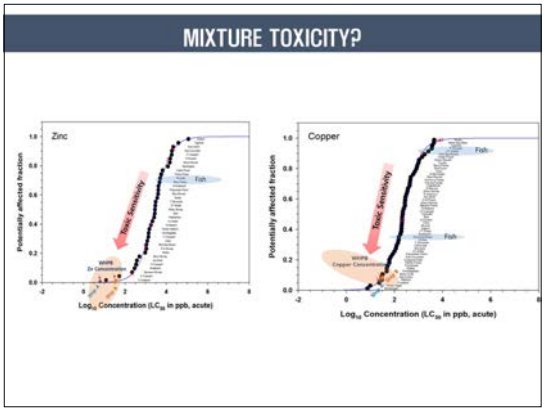
MIXTURE TOXICITY?
Zinc
Copper
Fish
Fish
Toxic Sensitivity
Toxic Sensitivity
Potentially affected fraction
Potentially affected fraction
Log10 Concentration (LC50 in ppb, acute)
Log10 Concentration (LC50 in ppb, acute)


경청해 주셔서 감사합니다!
SOUTH SEA RESEARCH INSTITUTE, KIOST

Dev. Reprod. Vol 26, 2022 (Suppl. 1). pp 41

Drug-induced renal injury and regeneration in zebrafish model

강영선

고려대학교

Aug 19, 2022

Drug-induced renal injury and regeneration in zebrafish model

Department of Nephrology, Korea University Ansan Hospital

Young Sun Kang, M.D.

Comparison between human nephron and zebrafish pronephros

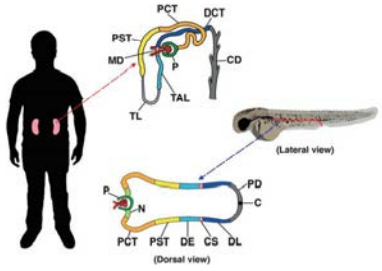

Results Probl Cell Differ. 2017;60:55-75. Zebrafish as a Model of Kidney Disease. Morales EE, Wingert RA.

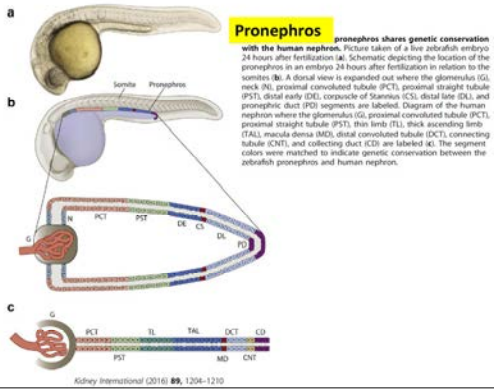

Kidney International (2016) 89, 1204–1210

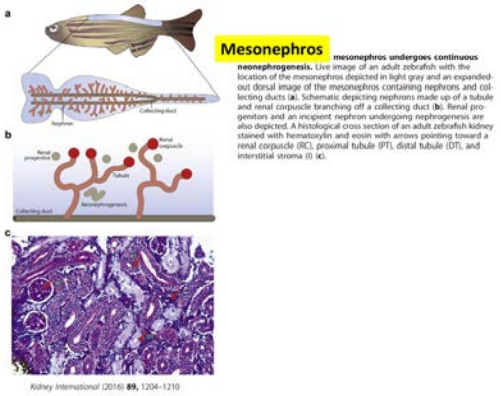

Kidney International (2016) 89, 1204–1210

Zebrafish Models

- Acute Kidney Injury (AKI) >> Proximal tubular injury

  Gentamycin, Cisplatin, Puromycin, Adriamycin

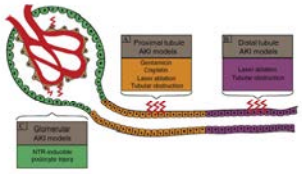

Gentamicin-induced kidney injury

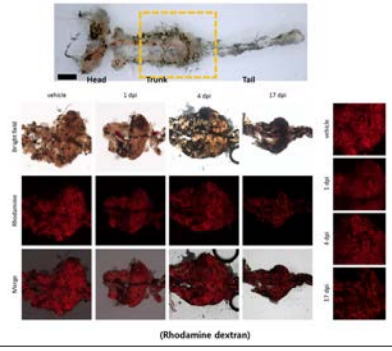

(Rhodamine dextran)

SGLT2 in the diabetic kidney.

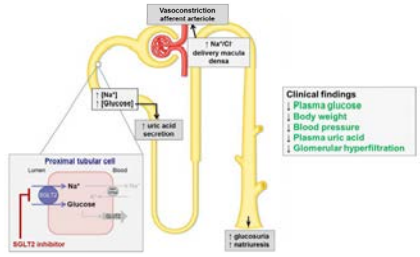

Erik J.M. van Bommel et al. CJASN doi:10.2215/CJN.06080616

***slc5a2*/SGLT2**

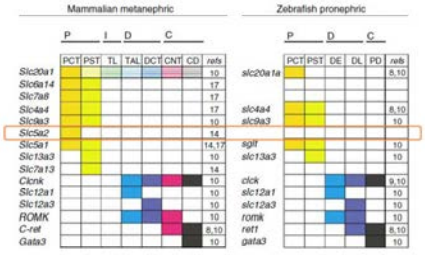

Kidney Int. 2008 May;73(10):1120-7. **The zebrafish pronephros: a model to study nephron segmentation.** Wingert RA, Davidson AJ

***slc5a2* expression in zebrafish nephros**

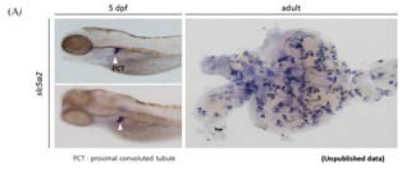

Puromycin; *slc5a2* expression as a marker

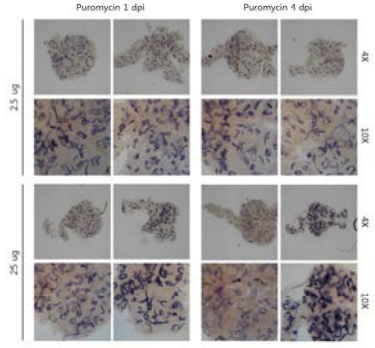

The effect of *sglt2 inhibitor* on gentamicin-induced kidney injury and regeneration

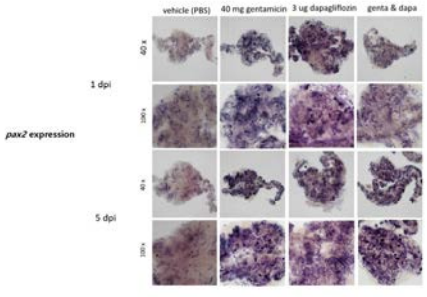

The effect of new drug on renal injury and regeneration?

; visfatin (nampt)

Nampt expressions in kidney of zebrafish

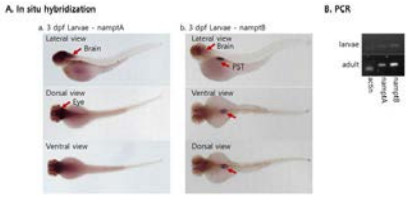

Figure 1. Nampt expression in the kidney of larvae and adult zebrafish (A) In situ hybridization (B) PCR

Nampt expressions in puromycin-induced renal injury and regeneration in adult zebrafish

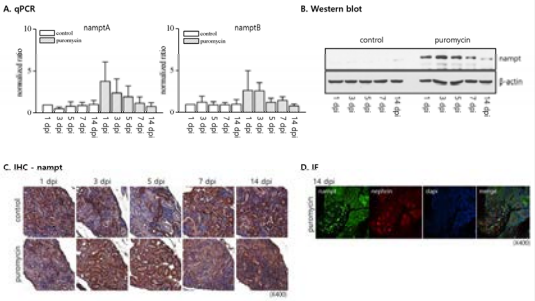

Figure 2. Nampt expressions in puromycin-induced kidney injury and regeneration in adult zebrafish (A) PCR (B) Western blot analysis (C) IHC (D) IF stain with nephrin

The effect of visfatin on puromycin-induced renal injury and regeneration

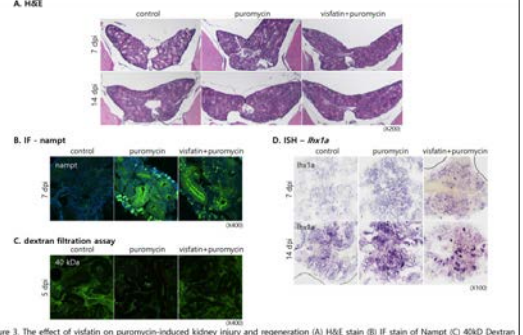

Figure 3. The effect of visfatin on puromycin-induced kidney injury and regeneration (A) H&E stain (B) IF stain of Nampt (C) 40kD Dextran filtration assay (D) In situ hybridization of Ihx1a

The effect of visfatin on puromycin-induced kidney and regeneration

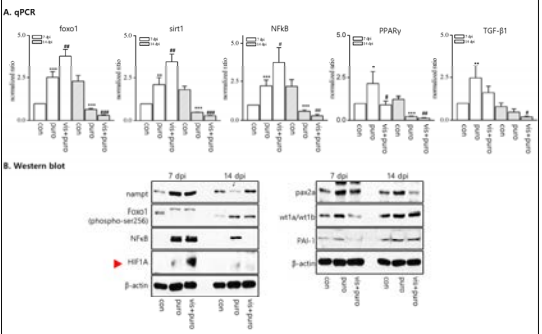

Figure 4. The effect of visfatin on puromycin-induced kidney and regeneration (A)Western blot analysis (B) RT-PCR

The proteinuric model in zebrafish ?

; the effect of sleep deprivation on proteinuria

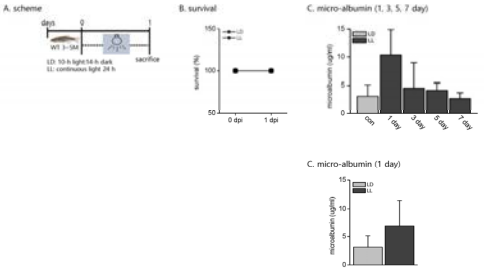

Nephrin (IF stain): Sleep deprivation (larva)

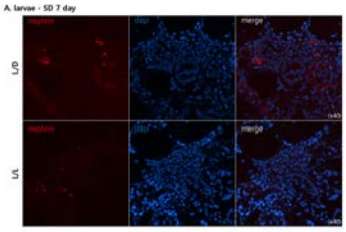

Nephrin (IF stain): sleep deprivation (adult zebrafish)

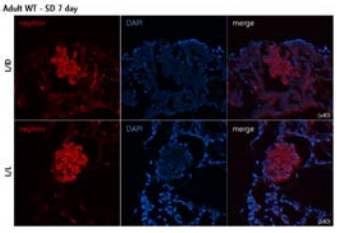

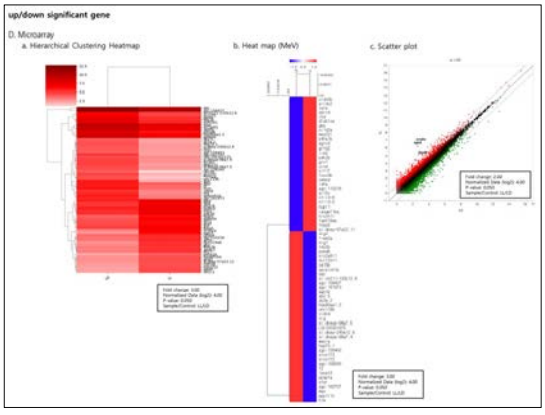

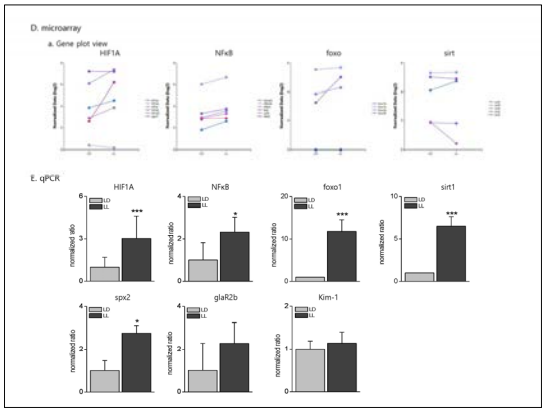

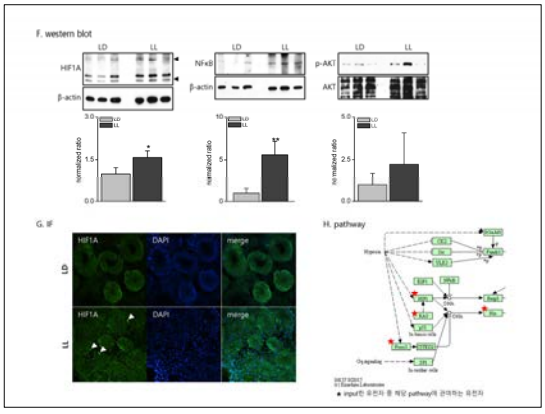

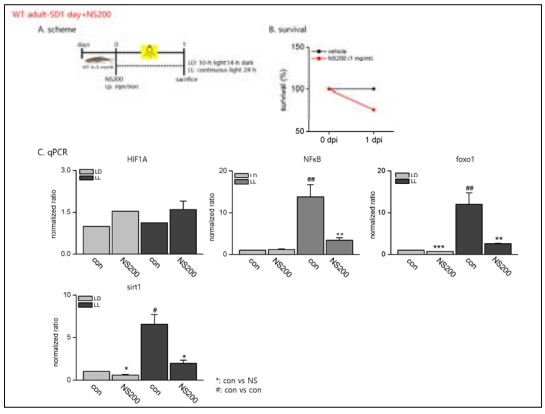

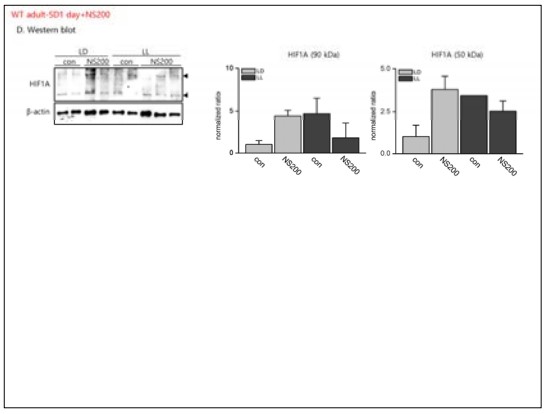
WT adult-SD1 day+NS200
D. Western blot
LD
LL
con
NS200
HIF1A
β-actin
HIF1A (90 kDa)
HIF1A (50 kDa)
normalized ratio

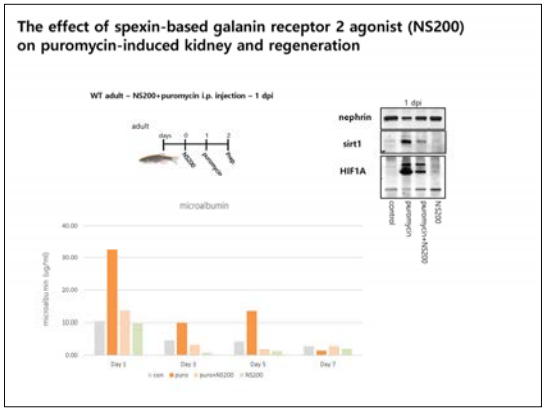
The effect of spexin-based galanin receptor 2 agonist (NS200) on puromycin-induced kidney and regeneration
WT adult – NS200+puromycin i.p. injection – 1 dpi
adult
nephrin
sirt1
HIF1A
1 dpi
microalbumin

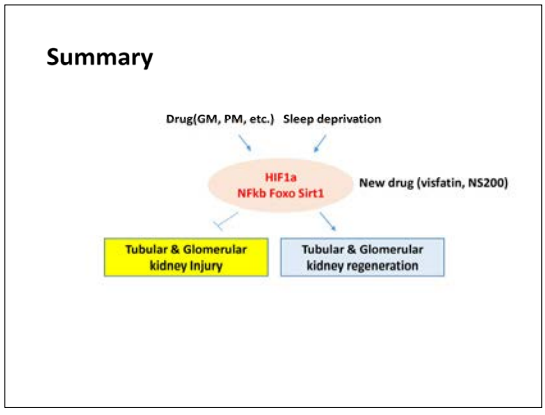
Summary
Drug(GM, PM, etc.) Sleep deprivation
HIF1a
NFkb Foxo Sirt1
New drug (visfatin, NS200)
Tubular & Glomerular kidney Injury
Tubular & Glomerular kidney regeneration

Dev. Reprod. Vol 26, 2022 (Suppl. 1). pp 46

영장류 및 인간화 마우스를 이용한 조혈계 질병 기전 연구

유경록

서울대학교

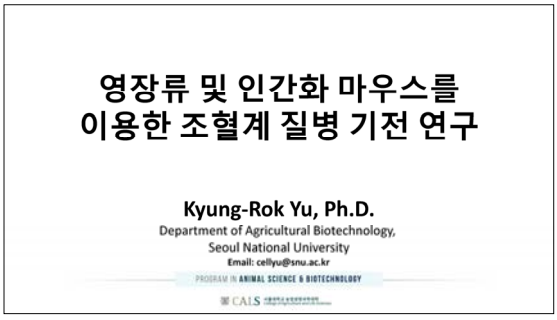

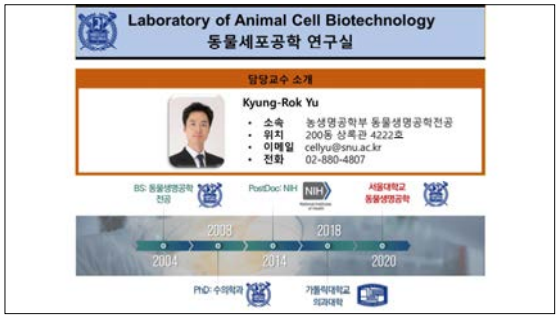

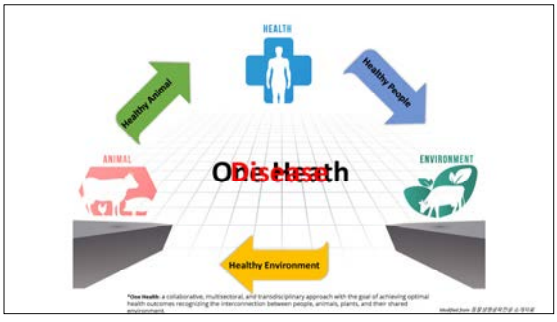

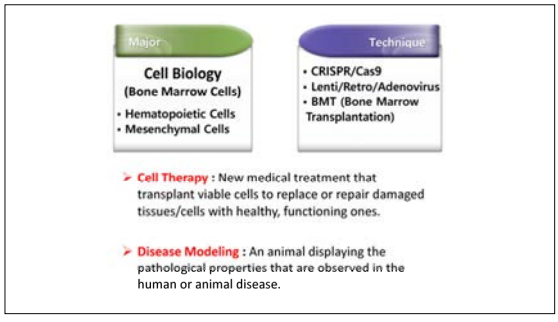

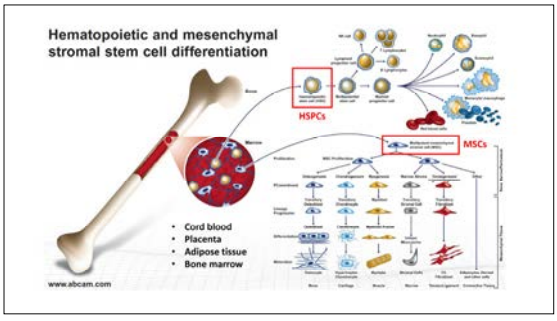

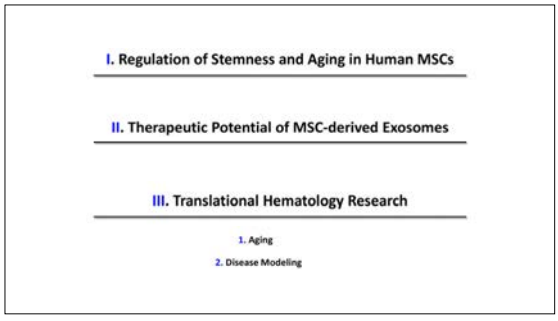

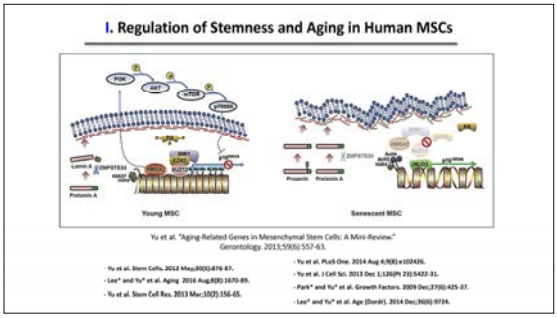
I. Regulation of Stemness and Aging in Human MSCs
Young MSC
Senescent MSC

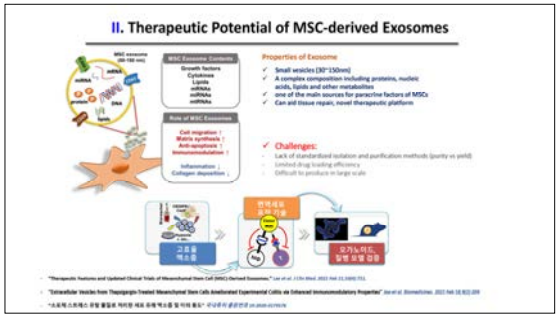
II. Therapeutic Potential of MSC-derived Exosomes
Properties of Exosome
Challenges:

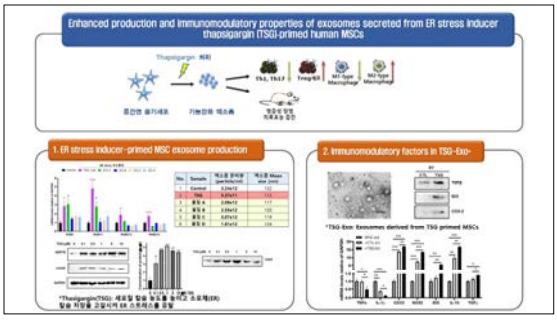
Enhanced production and immunomodulatory properties of exosomes secreted from ER stress inducer thapsigargin (TSG)-primed human MSCs
1. ER stress inducer-primed MSC exosome production
2. Immunomodulatory factors in TSG-Exo-

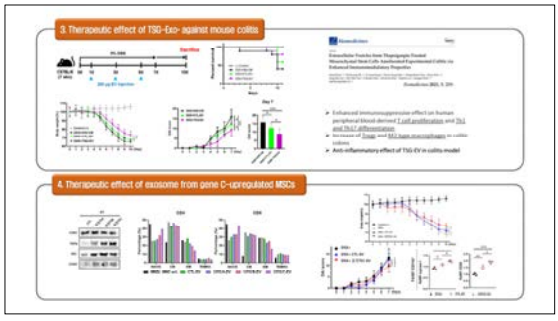
3. Therapeutic effect of TSG-Exo- against mouse colitis
4. Therapeutic effect of exosome from gene C-upregulated MSCs

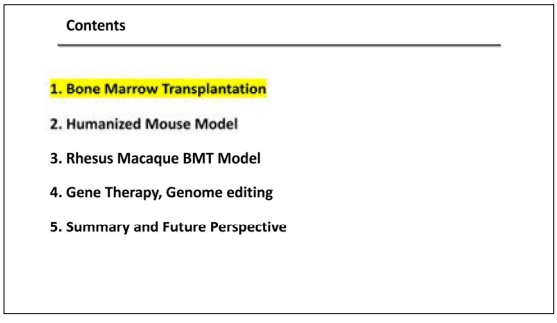
Contents
1. Bone Marrow Transplantation
2. Humanized Mouse Model
3. Rhesus Macaque BMT Model
4. Gene Therapy, Genome editing
5. Summary and Future Perspective

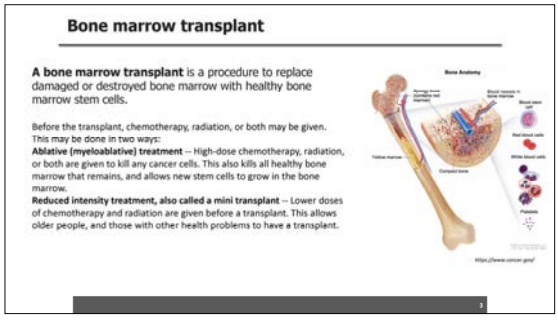
Bone marrow transplant
A bone marrow transplant is a procedure to replace damaged or destroyed bone marrow with healthy bone marrow stem cells.
Before the transplant, chemotherapy, radiation, or both may be given. This may be done in two ways:
Ablative (myeloablative) treatment -- High-dose chemotherapy, radiation, or both are given to kill any cancer cells. This also kills all healthy bone marrow that remains, and allows new stem cells to grow in the bone marrow.
Reduced intensity treatment, also called a mini transplant -- Lower doses of chemotherapy and radiation are given before a transplant. This allows older people, and those with other health problems to have a transplant.

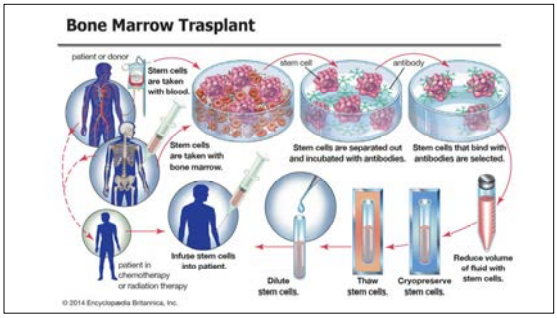
Bone Marrow Trasplant
patient or donor
Stem cells are taken with blood.
Stem cells are taken with bone marrow.
Infuse stem cells into patient.
patient in chemotherapy or radiation therapy
Dilute stem cells.
Thaw stem cells.
Cryopreserve stem cells.
Reduce volume of fluid with stem cells.
stem cell
antibody
Stem cells are separated out and incubated with antibodies.
Stem cells that bind with antibodies are selected.
© 2014 Encyclopaedia Britannica, Inc.

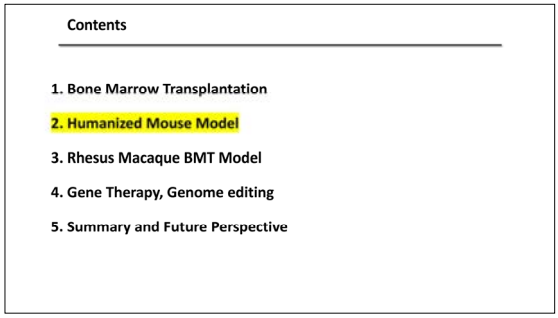
Contents
1. Bone Marrow Transplantation
2. Humanized Mouse Model
3. Rhesus Macaque BMT Model
4. Gene Therapy, Genome editing
5. Summary and Future Perspective

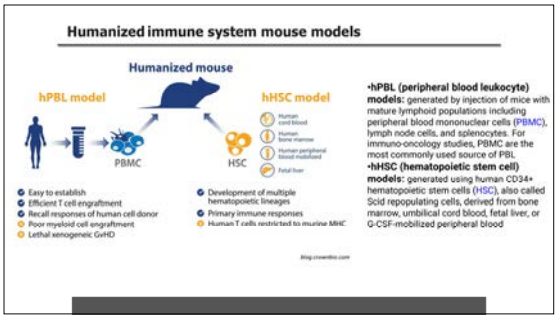
Humanized immune system mouse models
Humanized mouse
hPBL model
hHSC model
PBMC
HSC
Easy to establish
Efficient T cell engraftment
Recall responses of human cell donor
Poor myeloid cell engraftment
Lethal xenogeneic GvHD
Development of multiple hematopoietic lineages
Primary immune responses
Human T cells restricted to murine MHC
•hPBL (peripheral blood leukocyte) models: generated by injection of mice with mature lymphoid populations including peripheral blood mononuclear cells (PBMC), lymph node cells, and splenocytes. For immuno-oncology studies, PBMC are the most commonly used source of PBL
•hHSC (hematopoietic stem cell) models: generated using human CD34+ hematopoietic stem cells (HSC), also called Scid repopulating cells, derived from bone marrow, umbilical cord blood, fetal liver, or G-CSF-mobilized peripheral blood

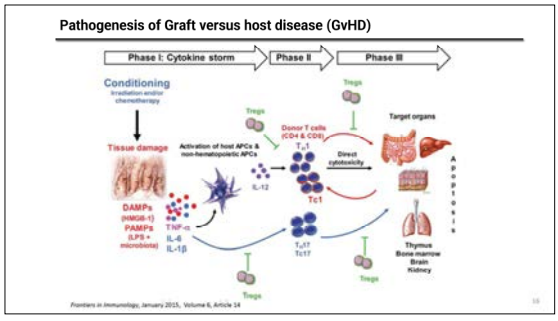
Pathogenesis of Graft versus host disease (GvHD)
Phase I: Cytokine storm
Phase II
Phase III
Conditioning
Tissue damage
DAMPs
PAMPs
Tregs
Target organs
Thymus
Bone marrow
Brain
Kidney
Apoptosis

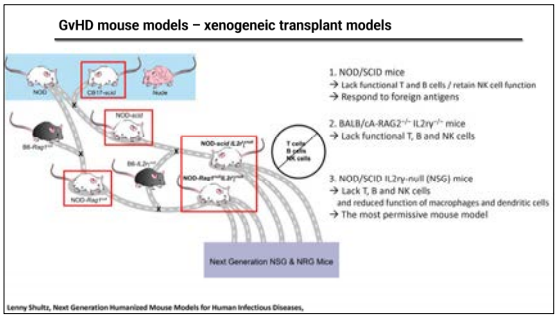
GvHD mouse models – xenogeneic transplant models
1. NOD/SCID mice
→ Lack functional T and B cells / retain NK cell function
→ Respond to foreign antigens
2. BALB/cA-RAG2−/− IL2rγ−/− mice
→ Lack functional T, B and NK cells
3. NOD/SCID IL2rγ-null (NSG) mice
→ Lack T, B and NK cells
and reduced function of macrophages and dendritic cells
→ The most permissive mouse model
Next Generation NSG & NRG Mice
Lenny Shultz, Next Generation Humanized Mouse Models for Human Infectious Diseases,

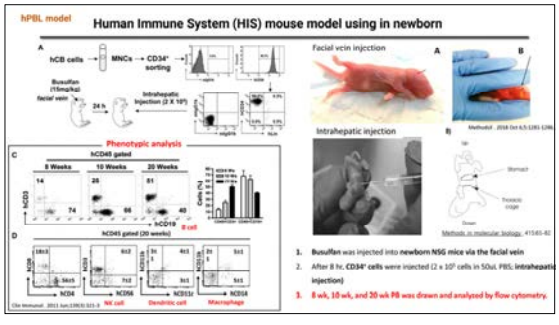
hPBL model
Human Immune System (HIS) mouse model using in newborn
hCB cells
MNCs → CD34+ sorting
Busulfan (15mg/kg) facial vein
24 h
Intrahepatic Injection (2 X 10⁵)
Facial vein injection
Intrahepatic injection
Phenotypic analysis
hCD45 gated
8 Weeks
10 Weeks
20 Weeks
hCD45 gated (20 weeks)
NK cell
Dendritic cell
Macrophage
1. Busulfan was injected into newborn NSG mice via the facial vein
2. After 8 hr, CD34+ cells were injected (2 x 10⁵ cells in 50uL PBS; intrahepatic injection)
3. 8 wk, 10 wk, and 20 wk PB was drawn and analyzed by flow cytometry.

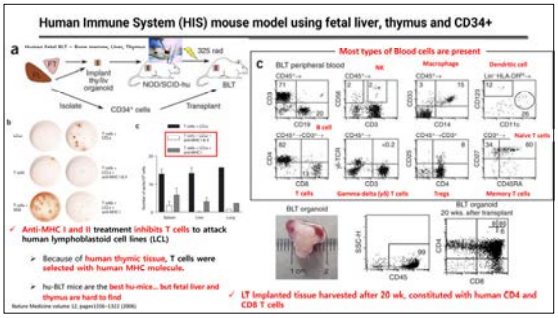

Contents

1. Bone Marrow Transplantation
2. Humanized Mouse Model
3. Rhesus Macaque BMT Model
4. Gene Therapy, Genome editing
5. Summary and Future Perspective

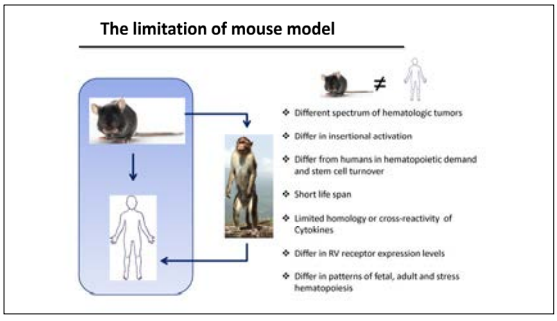

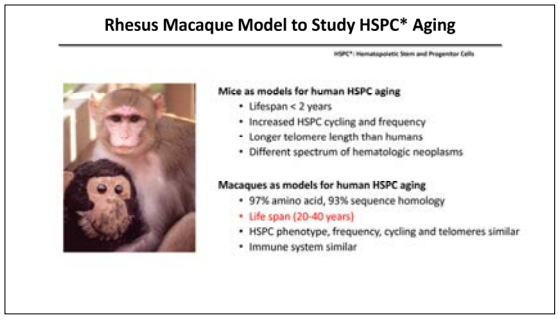

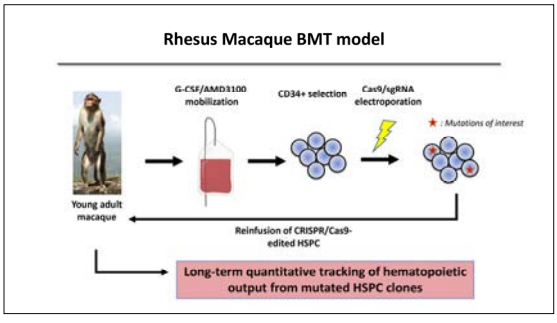

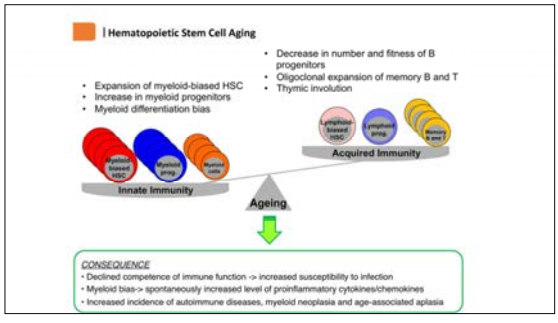

1. Clonal Tracking of Hematopoiesis in Young vs Aged Macaque

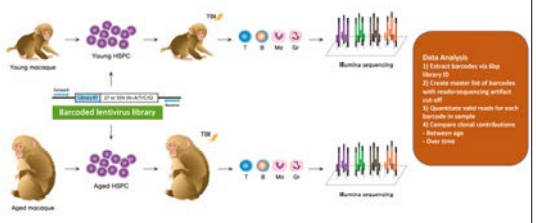

Aged macaques showed delayed emergence of multipotent clones

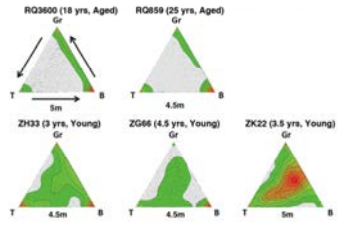

Clonal expansion of both multipotent and myeloid-, B-biased clones occurred in aged macaques

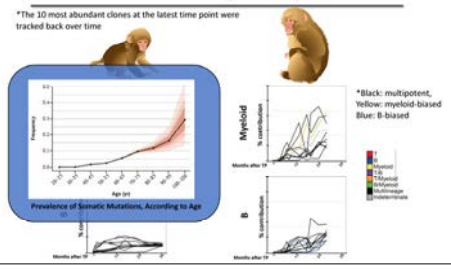

Contents

1. Bone Marrow Transplantation
2. Humanized Mouse Model
3. Rhesus Macaque BMT Model
4. Gene Therapy, Genome editing
5. Summary and Future Perspective

Gene Therapy

What is gene therapy?

- Gene therapy is an experimental technique that uses genes to treat or prevent disease.
- In the future, this technique may allow doctors to treat a disorder by inserting a gene into a patient's cells instead of using drugs or surgery.
- Researchers are testing several approaches to gene therapy, including:
  - Replacing a mutated gene that causes disease with a healthy copy of the gene.
  - Inactivating, or "knocking out," a mutated gene that is functioning improperly.
  - Introducing a new gene into the body to help fight a disease.

- NIH website

Integrating retroviruses

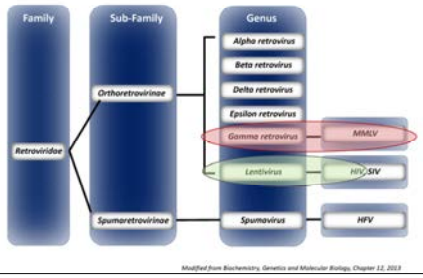

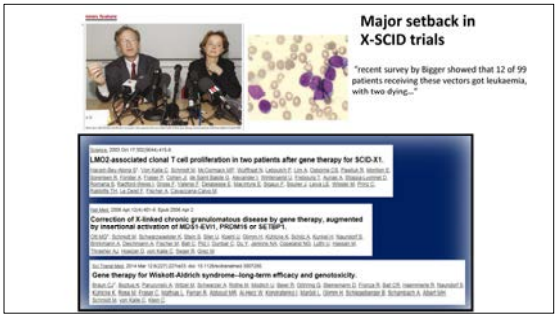

Genomic medicine harnesses the knowledge of genetics to guide the care of patients and create new treatments…

1. Gene augmentation (Gene Therapy) and
2. Genome editing. Each approach seeks to address genetically defined diseases at the level of DNA.

CRISPR/Cas9-mediated genome editing

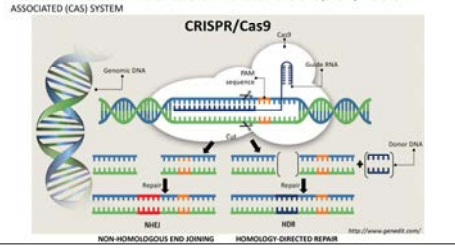

Strategy for therapeutic gene editing in HSPCs

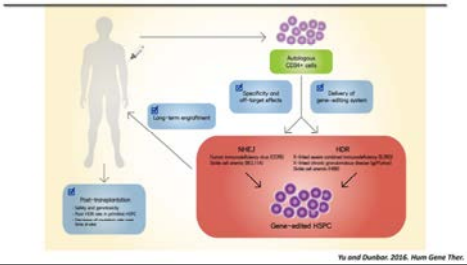

'Berlin patient'- Timothy Ray Brown

- In 2006, after living with the virus for 11 years and controlling his infection with antiretroviral drugs (ARVs), he learned that he had developed acute myeloid leukemia.
- Chemotherapy failed, and the next year Brown, an American then living in Berlin, received the first of two bone marrow transplants—a common treatment for this cancer—and ditched his ARVs
- Brown's blood over the past 7 years have found only traces of the viral genetic material, none of which can replicate.

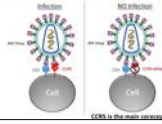

Generating Macaque Model via CRISPR/Cas9 Editing of HSPC

1. Rhesus Macaque CRISPR/Cas9 Model for PNH (Paroxysmal nocturnal hemoglobinuria) (PIGA)

2. Engineering The Hematopoietic System To Enable Antigen-Specific Targeting of Acute Myeloid Leukemia (CD33)

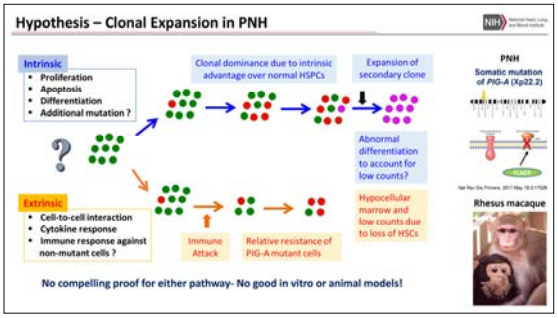

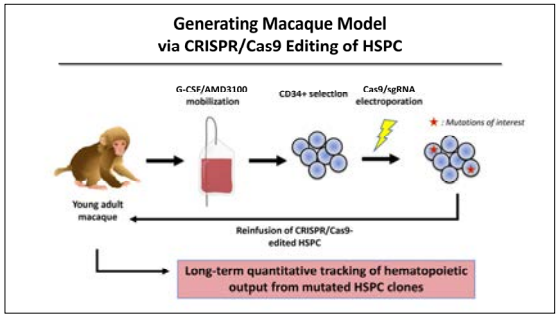

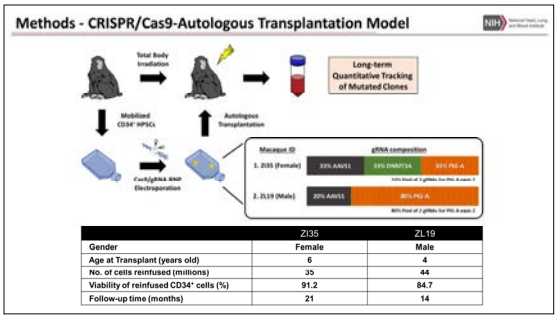

	ZI35	ZL19
Gender	Female	Male
Age at Transplant (years old)	6	4
No. of cells reinfused (millions)	35	44
Viability of reinfused CD34+ cells (%)	91.2	84.7
Follow-up time (months)	21	14

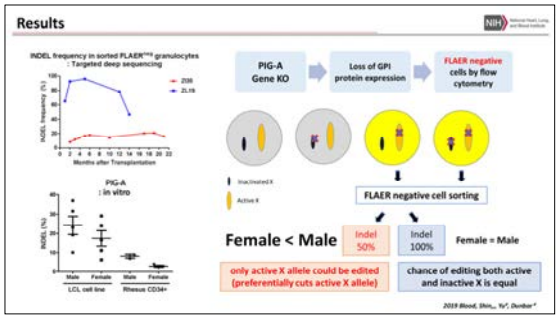

Genetic Inactivation of CD33 in Hematopoietic Stem Cells to Enable CAR T Cell Immunotherapy for Acute Myeloid Leukemia

Aim : generating a hematopoietic system resistant to CD33-targeted therapy and enabling specific targeting of AML with CAR T cells

Approach : CRISPR/Cas9 engineering of CD33 followed by CAR T cell administration

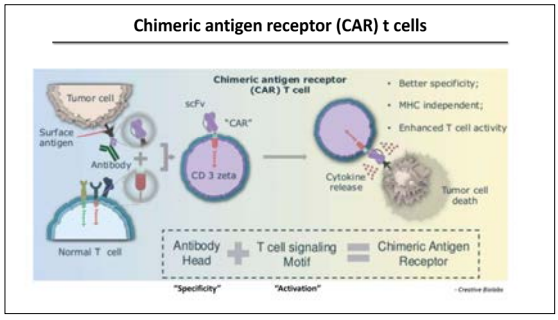

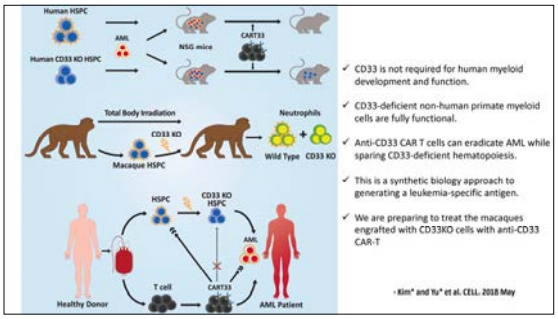
Human HSPC
AML
NSG mice
CART33
Human CD33 KO HSPC
Total Body Irradiation
Neutrophils
CD33 KO
Macaque HSPC
Wild Type
CD33 KO
HSPC
CD33 KO HSPC
AML
T cell
CART33
Healthy Donor
AML Patient
✓ CD33 is not required for human myeloid development and function.
✓ CD33-deficient non-human primate myeloid cells are fully functional.
✓ Anti-CD33 CAR T cells can eradicate AML while sparing CD33-deficient hematopoiesis.
✓ This is a synthetic biology approach to generating a leukemia-specific antigen.
✓ We are preparing to treat the macaques engrafted with CD33KO cells with anti-CD33 CAR-T
- Kim* and Yu* et al. CELL. 2018 May

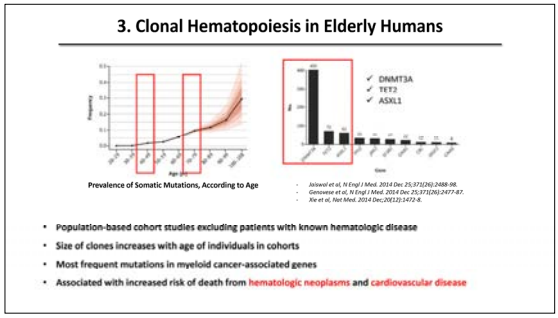
3. Clonal Hematopoiesis in Elderly Humans
Prevalence of Somatic Mutations, According to Age
✓ DNMT3A
✓ TET2
✓ ASXL1
Jaiswal et al, N Engl J Med. 2014 Dec 25;371(26):2488-98.
Genovese et al, N Engl J Med. 2014 Dec 25;371(26):2477-87.
Xie et al, Nat Med. 2014 Dec;20(12):1472-8.
• Population-based cohort studies excluding patients with known hematologic disease
• Size of clones increases with age of individuals in cohorts
• Most frequent mutations in myeloid cancer-associated genes
• Associated with increased risk of death from hematologic neoplasms and cardiovascular disease

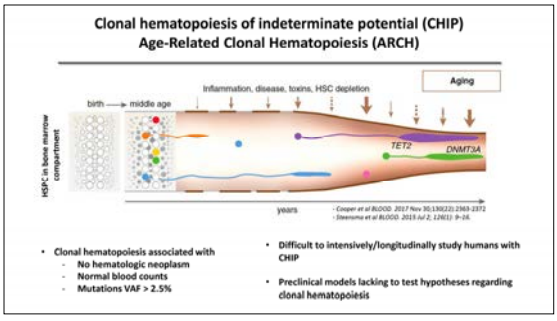
Clonal hematopoiesis of indeterminate potential (CHIP)
Age-Related Clonal Hematopoiesis (ARCH)
Aging
Inflammation, disease, toxins, HSC depletion
birth
middle age
HSPC in bone marrow compartment
TET2
DNMT3A
years
Cooper et al BLOOD. 2017 Nov 30;130(22):2369-2372
Steensma et al BLOOD. 2015 Jul 2; 126(1): 9-16.
• Clonal hematopoiesis associated with
- No hematologic neoplasm
- Normal blood counts
- Mutations VAF > 2.5%
• Difficult to intensively/longitudinally study humans with CHIP
• Preclinical models lacking to test hypotheses regarding clonal hematopoiesis

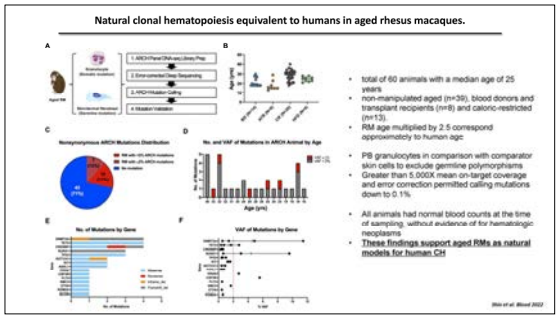
Natural clonal hematopoiesis equivalent to humans in aged rhesus macaques.
• total of 60 animals with a median age of 25 years
• non-manipulated aged (n=39), blood donors and transplant recipients (n=8) and caloric-restricted (n=13).
• RM age multiplied by 2.5 correspond approximately to human age
• PB granulocytes in comparison with comparator skin cells to exclude germline polymorphisms
• Greater than 5,000X mean on-target coverage and error correction permitted calling mutations down to 0.1%
• All animals had normal blood counts at the time of sampling, without evidence of for hematologic neoplasms
• These findings support aged RMs as natural models for human CH


Thank You!
Email: cellyu@snu.ac.kr
PROGRAM IN ANIMAL SCIENCE & BIOTECHNOLOGY
CALS

심포지엄 II
한국발생생물학회 젊은과학자

Dev. Reprod. Vol 26, 2022 (Suppl. 1). pp 57

Convergent differentiation of multiciliated cells

채신혁

UNIST

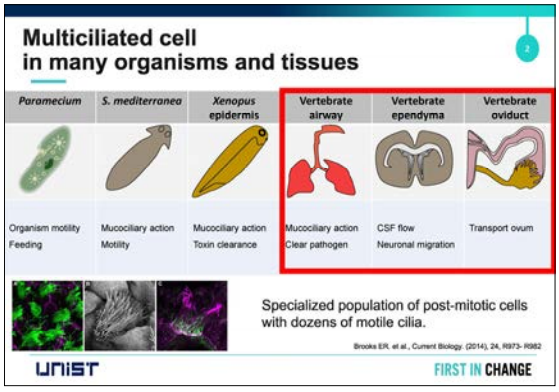

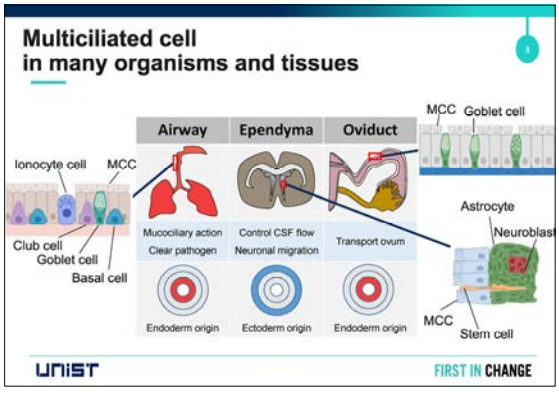

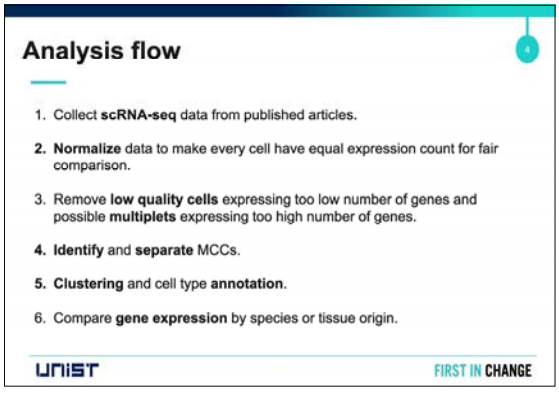

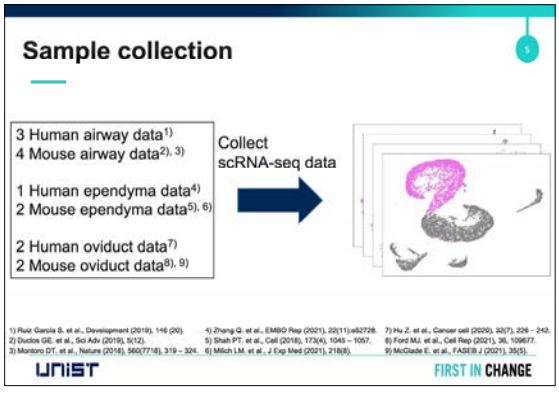

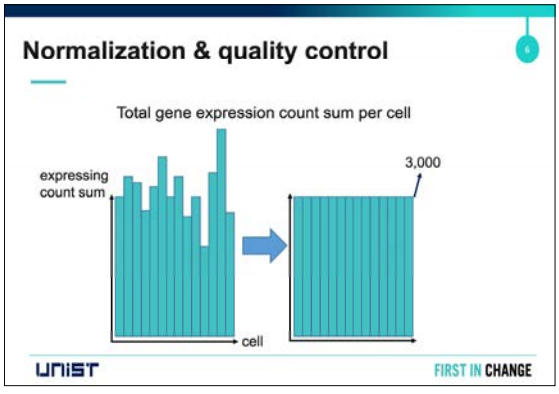

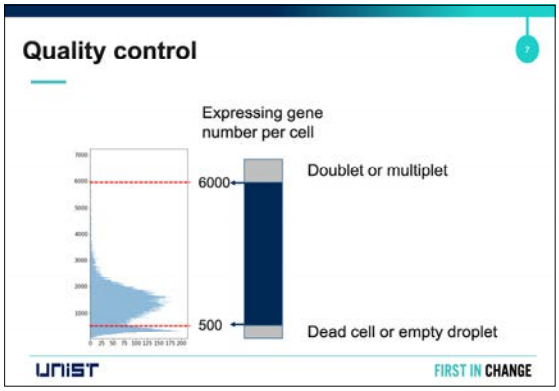
Quality control
Expressing gene number per cell
6000
500
Doublet or multiplet
Dead cell or empty droplet
UNIST
FIRST IN CHANGE

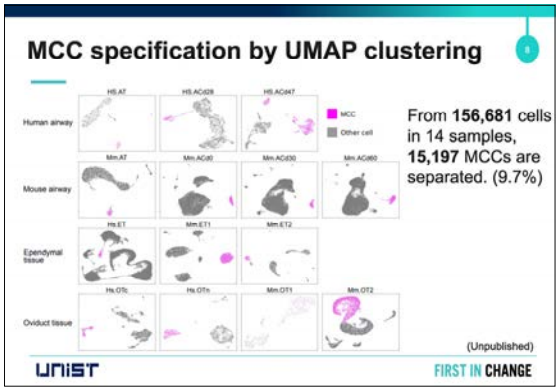
MCC specification by UMAP clustering
From 156,681 cells in 14 samples, 15,197 MCCs are separated. (9.7%)
(Unpublished)
UNIST
FIRST IN CHANGE

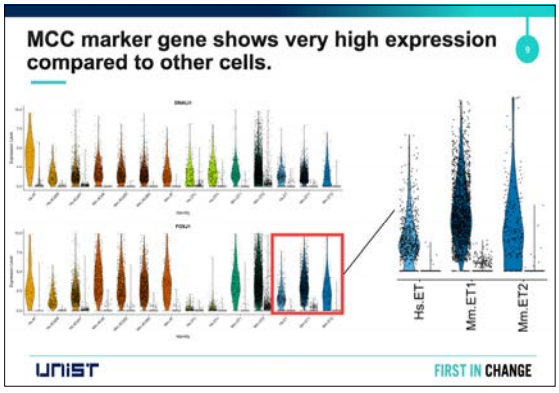
MCC marker gene shows very high expression compared to other cells.
Hs.ET
Mm.ET1
Mm.ET2
UNIST
FIRST IN CHANGE

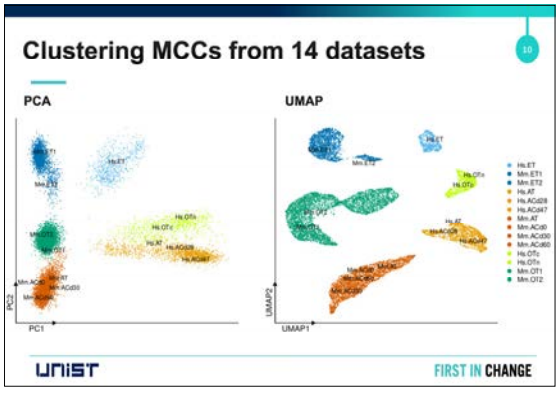
Clustering MCCs from 14 datasets
PCA
UMAP
PC1
PC2
UMAP1
UMAP2
UNIST
FIRST IN CHANGE

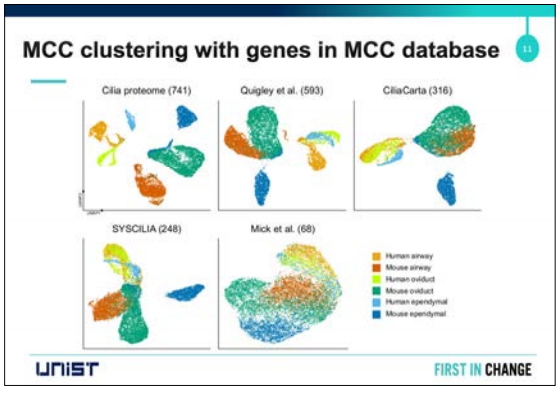
MCC clustering with genes in MCC database
Cilia proteome (741)
Quigley et al. (593)
CiliaCarta (316)
SYSCILIA (248)
Mick et al. (68)
Human airway
Mouse airway
Human oviduct
Mouse oviduct
Human ependymal
Mouse ependymal
UNIST
FIRST IN CHANGE

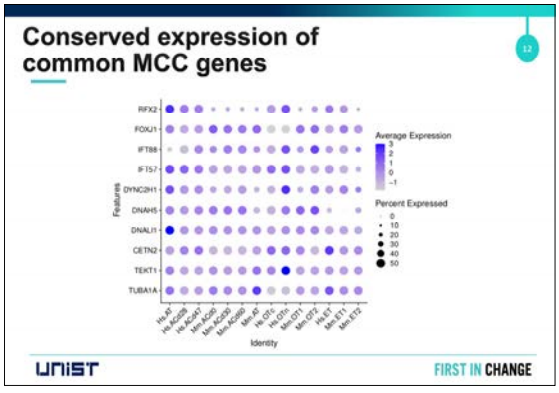
Conserved expression of common MCC genes
RFX2
FOXJ1
IFT88
IFT57
DYNC2H1
DNAH5
DNALI1
CETN2
TEKT1
TUBA1A
Features
Identity
Average Expression
Percent Expressed
UNIST
FIRST IN CHANGE

Conserved expression of MCC genes

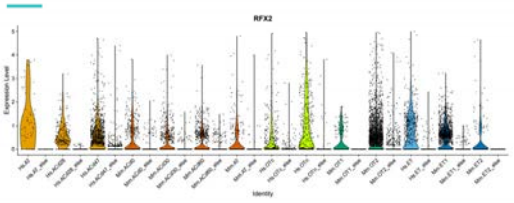

- Although RFX2 shows high expression level in human, we can find MCC specific expression in all samples.
- There are many RFX2 non-expressing cells in mouse samples.

UNIST FIRST IN CHANGE

Dot plots by genes with ciliopathies

- Conserved high expression level across all samples in every symptom
- No tissue specificity
- Some genes (OFD1, NEK10 …) are expressed human specifically.

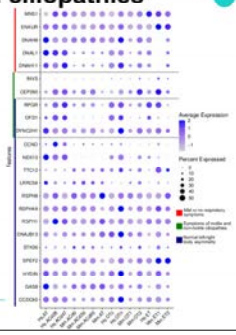

UNIST

GO of airway specific markers (40)

- **Epithelium development**
  PROM1, KRT4, SLITRK6, TBX1, FOXC1, FOXA1, SIX1
- **Sensory organ development**
  PROM1, AQP5, SLITRK6, TBX1, FOXC1, OTX1, SIX1
- **Tissue homeostasis**
  PROM1, PIGR, ZG16B, EPAS1, FOXC1, MUC4

Underbar : TFs

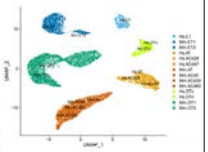

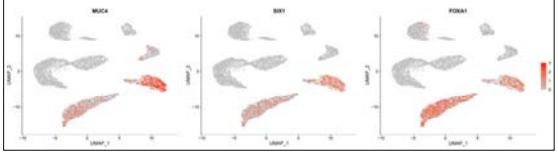

GO of oviduct specific markers (19)

- **Reproductive process**
  ESR1, WDR77, OVGP1, PANX1, STC1, GATA6
- **Regulation of apoptotic process**
  ESR1, PAX8, TCTN3, GATA6, AMIGO2

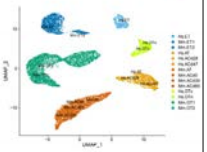

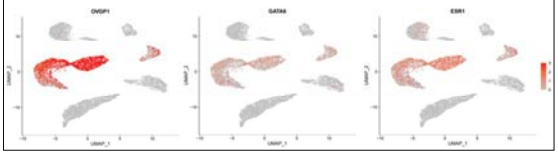

GO of ependymal specific markers (266)

- **NMDA glutamate receptor clustering**
  NLGN1, NRXN1, APOE, RELN
- **Cell-cell junction assembly**
  CDH2, PRKCA, MPDZ, ANK2, GJC1, TLN2, CLDN5, DCHS1, GJC1, GJA1, CDH7, CTNND2
- **Synapse assembly**
  CDH2, NLGN1, PTPRD, SPOCK2, DNER, NRXN1, IL1RAPL1, SDK2, GPM6A
- **Negative regulation of microtubule polymerization**
  MAP2, STMN2, CLIP3, TUBB4A

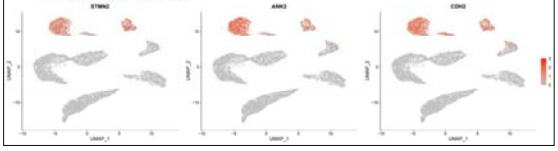

Sample specific marker genes

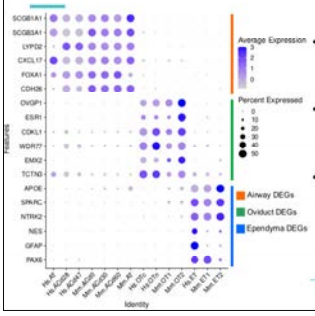

- Airway DEGs includes **club cell** markers such as SCGB1A1 and SCGB3A1.
- Oviduct DEGs includes **sex hormone** related genes such as ESR1 and OVGP1.
- Ependyma DEGs includes **radial glial cell** markers such as NES and GFAP.

FIRST IN CHANGE

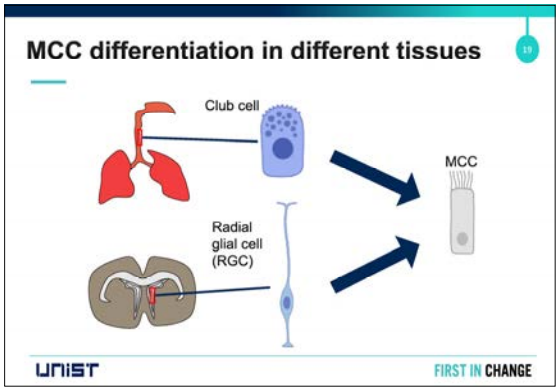
MCC differentiation in different tissues
Club cell
MCC
Radial glial cell (RGC)
UNIST
FIRST IN CHANGE

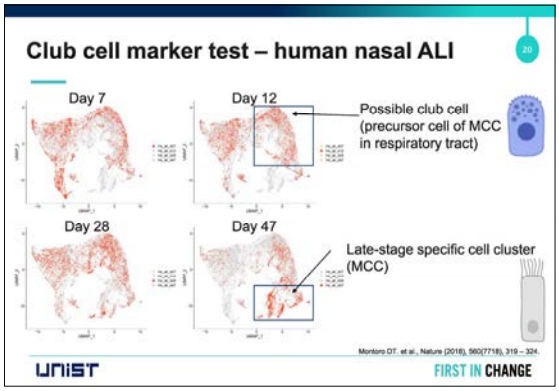
Club cell marker test – human nasal ALI
Day 7
Day 12
Possible club cell (precursor cell of MCC in respiratory tract)
Day 28
Day 47
Late-stage specific cell cluster (MCC)
UNIST
FIRST IN CHANGE

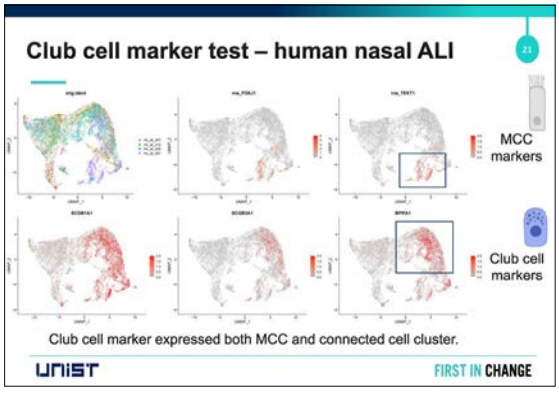
Club cell marker test – human nasal ALI
MCC markers
Club cell markers
Club cell marker expressed both MCC and connected cell cluster.
UNIST
FIRST IN CHANGE

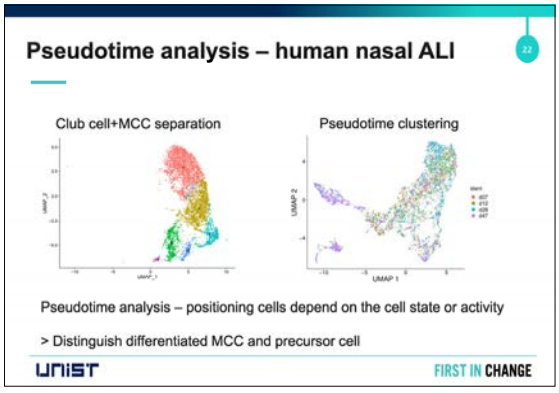
Pseudotime analysis – human nasal ALI
Club cell+MCC separation
Pseudotime clustering
Pseudotime analysis – positioning cells depend on the cell state or activity
> Distinguish differentiated MCC and precursor cell
UNIST
FIRST IN CHANGE

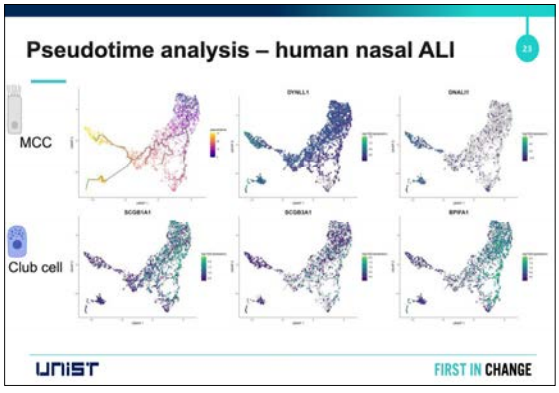
Pseudotime analysis – human nasal ALI
MCC
Club cell
UNIST
FIRST IN CHANGE

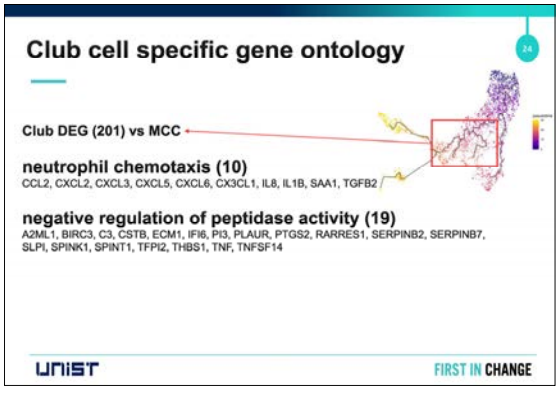
Club cell specific gene ontology
Club DEG (201) vs MCC
neutrophil chemotaxis (10)
CCL2, CXCL2, CXCL3, CXCL5, CXCL6, CX3CL1, IL8, IL1B, SAA1, TGFB2
negative regulation of peptidase activity (19)
A2ML1, BIRC3, C3, CSTB, ECM1, IFI6, PI3, PLAUR, PTGS2, RARRES1, SERPINB2, SERPINB7, SLPI, SPINK1, SPINT1, TFPI2, THBS1, TNF, TNFSF14
UNIST
FIRST IN CHANGE

RGC marker test – human fetal spinal cord

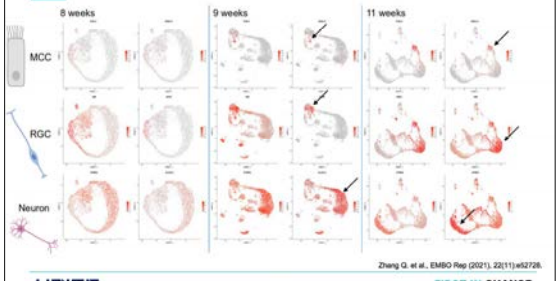

UNIST FIRST IN CHANGE

RGC marker test – human fetal spinal cord

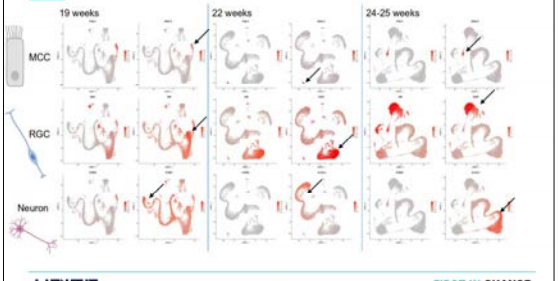

UNIST FIRST IN CHANGE

Pseudotime analysis – human fetal spinal cord

11 weeks + 19 weeks + 24-25 weeks
to see RGC to MCC development

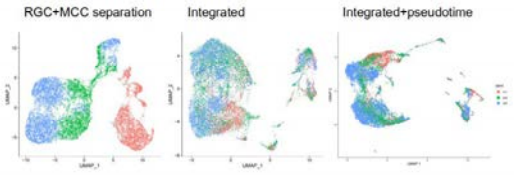

UNIST FIRST IN CHANGE

Pseudotime analysis – human fetal spinal cord

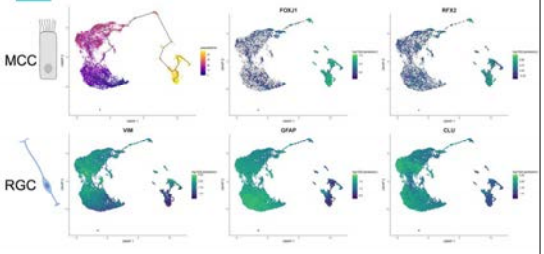

UNIST FIRST IN CHANGE

RGC specific gene ontology

RGC DEG (107) vs MCC

cholesterol biosynthetic process (10)
DHCR24, DHCR7, FDFT1, FDPS, HMGCR, HMGCS1, IDI1, INSIG1, MSMO1, MVD

cell adhesion (19)
AQP4, CD44, CDH15, CNN3, ID1, LAMA4, LGALS1, MYBPC1, NRP2, NTM, PCDH9, PRPH, ROM1, SLITRK2, SPARCL1, TGFBI, TJP2, TNC, WNT7B

neuron differentiation (17)
APOE, CRTAC1, ETV1, GAP43, GFAP, ID1, ID2, ID3, LGI4, NRP2, NTM, PRPH, PRRX1, ROM1, SLITRK2, TNC, WNT7B

UNIST FIRST IN CHANGE

Conclusion

- We can find MCCs from different tissues and species have **conserved MCC marker gene** expression.
- However, still MCCs from different tissues and species has different characteristics.
  - **Club cell marker** expression in airway MCCs
  - **RGC marker gene** expression in ependyma MCCs
- We can see **different MCC development** depend on the tissue.

UNIST FIRST IN CHANGE

Acknowledgement

Taejoon Lab.
- **Prof. Taejoon Kwon**
- Hwi Hyun
- Kujin Kwon
- Seongmin Yun
- Hyeongsun Jeong
- Kyungha Kim
- Seohyun Kim
- Jiwon Choi

UNIST FIRST IN CHANGE

THANK YOU

FIRST IN CHANGE

Samples

Label	Accession #	Species	Tissue	Description
Hs.AT	GSE131391	Human	Bronchial	Bronchial epithelium from smokers and non-smokers
Hs.ACd28	GSE121600	Human	Nasal epithelia	ALI culture of HAEC derived from nasal mucosa
Hs.ACd27	GSE121600	Human	Nasal epithelia	ALI culture of HAEC derived from nasal mucosa
Mm.AT	GSE103354	Mouse	Bronchia	Mouse tracheal epithelial cell
Mm.ACd0	GSE103354	Mouse	Bronchia	Differentiated mouse tracheal basal cell
Mm.ACd30	GSE103354	Mouse	Bronchia	Differentiated mouse tracheal basal cell
Mm.ACd60	GSE103354	Mouse	Bronchia	Differentiated mouse tracheal basal cell

UNIST FIRST IN CHANGE

Samples

Label	Accession #	Species	Tissue	Description
Hs.ET	GSE136719	Human	Spinal cord	Human fatal spinal cord data from 24–25-week prenatal baby
Mm.ET1	GSE162610	Mouse	Spinal cord	Uninjured spinal cord data from 8–10-week mice
Mm.ET2	GSE100320	Mouse	Brain	Ependymal cells and neuronal cells from 8-week mice
Hs.OTc	GSE132149	Human	Oviduct	Fallopian tube tissues from ovarian cancer patients
Hs.OTn	GSE139079	Human	Oviduct	Fallopian tube tissues from ovarian benign patients
Mm.OT1	GSE180102	Mouse	Oviduct	Fallopian tube tissues from mice in reproductive age
Mm.OT2	GSE164291	Mouse	Oviduct	Fallopian tube tissues from mice in reproductive age

UNIST FIRST IN CHANGE

Samples

1. Human nasal epithelial cell ALI (Hs.ACd28, Hs.ACd47)
- ALI culture of HAEC derived from nasal mucosa.
- Ruiz García S. et al., Development (2019), 146 (20).

2. Human bronchial epithelial cell (Hs.AT)
- Brushing from the human bronchus.
- Duclos GE. et al., Sci Adv (2019). 5(12).

3. Mouse bronchial cell (Mm.ACd0, Mm.ACd30, Mm.ACd60, Mm.AT)
- Cells after homeostatic turnover by treatment of tamoxifen to induce cell differentiation from basal cell of 6–12-week mice trachea (3 per time point).
- Montoro DT. et al., Nature (2018), 560(7718), 319 – 324.

UNIST FIRST IN CHANGE

Samples

4. Human fallopian tube (Hs.OTc, Hs.OTn)
- Human fallopian tube epithelial cells from 5 cancer and 5 benign patients.
- Hu Z. et al., Cancer cell (2020), 32(7), 226 – 242.

5. Mouse fallopian tube (Mm.OT1, Mm.OT2)
- Fallopian tube cells from mouse in reproductive age (2-4 months).
- Ford MJ. et al., Cell Rep (2021), 36, 109677.
- Oviduct from 8 ~ 10-week mice.
- McGlade E. et al., FASEB J (2021), 35(5).

UNIST FIRST IN CHANGE

Samples

6. Mouse SVZ (Mm.ET1)
- Ependymal cells and neuronal cell from 8-week mice (3).
- Shah PT. et al., Cell (2018), 173(4), 1045 – 1057.

7. Mouse spinal cord (Mm.ET2)
- Uninjured spinal cord data from 8–10-week mice.
- Milich LM. et al., J Exp Med (2021), 218(8).

8. Human spinal cord (Hs.ET)
- Human fatal spinal cord data from 24–25-week prenatal baby.
- Zhang Q. et al., EMBO Rep (2021), 22(11):e52728.

UNIST FIRST IN CHANGE

Marker gene selection

Marker gene selection rules

1. Expression of target tissue > Expression of else *2
2. 10% of target cells expressing the gene
3. No human – mouse expression difference (less than 2-fold)

UNIST FIRST IN CHANGE

Heatmap of DEGs from 14 datasets (Z-score)

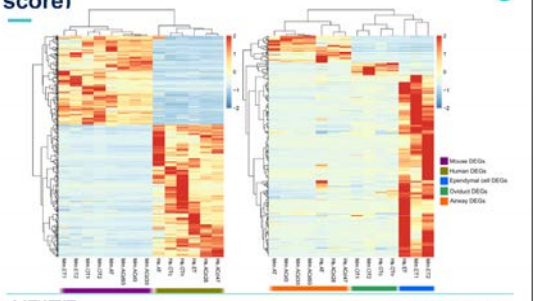

UNIST FIRST IN CHANGE

GO of human specific markers (386)

- **Deoxyribonucleotide metabolic process**
DCTD, DERA, DUT, DCK, NUDT15, NEIL1, TYMP, NEIL2
- **Telomere maintenance**
ZBTB48, DCLRE1C, RAD51C, XRCC6, APEX1, PRKDC, ERCC1
- **Cytochrome complex assembly**
COA4, PET117, LYRM7, TACO1, SCO1
- **Somatic diversification of immune receptors**
ADAR, DCLRE1C, TCF7, PRKDC, ERCC1

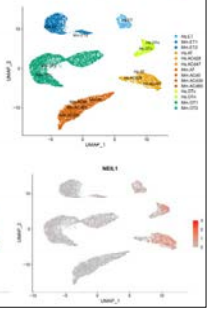

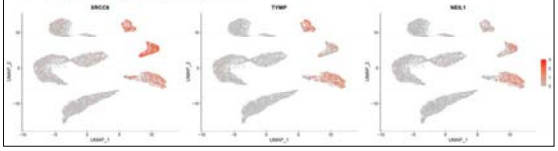

UNIST FIRST IN CHANGE

GO of mouse specific markers (262)

- **Regulation of lipid biosynthetic process**
FITM2, PLIN5, SIRT3, ATP1A1, ABCA3, SREBF2, NR1D1, ACADL, DGAT2
- **Polyol metabolic process**
PCBD2, SPTLC3, SYNJ1, NAAA, GALK1, DGAT2, SGPP1, ITPKA
- **Regulation of steroid metabolic process**
FMO5, ATP1A1, SREBF2, NR1D1, ACADL, KIT, DGAT2
- **Regulation of dendrite development**
FBXW8, DAB2IP, ANAPC2, STK11, NEDD4, GSK3B, ITPKA
- **Regulation of epidermal growth factor receptor signaling pathway**
DAB2IP, HAP1, PTPRJ, CDH13, HBEGF

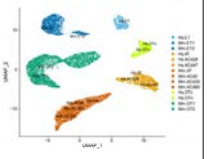

UNIST FIRST IN CHANGE

GO of mouse specific markers (262)

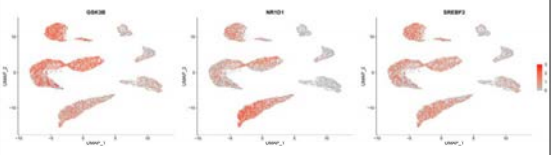

UNIST FIRST IN CHANGE

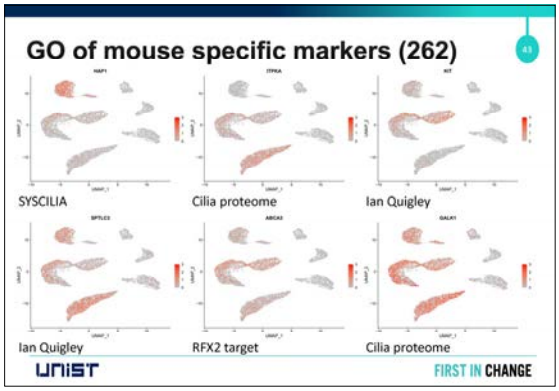
GO of mouse specific markers (262)
43
SYSCILIA
Cilia proteome
Ian Quigley
Ian Quigley
RFX2 target
Cilia proteome
UNIST
FIRST IN CHANGE

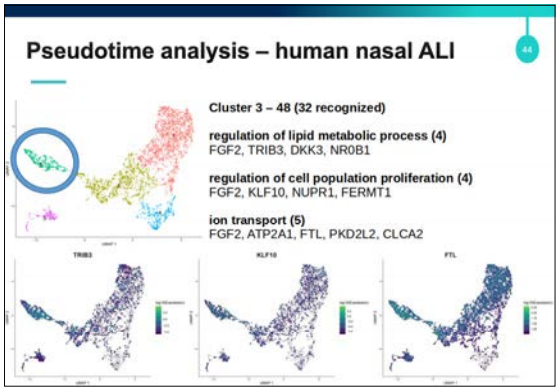
Pseudotime analysis – human nasal ALI
44
Cluster 3 – 48 (32 recognized)
regulation of lipid metabolic process (4)
FGF2, TRIB3, DKK3, NR0B1
regulation of cell population proliferation (4)
FGF2, KLF10, NUPR1, FERMT1
ion transport (5)
FGF2, ATP2A1, FTL, PKD2L2, CLCA2
TRIB3
KLF10
FTL

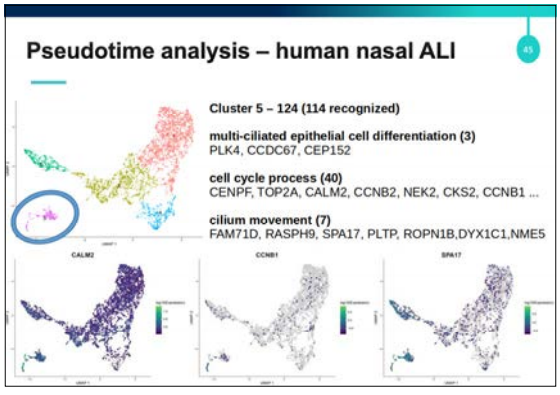
Pseudotime analysis – human nasal ALI
45
Cluster 5 – 124 (114 recognized)
multi-ciliated epithelial cell differentiation (3)
PLK4, CCDC67, CEP152
cell cycle process (40)
CENPF, TOP2A, CALM2, CCNB2, NEK2, CKS2, CCNB1 ...
cilium movement (7)
FAM71D, RASPH9, SPA17, PLTP, ROPN1B,DYX1C1,NME5
CALM2
CCNB1
SPA17

Dev. Reprod. Vol 26, 2022 (Suppl. 1). pp 65

Establishment of a male fertility prediction model with sperm RNA markers in pigs as a translational animal model

방원기

중앙대학교

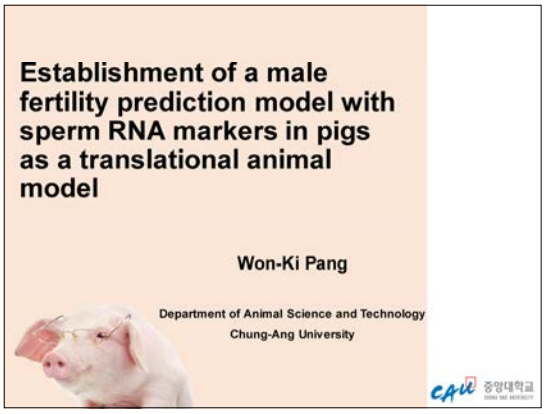

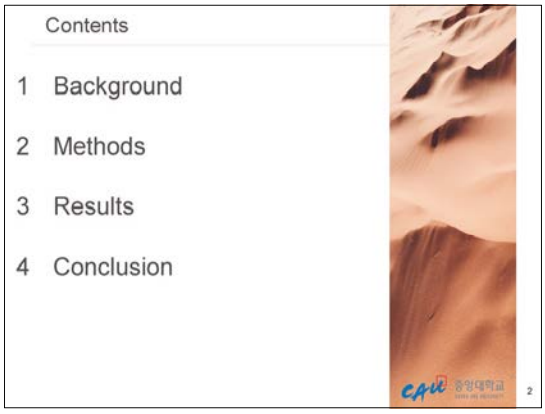

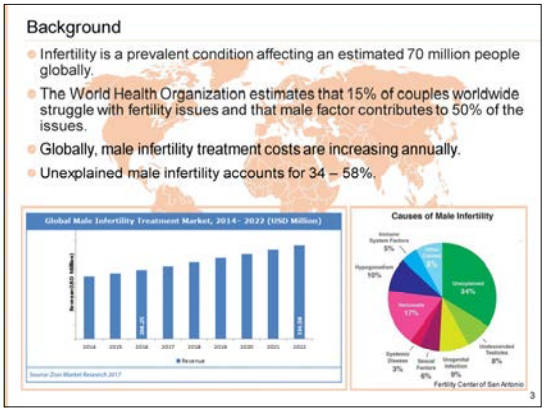

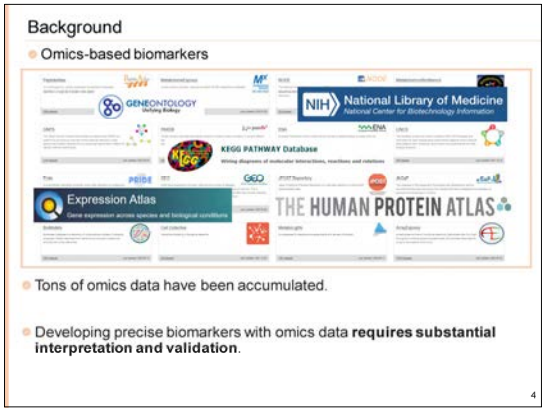

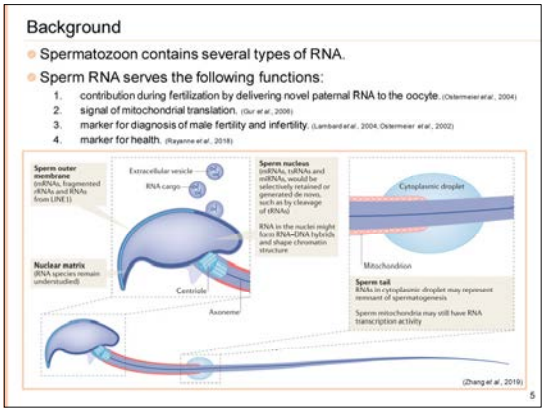

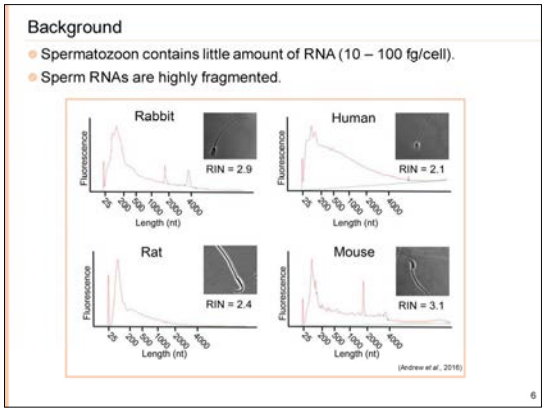

Background

- Optimization of sperm RNA processing (Pang et al., 2020)

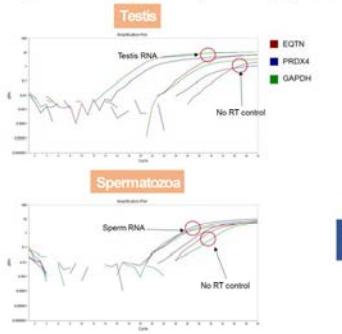

MIQE
Sample storage
RNA isolation
cDNA synthesis
RT-qPCR
Optimization of Sperm RNA Processing

7

Background

- Pig is one of the best translational animal model for studying male fertility.
  1. High physiological similarity with human.
  2. Huge amount and accurate fertility data acquisition through artificial insemination results.

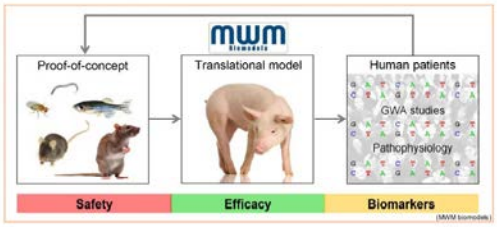

8

Background

- Single marker vs multiple marker

- A major benefit of the single marker is **simplicity**
- Fertilization is not controlled by a single gene – **Polygenic trait**

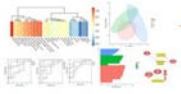

- Multiple marker approach has following benefits
  - ✓ **Higher diagnostic value**
  - ✓ **Easy to adjust**

9

Objective

To establish an accurate porcine fertility prediction model with sperm RNA markers related with acrosome reaction and sperm-egg fusion.

10

Methods

- Animal
  - Sexually matured (body weight over 90 kg and age between 9 to 24 months)
  - All boars and sows used in the experiment were reared at 20 ± 5°C under a 2:1 light/dark cycle, continuous air circulation, and appropriate feed and water.

- Male fertility prediction model
  - The acrosome reaction & sperm-egg fusion related genes are listed from Gene Ontology database.

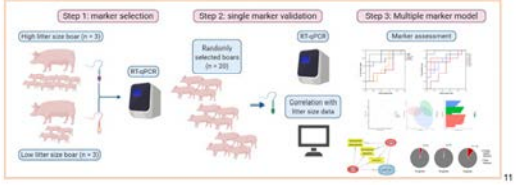

11

Results

Table 1. Functional parameters of spermatozoa and litter size of the high- and low-fertility groups.

	High fertility	Low fertility
Litter size	13.97 ± 0.07*	11.17 ± 0.13
MOT (%)	72.94 ± 18.26	70.19 ± 14.68
HYP (%)	13.19 ± 6.80	12.67 ± 7.57
VCL (μm/s)	134.59 ± 21.57	134.21 ± 25.00
VSL (μm/s)	58.66 ± 9.32	65.51 ± 16.53
VAP (μm/s)	69.96 ± 11.02	74.29 ± 14.75
LIN (%)	43.87 ± 3.14	49.25 ± 7.96
BCF (Hz)	13.75 ± 1.10	14.09 ± 1.28
WOB (%)	52.10 ± 1.90	55.94 ± 5.31
ALH (μm)	5.96 ± 0.92	6.01 ± 1.01
AR (%)	2.68 ± 0.88	8.20 ± 6.95
F (%)	65.24 ± 10.42	76.92 ± 9.32
B (%)	32.08 ± 10.58	14.88 ± 2.80

MOT = motility; HYP = hyperactivation; VCL = curvilinear velocity; VSL = straight line velocity; VAP = average path velocity; LIN = linearity; BCF = beat cross frequency; WOB = wobble; ALH = mean amplitude of head lateral displacement; AR = acrosome reacted; F = normal; B = capacitated. Data are expressed as mean ± SEM. *$P < 0.05$.

12

Results

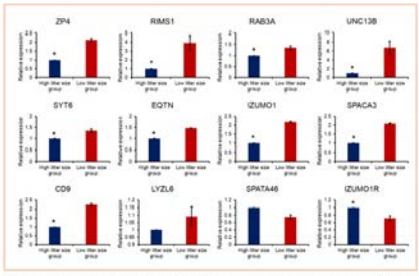

Figure 1. The expression pattern of target genes in the high- and low-fertility groups. Relative mRNA expression of selected genes in the high- and low-fertility groups. (n = 3). * $P < 0.05$.

13

Results

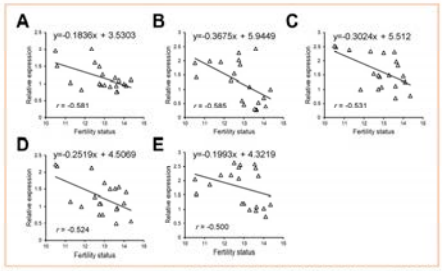

Figure 2. Linear regression test. Linear regression of (B) EQTN. (C) ZP4. (D) UNC13B. (E) RIMS1. and (F) SPACA3 and fertility status of 20 randomly selected pigs. r, Pearson coefficient; $P < 0.05$.

14

Results

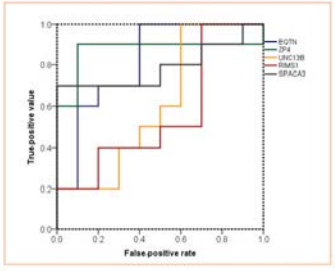

Figure 3. The receiver operating characteristic curve. The receiver operating characteristic curve of EQTN, ZP4, UNC13B, RIMS1, and SPACA3 for single marker evaluation.

15

Results

Table 2. Male fertility prediction value of single markers.

Gene	Cut-off value	AUC	Sensitivity (%)	Specificity (%)	NPV (%)	PPV (%)	OA (%)
EQTN	1.0	0.8	70.0	70.0	70.0	70.0	70.0
ZP4	1.2	0.9	90.0	90.0	90.0	90.0	90.0
UNC13B	1.5	0.6	60.0	50.0	55.6	54.5	55.0
RIMS1	1.1	0.6	50.0	40.0	44.4	45.5	45.0
SPACA3	2.0	0.8	70.0	70.0	70.0	70.0	70.0

AUC = Area under the curve. Sensitivity is the percentage of pigs showing true-positive results when tested with mRNA expression. Specificity is the percentage of pigs showing true-negative results. The positive predictive value (PPV) is the percentage of pigs that tested as positive and simultaneously showed true-positive litter size. The negative predictive value (NPV) is the percentage of pigs that tested as negative and simultaneously showed true-negative litter size. OA = overall accuracy.

16

Results

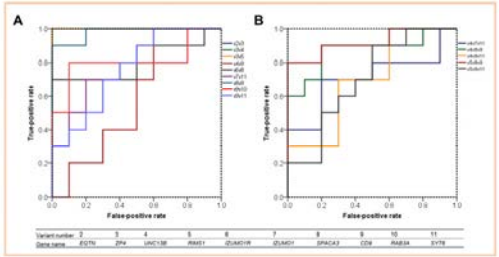

Figure 4. Assessment of multiple fertility markers. (A) The receiver operating characteristic curve of the predictive ability of the two-gene marker models for male fertility prediction. (B) The receiver operating characteristic curve of the predictive ability of the three-gene marker models for male fertility prediction.

17

Results

Table 3. Male fertility prediction value of multiple marker models.

Prediction model	AUC	Sensitivity (%)	Specificity (%)	NPV (%)	PPV (%)	OA (%)
EQTN-ZP4	1.0	100.0	100.0	100.0	100.0	100.0
ZP4-UNC13B	1.0	100.0	100.0	100.0	100.0	100.0
ZP4-RIMS1	1.0	100.0	100.0	100.0	100.0	100.0
UNC13B-CD9	0.6	50.0	50.0	50.0	50.0	50.0
IZUMO1R-SPACA3	0.8	70.0	60.0	66.7	63.6	65.0
IZUMO1-SYT6	0.7	70.0	60.0	66.7	63.6	65.0
SPACA3-CD9	1.0	90.0	80.0	88.9	81.8	85.0
CD9-RAB3A	0.8	80.0	80.0	80.0	80.0	80.0
CD9-SYT6	0.8	70.0	70.0	70.0	70.0	70.0
UNC13B-IZUMO1-SYT6	0.7	70.0	60.0	66.7	63.6	65.0
UNC13B-SPACA3-CD9	0.9	80.0	80.0	80.0	80.0	80.0
UNC13B-CD9-SYT6	0.7	70.0	70.0	70.0	70.0	70.0
RIMS1-SPACA3-CD9	0.9	80.0	80.0	80.0	80.0	80.0
RIMS1-CD9-SYT6	0.7	70.0	60.0	66.7	63.6	65.0

AUC = Area under the curve. Sensitivity is the percentage of pigs showing true-positive results when tested with mRNA expression. Specificity is the percentage of pigs showing true-negative results. The positive predictive value (PPV) is the percentage of pigs that tested as positive and simultaneously has a true-positive litter size. The negative predictive value (NPV) is the percentage of pigs that tested as negative or simultaneously had a true-negative litter size. OA = overall accuracy.

18

Results

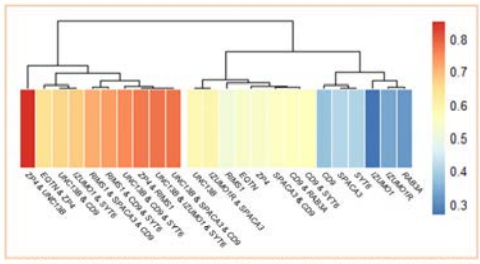

Figure 5. Heatmap analysis. Heatmap showing the coefficient values of the multiple-marker prediction models and single markers.

19

Results

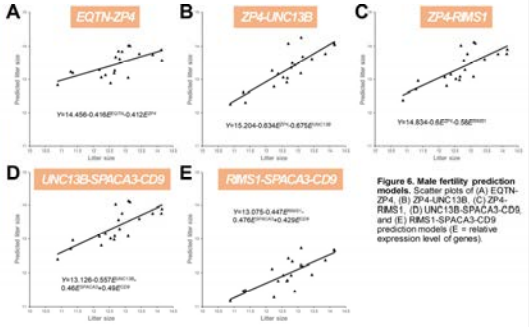

Figure 6. Male fertility prediction models. Scatter plots of (A) EQTN-ZP4, (B) ZP4-UNC13B, (C) ZP4-RIMS1, (D) UNC13B-SPACA3-CD9, and (E) RIMS1-SPACA3-CD9 prediction models (E = relative expression level of genes).

20

Results

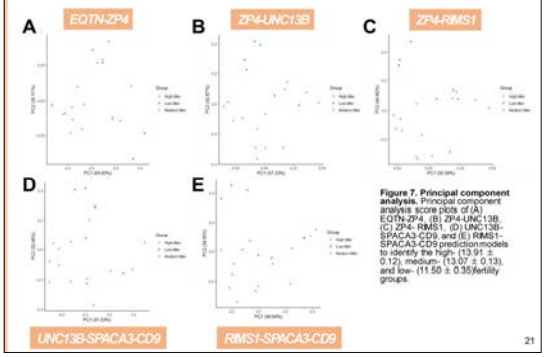

Figure 7. Principal component analysis. Principal component analysis score plots of (A) EQTN-ZP4, (B) ZP4-UNC13B, (C) ZP4- RIMS1, (D) UNC13B-SPACA3-CD9, and (E) RIMS1-SPACA3-CD9 prediction models to identify the high- (13.91 ± 0.12), medium- (13.07 ± 0.13), and low- (11.50 ± 0.35)fertility groups.

21

Results

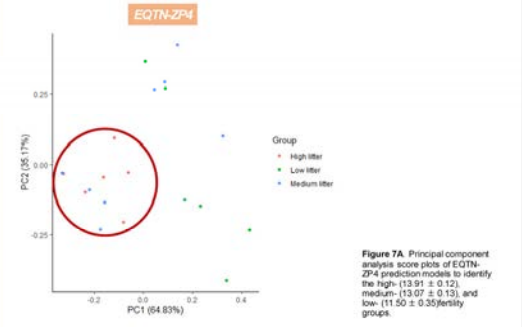

Figure 7A. Principal component analysis score plots of EQTN-ZP4 prediction models to identify the high- (13.91 ± 0.12), medium- (13.07 ± 0.13), and low- (11.50 ± 0.35)fertility groups.

22

Results

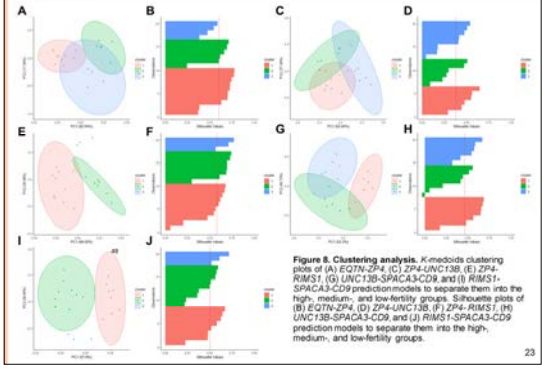

Figure 8. Clustering analysis. *K*-medoids clustering plots of (A) *EQTN-ZP4*, (C) *ZP4-UNC13B*, (E) *ZP4-RIMS1*, (G) *UNC13B-SPACA3-CD9*, and (I) *RIMS1-SPACA3-CD9* prediction models to separate them into the high-, medium-, and low-fertility groups. Silhouette plots of (B) *EQTN-ZP4*, (D) *ZP4-UNC13B*, (F) *ZP4- RIMS1*, (H) *UNC13B-SPACA3-CD9*, and (J) *RIMS1-SPACA3-CD9* prediction models to separate them into the high-, medium-, and low-fertility groups.

23

Results

Table 4. Average litter size of high-, medium-, and low-fertility groups after clustering.

Marker combination	High-fertility *K*-medoids clustering and silhouette plotting	Medium fertility *K*-medoids clustering and silhouette plotting	Low-fertility *K*-medoids clustering and silhouette plotting
EQTN-ZP4	14.05 ± 0.12a	13.45 ± 0.10a	12.02 ± 0.29b
ZP4-UNC13B	13.82 ± 0.10a	12.91 ± 0.08b	11.50 ± 0.35c
ZP4-RIMS1	14.15 ± 0.11a	13.49 ± 0.10b	12.02 ± 0.29b
UNC13B-SPACA3-CD9	13.91 ± 0.12a	13.12 ± 0.13b	11.67 ± 0.35b
RIMS1-SPACA3-CD9	14.15 ± 0.11a	13.35 ± 0.12b	11.81 ± 0.33b

Data are expressed as mean ± SEM. a,b,c $P < 0.05$.

24

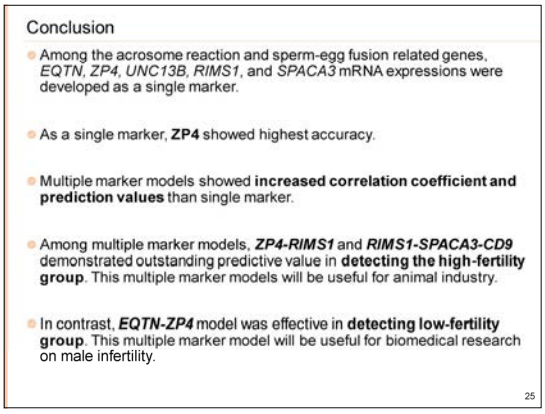
Conclusion
Among the acrosome reaction and sperm-egg fusion related genes, EQTN, ZP4, UNC13B, RIMS1, and SPACA3 mRNA expressions were developed as a single marker.
As a single marker, ZP4 showed highest accuracy.
Multiple marker models showed increased correlation coefficient and prediction values than single marker.
Among multiple marker models, ZP4-RIMS1 and RIMS1-SPACA3-CD9 demonstrated outstanding predictive value in detecting the high-fertility group. This multiple marker models will be useful for animal industry.
In contrast, EQTN-ZP4 model was effective in detecting low-fertility group. This multiple marker model will be useful for biomedical research on male infertility.
25

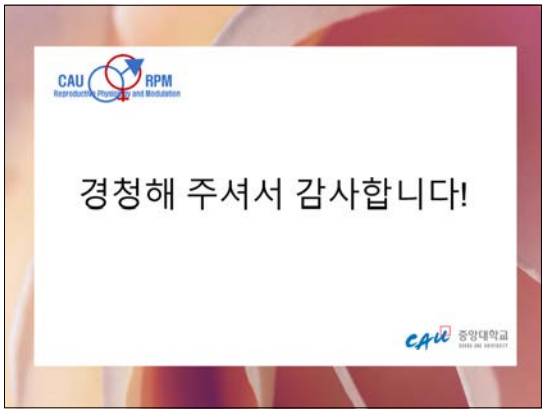
CAU RPM
경청해 주셔서 감사합니다!
CAU 중앙대학교

Dev. Reprod. Vol 26, 2022 (Suppl. 1). pp 70

Energy pathways involved in the maturation of the Pacific oyster, *Crassostrea gigas*

Su-jin Park[1], Soyeon Hwang[1], Yein Lee[1], *Youn Hee Choi[1,2]

[1]Department of Fisheries Biology, Pukyong National University

[2]Devision of Fisheries Life Sciences, Pukyong National University

(unichoi@pknu.ac.kr)

The Pacific oyster *Crassostrea gigas* is commercially-important aquaculture species worldwide. In marine bivalves like *C. gigas*, glycogen is used as energy storage for maturation and to provide energy for gametogenic development and maintenance. The stored glycogen is broken down into glucose when needed and used for energy production or blood sugar control. Additionally, it is known that growth factors inactivate glycogen synthase kinase 3 (GSK3) through phosphorylation, promote glycogen synthase (GS) activity, and regulate glucose synthesis and glycogen metabolism. Various signal transductions regulate GSK3 activity, and examples of phosphorylating enzymes capable of inducing such phosphorylation include protein kinase B (Akt). Therefore, this study was confirmed to investigate the relationship between GSK-3 and glycogenolysis/glycogenesis and compare the reproductive cycle of the *C. gigas* to the energy pathway.

Fifty oysters were randomly collected monthly for one year from the long-line culture system in Jaran Bay, Tongyeong, twenty of which were fixed in 4% paraformaldehyde for histological observation. To confirm changes in the GSK3 mRNA expression, gonads and adductor muscles were subjected to Reverse Transcription PCR (RT-PCR) and fluorescence in situ hybridization (FISH) methods, and the AKT/GSK3 signaling pathway in the gonads was analyzed using western-blot.

The expression of GSK3 mRNA levels in the female gonad was highest in October when spawning occurred after maturation, and the lowest expression was shown in July when spawning and spent. Similarly, in the male gonad, the expression of GSK3 mRNA levels was lowest in July. Also, in the adductor muscle, males and females showed the highest expression in April and low in July and October, when spawning and spent. This pattern was similar to the result confirming that GSK3 mRNA was detected in female and male gonad and adductor muscle by the FISH method. Furtherly observed that matured and spawned oysters from April to July exhibited higher AKT activities and lower GSK3 activities. In conclusion, GSK3 expression appears high at the time of ripe, inhibiting the synthesis of glycogen is used as energy for maturation, and glycogen synthesis occurs for energy storage during degeneration.

Key words: *Crassostrea gigas*, GSK3, energy, glycogen, maturation

심포지엄 Ⅲ
한국발생생물학회 신진과학자

Dev. Reprod. Vol 26, 2022 (Suppl. 1). pp 73

Effects of environmental stressors in antioxidant response of bay scallop *Argopecten irradians*

송진아

한국해양과학기술원

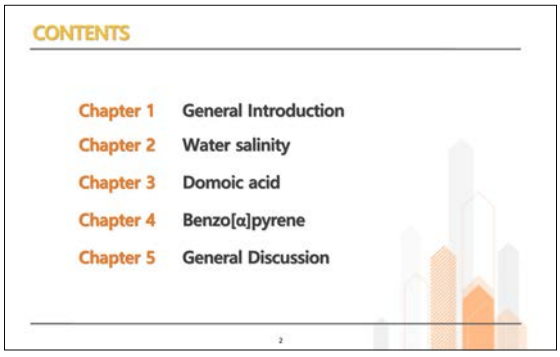

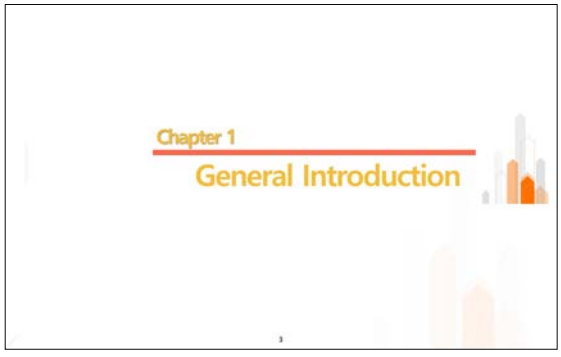

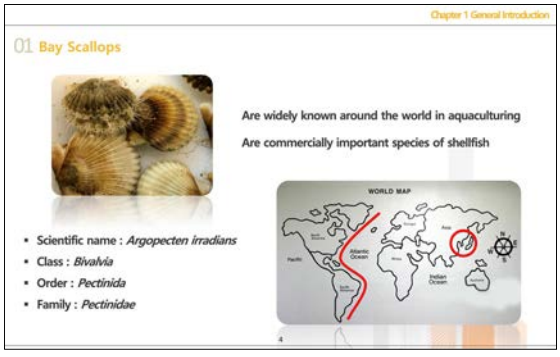

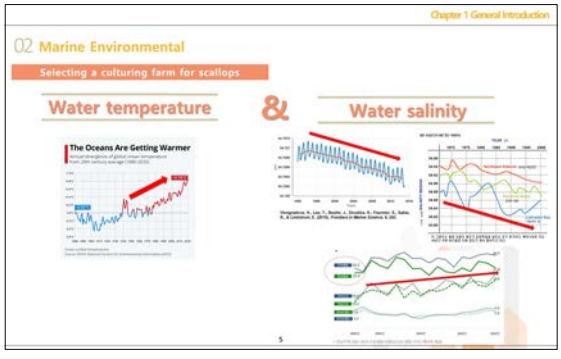

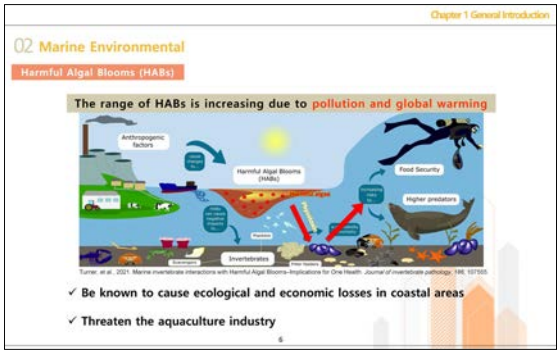

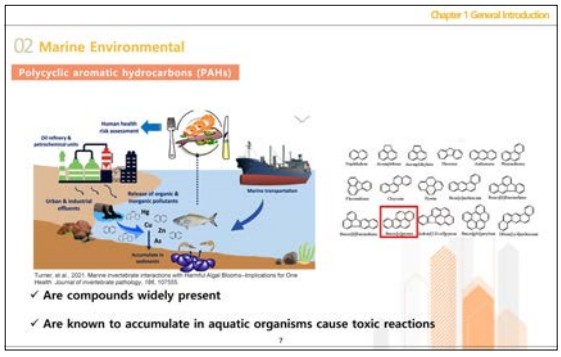
Chapter 1 General Introduction
02 Marine Environmental
Polycyclic aromatic hydrocarbons (PAHs)
✓ Are compounds widely present
✓ Are known to accumulate in aquatic organisms cause toxic reactions

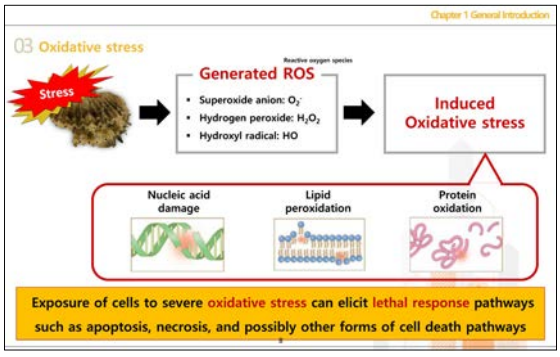
Chapter 1 General Introduction
03 Oxidative stress
Stress
Generated ROS
Superoxide anion: O_2^-
Hydrogen peroxide: H_2O_2
Hydroxyl radical: HO
Induced Oxidative stress
Nucleic acid damage
Lipid peroxidation
Protein oxidation
Exposure of cells to severe oxidative stress can elicit lethal response pathways such as apoptosis, necrosis, and possibly other forms of cell death pathways

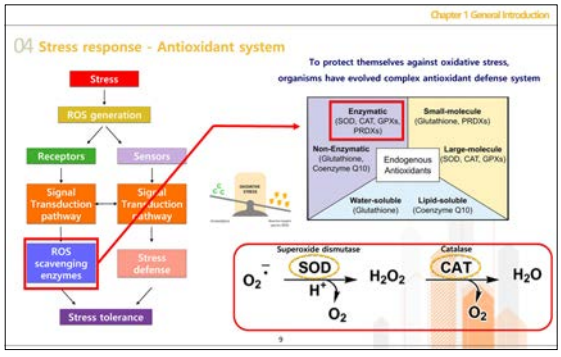
Chapter 1 General Introduction
04 Stress response - Antioxidant system
To protect themselves against oxidative stress, organisms have evolved complex antioxidant defense system
Stress
ROS generation
Receptors
Sensors
Signal Transduction pathway
ROS scavenging enzymes
Stress defense
Stress tolerance
Enzymatic (SOD, CAT, GPXs, PRDXs)
Small-molecule (Glutathione, PRDXs)
Non-Enzymatic (Glutathione, Coenzyme Q10)
Endogenous Antioxidants
Large-molecule (SOD, CAT, GPXs)
Water-soluble (Glutathione)
Lipid-soluble (Coenzyme Q10)
Superoxide dismutase
Catalase
SOD
CAT

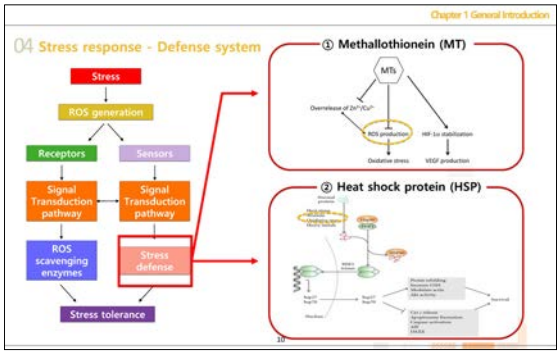
Chapter 1 General Introduction
04 Stress response - Defense system
① Methallothionein (MT)
② Heat shock protein (HSP)
Stress
ROS generation
Receptors
Sensors
Signal Transduction pathway
ROS scavenging enzymes
Stress defense
Stress tolerance

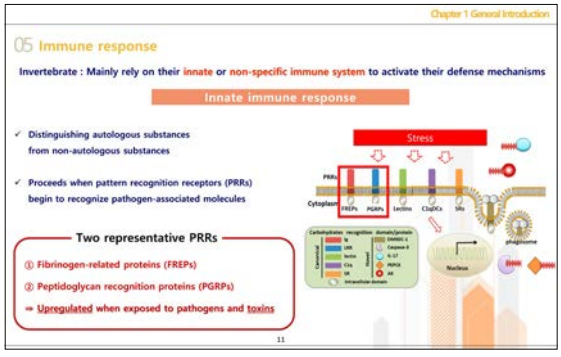
Chapter 1 General Introduction
05 Immune response
Invertebrate : Mainly rely on their innate or non-specific immune system to activate their defense mechanisms
Innate immune response
✓ Distinguishing autologous substances from non-autologous substances
✓ Proceeds when pattern recognition receptors (PRRs) begin to recognize pathogen-associated molecules
Two representative PRRs
① Fibrinogen-related proteins (FREPs)
② Peptidoglycan recognition proteins (PGRPs)
⇒ Upregulated when exposed to pathogens and toxins
Stress
Cytoplasm
Nucleus
phagosome

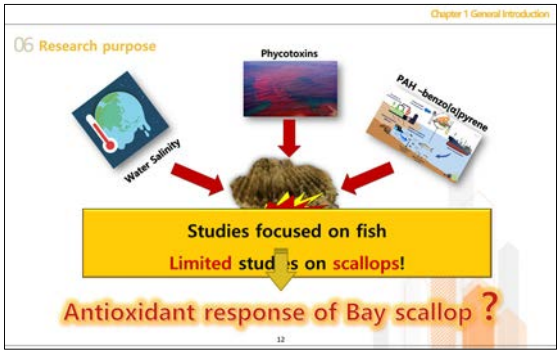
Chapter 1 General Introduction
06 Research purpose
Phycotoxins
Water Salinity
PAH -benzo[a]pyrene
Studies focused on fish
Limited studies on scallops!
Antioxidant response of Bay scallop ?

Chapter 2

Water salinity changes

13

Chapter 3 Introduction

01 Water salinity

✓ Is one of the factors limiting the area where stable aquaculture is possible

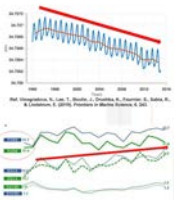

Cultured scallops are frequently exposed to salinity changes

14

Chapter 3 Introduction

03 Research purpose

Water salinity change

High or low salinity

SOD
CAT
H_2O_2
LPO
DNA damage
Apoptosis

Antioxidant system

The changes in oxidative stress and apoptosis on exposing bay scallops to an environment of rapid salinity changes were investigated

15

Chapter 3 Materials and Methods

05 Experimental design

✓ Species : *A. irradians* (55.0 ± 2.1 mm)

✓ Water quality : 17 °C and 35 psu

✓ Salinity

Instant Ocean synthetic sea salt (Aquarium Systems, USA)

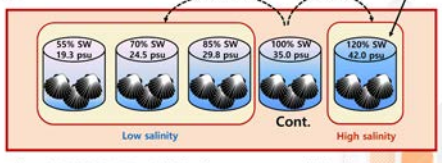

✓ Sampling : 0, 6, 12, 24, 48, and 72 h after exposure to salinity change

16

Chapter 3 Results

07 SOD mRNA and protein expression, activity

SOD mRNA and activity

① Salinity change

② Exposure time

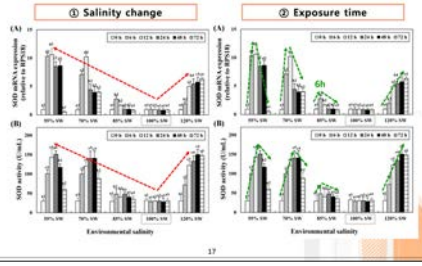

17

Chapter 3 Results

07 SOD mRNA and protein expression, activity

SOD protein

Western blot

IHC

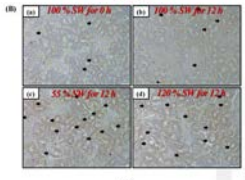

18

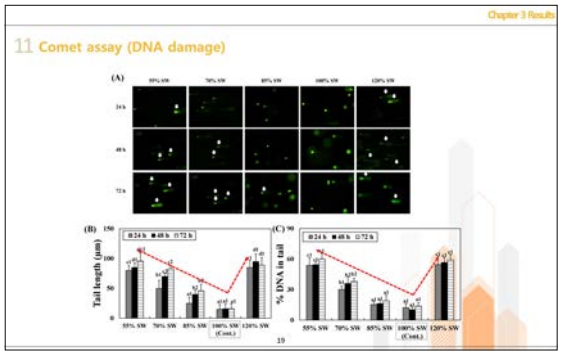
Chapter 3 Results
11 Comet assay (DNA damage)
(A)
(B)
Tail length (um)
(C)
% DNA in tail
55% SW
70% SW
85% SW
100% SW (Cont.)
120% SW
19

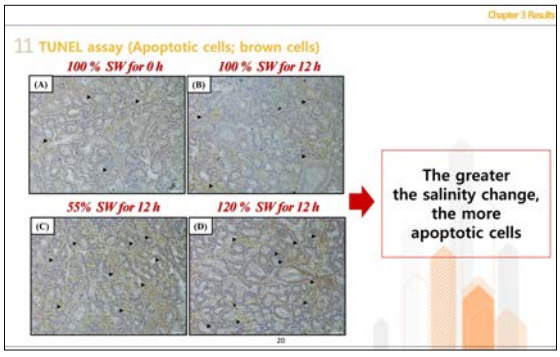
Chapter 3 Results
11 TUNEL assay (Apoptotic cells; brown cells)
100 % SW for 0 h
100 % SW for 12 h
55% SW for 12 h
120 % SW for 12 h
(A)
(B)
(C)
(D)
The greater the salinity change, the more apoptotic cells
20

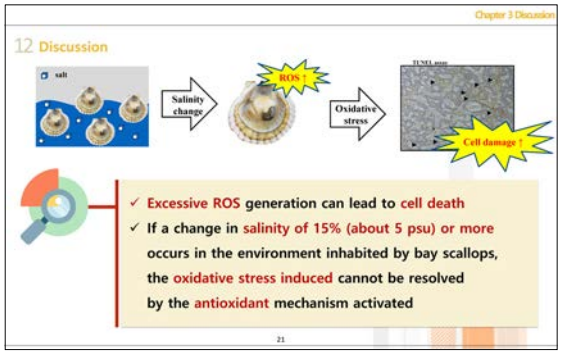
Chapter 3 Discussion
12 Discussion
salt
Salinity change
ROS ↑
Oxidative stress
Cell damage ↑
✓ Excessive ROS generation can lead to cell death
✓ If a change in salinity of 15% (about 5 psu) or more occurs in the environment inhabited by bay scallops, the oxidative stress induced cannot be resolved by the antioxidant mechanism activated
21

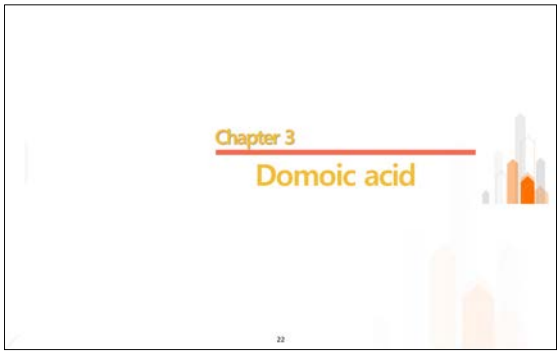
Chapter 3
Domoic acid
22

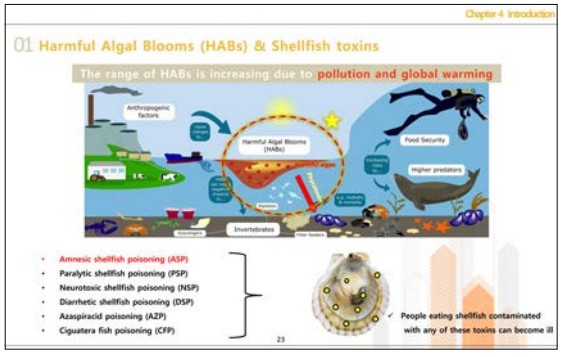
Chapter 4 Introduction
01 Harmful Algal Blooms (HABs) & Shellfish toxins
The range of HABs is increasing due to pollution and global warming
Anthropogenic factors
Harmful Algal Blooms (HABs)
Food Security
Higher predators
Invertebrates
Amnesic shellfish poisoning (ASP)
Paralytic shellfish poisoning (PSP)
Neurotoxic shellfish poisoning (NSP)
Diarrhetic shellfish poisoning (DSP)
Azaspiracid poisoning (AZP)
Ciguatera fish poisoning (CFP)
People eating shellfish contaminated with any of these toxins can become ill
23

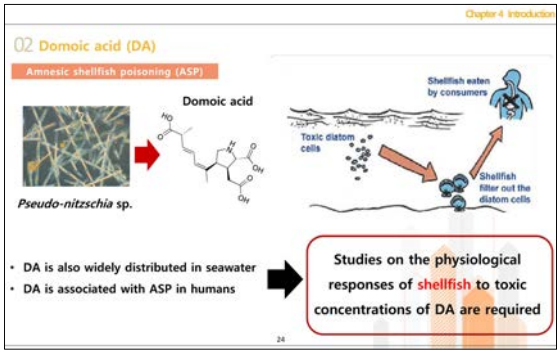
Chapter 4 Introduction
02 Domoic acid (DA)
Amnesic shellfish poisoning (ASP)
Domoic acid
Pseudo-nitzschia sp.
Shellfish eaten by consumers
Toxic diatom cells
Shellfish filter out the diatom cells
• DA is also widely distributed in seawater
• DA is associated with ASP in humans
Studies on the physiological responses of shellfish to toxic concentrations of DA are required
24

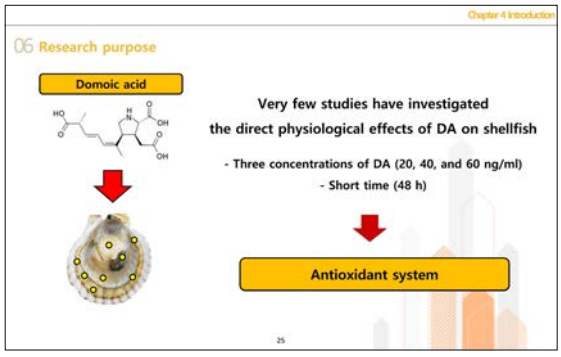
Chapter 4 Introduction
06 Research purpose
Domoic acid
Very few studies have investigated
the direct physiological effects of DA on shellfish
- Three concentrations of DA (20, 40, and 60 ng/ml)
- Short time (48 h)
Antioxidant system

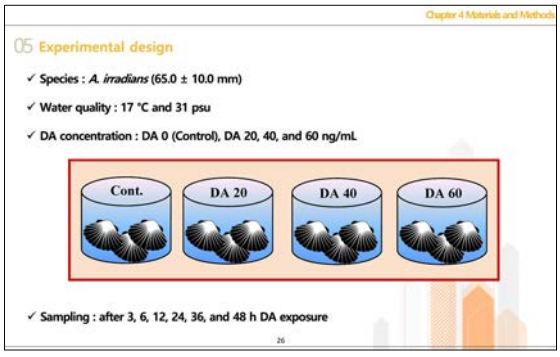
Chapter 4 Materials and Methods
05 Experimental design
✓ Species : A. irradians (65.0 ± 10.0 mm)
✓ Water quality : 17 °C and 31 psu
✓ DA concentration : DA 0 (Control), DA 20, 40, and 60 ng/mL
Cont.
DA 20
DA 40
DA 60
✓ Sampling : after 3, 6, 12, 24, 36, and 48 h DA exposure

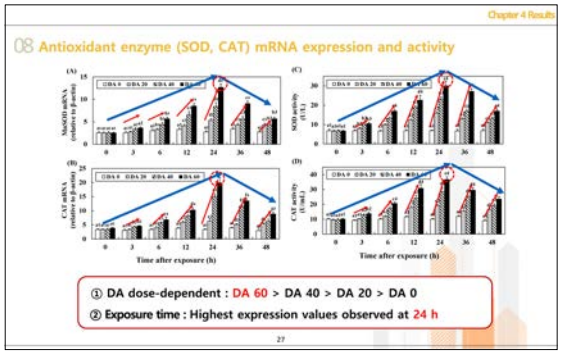
Chapter 4 Results
08 Antioxidant enzyme (SOD, CAT) mRNA expression and activity
Time after exposure (h)
① DA dose-dependent : DA 60 > DA 40 > DA 20 > DA 0
② Exposure time : Highest expression values observed at 24 h

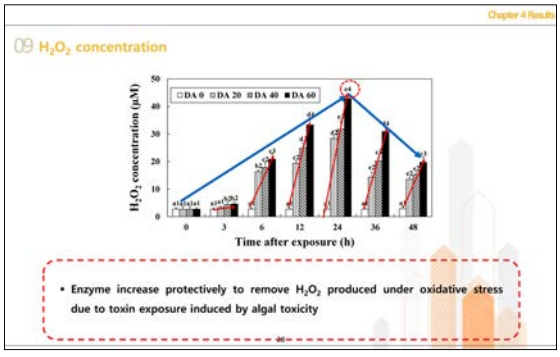
Chapter 4 Results
09 H2O2 concentration
H2O2 concentration (μM)
Time after exposure (h)
▪ Enzyme increase protectively to remove H2O2 produced under oxidative stress
due to toxin exposure induced by algal toxicity

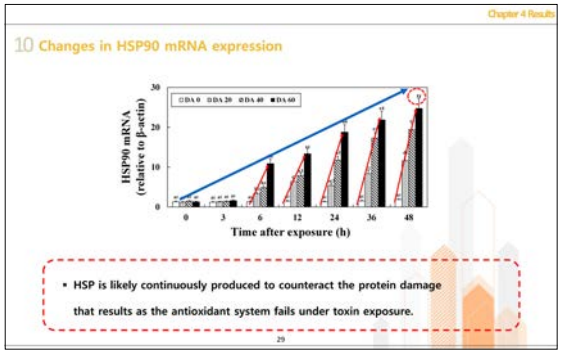
Chapter 4 Results
10 Changes in HSP90 mRNA expression
HSP90 mRNA
(relative to β-actin)
Time after exposure (h)
▪ HSP is likely continuously produced to counteract the protein damage
that results as the antioxidant system fails under toxin exposure.

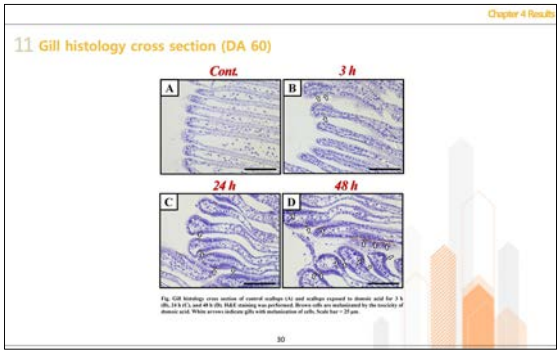
Chapter 4 Results
11 Gill histology cross section (DA 60)
Cont.
3 h
24 h
48 h
A
B
C
D

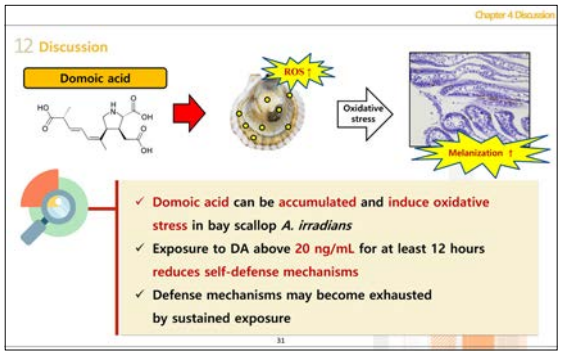
Chapter 4 Discussion
12 Discussion
Domoic acid
ROS ↑
Oxidative stress
Melanization ↑
✓ Domoic acid can be accumulated and induce oxidative stress in bay scallop A. irradians
✓ Exposure to DA above 20 ng/mL for at least 12 hours reduces self-defense mechanisms
✓ Defense mechanisms may become exhausted by sustained exposure
31

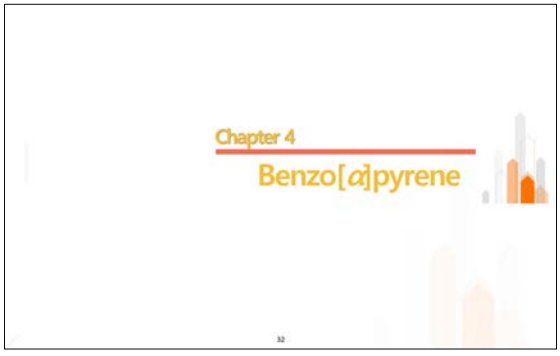
Chapter 4
Benzo[a]pyrene
32

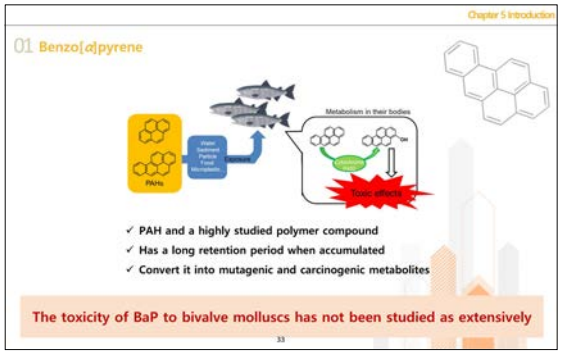
Chapter 5 Introduction
01 Benzo[a]pyrene
PAHs
Metabolism in their bodies
Toxic effects
✓ PAH and a highly studied polymer compound
✓ Has a long retention period when accumulated
✓ Convert it into mutagenic and carcinogenic metabolites
The toxicity of BaP to bivalve molluscs has not been studied as extensively
33

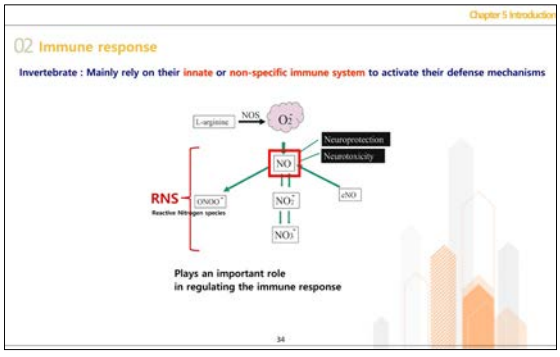
Chapter 5 Introduction
02 Immune response
Invertebrate : Mainly rely on their innate or non-specific immune system to activate their defense mechanisms
L-arginine
NOS
Neuroprotection
Neurotoxicity
RNS
Reactive Nitrogen species
Plays an important role
in regulating the immune response
34

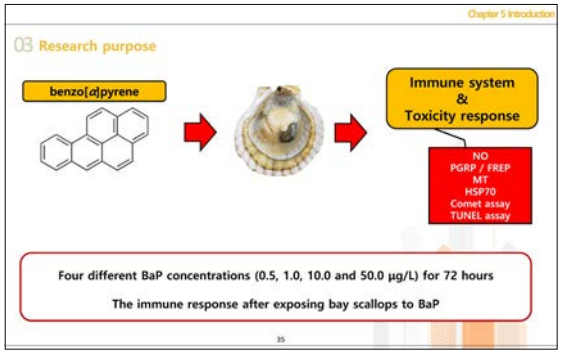
Chapter 5 Introduction
03 Research purpose
benzo[a]pyrene
Immune system
&
Toxicity response
NO
PGRP / FREP
MT
HSP70
Comet assay
TUNEL assay
Four different BaP concentrations (0.5, 1.0, 10.0 and 50.0 μg/L) for 72 hours
The immune response after exposing bay scallops to BaP
35

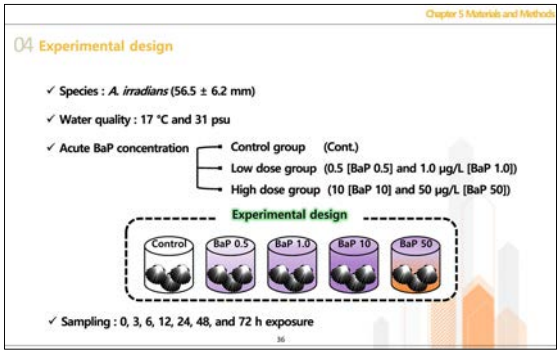
Chapter 5 Materials and Methods
04 Experimental design
✓ Species : A. irradians (56.5 ± 6.2 mm)
✓ Water quality : 17 °C and 31 psu
✓ Acute BaP concentration
Control group (Cont.)
Low dose group (0.5 [BaP 0.5] and 1.0 μg/L [BaP 1.0])
High dose group (10 [BaP 10] and 50 μg/L [BaP 50])
Experimental design
Control
BaP 0.5
BaP 1.0
BaP 10
BaP 50
✓ Sampling : 0, 3, 6, 12, 24, 48, and 72 h exposure
36

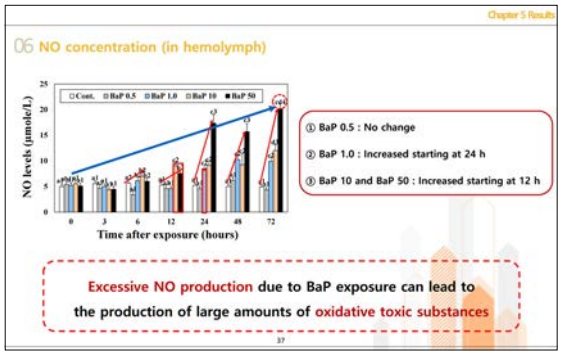
Chapter 5 Results
06 NO concentration (in hemolymph)
NO levels (μmole/L)
Time after exposure (hours)
① BaP 0.5 : No change
② BaP 1.0 : Increased starting at 24 h
③ BaP 10 and BaP 50 : Increased starting at 12 h
Excessive NO production due to BaP exposure can lead to
the production of large amounts of oxidative toxic substances

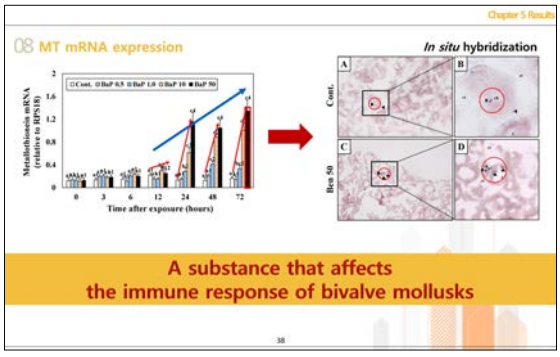
Chapter 5 Results
08 MT mRNA expression
In situ hybridization
Time after exposure (hours)
A substance that affects
the immune response of bivalve mollusks

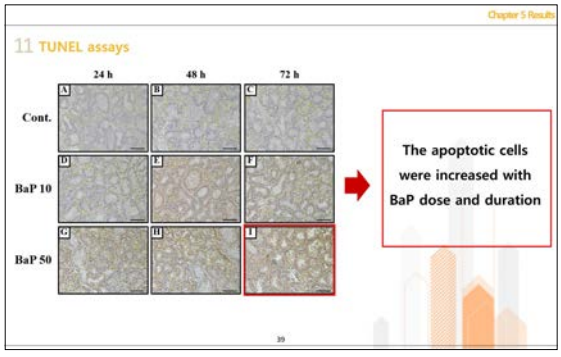
Chapter 5 Results
11 TUNEL assays
24 h
48 h
72 h
Cont.
BaP 10
BaP 50
The apoptotic cells
were increased with
BaP dose and duration

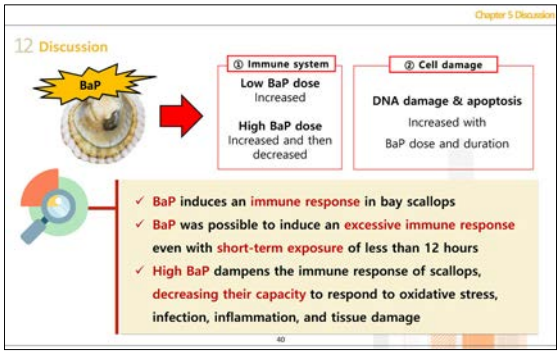
Chapter 5 Discussion
12 Discussion
BaP
① Immune system
Low BaP dose
Increased
High BaP dose
Increased and then
decreased
② Cell damage
DNA damage & apoptosis
Increased with
BaP dose and duration
✓ BaP induces an immune response in bay scallops
✓ BaP was possible to induce an excessive immune response
even with short-term exposure of less than 12 hours
✓ High BaP dampens the immune response of scallops,
decreasing their capacity to respond to oxidative stress,
infection, inflammation, and tissue damage

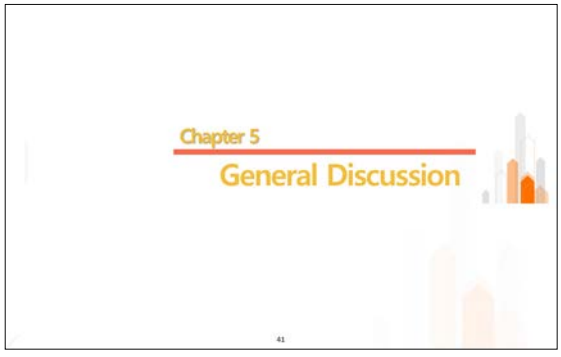
Chapter 5
General Discussion


Chapter 7 General Discussion
Environmental Stressors to bay scallops
Various features of bay scallops
✓ Are widely known around the world in aquaculturing
✓ Are commercially important species of shellfish
Main problem
Since shellfish do not have a wide range of movement like fish
Environmental factors have a direct or indirect effect on the physiological response
However! physiological studies on bay scallops
have not been actively conducted

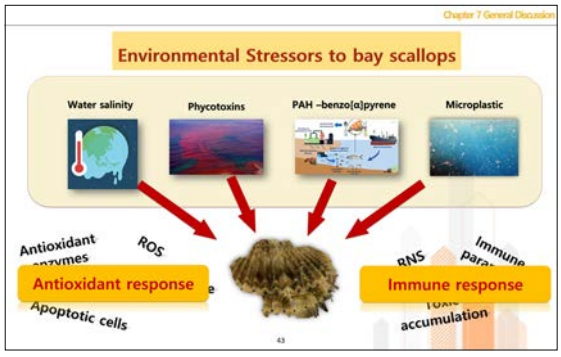
Chapter 7 General Discussion
Environmental Stressors to bay scallops
Water salinity
Phycotoxins
PAH –benzo(α)pyrene
Microplastic
Antioxidant
ROS
Antioxidant response
Apoptotic cells
RNS
Immune response
accumulation
43


Thanks for listening!
44

Dev. Reprod. Vol 26, 2022 (Suppl. 1). pp 81

Zebrafish as a model system to investigate human liver diseases

Azra Memon[1], Siyeo Lee[2], *Tae-Young Choi[1,2]

[1]Department of Pathology, Digestive Disease Research Institute, Wonkwang University School of Medicine

[2]Department of Biomedical Science, Graduate School, Wonkwang University

(azra1979@wku.ac.kr)

The zebrafish (*Danio rerio*) is becoming a useful vertebrate model organism in developmental biology. Zebrafish models are critical for advancing our understanding of human pathogenesis and are a popular model for liver diseases allowing researchers to identify therapeutic targets and test novel drugs. The larval transparency of the zebrafish is a great advantage for real-time imaging in hepatic studies.

Part I, Here we describe *epcam* mutants in zebrafish as a helpful model system to investigate Primary biliary cholangitis (PBC), formerly known as primary biliary cirrhosis. PBC is a disease that harms the liver's ability to function. In people with PBC, the bile ducts become injured, then inflamed, and eventually permanently damaged. our findings suggest that *epcam* positively regulates liver development and liver regeneration and plays a potential role in bile duct formation in regenerative response.

Part II. A large number of heritable and acquired diseases are related to the interruption of liver function. Zebrafish can be a valuable model system to investigate a rare inherited disorder Sjogren–Larsson syndrome (SLS). SLS is a rare autosomal recessive condition characterized by significant ichthyosis symptoms, mental retardation, and spasticity due to a defect of the fatty aldehyde dehydrogenase (FALDH), which is related to mutations in the Aldehyde Dehydrogenase 3 Family Member A2 (ALDH3A2) gene. FALDH, a key component of the detoxification pathway of aldehydes arising from lipid peroxidation and the enzymatic function of ALDH3A2 is well-known, but the disease model is necessary to investigate the molecular mechanisms of which fatty aldehyde or of which metabolic liver pathway mainly contributes to the pathogenesis of SLS ichthyosis symptoms.

Even though zebrafish have advanced our understanding of liver diseases as well as liver cancer and regeneration, the disease model is necessary to investigate the molecular mechanisms of inherited and acquired liver diseases as well as liver primary biliary cirrhosis.

Key words: zebrafish, liver diseases, EpCam, primary biliary cirrhosis (PBC), Sjogren-Larsson syndrome (SLS)

Dev. Reprod. Vol 26, 2022 (Suppl. 1). pp 82

Autophagic induction and dual functions of trehalose via PI3K/Akt and VPS34/mTOR pathways on porcine oocyte and cumulus cells

채련

충북대학교

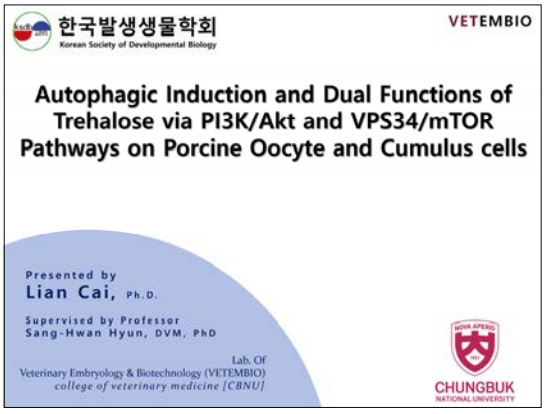

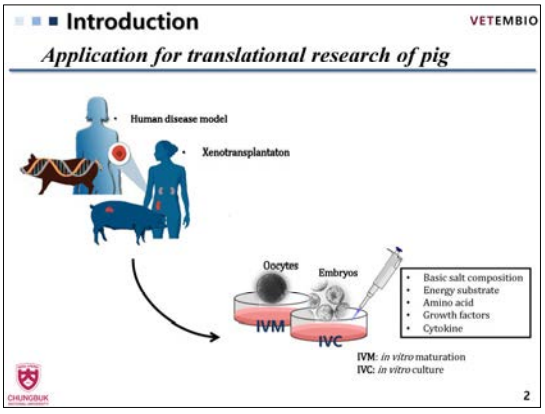

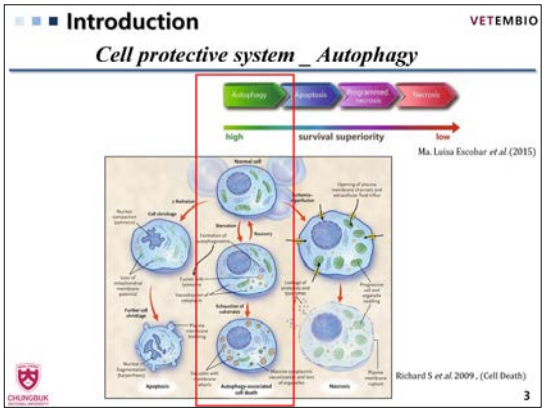

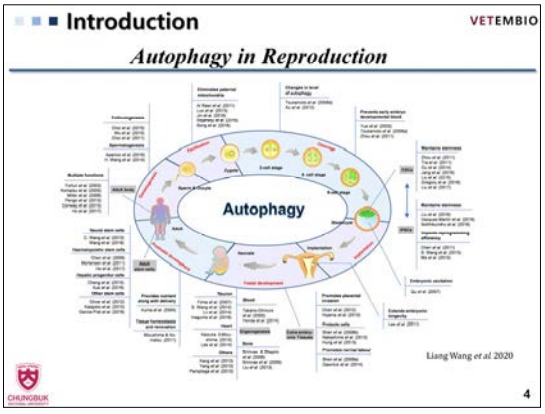

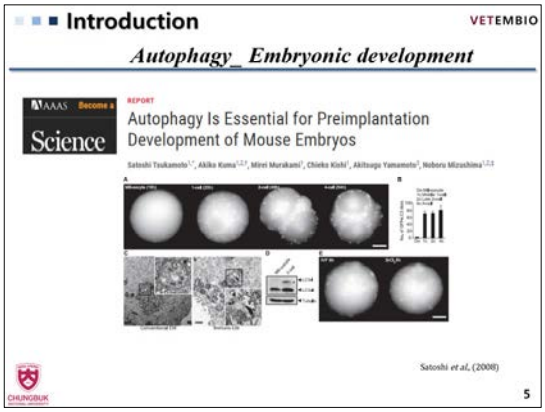

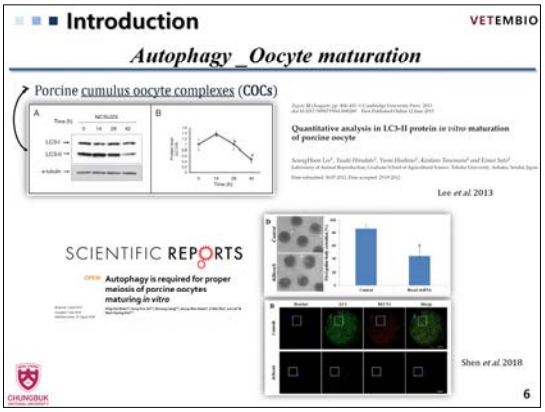

Introduction

VETEMBIO

Effects of autophagy activator in oocyte maturation

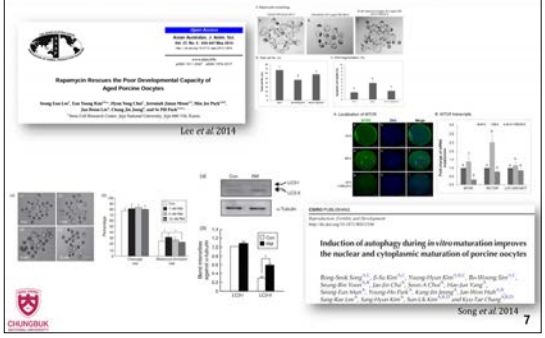

7

Introduction

VETEMBIO

Regulation of key cellular processes of mTOR

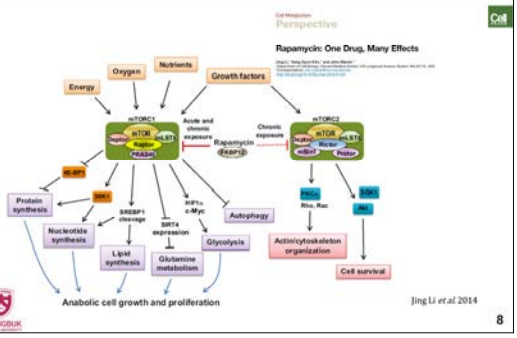

8

Introduction

What is Trehalose?

VETEMBIO

- Trehalose
  - ✓ A naturally occurring disaccharide present in a diverse range of organisms: plants, bacteria, yeast, and fungi.
  - ✓ Has been reported to have cytoprotective effects in response to various stress conditions : Oxidative damage, Dehydration, Temperature changes.
  - ✓ Is a novel autophagy activator in many cells, acting through an mTOR-independent pathway (Lee et. al., 2018).
  - ✓ Reduce apoptosis in an autophagy-dependent manner (Tang et. al., 2017).

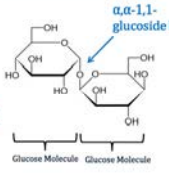

9

Introduction

Supplementation trehalose during IVM _ Porcine embronic development capacity

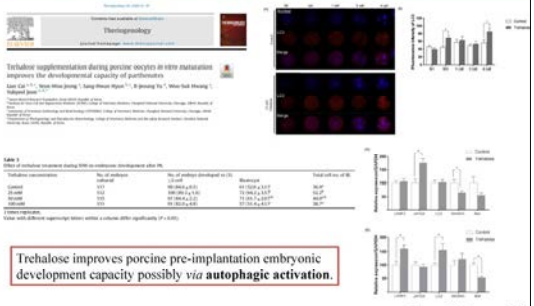

Trehalose improves porcine pre-implantation embryonic development capacity possibly *via* **autophagic activation**.

Cai et al. 2020

10

Introduction

Trehalose : Autophagic inducer? or blocker ?

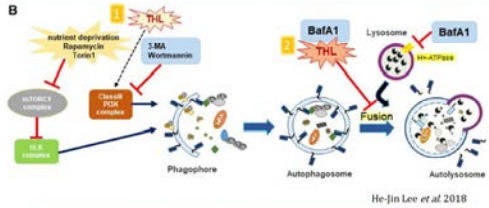

- **The role of trehalose (THL) on autophagy process was controversial**
  - 1) Induce autophagy *via* Class III PI3K (VPS34) complex activation
  - 2) Block autophagic flux similarly to BafA1

11

Introduction

VETEMBIO

Autophagic mechanism of trahalose _<1>

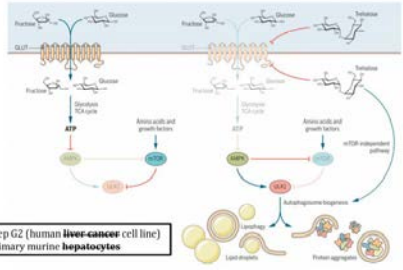

- Hep G2 (human ~~liver cancer~~ cell line)
- Primary murine ~~hepatocytes~~

Pablo Mardones et al. 2016

12

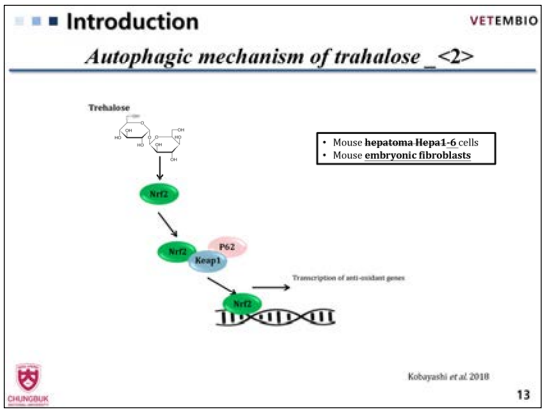
Introduction
VETEMBIO
Autophagic mechanism of trahalose _ <2>
Trehalose
Nrf2
Keap1
P62
Transcription of anti-oxidant genes
• Mouse hepatoma Hepa1-6 cells
• Mouse embryonic fibroblasts
Kobayashi et al. 2018
13

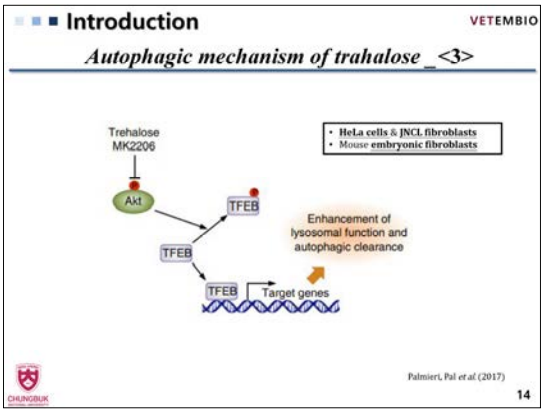
Introduction
VETEMBIO
Autophagic mechanism of trahalose _ <3>
Trehalose
MK2206
Akt
TFEB
Enhancement of lysosomal function and autophagic clearance
Target genes
• HeLa cells & JNCL fibroblasts
• Mouse embryonic fibroblasts
Palmieri, Pal et al. (2017)
14

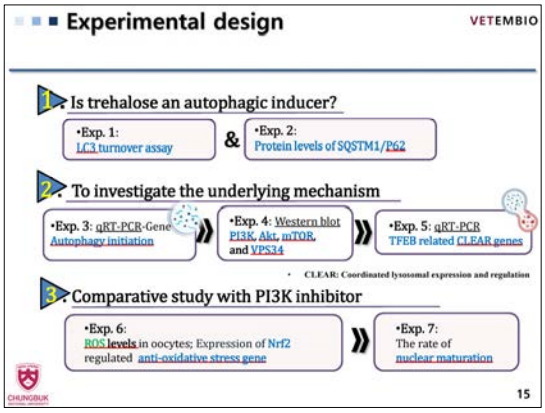
Experimental design
VETEMBIO
1. Is trehalose an autophagic inducer?
•Exp. 1: LC3 turnover assay
&
•Exp. 2: Protein levels of SQSTM1/P62
2. To investigate the underlying mechanism
•Exp. 3: qRT-PCR-Gene Autophagy initiation
•Exp. 4: Western blot PI3K, Akt, mTOR, and VPS34
•Exp. 5: qRT-PCR TFEB related CLEAR genes
• CLEAR: Coordinated lysosomal expression and regulation
3. Comparative study with PI3K inhibitor
•Exp. 6: ROS levels in oocytes; Expression of Nrf2 regulated anti-oxidative stress gene
•Exp. 7: The rate of nuclear maturation
15

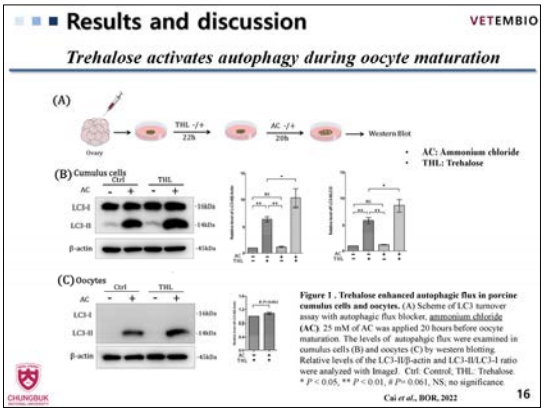
Results and discussion
VETEMBIO
Trehalose activates autophagy during oocyte maturation
(A)
Ovary
Western Blot
• AC: Ammonium chloride
• THL: Trehalose
(B) Cumulus cells
Ctrl
THL
AC
LC3-I
LC3-II
β-actin
(C) Oocytes
Figure 1 . Trehalose enhanced autophagic flux in porcine cumulus cells and oocytes. (A) Scheme of LC3 turnover assay with autophagic flux blocker, ammonium chloride (AC). 25 mM of AC was applied 20 hours before oocyte maturation. The levels of autophagic flux were examined in cumulus cells (B) and oocytes (C) by western blotting. Relative levels of the LC3-II/β-actin and LC3-II/LC3-I ratio were analyzed with ImageJ. Ctrl: Control; THL: Trehalose. * P < 0.05, ** P < 0.01, # P= 0.061, NS; no significance.
Cui et al., BOR, 2022
16

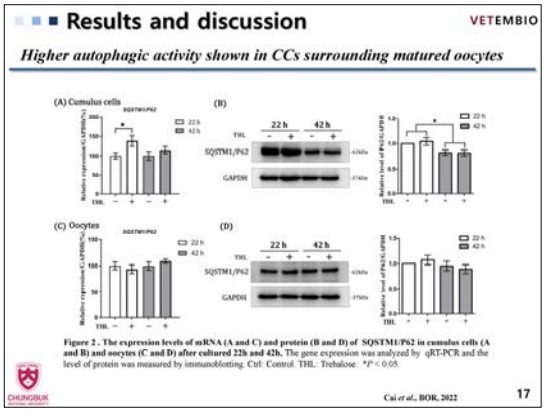
Results and discussion
VETEMBIO
Higher autophagic activity shown in CCs surrounding matured oocytes
(A) Cumulus cells
(B)
(C) Oocytes
(D)
22 h
42 h
THL
SQSTM1/P62
GAPDH
Figure 2 . The expression levels of mRNA (A and C) and protein (B and D) of SQSTM1/P62 in cumulus cells (A and B) and oocytes (C and D) after cultured 22h and 42h. The gene expression was analyzed by qRT-PCR and the level of protein was measured by immunoblotting. Ctrl: Control. THL: Trehalose. *P < 0.05.
Cui et al., BOR, 2022
17

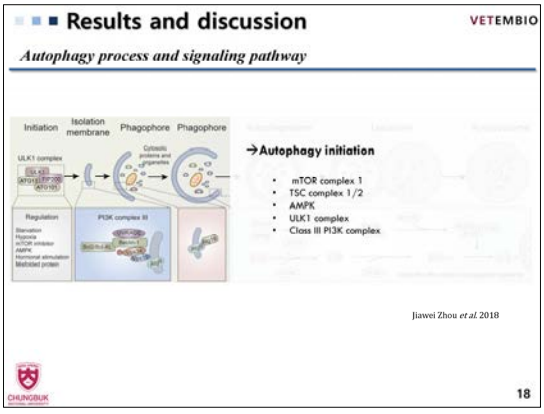
Results and discussion
VETEMBIO
Autophagy process and signaling pathway
Initiation
Isolation membrane
Phagophore
Phagophore
ULK1 complex
Regulation
PI3K complex III
→Autophagy initiation
• mTOR complex 1
• TSC complex 1/2
• AMPK
• ULK1 complex
• Class III PI3K complex
Jiawei Zhou et al. 2018
18

Results and discussion

VETEMBIO

Trehalose inhibites PI3K/Akt/mTOR pathway & activate VPS34 complex

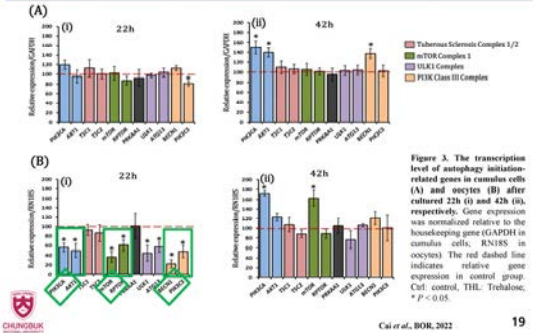

Figure 3. The transcription level of autophagy initiation-related genes in cumulus cells (A) and oocytes (B) after cultured 22h (i) and 42h (ii), respectively. Gene expression was normalized relative to the housekeeping gene (GAPDH in cumulus cells; RN18S in oocytes). The red dashed line indicates relative gene expression in control group. Ctrl: control, THL: Trehalose, * $P < 0.05$.

Cai *et al.*, BOR, 2022

Results and discussion

VETEMBIO

Trehalose inhibits PI3K/Akt/mTOR pathway in CCs

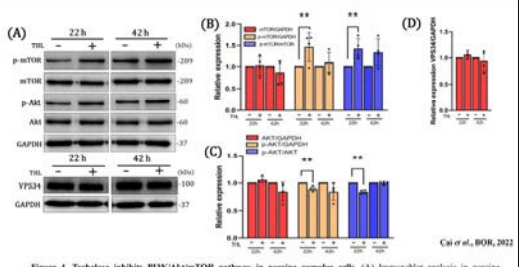

Figure 4. Trehalose inhibits PI3K/Akt/mTOR pathway in porcine cumulus cells. (A) Immunoblot analysis in porcine cumulus cells with or without 25mM trehalose after the COCs were cultured 22h and 42h, respectively. (B-D) Quantification of the levels of mTOR and phospho-mTOR (B), Akt and phospho-Akt (C), and VPS34 (D) with imagJ. GAPDH was used as loading control for immunoblot. THL: Trehalose * $P < 0.05$, ** $P < 0.01$. Data represent means ± SEM.

Cai *et al.*, BOR, 2022

Results and discussion

VETEMBIO

Trehalose inhibits PI3K/Akt/mTOR pathway & activates VPS34 complex in oocytes

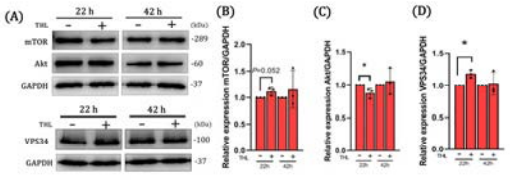

Figure 5. Trehalose inhibits PI3K/Akt/mTOR pathway and activates VPS34 complex in porcine oocytes. (A) Immunoblot analysis in porcine oocytes with or without 25mM trehalose after the COCs were cultured 22h and 42h, respectively. (B-D) Quantification of the levels of mTOR (B), Akt (C), and VPS34 (D) with imagJ. GAPDH was used as loading control for immunoblot. THL: Trehalose * $P < 0.05$, Data represent means ± SEM.

Cai *et al.*, BOR, 2022

Results and discussion

VETEMBIO

TFEB mediated lysosomal function and autophagic clearance genes

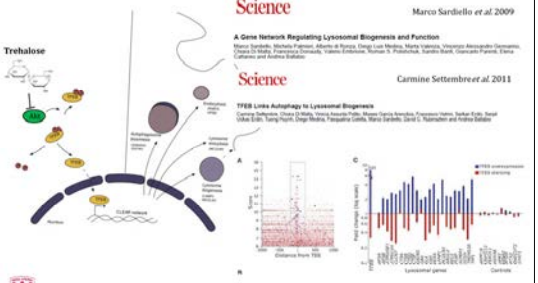

Results and discussion

VETEMBIO

Trehalose upregulates the levels of CLEAR genes specifically in porcine CCs

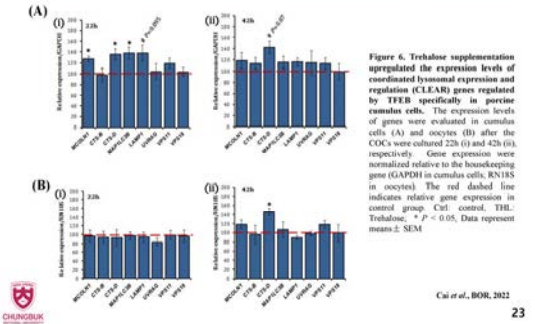

Figure 6. Trehalose supplementation upregulated the expression levels of coordinated lysosomal expression and regulation (CLEAR) genes regulated by TFEB specifically in porcine cumulus cells. The expression levels of genes were evaluated in cumulus cells (A) and oocytes (B) after the COCs were cultured 22h (i) and 42h (ii), respectively. Gene expression were normalized relative to the housekeeping gene (GAPDH in cumulus cells; RN18S in oocytes). The red dashed line indicates relative gene expression in control group. Ctrl: control, THL: Trehalose, * $P < 0.05$, Data represent means ± SEM

Cai *et al.*, BOR, 2022

Results and discussion

VETEMBIO

Phospho-Akt related to meiotic division in porcine oocytes

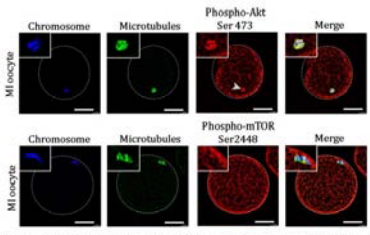

Figure 7. Immunolocalization of phospho-Akt Ser 473 and phospho-mTOR Ser 2448 in porcine metaphase I (MI) stage oocytes. The fluorescence imaging of phospho-Akt (red), phospho-mTOR (red), microtubule (green), and chromosome (blue) were detected by confocal microscopy. Arrows indicate the distribution of phospho-Akt Ser 473 in oocyte spindle. Scale bar = 50μm.

Cai *et al.*, BOR, 2022

Results and discussion

VETEMBIO

Trehalose has a synergistic effect with PI3K inhibitor (Wortmannin)

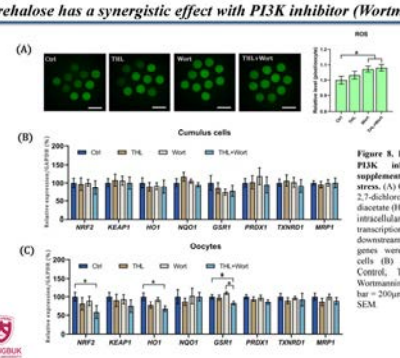

Figure 8. Effects of trehalose and PI3K inhibitor (Wortmannin) supplementation on the oxidative stress. (A) Oocytes were stained with 2,7-dichlorodihydrofluorescein diacetate (H2DCFH-DA) to detect the intracellular levels of ROS. mRNA transcriptional levels of *Nrf2* and its downstream oxidative stress related genes were evaluated in cumulus cells (B) and oocytes (C). Ctrl: Control, THL: Trehalose, Wort: Wortmannin (10nM). $P < 0.05$. Scale bar = 200μm, Data represent means ± SEM.

Cai *et al.*, BOR, 2022

CHUNGBUK

25

Results and discussion

VETEMBIO

Trehalose not has exactly the same effect with PI3K inhibitor (wortmannin)

Table 1. Effect of trehalose and wortmannin supplementation on nuclear maturation of porcine oocytes

Group	No. oocytes cultured for maturation (3)*	No. (%) of oocytes at the stage of			
		Germinal vesicle (%)	Metaphase I (%)	Anaphase I and Telophase I (%)	Metaphase II (%)
Control	139	0 (0.0 ± 0.0)	15 (10.8 ± 3.0)[a]	4 (2.9 ± 2.2)	120 (86.3 ± 2.0)[b]
THL	148	0 (0.0 ± 0.0)	15 (10.1 ± 0.9)[a]	7 (4.7 ± 1.9)	126 (85.1 ± 1.1)[b]
Wort	143	1 (0.7 ± 0.7)	26 (18.2 ± 3.8)[ab]	19 (13.3 ± 8.7)	97 (67.8 ± 5.7)[a]
Wort+THL	135	0 (0.0 ± 0.0)	32 (23.7 ± 4.2)[b]	17 (12.6 ± 3.1)	86 (63.7 ± 4.8)[a]

a and b: Values with different superscripts within the same column differ significantly ($P < 0.05$).
Wort: Wortmannin (10 nM), THL: Trehalose
* Replication number.
The data are mean ± SEM.

Cai *et al.*, BOR, 2022

CHUNGBUK

26

Summary

VETEMBIO

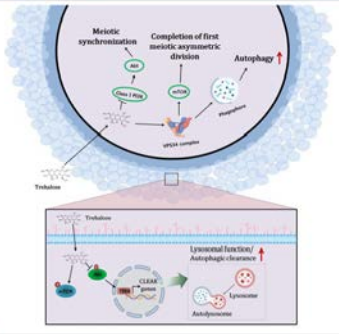

Figure 9. Schematic diagram for trehalose underlying mechanism in cumulus oocyte complexes (COCs). Trehalose inhibits PI3K/Akt/mTOR pathway both in cumulus cells and oocytes, whereas playing different roles, respectively. Meiotic synchronization was induced in oocytes, and the lysosomal function/ autophagic clearance was improved in cumulus cells. In oocytes, the autophagic initiation was induced *via* VPS34 complex activation. Trehalose dose not influence AMPK-dependent or Nrf2-dependent pathway in cumulus cells and oocytes.

Cai *et al.*, BOR, 2022

CHUNGBUK

27

Acknowledgement

Supervisor
Prof. Sang-Hwan Hyun

Colleagues
Prof. Yubyeol Jeon
Prof. Eunhye Kim
Joohyeong Lee, Ph.D.
Junchul David Yoon, Ph.D.
Seonung Hwang, Ph.D.
Mirae Kim, Ph.D.
Gahye Kim
Hyerin Choi
Dongjin Oh
Suin Lee
Jawad Ali
Jiyoung Jeong
Sohee Kim
Haomiao Zheng

CHUNGBUK

VETEMBIO

심포지엄 Ⅳ

Dev. Reprod. Vol 26, 2022 (Suppl. 1). pp 89

Metabolic restructuring and cell fate conversion through controlling cellular organelles

이만렬

순천향대학교

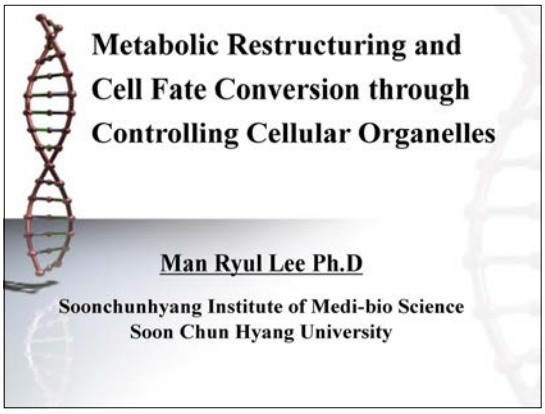

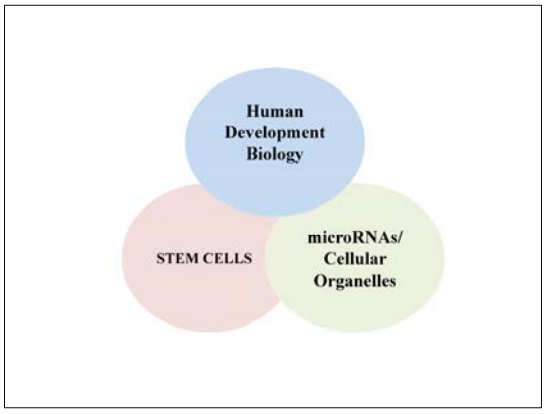

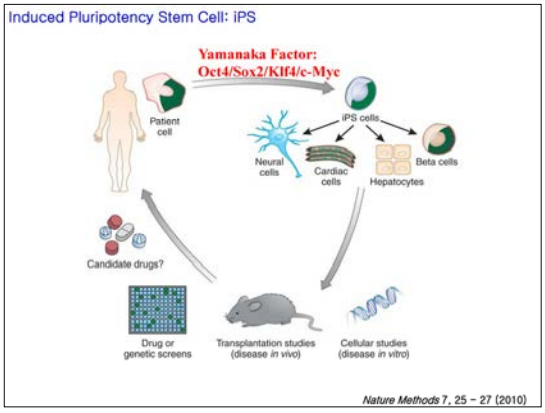

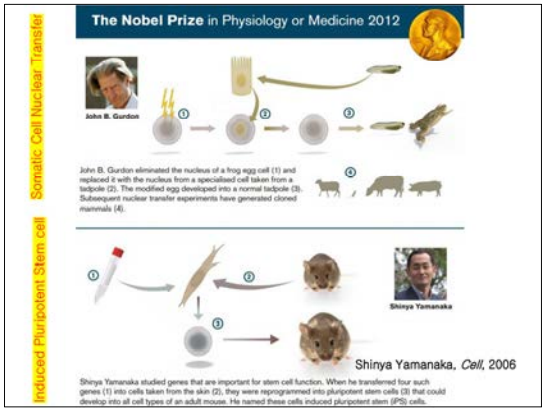

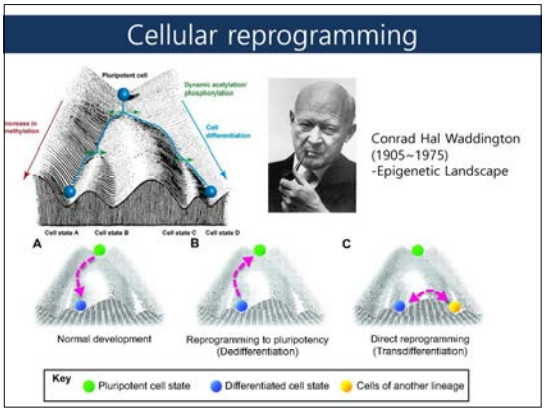

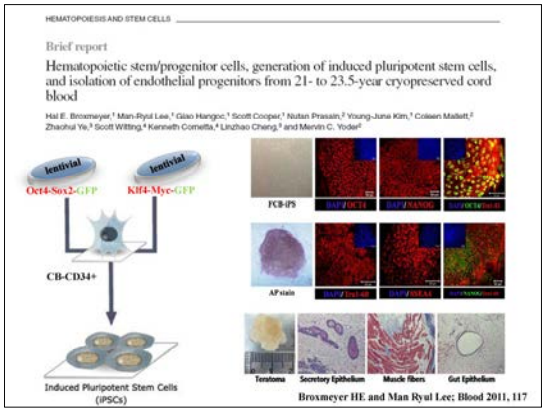

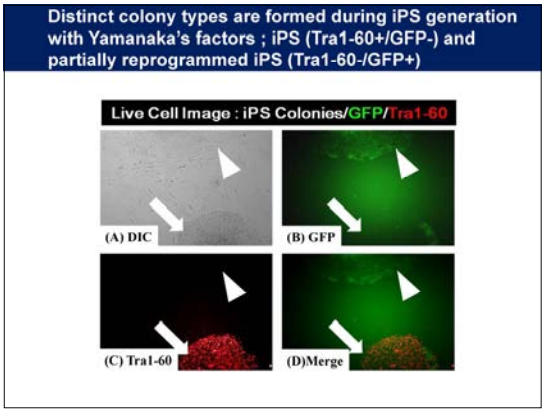
Distinct colony types are formed during iPS generation with Yamanaka's factors ; iPS (Tra1-60+/GFP-) and partially reprogrammed iPS (Tra1-60-/GFP+)
Live Cell Image : iPS Colonies/GFP/Tra1-60
(A) DIC
(B) GFP
(C) Tra1-60
(D)Merge

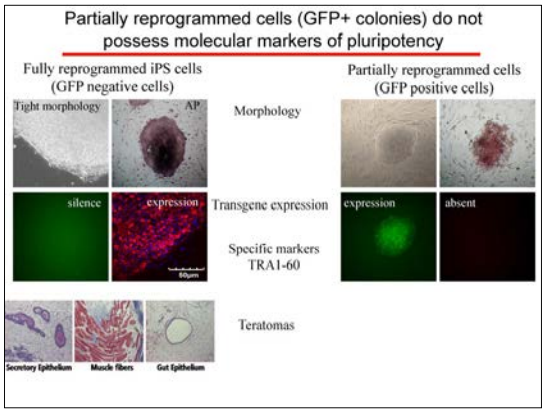
Partially reprogrammed cells (GFP+ colonies) do not possess molecular markers of pluripotency
Fully reprogrammed iPS cells (GFP negative cells)
Partially reprogrammed cells (GFP positive cells)
Tight morphology
AP
Morphology
silence
expression
Transgene expression
expression
absent
Specific markers TRA1-60
Teratomas
Secretory Epithelium
Muscle fibers
Gut Epithelium

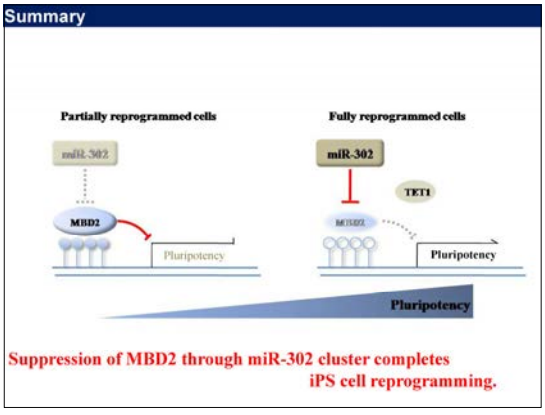
Summary
Partially reprogrammed cells
Fully reprogrammed cells
miR-302
MBD2
TET1
Pluripotency
Pluripotency
Suppression of MBD2 through miR-302 cluster completes iPS cell reprogramming.

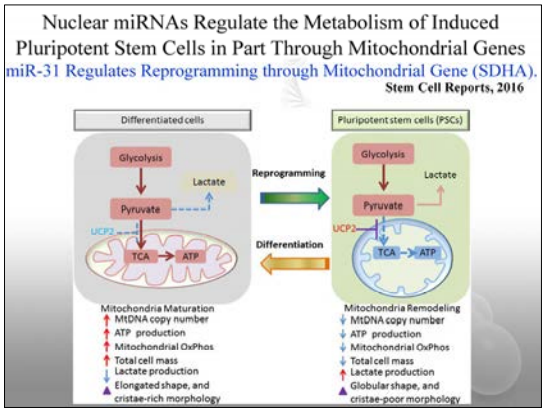
Nuclear miRNAs Regulate the Metabolism of Induced Pluripotent Stem Cells in Part Through Mitochondrial Genes
miR-31 Regulates Reprogramming through Mitochondrial Gene (SDHA).
Stem Cell Reports, 2016
Differentiated cells
Pluripotent stem cells (PSCs)
Glycolysis
Lactate
Pyruvate
UCP2
TCA
ATP
Reprogramming
Differentiation
Mitochondria Maturation
MtDNA copy number
ATP production
Mitochondrial OxPhos
Total cell mass
Lactate production
Elongated shape, and cristae-rich morphology
Mitochondria Remodeling
MtDNA copy number
ATP production
Mitochondrial OxPhos
Total cell mass
Lactate production
Globular shape, and cristae-poor morphology

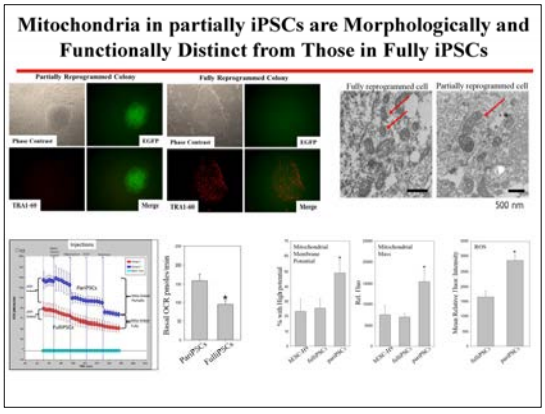
Mitochondria in partially iPSCs are Morphologically and Functionally Distinct from Those in Fully iPSCs
Partially Reprogrammed Colony
Fully Reprogrammed Colony
Phase Contrast
EGFP
TRA1-60
Merge
Fully reprogrammed cell
Partially reprogrammed cell
500 nm

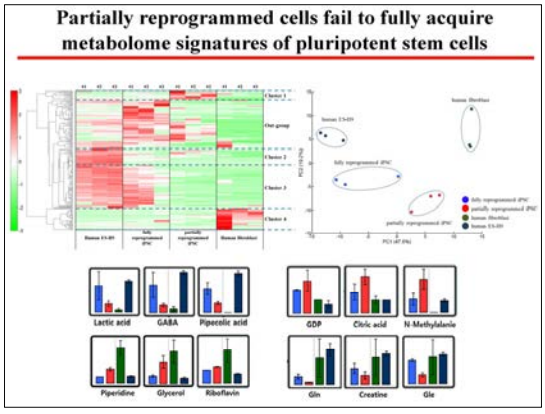
Partially reprogrammed cells fail to fully acquire metabolome signatures of pluripotent stem cells
Lactic acid
GABA
Pipecolic acid
GDP
Citric acid
N-Methylalanie
Piperidine
Glycerol
Riboflavin
Gln
Creatine
Gle

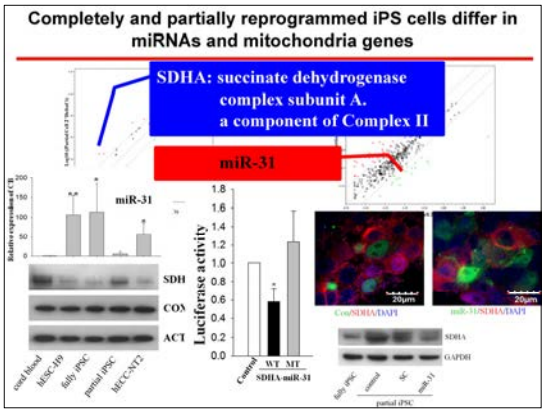
Completely and partially reprogrammed iPS cells differ in miRNAs and mitochondria genes
SDHA: succinate dehydrogenase complex subunit A. a component of Complex II
miR-31
Luciferase activity
SDH
COX
ACT
SDHA
GAPDH

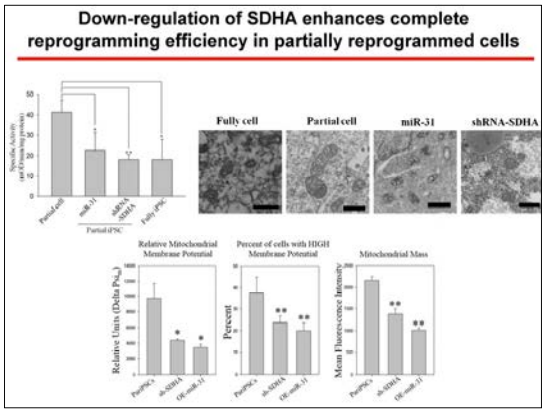
Down-regulation of SDHA enhances complete reprogramming efficiency in partially reprogrammed cells
Fully cell
Partial cell
miR-31
shRNA-SDHA
Relative Mitochondrial Membrane Potential
Percent of cells with HIGH Membrane Potential
Mitochondrial Mass
Percent

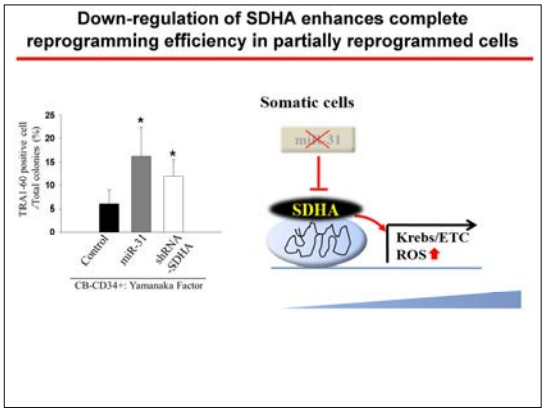
Down-regulation of SDHA enhances complete reprogramming efficiency in partially reprogrammed cells
TRA1-60 positive cell /Total colonies (%)
Control
miR-31
shRNA -SDHA
CB-CD34+: Yamanaka Factor
Somatic cells
miR-31
SDHA
Krebs/ETC
ROS

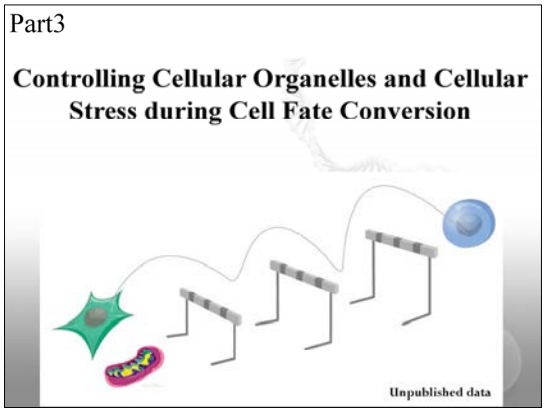
Part3
Controlling Cellular Organelles and Cellular Stress during Cell Fate Conversion
Unpublished data

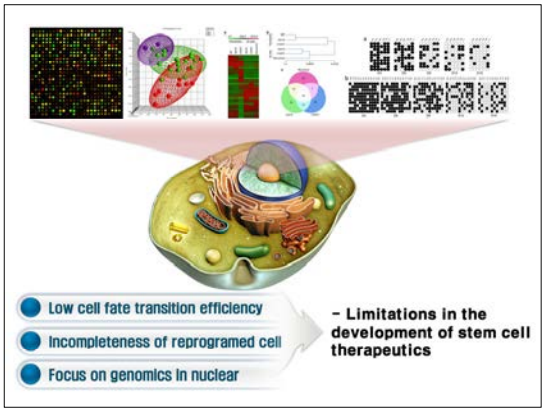
Low cell fate transition efficiency
Incompleteness of reprogramed cell
Focus on genomics in nuclear
- Limitations in the development of stem cell therapeutics

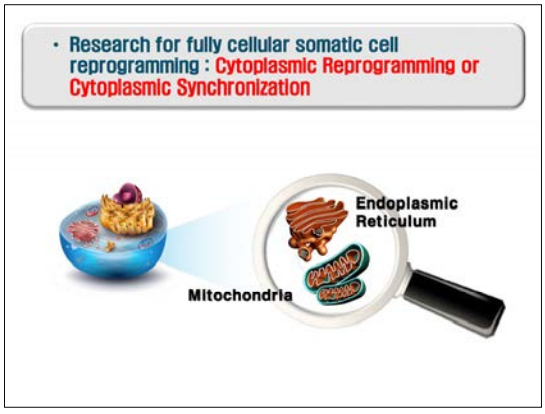
· Research for fully cellular somatic cell reprogramming : Cytoplasmic Reprogramming or Cytoplasmic Synchronization
Endoplasmic Reticulum
Mitochondria

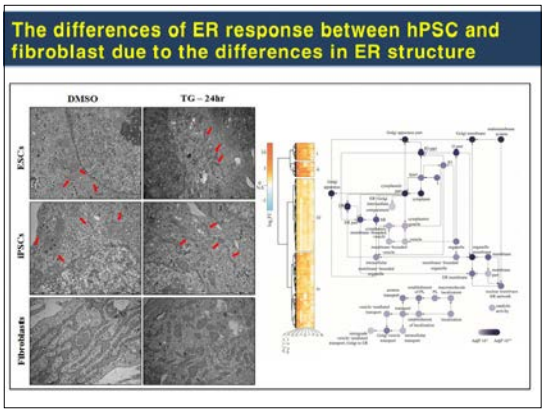
The differences of ER response between hPSC and fibroblast due to the differences in ER structure
DMSO
TG – 24hr
ESCs
iPSCs
Fibroblasts

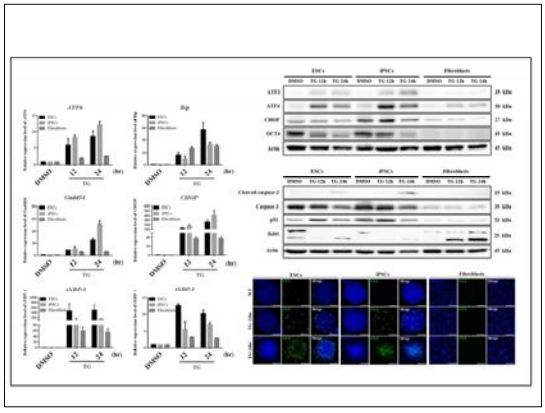

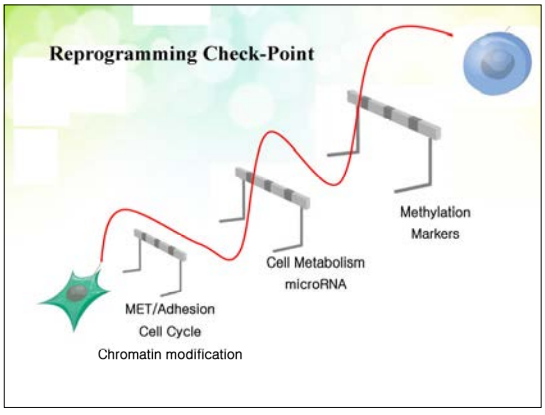
Reprogramming Check-Point
Methylation Markers
Cell Metabolism microRNA
MET/Adhesion
Cell Cycle
Chromatin modification


Acknowledgments & Introduction of Collaborators
Hal E. Broxmeyer, Ph.D. IUSM
Charlie Mantel, Scott Cooper,
Mervin Yoder, MD. IUSM
Nutan Prasain, Ph.D
Jaeseok Han, Ph.D. SIMS
STEMOPIA Lab.
Jae Hyen Kwon, Yena Song, Hyun Kyu Kim
Dr. Jae Sang Oh

Dev. Reprod. Vol 26, 2022 (Suppl. 1). pp 93

Lineage recording and tracing: single-cell technology unravels epigenetic regulation of cell fate decisions

김익수

가천대학교

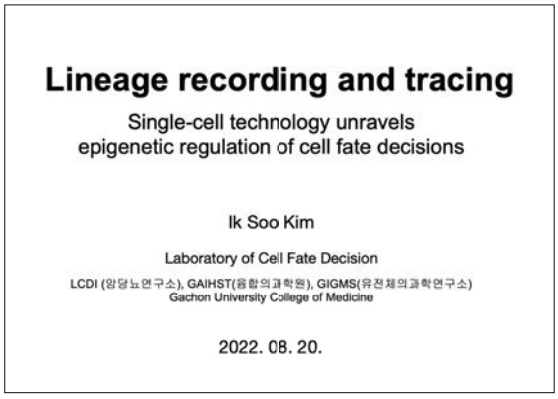

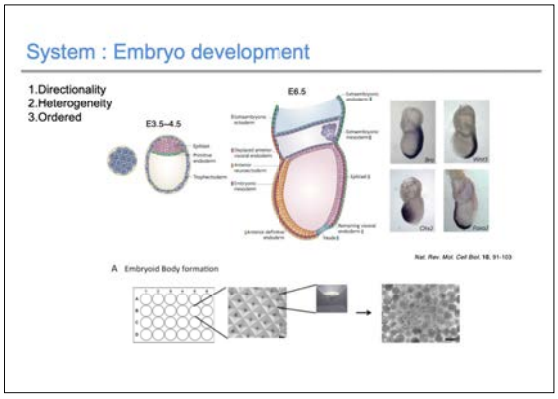

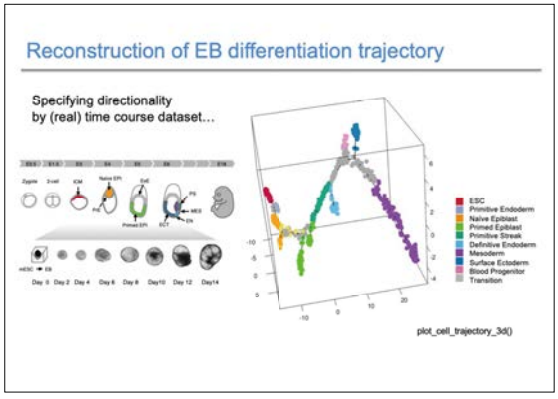

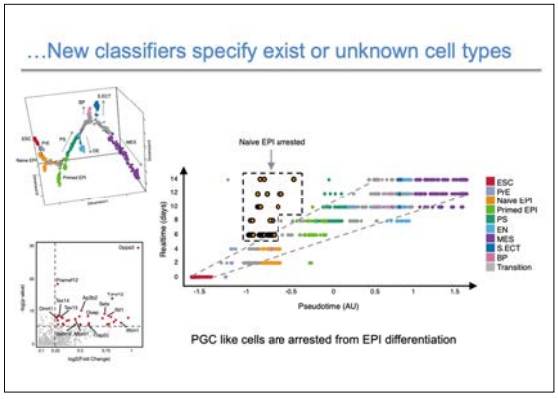

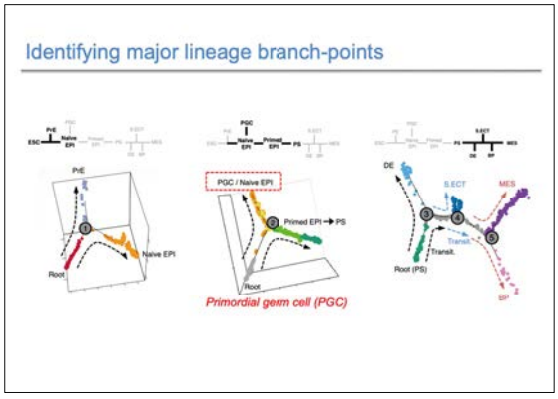

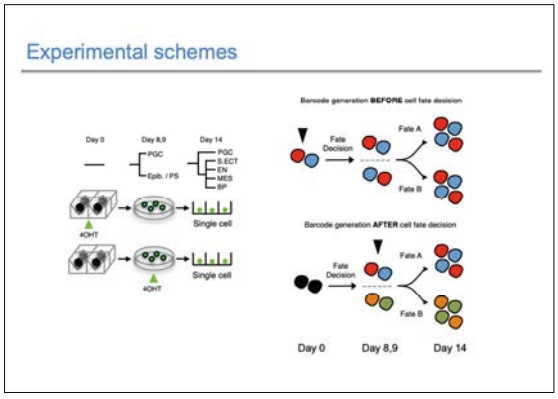

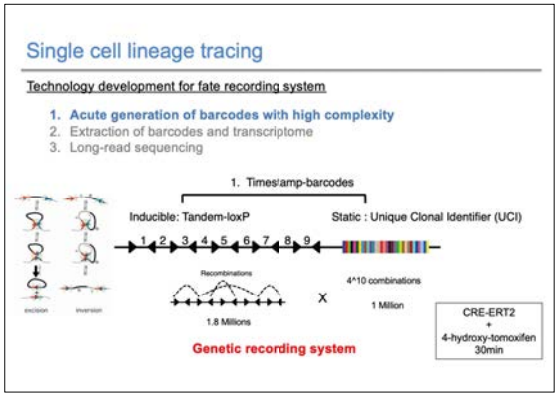
Single cell lineage tracing
Technology development for fate recording system
1. Acute generation of barcodes with high complexity
2. Extraction of barcodes and transcriptome
3. Long-read sequencing
1. Times/amp-barcodes
Inducible: Tandem-loxP
Static : Unique Clonal Identifier (UCI)
Recombinations
1.8 Millions
4^10 combinations
1 Million
CRE-ERT2
+
4-hydroxy-tomoxifen
30min
Genetic recording system

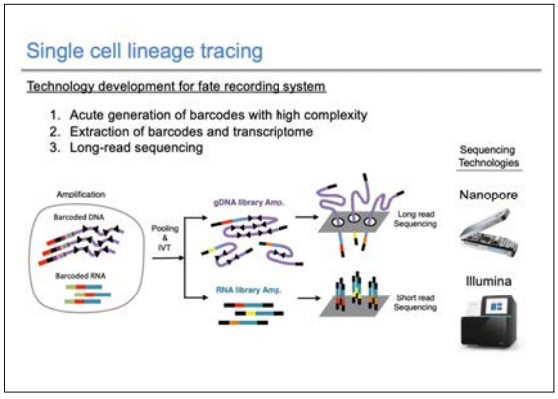
Single cell lineage tracing
Technology development for fate recording system
1. Acute generation of barcodes with high complexity
2. Extraction of barcodes and transcriptome
3. Long-read sequencing
Sequencing Technologies
Nanopore
Illumina
Amplification
Barcoded DNA
Barcoded RNA
Pooling & IVT
gDNA library Amp.
RNA library Amp.
Long read Sequencing
Short read Sequencing

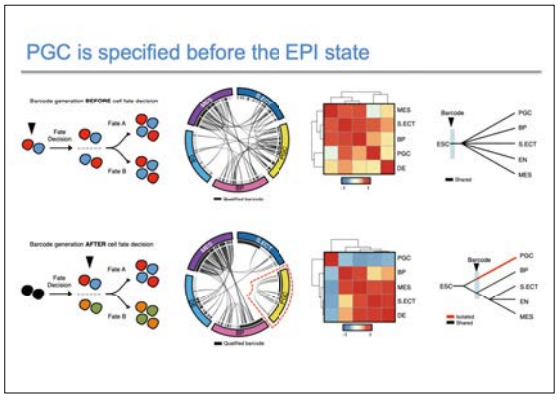
PGC is specified before the EPI state

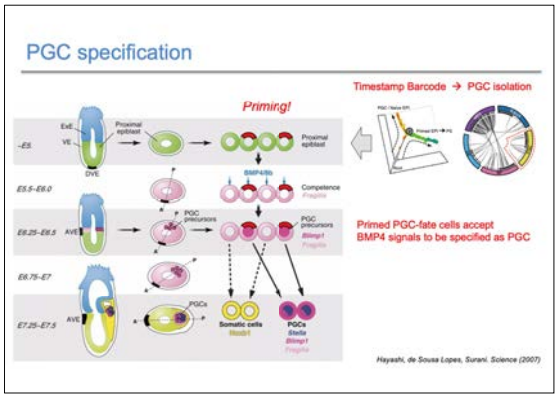
PGC specification
Timestamp Barcode → PGC isolation
Priming!
Primed PGC-fate cells accept BMP4 signals to be specified as PGC
Hayashi, de Sousa Lopes, Surani. Science (2007)


Acknowledgements
Lab of Cell Fate Decision
LCDI (Lee Gil Ya Cancer and Diabetes Institute)
GAIHST (Gachon Advanced Institute for Health Sciences & Technology)
Department of Microbiology, Gachon University College of Medicine
Jung, Jiyeong, Post.Doc.
Lee, Goeun, Research scientist
Lee, Yunjae, Undergraduate, Intern
Harvard Medical School,
Broad Institute of Harvard and MIT
Brad Bernstein Lab Epigenomics group
Funding sources :
Samsung Science and Technology Foundation
General Research Program
Bio & Medical Technology Development Program
Medical Research Center (CidMRC)

Dev. Reprod. Vol 26, 2022 (Suppl. 1). pp 95

Effect of nanoplastics on the behavioral and nutritional characteristics of aquatic organisms

채유은

안전성평가연구소 생태위해성평가센터

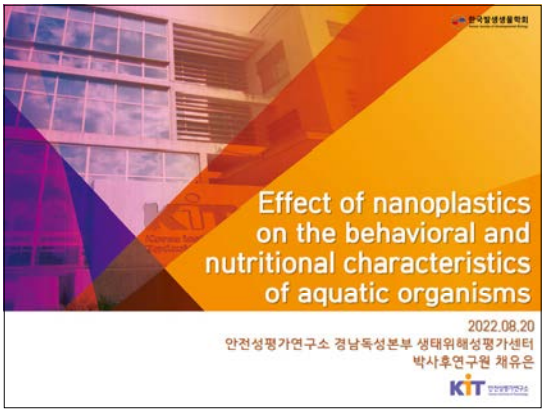

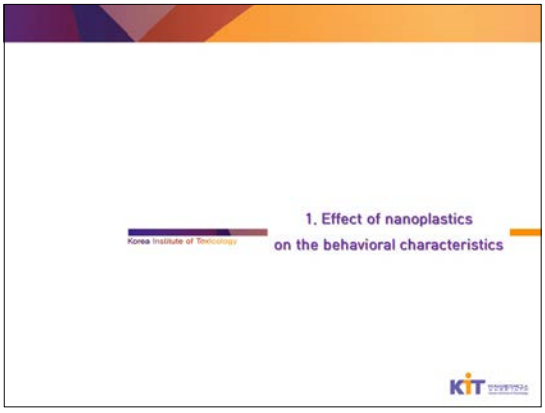

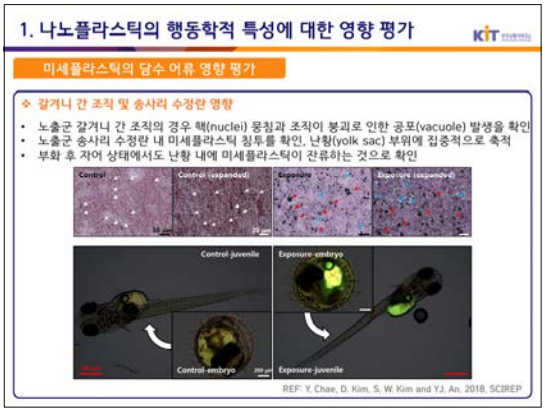

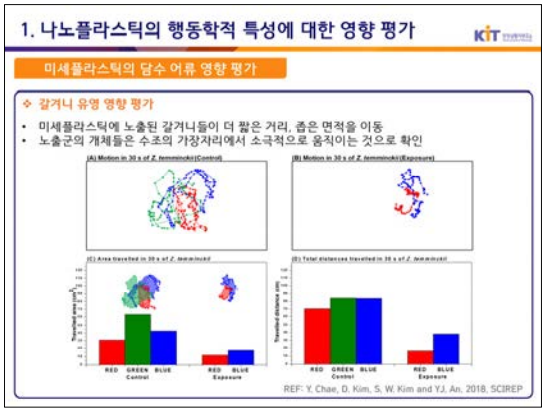

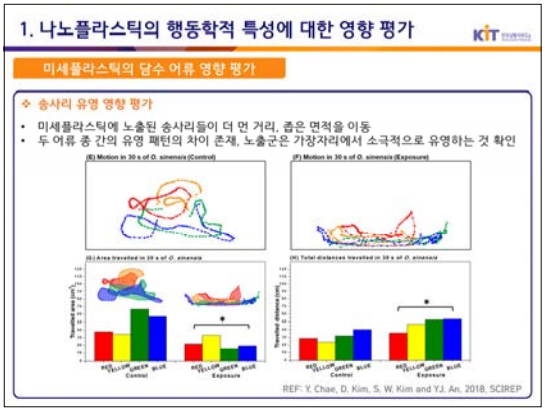
1. 나노플라스틱의 행동학적 특성에 대한 영향 평가
미세플라스틱의 담수 어류 영향 평가
❖ 송사리 유영 영향 평가
• 미세플라스틱에 노출된 송사리들이 더 먼 거리, 좁은 면적을 이동
• 두 어류 종 간의 유영 패턴의 차이 존재, 노출군은 가장자리에서 소극적으로 유영하는 것 확인
REF: Y. Chae, D. Kim, S. W. Kim and Y.J. An, 2018, SCIREP

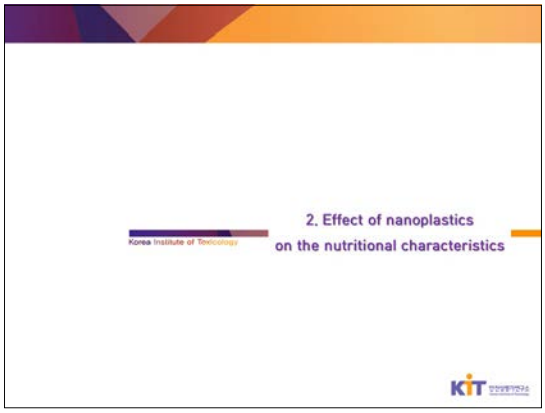
2. Effect of nanoplastics
on the nutritional characteristics
Korea Institute of Toxicology


2. 나노플라스틱의 영양학적 특성에 대한 영향 평가
미세플라스틱의 해양 생물 영향 평가
시험종 | 시험물질 | 노출 매체 | 노출 기간 | 측정 항목(정성) | 측정 항목(정량)
Mytilus galloprovincialis (지중해담치) → Litopenaeus vannamei (흰다리새우)
폴리스티렌 MP (44 nm) | 인공해수 | 21일 | 담치 내 미세플라스틱 흡착, 새우 내 미세플라스틱 전이 | 새우의 신체적 영향, 생화학적 영향, 영양학적 영향
1. 지중해담치를 미세플라스틱에 1시간 노출
2. 미세플라스틱에 노출된 지중해담치를 흰다리새우에게 21일간 먹이로 배급(먹이노출),
먹이노출 후 흰다리새우의 신체적, 생화학적, 영양학적 영향을 평가함
1
2
21 days feeding
신체적 영향 | • 총장, 총 습중량, 신체 질량 지수, 가식부 습중량, 가식부 건중량, 가식부 수분 함량
생화학적 영향 | • 장 내 미생물 활성, 글루타티온 S-전달효소(GST) 활성, 초과산화물 불균등화효소(SOD) 활성
영양학적 영향 | • 가식부의 조단백, 조지방, 20개 필수 아미노산, 37개 지방산
REF: Y. Chae, D. Kim, M.J. Choi, Y. Cho and Y.J. An, 2019, ENVINT


2. 나노플라스틱의 영양학적 특성에 대한 영향 평가
미세플라스틱의 해양 생물 영향 평가
시험종 | 시험물질 | 노출 매체 | 노출 기간 | 측정 항목(정성) | 측정 항목(정량)
Mytilus galloprovincialis (지중해담치) → Litopenaeus vannamei (흰다리새우)
폴리스티렌 MP (44 nm) | 인공해수 | 21일 | 담치 내 미세플라스틱 흡착, 새우 내 미세플라스틱 전이 | 새우의 신체적 영향, 생화학적 영향, 영양학적 영향
- 실험실 내 모의생태계 조성
- 흰다리새우를 이용한 나노플라스틱의 아만성(21d) 영향 평가
- 나노플라스틱이 흰다리새우의 신체적, 생화학적, 영양학적 특성에 영향을 미치는 것을 확인
REF: Y. Chae, D. Kim, M.J. Choi, Y. Cho and Y.J. An, 2019, ENVINT


2. 나노플라스틱의 영양학적 특성에 대한 영향 평가
미세플라스틱의 해양 생물 영향 평가
❖ 담치 내 미세플라스틱 축적
• 담치를 미세플라스틱에 한 시간 동안 노출하여 이를 먹이 노출에 사용
- 미세플라스틱에 노출된 담치를 현미경으로 관찰한 결과, 미세플라스틱이 담치의 연조직 내 기관, 특히 아가미(gill)에 다량 부착된 것을 확인
- 미세플라스틱이 먹이(담치)를 통해 상위 영양단계 생물 종인 새우에 먹이 노출
• 한 시간의 노출 이후 치사에 이른 담치는 발생하지 않았음
gill
intestine
rectum
stomach
foot retractor muscle
byssal retractor muscle
anus
labial palp
mantle
anterior adductor muscle
foot
posterior adductor muscle
byssal threads
Control
Exposure
REF: Y. Chae, D. Kim, M.J. Choi, Y. Cho and Y.J. An, 2019, ENVINT

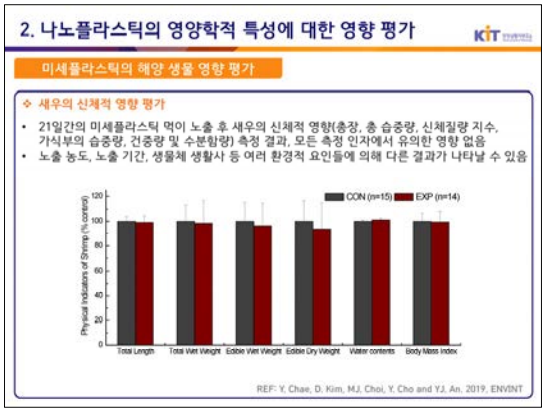
2. 나노플라스틱의 영양학적 특성에 대한 영향 평가
미세플라스틱의 해양 생물 영향 평가
❖ 새우의 신체적 영향 평가
• 21일간의 미세플라스틱 먹이 노출 후 새우의 신체적 영향(총장, 총 습중량, 신체질량 지수, 가식부의 습중량, 건중량 및 수분함량) 측정 결과, 모든 측정 인자에서 유의한 영향 없음
• 노출 농도, 노출 기간, 생물체 생활사 등 여러 환경적 요인들에 의해 다른 결과가 나타날 수 있음
CON (n=15)
EXP (n=14)
Physical indicators of Shrimp (% control)
Total Length
Total Wet Weight
Edible Wet Weight
Edible Dry Weight
Water contents
Body Mass Index
REF: Y. Chae, D. Kim, M.J. Choi, Y. Cho and Y.J. An, 2019, ENVINT

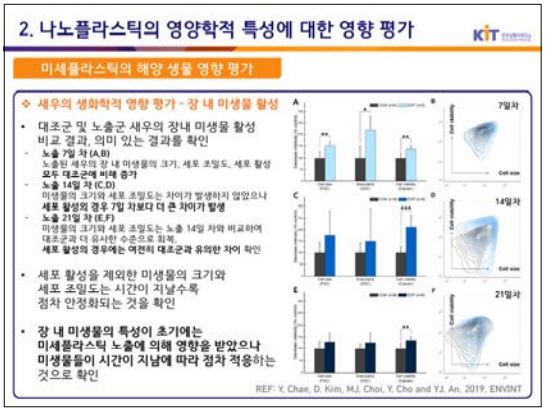
2. 나노플라스틱의 영양학적 특성에 대한 영향 평가
KIT
미세플라스틱의 해양 생물 영향 평가
❖ 새우의 생화학적 영향 평가 - 장 내 미생물 활성
• 대조군 및 노출군 새우의 장내 미생물 활성 비교 결과, 의미 있는 결과를 확인
- 노출 7일 차 (A,B)
노출된 새우의 장 내 미생물의 크기, 세포 조밀도, 세포 활성 모두 대조군에 비해 증가
- 노출 14일 차 (C,D)
미생물의 크기와 세포 조밀도는 차이가 발생하지 않았으나 세포 활성의 경우 7일 차보다 더 큰 차이가 발생
- 노출 21일 차 (E,F)
미생물의 크기와 세포 조밀도는 노출 14일 차와 비교하여 대조군과 더 유사한 수준으로 회복,
세포 활성의 경우에는 여전히 대조군과 유의한 차이 확인
• 세포 활성을 제외한 미생물의 크기와 세포 조밀도는 시간이 지날수록 점차 안정화되는 것을 확인
• 장 내 미생물의 특성이 초기에는 미세플라스틱 노출에 의해 영향을 받았으나 미생물들이 시간이 지남에 따라 점차 적응하는 것으로 확인
7일차
14일차
21일차
REF: Y. Chae, D. Kim, M.J. Choi, Y. Cho and Y.J. An. 2019. ENVINT

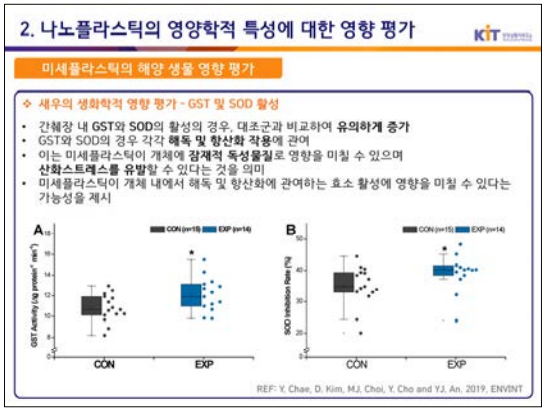
2. 나노플라스틱의 영양학적 특성에 대한 영향 평가
KIT
미세플라스틱의 해양 생물 영향 평가
❖ 새우의 생화학적 영향 평가 - GST 및 SOD 활성
• 간췌장 내 GST와 SOD의 활성의 경우, 대조군과 비교하여 유의하게 증가
• GST와 SOD의 경우 각각 해독 및 항산화 작용에 관여
• 이는 미세플라스틱이 개체에 잠재적 독성물질로 영향을 미칠 수 있으며 산화스트레스를 유발할 수 있다는 것을 의미
• 미세플라스틱이 개체 내에서 해독 및 항산화에 관여하는 효소 활성에 영향을 미칠 수 있다는 가능성을 제시
A
B
CON (n=15) EXP (n=14)
GST Activity (/g protein* min-1)
SOD Inhibition Rate (%)
CON
EXP
REF: Y. Chae, D. Kim, M.J. Choi, Y. Cho and Y.J. An. 2019. ENVINT

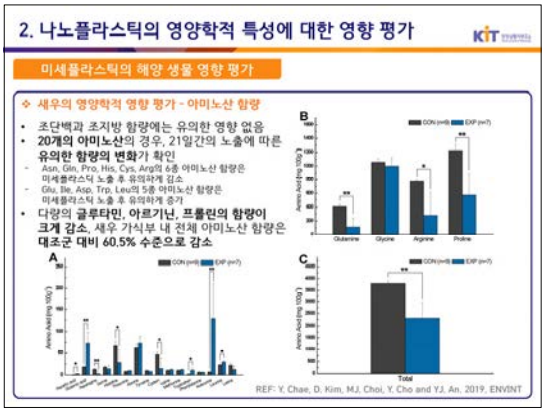
2. 나노플라스틱의 영양학적 특성에 대한 영향 평가
KIT
미세플라스틱의 해양 생물 영향 평가
❖ 새우의 영양학적 영향 평가 - 아미노산 함량
• 조단백과 조지방 함량에는 유의한 영향 없음
• 20개의 아미노산의 경우, 21일간의 노출에 따른 유의한 함량의 변화가 확인
- Asn, Gln, Pro, His, Cys, Arg의 6종 아미노산 함량은 미세플라스틱 노출 후 유의하게 감소
- Glu, Ile, Asp, Trp, Leu의 5종 아미노산 함량은 미세플라스틱 노출 후 유의하게 증가
• 다량의 글루타민, 아르기닌, 프롤린의 함량이 크게 감소, 새우 가식부 내 전체 아미노산 함량은 대조군 대비 60.5% 수준으로 감소
A
B
C
Glutamine
Glycine
Arginine
Proline
Total
REF: Y. Chae, D. Kim, M.J. Choi, Y. Cho and Y.J. An. 2019. ENVINT

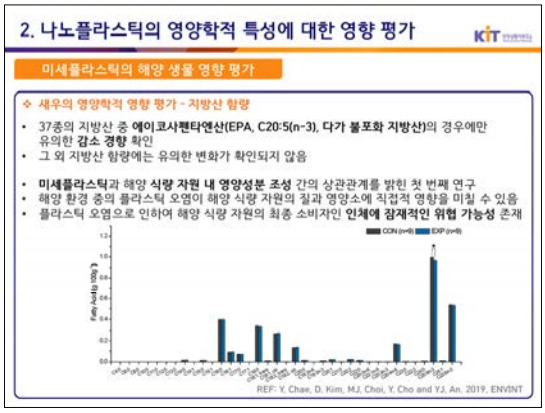
2. 나노플라스틱의 영양학적 특성에 대한 영향 평가
KIT
미세플라스틱의 해양 생물 영향 평가
❖ 새우의 영양학적 영향 평가 - 지방산 함량
• 37종의 지방산 중 에이코사펜타엔산(EPA, C20:5(n-3), 다가 불포화 지방산)의 경우에만 유의한 감소 경향 확인
• 그 외 지방산 함량에는 유의한 변화가 확인되지 않음
• 미세플라스틱과 해양 식량 자원 내 영양성분 조성 간의 상관관계를 밝힌 첫 번째 연구
• 해양 환경 중의 플라스틱 오염이 해양 식량 자원의 질과 영양소에 직접적 영향을 미칠 수 있음
• 플라스틱 오염으로 인하여 해양 식량 자원의 최종 소비자인 인체에 잠재적인 위협 가능성 존재
CON (n=6) EXP (n=8)
REF: Y. Chae, D. Kim, M.J. Choi, Y. Cho and Y.J. An. 2019. ENVINT


3. Significance of research
Korea Institute of Toxicology
KIT

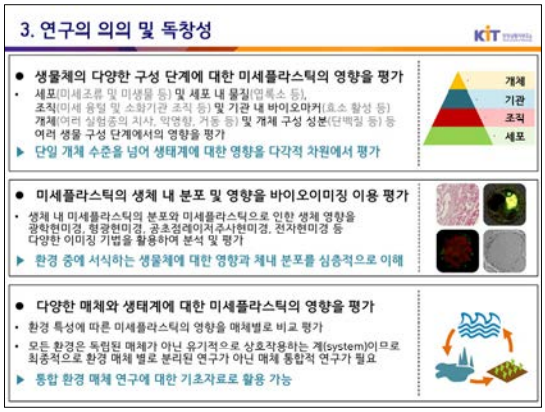
3. 연구의 의의 및 독창성
KIT
● 생물체의 다양한 구성 단계에 대한 미세플라스틱의 영향을 평가
• 세포(미세조류 및 미생물 등) 및 세포 내 물질(엔록소 등),
조직(미세 융털 및 소화기관 조직 등) 및 기관 내 바이오마커(효소 활성 등)
개체(여러 실험종의 지사, 먹영향, 거동 등) 및 개체 구성 성분(단백질 등) 등
여러 생물 구성 단계에서의 영향을 평가
▶ 단일 개체 수준을 넘어 생태계에 대한 영향을 다각적 차원에서 평가
개체
기관
조직
세포
● 미세플라스틱의 생체 내 분포 및 영향을 바이오이미징 이용 평가
• 생체 내 미세플라스틱의 분포와 미세플라스틱으로 인한 생체 영향을 광학현미경, 형광현미경, 공초점레이저주사현미경, 전자현미경 등 다양한 이미징 기법을 활용하여 분석 및 평가
▶ 환경 중에 서식하는 생물체에 대한 영향과 체내 분포를 심층적으로 이해
● 다양한 매체와 생태계에 대한 미세플라스틱의 영향을 평가
• 환경 특성에 따른 미세플라스틱의 영향을 매체별로 비교 평가
• 모든 환경은 독립된 매체가 아닌 유기적으로 상호작용하는 계(system)이므로 최종적으로 환경 매체 별로 분리된 연구가 아닌 매체 통합적 연구가 필요
▶ 통합 환경 매체 연구에 대한 기초자료로 활용 가능


감사합니다 ☺

Dev. Reprod. Vol 26, 2022 (Suppl. 1). pp 99

Chemokine regulates eye morphogenesis in *Xenopus*

정호성

연세대학교

(HJUNG@yuhs.ac)

심포지엄 V

Dev. Reprod. Vol 26, 2022 (Suppl. 1). pp 103

지속 가능한 미래 생물자원 확보를 위한 남극 어류 연구

김진형

한국해양과학기술원 극지연구소

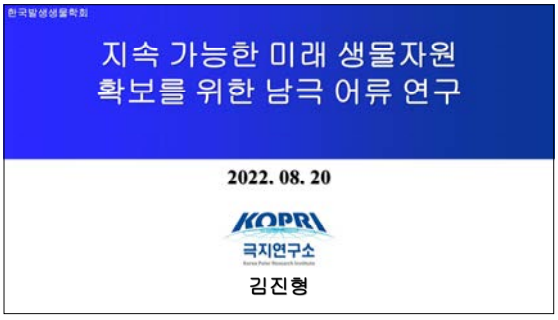

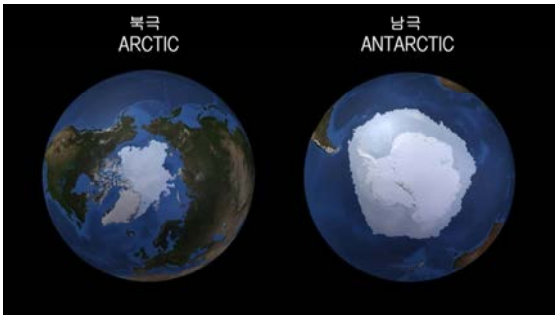

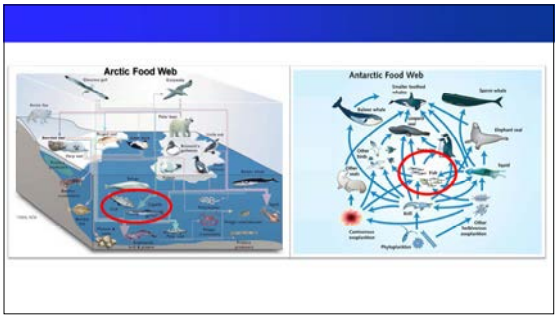

몸속 부동액
결빙방지단백질

뼈대 없는 가문

피는 물보다 진하다!

차원이 다른 생체 시계!

미래의 수산자원

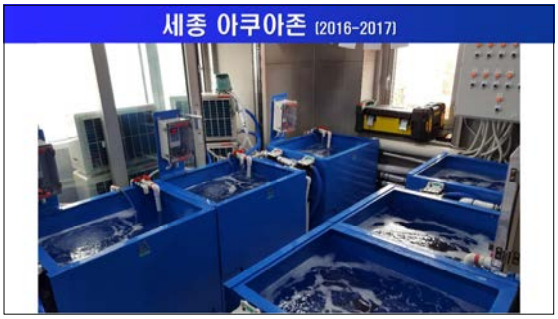
세종 아쿠아존 (2016-2017)


KOPRI 아쿠아리움 (2018)


Thank you
https://www.kopri.re.kr
kimjh@kopri.re.kr

Dev. Reprod. Vol 26, 2022 (Suppl. 1). pp 106

Enhanced hepatic functionality in long-term cultured 3D spheroids of zebrafish liver cells

김용준

한국과학기술연구원 환경안정성연구단

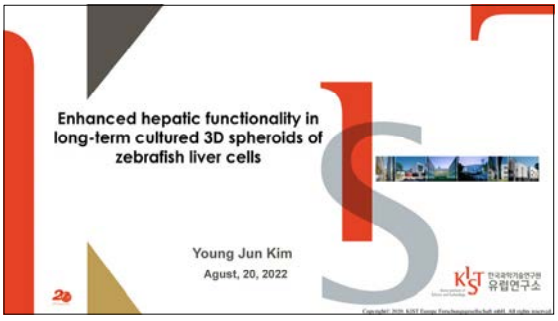

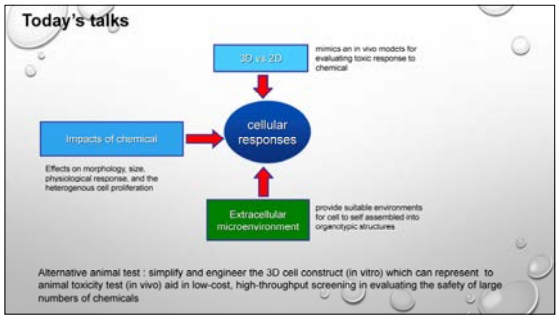

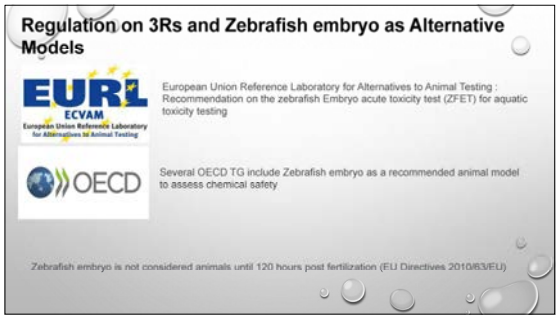

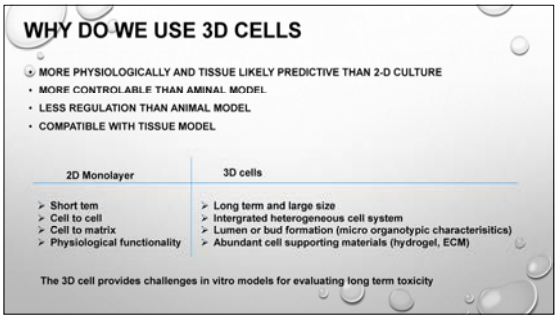

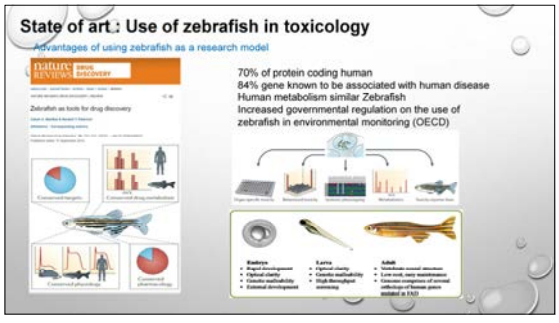

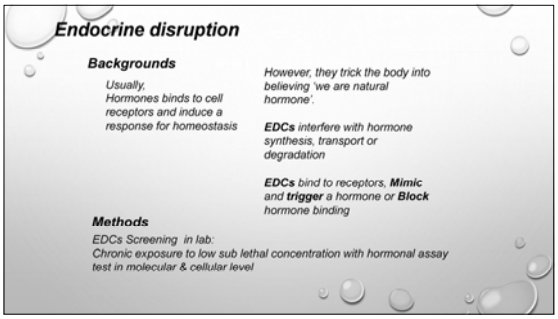
Endocrine disruption
Backgrounds
Usually,
Hormones binds to cell receptors and induce a response for homeostasis
However, they trick the body into believing 'we are natural hormone'.
EDCs interfere with hormone synthesis, transport or degradation
EDCs bind to receptors, Mimic and trigger a hormone or Block hormone binding
Methods
EDCs Screening in lab:
Chronic exposure to low sub lethal concentration with hormonal assay test in molecular & cellular level

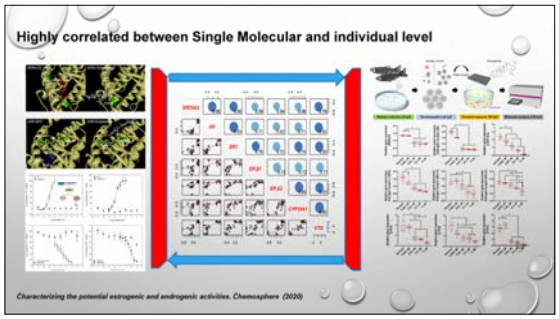
Highly correlated between Single Molecular and individual level
Characterizing the potential estrogenic and androgenic activities. Chemosphere (2020)

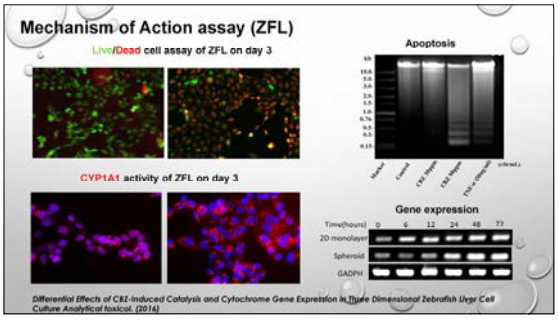
Mechanism of Action assay (ZFL)
Live/Dead cell assay of ZFL on day 3
CYP1A1 activity of ZFL on day 3
Apoptosis
Gene expression
Time(hours) 0 6 12 24 48 72
2D monolayer
Spheroid
GADPH
Differential Effects of CB1-Induced Catalysis and Cytochrome Gene Expression in Three Dimensional Zebrafish Liver Cell Culture Analytical toxicol. (2016)

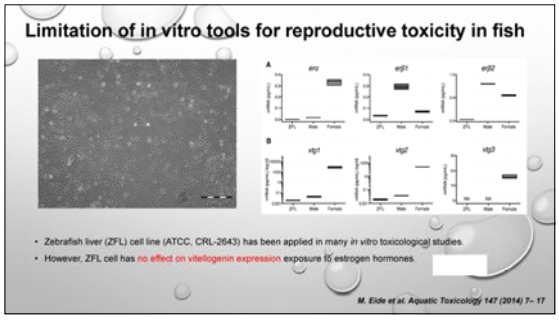
Limitation of in vitro tools for reproductive toxicity in fish
Zebrafish liver (ZFL) cell line (ATCC, CRL-2643) has been applied in many in vitro toxicological studies.
However, ZFL cell has no effect on vitellogenin expression exposure to estrogen hormones.
M. Eide et al. Aquatic Toxicology 147 (2014) 7– 17

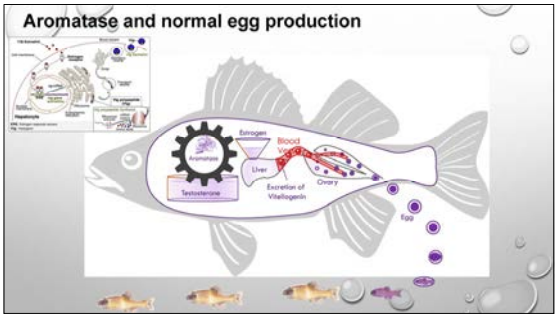
Aromatase and normal egg production
Estrogen
Blood Vessel
Liver
Excretion of Vitellogenin
Ovary
Egg
Testosterone

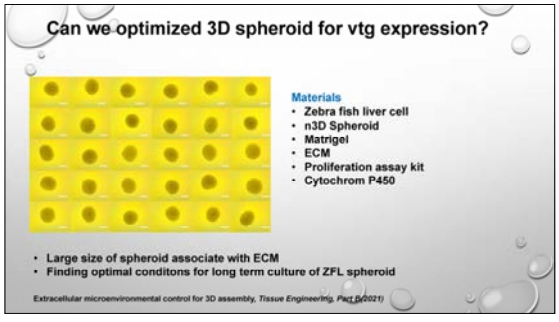
Can we optimized 3D spheroid for vtg expression?
Materials
Zebra fish liver cell
n3D Spheroid
Matrigel
ECM
Proliferation assay kit
Cytochrom P450
Large size of spheroid associate with ECM
Finding optimal conditons for long term culture of ZFL spheroid
Extracellular microenvironmental control for 3D assembly, Tissue Engineering, Part D(2021)

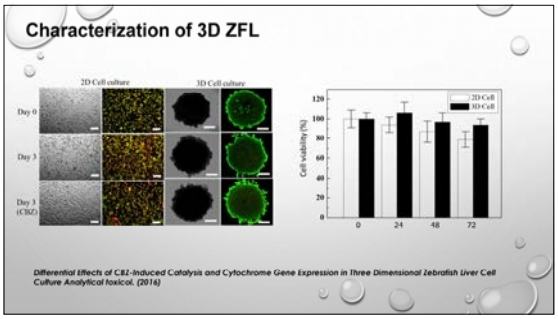
Characterization of 3D ZFL
2D Cell culture
3D Cell culture
Day 0
Day 3
Day 3 (CBZ)
Cell viability (%)
2D Cell
3D Cell
0
24
48
72
Differential Effects of CBZ-Induced Catalysis and Cytochrome Gene Expression in Three Dimensional Zebrafish Liver Cell Culture Analytical toxicol. (2016)

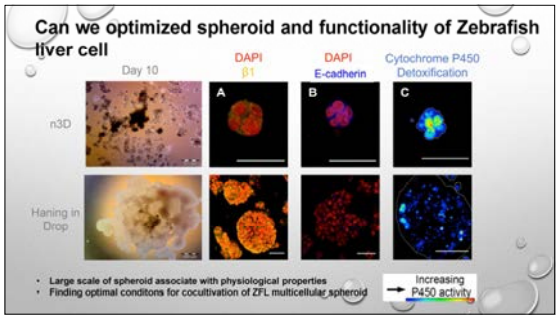
Can we optimized spheroid and functionality of Zebrafish liver cell
Day 10
DAPI
β1
DAPI
E-cadherin
Cytochrome P450
Detoxification
n3D
Haning in Drop
A
B
C
Large scale of spheroid associate with physiological properties
Finding optimal conditons for cocultivation of ZFL multicellular spheroid
increasing P450 activity

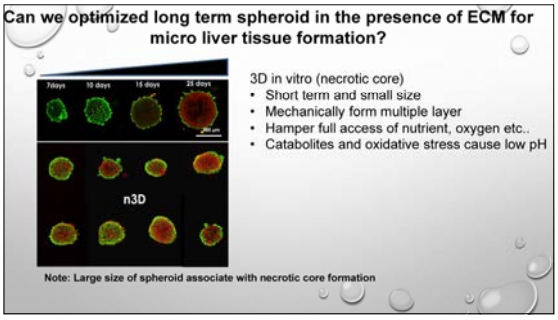
Can we optimized long term spheroid in the presence of ECM for micro liver tissue formation?
7days
10 days
15 days
20 days
n3D
3D in vitro (necrotic core)
Short term and small size
Mechanically form multiple layer
Hamper full access of nutrient, oxygen etc..
Catabolites and oxidative stress cause low pH
Note: Large size of spheroid associate with necrotic core formation

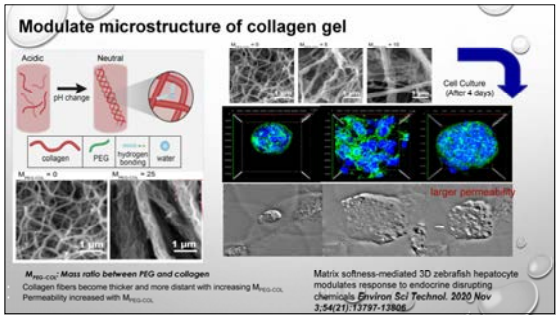
Modulate microstructure of collagen gel
Acidic
Neutral
pH change
collagen
PEG
hydrogen bonding
water
1 μm
Cell Culture (After 4 days)
larger permeability
Matrix softness-mediated 3D zebrafish hepatocyte modulates response to endocrine disrupting chemicals Environ Sci Technol. 2020 Nov 3;54(21):13797-13806.

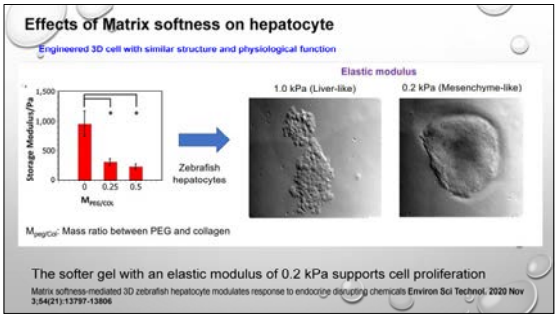
Effects of Matrix softness on hepatocyte
Engineered 3D cell with similar structure and physiological function
Elastic modulus
1.0 kPa (Liver-like)
0.2 kPa (Mesenchyme-like)
Storage Modulus/Pa
Zebrafish hepatocytes
Mass ratio between PEG and collagen
The softer gel with an elastic modulus of 0.2 kPa supports cell proliferation
Matrix softness-mediated 3D zebrafish hepatocyte modulates response to endocrine disrupting chemicals Environ Sci Technol. 2020 Nov 3;54(21):13797-13806

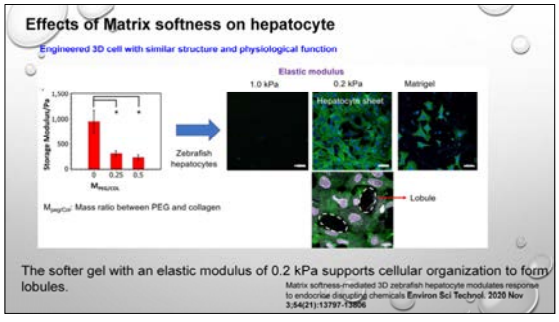
Effects of Matrix softness on hepatocyte
Engineered 3D cell with similar structure and physiological function
Elastic modulus
1.0 kPa
0.2 kPa
Matrigel
Hepatocyte sheet
Zebrafish hepatocytes
Lobule
Mass ratio between PEG and collagen
The softer gel with an elastic modulus of 0.2 kPa supports cellular organization to form lobules.
Matrix softness-mediated 3D zebrafish hepatocyte modulates response to endocrine disrupting chemicals Environ Sci Technol. 2020 Nov 3;54(21):13797-13806

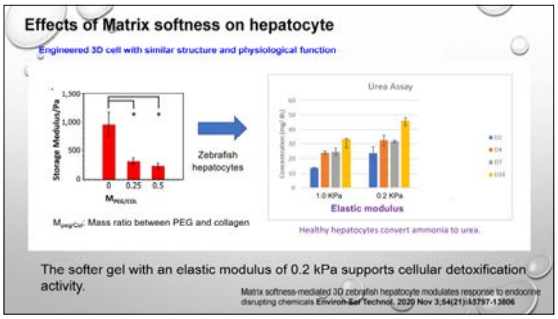
Effects of Matrix softness on hepatocyte
Engineered 3D cell with similar structure and physiological function
Storage Modulus/Pa
Zebrafish hepatocytes
Urea Assay
1.0 KPa
0.2 KPa
Elastic modulus
Healthy hepatocytes convert ammonia to urea.
The softer gel with an elastic modulus of 0.2 kPa supports cellular detoxification activity.

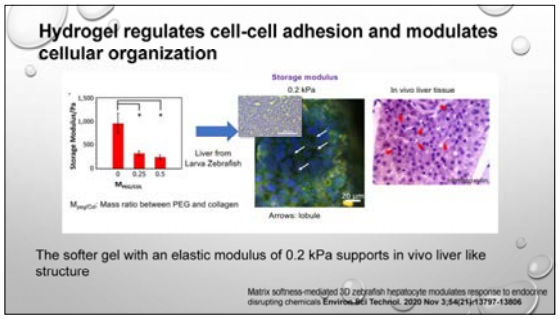
Hydrogel regulates cell-cell adhesion and modulates cellular organization
Storage modulus
0.2 kPa
In vivo liver tissue
Liver from Larva Zebrafish
Arrows: lobule
The softer gel with an elastic modulus of 0.2 kPa supports in vivo liver like structure

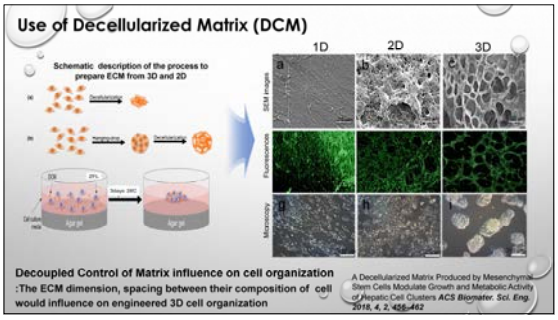
Use of Decellularized Matrix (DCM)
1D
2D
3D
Schematic description of the process to prepare ECM from 3D and 2D
Decoupled Control of Matrix influence on cell organization
:The ECM dimension, spacing between their composition of cell would influence on engineered 3D cell organization

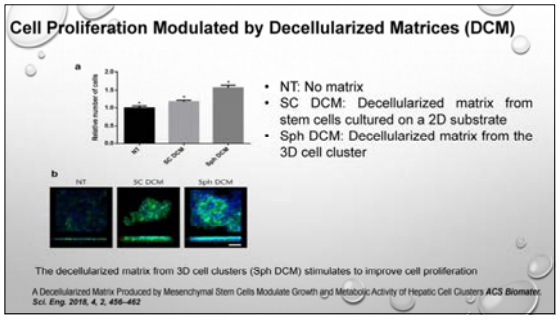
Cell Proliferation Modulated by Decellularized Matrices (DCM)
NT: No matrix
SC DCM: Decellularized matrix from stem cells cultured on a 2D substrate
Sph DCM: Decellularized matrix from the 3D cell cluster
The decellularized matrix from 3D cell clusters (Sph DCM) stimulates to improve cell proliferation

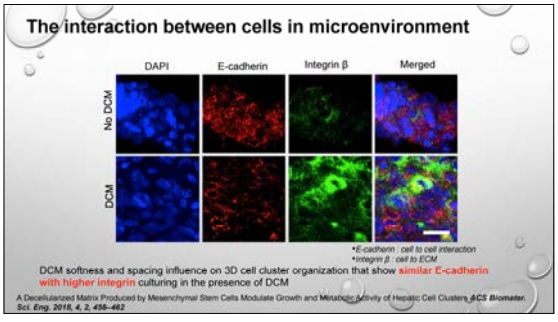
The interaction between cells in microenvironment
DAPI
E-cadherin
Integrin β
Merged
No DCM
DCM
DCM softness and spacing influence on 3D cell cluster organization that show similar E-cadherin with higher integrin culturing in the presence of DCM

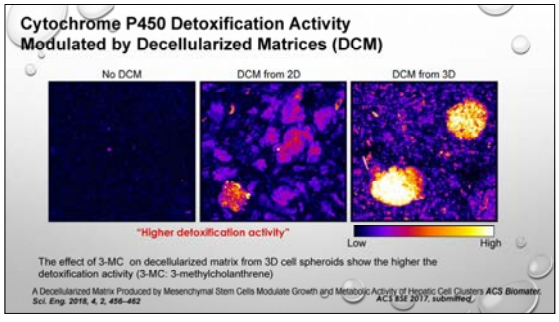
Cytochrome P450 Detoxification Activity Modulated by Decellularized Matrices (DCM)
No DCM
DCM from 2D
DCM from 3D
"Higher detoxification activity"
Low
High
The effect of 3-MC on decellularized matrix from 3D cell spheroids show the higher the detoxification activity (3-MC: 3-methylcholanthrene)

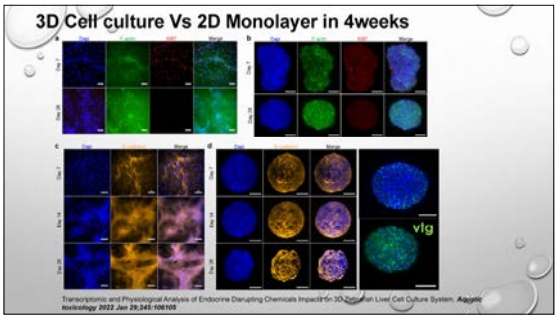
3D Cell culture Vs 2D Monolayer in 4weeks
vtg

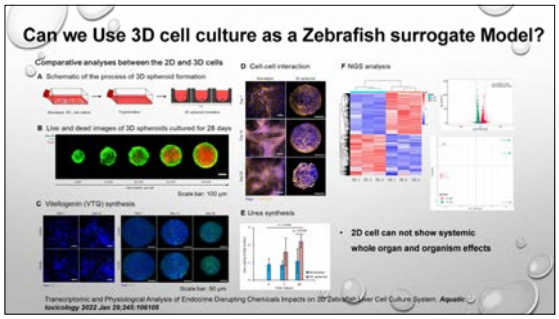
Can we Use 3D cell culture as a Zebrafish surrogate Model?
Comparative analyses between the 2D and 3D cells
A Schematic of the process of 3D spheroid formation
B Live and dead images of 3D spheroids cultured for 28 days
C Vitellogenin (VTG) synthesis
D Cell-cell interaction
E Urea synthesis
F NGS analysis
2D cell can not show systemic whole organ and organism effects

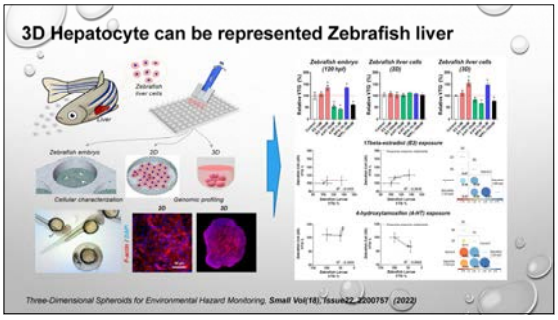
3D Hepatocyte can be represented Zebrafish liver
Three-Dimensional Spheroids for Environmental Hazard Monitoring, Small Vol(18), Issue22, 2200757, (2022)

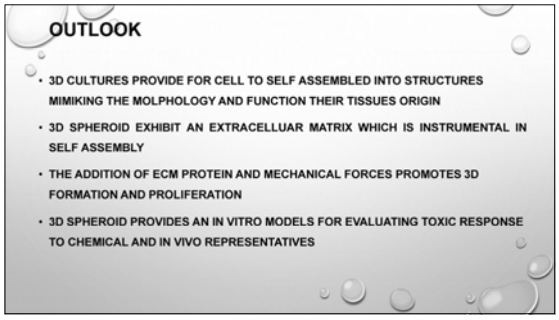
OUTLOOK
• 3D CULTURES PROVIDE FOR CELL TO SELF ASSEMBLED INTO STRUCTURES MIMIKING THE MOLPHOLOGY AND FUNCTION THEIR TISSUES ORIGIN
• 3D SPHEROID EXHIBIT AN EXTRACELLUAR MATRIX WHICH IS INSTRUMENTAL IN SELF ASSEMBLY
• THE ADDITION OF ECM PROTEIN AND MECHANICAL FORCES PROMOTES 3D FORMATION AND PROLIFERATION
• 3D SPHEROID PROVIDES AN IN VITRO MODELS FOR EVALUATING TOXIC RESPONSE TO CHEMICAL AND IN VIVO REPRESENTATIVES


Germany
감사합니다!
Thank you for your attention!
Vielen Dank fuer Ihre Aufmerksamkeit!

Dev. Reprod. Vol 26, 2022 (Suppl. 1). pp 111

Tumor-host interaction regulates cancer anorexia

염은별

경북대학교

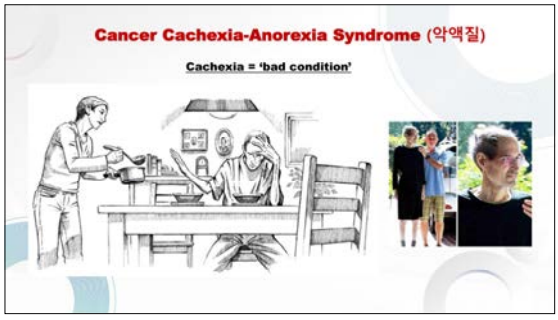

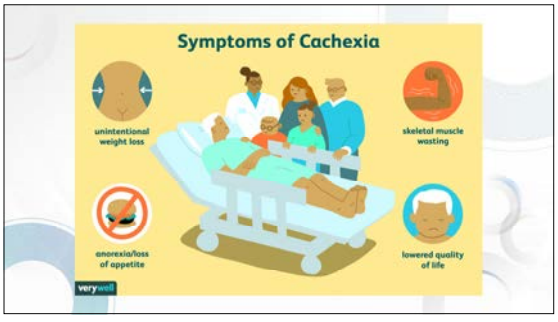

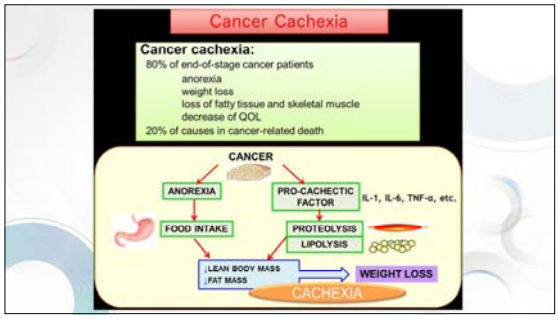

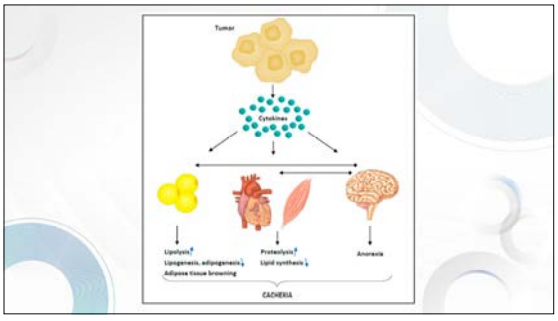

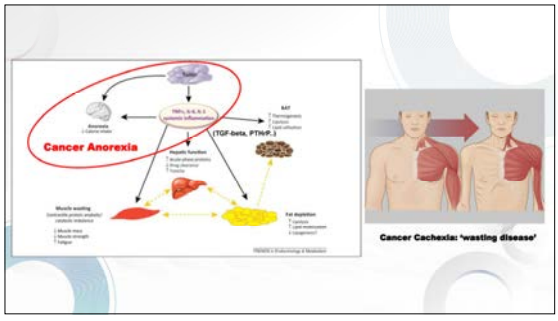

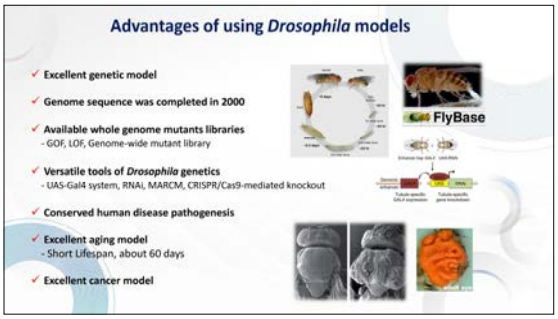
Advantages of using Drosophila models
Excellent genetic model
Genome sequence was completed in 2000
Available whole genome mutants libraries
- GOF, LOF, Genome-wide mutant library
Versatile tools of Drosophila genetics
- UAS-Gal4 system, RNAi, MARCM, CRISPR/Cas9-mediated knockout
Conserved human disease pathogenesis
Excellent aging model
- Short Lifespan, about 60 days
Excellent cancer model
FlyBase

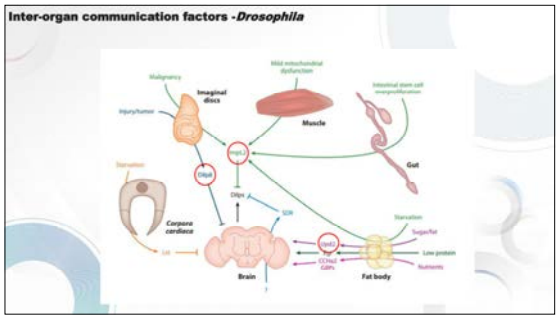
Inter-organ communication factors -Drosophila
Imaginal discs
Muscle
Gut
Corpora cardiaca
Brain
Fat body

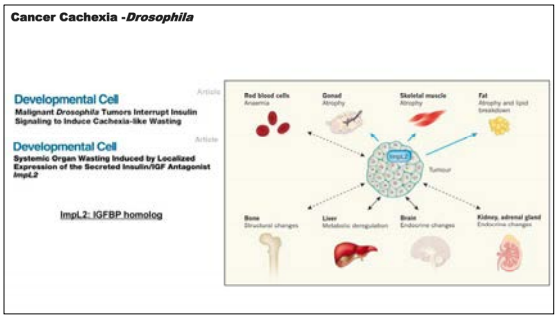
Cancer Cachexia -Drosophila
Developmental Cell
Malignant Drosophila Tumors Interrupt Insulin Signaling to Induce Cachexia-like Wasting
Developmental Cell
Systemic Organ Wasting Induced by Localized Expression of the Secreted Insulin/IGF Antagonist ImpL2
ImpL2: IGFBP homolog
Red blood cells
Gonad
Skeletal muscle
Fat
Tumour
Bone
Liver
Brain
Kidney, adrenal gland

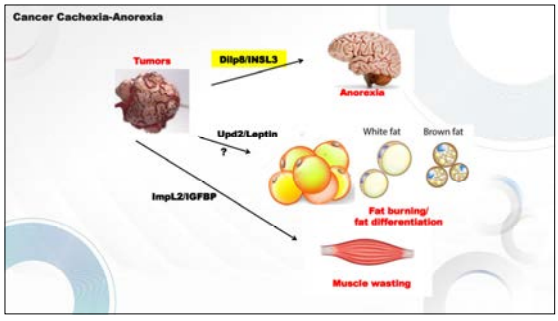
Cancer Cachexia-Anorexia
Tumors
Dilp8/INSL3
Anorexia
Upd2/Leptin
?
White fat
Brown fat
ImpL2/IGFBP
Fat burning/
fat differentiation
Muscle wasting

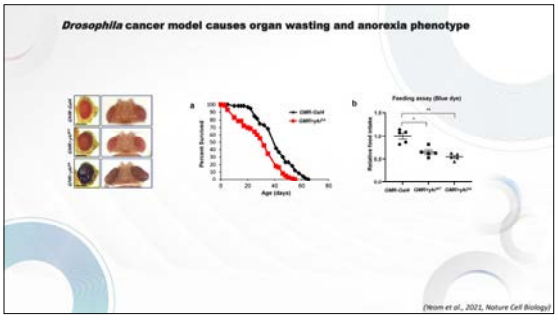
Drosophila cancer model causes organ wasting and anorexia phenotype
a
b
Age (days)
Feeding assay (Blue dye)
(Hoon et al., 2021, Nature Cell Biology)

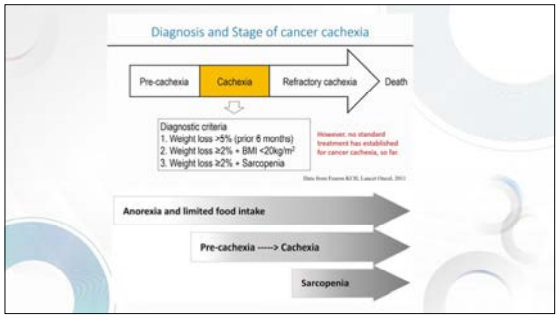
Diagnosis and Stage of cancer cachexia
Pre-cachexia
Cachexia
Refractory cachexia
Death
Diagnostic criteria
1. Weight loss >5% (prior 6 months)
2. Weight loss ≥2% + BMI <20kg/m²
3. Weight loss ≥2% + Sarcopenia
Anorexia and limited food intake
Pre-cachexia -----> Cachexia
Sarcopenia

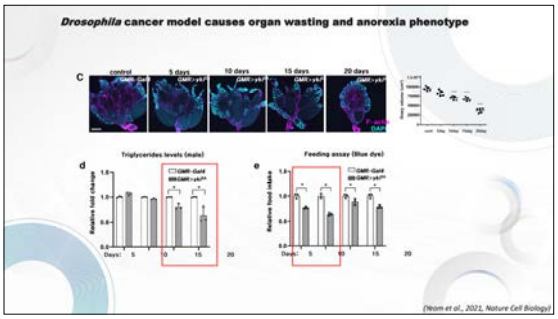
Drosophila cancer model causes organ wasting and anorexia phenotype
control
5 days
10 days
15 days
20 days
Triglycerides levels (male)
Feeding assay (Blue dye)
(Yeom et al., 2021, Nature Cell Biology)

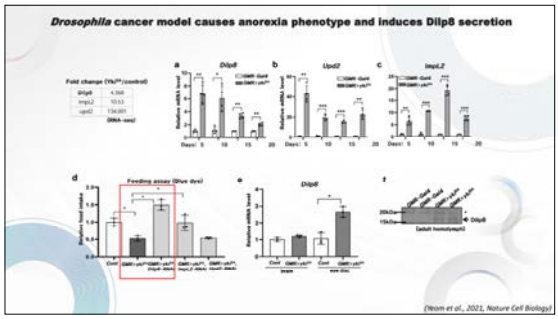
Drosophila cancer model causes anorexia phenotype and induces Dilp8 secretion
Dilp8
Upd2
Imp-L2
Feeding assay (Blue dye)
(Yeom et al., 2021, Nature Cell Biology)

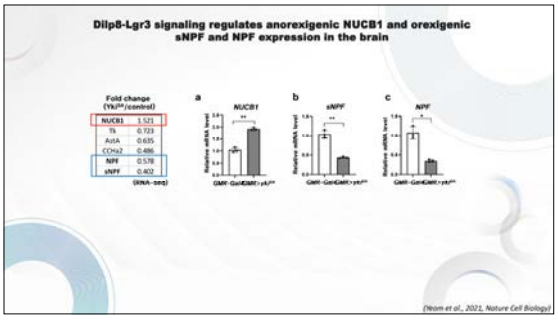
Dilp8-Lgr3 signaling regulates anorexigenic NUCB1 and orexigenic sNPF and NPF expression in the brain
Fold change (Yki3SA/control)
NUCB1 1.521
Tk 0.723
AstA 0.635
CCHa2 0.486
NPF 0.578
sNPF 0.402
(RNA-seq)
NUCB1
sNPF
NPF
(Yeom et al., 2021, Nature Cell Biology)

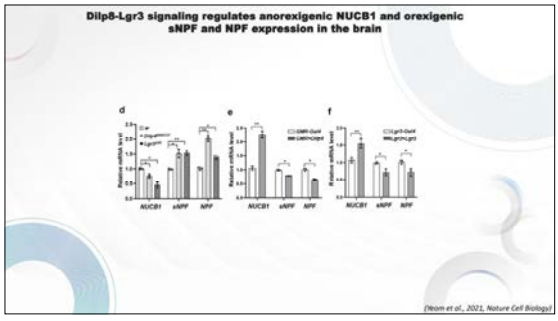
Dilp8-Lgr3 signaling regulates anorexigenic NUCB1 and orexigenic sNPF and NPF expression in the brain
(Yeom et al., 2021, Nature Cell Biology)

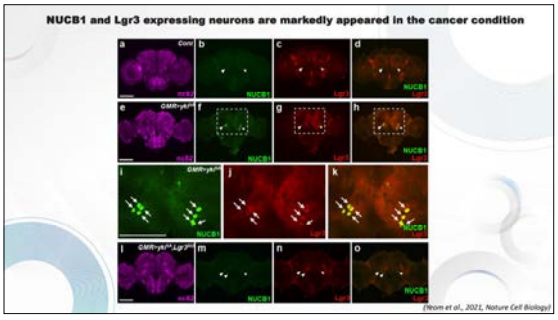
NUCB1 and Lgr3 expressing neurons are markedly appeared in the cancer condition
Cont
(Yeom et al., 2021, Nature Cell Biology)

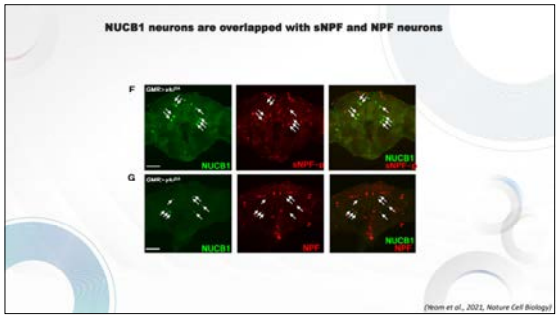
NUCB1 neurons are overlapped with sNPF and NPF neurons
(Yeom et al., 2021, Nature Cell Biology)

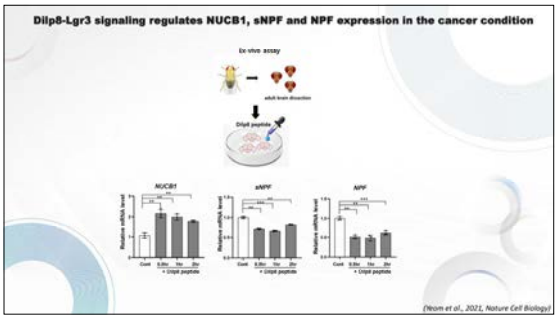
Dilp8-Lgr3 signaling regulates NUCB1, sNPF and NPF expression in the cancer condition
Ex vivo assay
Dilp8 peptide
NUCB1
sNPF
NPF
Cont
0.5hr
1hr
2hr
+ Dilp8 peptide
(Yeom et al., 2021, Nature Cell Biology)

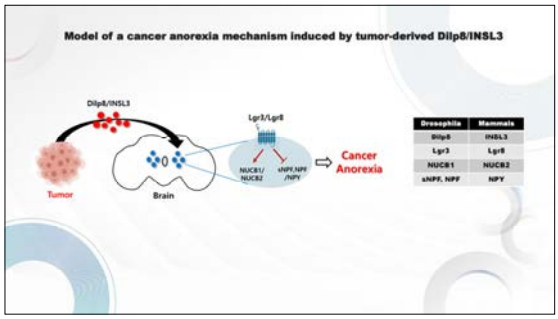
Model of a cancer anorexia mechanism induced by tumor-derived Dilp8/INSL3
Dilp8/INSL3
Lgr3/Lgr8
Tumor
Brain
NUCB1/ NUCB2
sNPF,NPF /NPY
Cancer Anorexia
Drosophila
Mammals
Dilp8
INSL3
Lgr3
Lgr8
NUCB1
NUCB2
sNPF, NPF
NPY

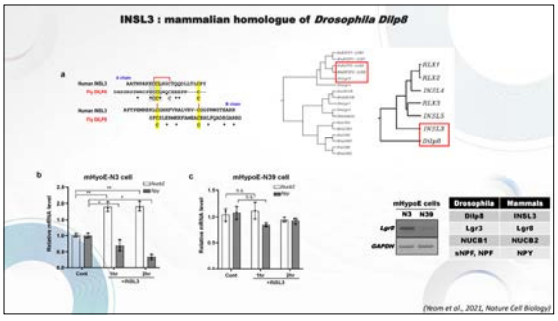
INSL3 : mammalian homologue of Drosophila Dilp8
mHypoE-N3 cell
mHypoE-N39 cell
Cont
1hr
2hr
+INSL3
mHypoE cells
N3
N39
Lgr3
GAPDH
Drosophila
Mammals
Dilp8
INSL3
Lgr3
Lgr8
NUCB1
NUCB2
sNPF, NPF
NPY
(Yeom et al., 2021, Nature Cell Biology)

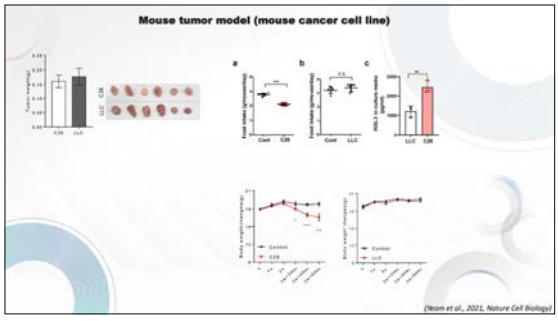
Mouse tumor model (mouse cancer cell line)
Cont
C26
LLC
(Yeom et al., 2021, Nature Cell Biology)

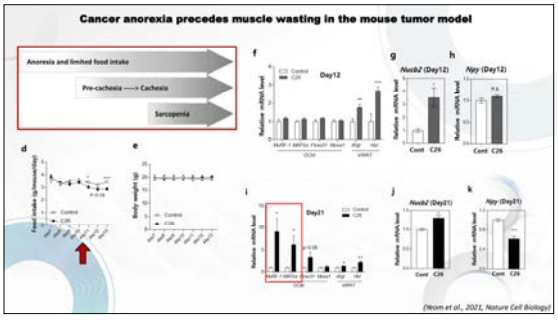
Cancer anorexia precedes muscle wasting in the mouse tumor model
Anorexia and limited food intake
Pre-cachexia ——> Cachexia
Sarcopenia
Day12
Nucb2 (Day12)
Npy (Day12)
Day21
Nucb2 (Day21)
Npy (Day21)
Cont
C26
(Yeom et al., 2021, Nature Cell Biology)

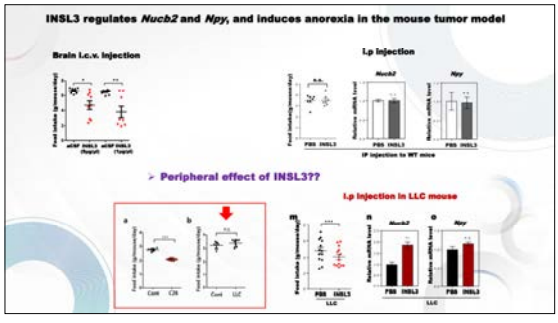
INSL3 regulates Nucb2 and Npy, and induces anorexia in the mouse tumor model
Brain i.c.v. injection
Lp injection
Nucb2
Npy
PBS
INSL3
IP injection to WT mice
Peripheral effect of INSL3??
Lp injection in LLC mouse
Cont
C26
LLC

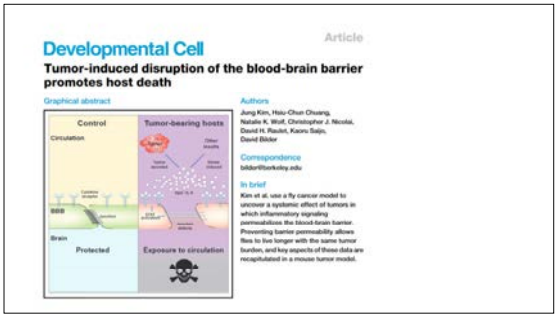
Developmental Cell
Article
Tumor-induced disruption of the blood-brain barrier promotes host death
Graphical abstract
Control
Tumor-bearing hosts
Circulation
BBB
Brain
Protected
Exposure to circulation
Authors
Correspondence
In brief

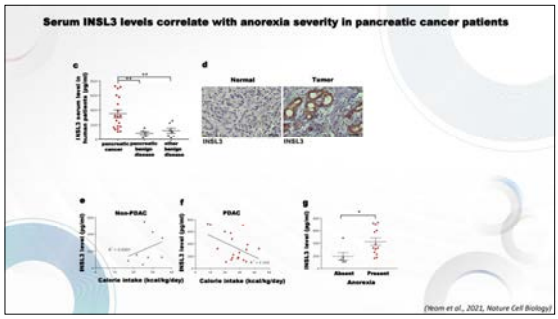
Serum INSL3 levels correlate with anorexia severity in pancreatic cancer patients
Normal
Tumor
INSL3
Non-PDAC
PDAC
Calorie intake (kcal/kg/day)
Absent
Present
Anorexia
(Yeom et al., 2021, Nature Cell Biology)

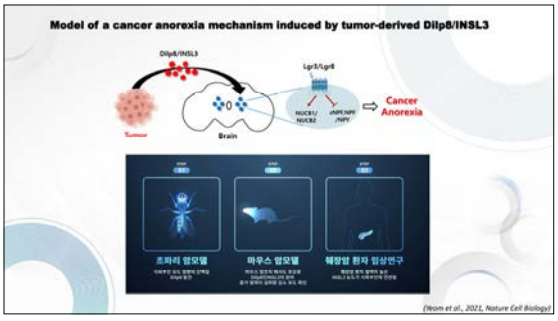
Model of a cancer anorexia mechanism induced by tumor-derived Dilp8/INSL3
Dilp8/INSL3
Lgr3/Lgr8
Tumor
Brain
Cancer Anorexia
초파리 암모델
마우스 암모델
췌장암 환자 임상연구
(Yeom et al., 2021, Nature Cell Biology)


Acknowledgements
KRIBB
Dr. Kweon Yu
Dr. Kyu-Sun Lee
Collaborators
Prof. Jae Myung Suh (KAIST)
Heymi Shin (KAIST)
Prof. Song-Cheol Kim (아산병원)
Dr. Eunsung Jun (아산병원)


경청해 주셔서 감사합니다
경북대학교

Dev. Reprod. Vol 26, 2022 (Suppl. 1). pp 116

Cardiotoxicity evaluation of drugs using human PSC-derived cardiomyocytes

문성환

상지대학교

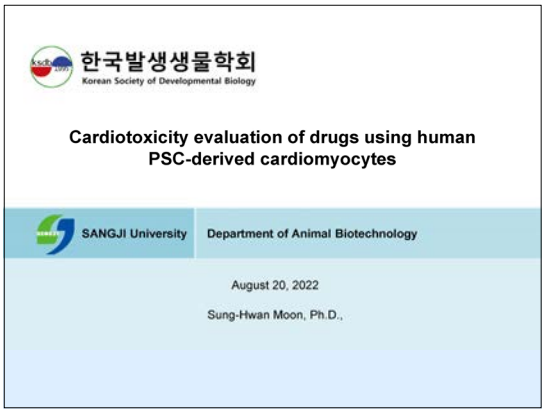

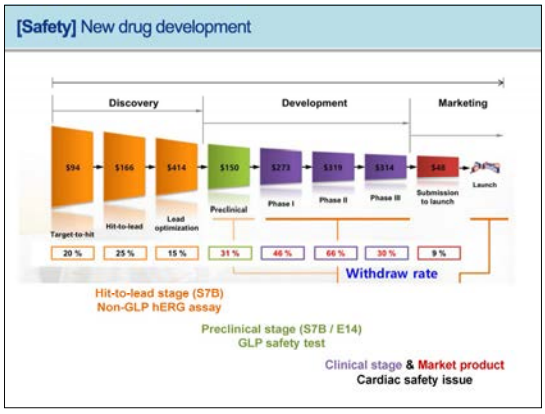

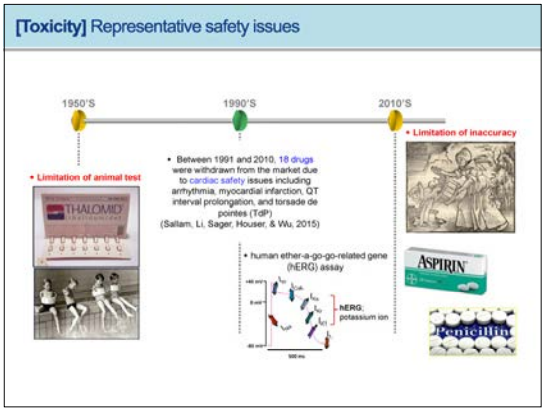

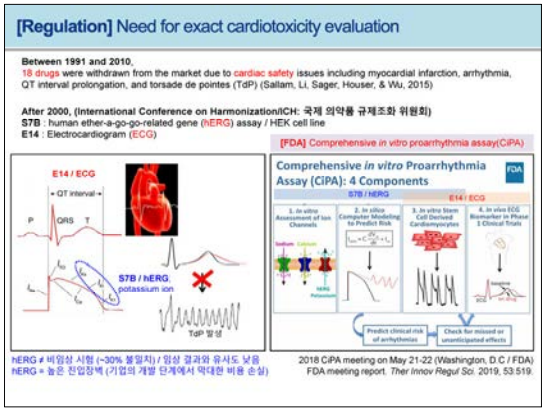

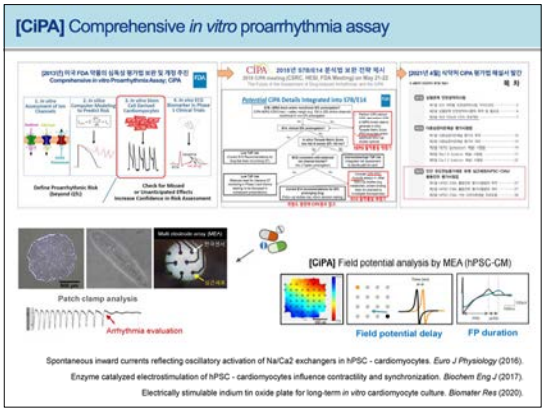

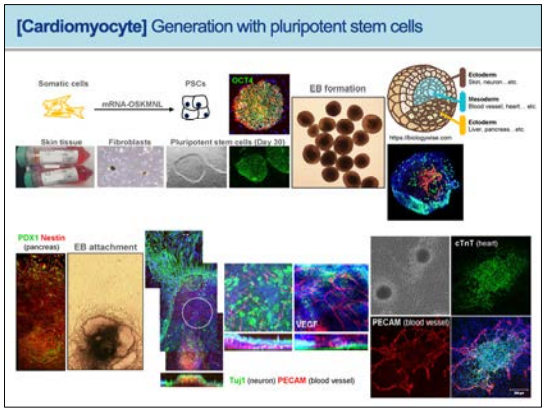


[Establishment] Information sharing
Sarcomere
20 μm
Ca²⁺ influx
국가줄기세포은행

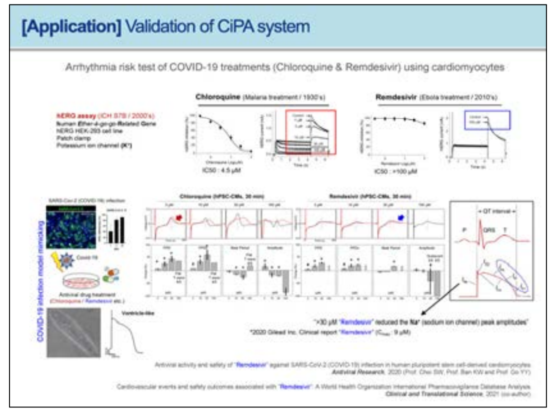
[Application] Validation of CiPA system
Arrhythmia risk test of COVID-19 treatments (Chloroquine & Remdesivir) using cardiomyocytes
Chloroquine (Malaria treatment / 1930's)
Remdesivir (Ebola treatment / 2010's)
hERG assay (ICH S7B / 2000's)
Human Ether-à-go-go-Related Gene
hERG HEK-293 cell line
Patch clamp
Potassium ion channel (K⁺)
IC50 : 4.5 μM
IC50 : >100 μM
COVID-19 infection model mimicking
QT interval
P
QRS
T
Ventricle-like


[Thanks to…] Research networks & grants
T&R Biofab Pangyo Stem Cell Research Institute
SEOUL ST. MARY'S HOSPITAL
Prof. Hoon-Jun Park
Prof. Kiwon Ban
Dr. Soon-Jung Park
Yun-Gwi Park
Yeo-Jin Son
Grant No. 21A0403L1 (중견)
Grant No. 2022R1A2C1006622
Grant No. HI20C0184


한국발생생물학회
Korean Society of Developmental Biology
Thank you very much for your attention !!!

의학 심포지엄 Session 1

불응성 자궁내막 및
아셔만 증후군의 치료

Dev. Reprod. Vol 26, 2022 (Suppl. 1). pp 121

불응성 자궁내막 및 아셔만 증후군의 치료: 약물치료

채수진

아이오라 여성의원

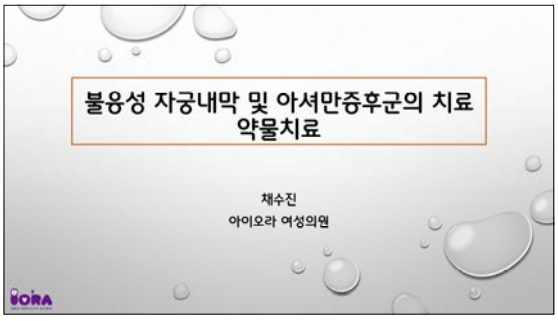

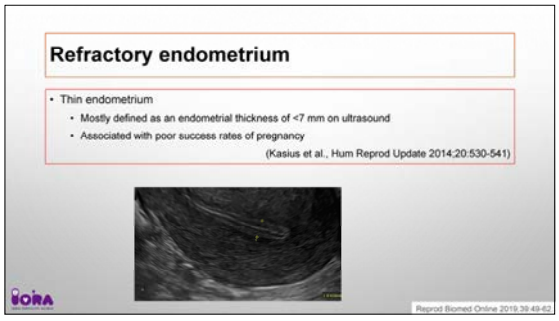

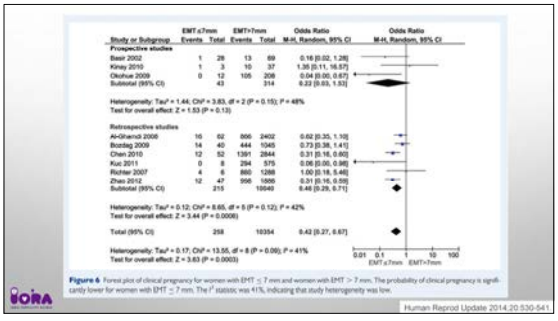

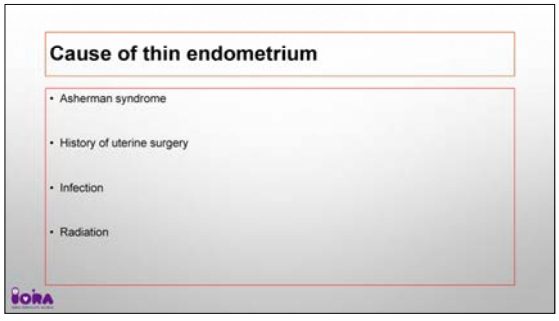

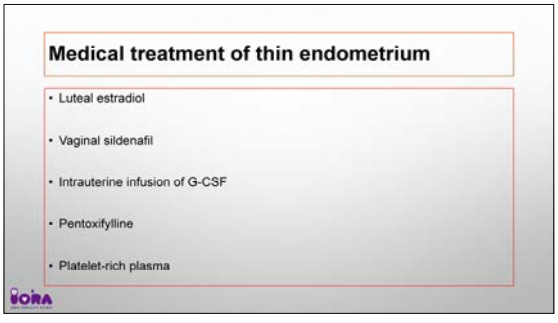

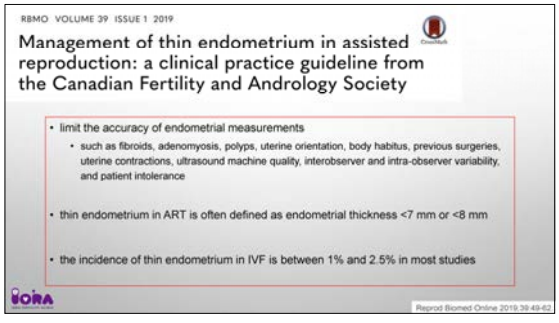

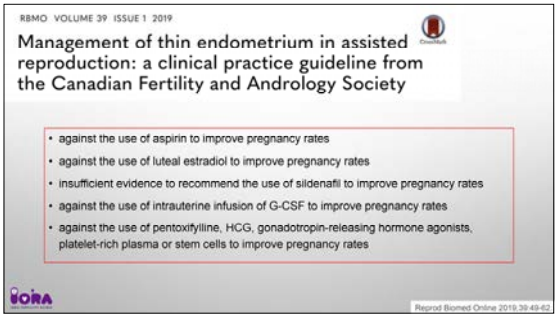
RBMO VOLUME 39 ISSUE 1 2019
Management of thin endometrium in assisted reproduction: a clinical practice guideline from the Canadian Fertility and Andrology Society
• against the use of aspirin to improve pregnancy rates
• against the use of luteal estradiol to improve pregnancy rates
• insufficient evidence to recommend the use of sildenafil to improve pregnancy rates
• against the use of intrauterine infusion of G-CSF to improve pregnancy rates
• against the use of pentoxifylline, HCG, gonadotropin-releasing hormone agonists, platelet-rich plasma or stem cells to improve pregnancy rates
Reprod Biomed Online 2019;39:49-62

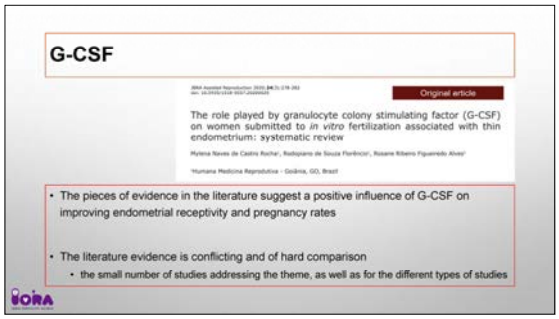
G-CSF
Original article
The role played by granulocyte colony stimulating factor (G-CSF) on women submitted to in vitro fertilization associated with thin endometrium: systematic review
• The pieces of evidence in the literature suggest a positive influence of G-CSF on improving endometrial receptivity and pregnancy rates
• The literature evidence is conflicting and of hard comparison
• the small number of studies addressing the theme, as well as for the different types of studies

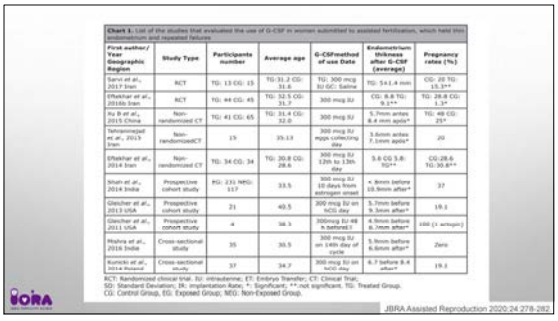
Chart 1: List of the studies that evaluated the use of G-CSF in women submitted to assisted fertilization, which held thin endometrium and repeated failures
JBRA Assisted Reproduction 2020;24:278-282

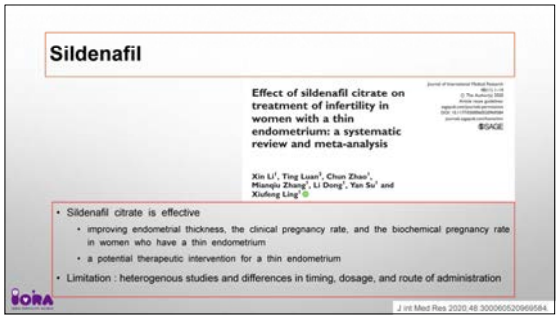
Sildenafil
Effect of sildenafil citrate on treatment of infertility in women with a thin endometrium: a systematic review and meta-analysis
Xin Li, Ting Luan, Chun Zhao, Mianqiu Zhang, Li Dong, Yan Su and Xiufang Ling
• Sildenafil citrate is effective
• improving endometrial thickness, the clinical pregnancy rate, and the biochemical pregnancy rate in women who have a thin endometrium
• a potential therapeutic intervention for a thin endometrium
• Limitation : heterogenous studies and differences in timing, dosage, and route of administration
J Int Med Res 2020;48:300060520969584

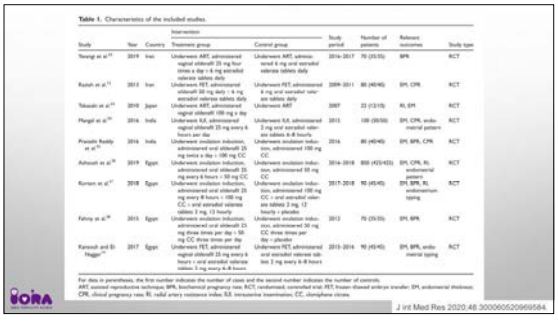
Table 1. Characteristics of the included studies.
J Int Med Res 2020;48:300060520969584

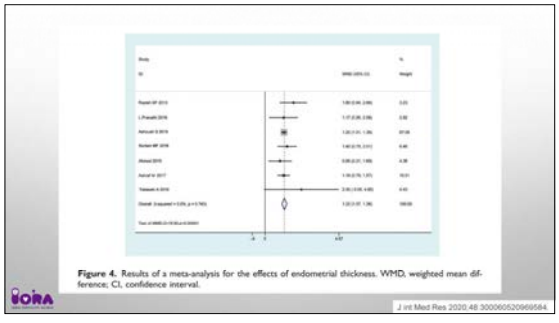
Figure 4. Results of a meta-analysis for the effects of endometrial thickness. WMD, weighted mean difference; CI, confidence interval.
J Int Med Res 2020;48:300060520969584

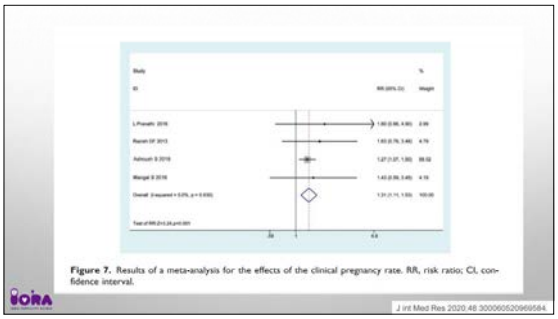

Figure 7. Results of a meta-analysis for the effects of the clinical pregnancy rate. RR, risk ratio; CI, confidence interval.

J Int Med Res 2020;48:300060520969584

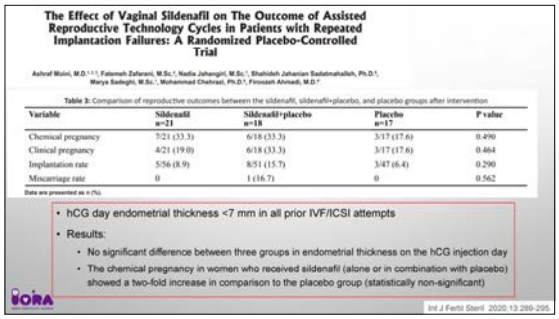

The Effect of Vaginal Sildenafil on The Outcome of Assisted Reproductive Technology Cycles in Patients with Repeated Implantation Failures: A Randomized Placebo-Controlled Trial

Table 3: Comparison of reproductive outcomes between the sildenafil, sildenafil+placebo, and placebo groups after intervention

Variable	Sildenafil n=21	Sildenafil+placebo n=18	Placebo n=17	P value
Chemical pregnancy	7/21 (33.3)	6/18 (33.3)	3/17 (17.6)	0.490
Clinical pregnancy	4/21 (19.0)	6/18 (33.3)	3/17 (17.6)	0.464
Implantation rate	5/56 (8.9)	8/51 (15.7)	3/47 (6.4)	0.290
Miscarriage rate	0	1 (16.7)	0	0.562

Data are presented as n (%).

- hCG day endometrial thickness <7 mm in all prior IVF/ICSI attempts
- Results:
  - No significant difference between three groups in endometrial thickness on the hCG injection day
  - The chemical pregnancy in women who received sildenafil (alone or in combination with placebo) showed a two-fold increase in comparison to the placebo group (statistically non-significant)

Int J Fertil Steril 2020;13:289-295

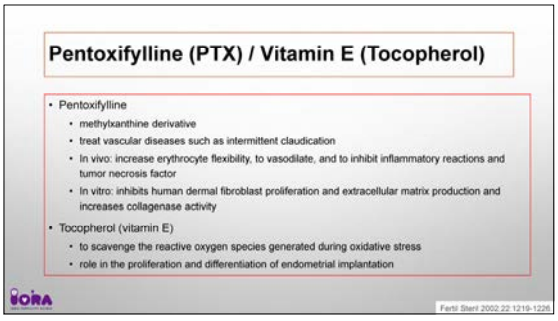

Pentoxifylline (PTX) / Vitamin E (Tocopherol)

- Pentoxifylline
  - methylxanthine derivative
  - treat vascular diseases such as intermittent claudication
  - In vivo: increase erythrocyte flexibility, to vasodilate, and to inhibit inflammatory reactions and tumor necrosis factor
  - In vitro: inhibits human dermal fibroblast proliferation and extracellular matrix production and increases collagenase activity
- Tocopherol (vitamin E)
  - to scavenge the reactive oxygen species generated during oxidative stress
  - role in the proliferation and differentiation of endometrial implantation

Fertil Steril 2002;22:1219-1226

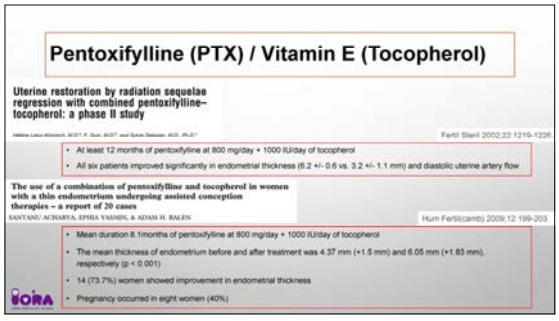

Pentoxifylline (PTX) / Vitamin E (Tocopherol)

Uterine restoration by radiation sequelae regression with combined pentoxifylline–tocopherol: a phase II study

Fertil Steril 2002;22:1219-1226

- At least 12 months of pentoxifylline at 800 mg/day + 1000 IU/day of tocopherol
- All six patients improved significantly in endometrial thickness (6.2 +/- 0.6 vs. 3.2 +/- 1.1 mm) and diastolic uterine artery flow

The use of a combination of pentoxifylline and tocopherol in women with a thin endometrium undergoing assisted conception therapies – a report of 20 cases

SANTANU ACHARYA, EPSHA YASMIN, & ADAM H. BALEN

Hum Fertil(camb) 2009;12:199-203

- Mean duration 8.1months of pentoxifylline at 800 mg/day + 1000 IU/day of tocopherol
- The mean thickness of endometrium before and after treatment was 4.37 mm (+1.5 mm) and 6.05 mm (+1.83 mm), respectively ($p < 0.001$)
- 14 (73.7%) women showed improvement in endometrial thickness
- Pregnancy occurred in eight women (40%)

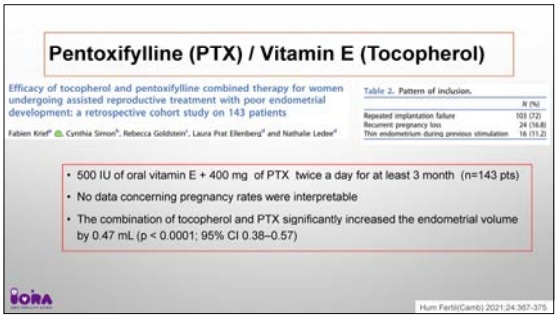

Pentoxifylline (PTX) / Vitamin E (Tocopherol)

Efficacy of tocopherol and pentoxifylline combined therapy for women undergoing assisted reproductive treatment with poor endometrial development: a retrospective cohort study on 143 patients

Fabien Krief[a], Cynthia Simon[b], Rebecca Goldstein[c], Laura Prat Ellenberg[d] and Nathalie Ledee[d]

Table 2. Pattern of inclusion.

	N (%)
Repeated implantation failure	103 (72)
Recurrent pregnancy loss	24 (16.8)
Thin endometrium during previous stimulation	16 (11.2)

- 500 IU of oral vitamin E + 400 mg of PTX twice a day for at least 3 month (n=143 pts)
- No data concerning pregnancy rates were interpretable
- The combination of tocopherol and PTX significantly increased the endometrial volume by 0.47 mL ($p < 0.0001$; 95% CI 0.38–0.57)

Hum Fertil(Camb) 2021;24:367-375

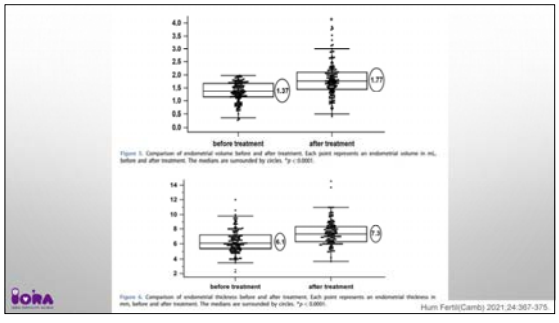

Hum Fertil(Camb) 2021;24:367-375

Platelet-Rich Plasma

- Support the regeneration and repair processes of damaged tissues, cells using growth factors present in platelet granularities

Table 1. Dohan- Ehrenfest PRP classification.

Preparation	Acronym	Leukocytes	Fibrin Density
Pure platelet rich plasma	P-PRP	Poor	Low
Leukocyte and platelet rich plasma	L-PRP	Rich	Low
Pure platelet rich fibrin	P-PRF	Poor	High
Leukocyte and platelet rich fibrin	L-PRF	Rich	High

Int J Environ Res Public Health 2022;19:5284

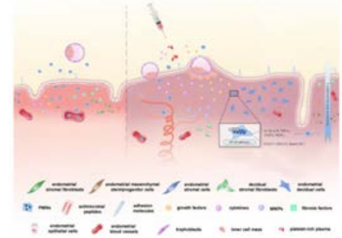

FIGURE 1 | The potential mechanisms of PRP on endometrial receptivity in assisted reproductive technology. PRP might improve the endometrial receptivity through the improvement of cell proliferation, vascularization, anti-inflammatory properties and the reduction in the degree of fibrosis, with the help of the concentrated peptides, GFs and cytokines in PRP.

Frontiers in Endocrinology 2021;12:707584

Platelet-Rich Plasma

Table 2. Specification of different PRP kits.

Kit Brand Name	Whole Blood Volume (mL)	Centrifugation	Time (min)	Final Volume of PRP (mL)	Platelet Concentration Compared to Whole Blood (Times)	Leukocyte	Activator
ACP-DS (Arthrex, Naples, FL, USA)	9	single	5	3	2-3	-	-
RegenKit® A-PRP (Regen Lab SA, Le Mont-sur-Lausanne, Switzerland)	10	single	8	5	1.6	-	-
GPS (Biomet, Zimmer GmbH, Zug, Switzerland)	27-110	single	15	3-12	3-8	+	TA/$CaCl_2$
Magellan (Medtronic, Minneapolis, MN, USA)	30-60	double	4-6	6	3-7	+	$CaCl_2$
PRGF (BTI, Biotechnology Institute, Vitoria, Alava, Spain)	9-72	single	8	4-32	2-3	-	$CaCl_2$
SmartPrep (Harvest Technologies, Plymouth, MA, USA)	20-120	double	14	3-20	4-6	+	TB/$CaCl_2$
Novang A-PRP (Novang, Kielce, Poland)	10	single	8	6-20	4	+	-

$CaCl_2$—Calcium chloride; TA—Autologous thrombin; TB—Bovine thrombin.

Int J Environ Res Public Health 2022;19:5284

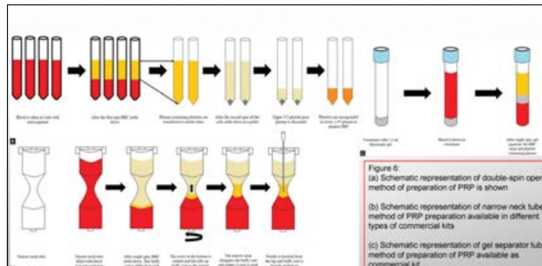

Figure 6:
(a) Schematic representation of double-spin open method of preparation of PRP is shown
(b) Schematic representation of narrow neck tube method of PRP preparation available in different types of commercial kits
(c) Schematic representation of gel separator tube method of preparation of PRP available as commercial kit

Indian Dermatol Online J 2021;12:S12-23

Platelet-rich plasma

Intrauterine infusion of autologous platelet rich plasma in women undergoing assisted reproduction: a systematic review and meta-analysis

Arezoo Maleki-Hagiagha, Maryam Razavi, Safoura Rouholamin, Mahroo Rezaeinejad, Saman Maroufizadeh, Mahdi Sepidarkish

J Reprod Immunol 2020;137:103078

- Intra-uterine administration of PRP increases the clinical pregnancy rate in women experienced frozen-thawed ET cycle
- More randomized clinical trials with larger sample sizes are needed

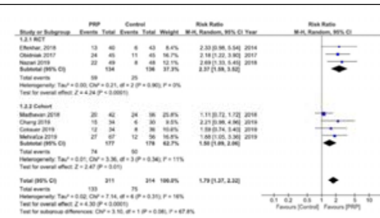

Figure 3: Forest plot detailed risk ratio (RR) and 95% confidence intervals for clinical pregnancy rate in the RCT and cohort studies for platelet rich plasma and control groups.

J Reprod Immunol 2020;137:103078

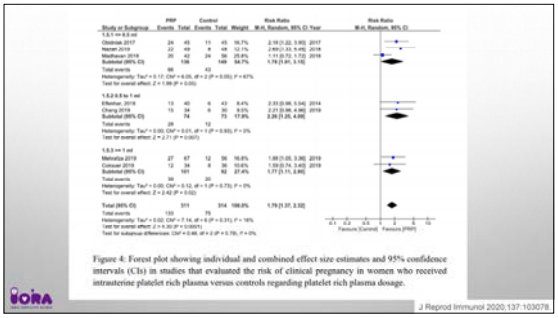

Figure 4: Forest plot showing individual and combined effect size estimates and 95% confidence intervals (CIs) in studies that evaluated the risk of clinical pregnancy in women who received intrauterine platelet rich plasma versus controls regarding platelet rich plasma dosage.

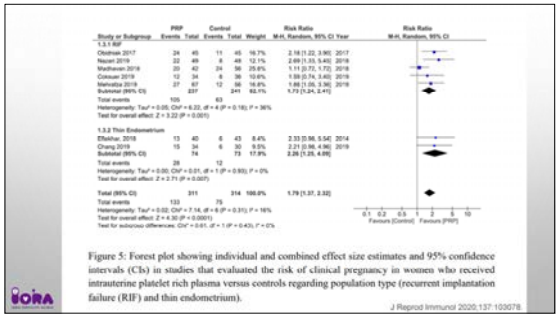

Figure 5: Forest plot showing individual and combined effect size estimates and 95% confidence intervals (CIs) in studies that evaluated the risk of clinical pregnancy in women who received intrauterine platelet rich plasma versus controls regarding population type (recurrent implantation failure (RIF) and thin endometrium).

Journal of Assisted Reproduction and Genetics
https://doi.org/10.1007/s10815-021-02146-9

REVIEW

A narrative review of platelet-rich plasma (PRP) in reproductive medicine

Fady I. Sharara[1,2] · Latashia-Lika Lelea[3] · Sara Rahman[1] · Jordan S. Klebanoff[4] · Gaby N. Moawad[2,5]

J Assist Reprod Genet 2021;38(5):1003-1012.

- Limited literature shows promise in increasing endometrial thickness, increasing AMH, and decreasing FSH levels, as well as increasing chemical and clinical pregnancy rates
- The lack of standardization of PRP preparation
- The lack of large RCTs
- PRP use should be considered experimental

Table 1. Studies evaluating PRP and thin endometrium

Author	Study design	Level of evidence	Control group (n)	Intervention group (n)	Endometrium prior to intervention (mm)	Endometrium post intervention (mm)	p value	p value		
								Clinical	Chemical	Clinical
Chang et al. (2015) [7]	Cohort	3	-	5	5.9–6.6	>7	-	80	-	
Zahedmodarres-et al. (2017)	Cohort	3	-	10	4–6	7.1–7.5	-	40	-	
Eftekhar et al. (2018) [6]	RCT	2	33	33	6.09±0.47	8.67±0.64	0.001	32.5	0.091	0.044
Chang et al. (2019) [21]	Prospective cohort	3	30	34	6.32±0.54	7.65±0.22	<0.05	44.12	-	0.036
Kim et al. (2019) [2]	Prospective cohort	3	-	20	4–6.8	4.2–9.1	0.070	30	0.020	
Nazari et al. (2019) [9]	Double-blind RCT	2	30	30	4.92±0.67	7.21±0.18	<0.001	33.3	0.031	0.048
Frantz et al. (2020) [22]	Retrospective case series	4	-	21	<5	-	-	66.7	-	

PRP platelet-rich plasma, *HRT* hormone replacement therapy, *eSF* human endometrial stromal fibroblasts, *eMSC* endometrial mesenchymal stem cells, *BM-MSC* bone marrow–derived mesenchymal stem cells, *IC* Ishikawa endometrial adenocarcinoma cells

Platelet-Rich Plasma as a Potential New Strategy in the Endometrium Treatment in Assisted Reproductive Technology

Yunying Lin[1,2†], Jia Qi[1,2†] and Yun Sun[1,2*]

[1] Center for Reproductive Medicine, Renji Hospital, School of Medicine, Shanghai Jiao Tong University, Shanghai, China,
[2] Shanghai Key Laboratory for Assisted Reproduction and Reproductive Genetics, Shanghai, China

- Most studies suggested that PRP treatment resulted in positive reproductive results in patients with thin endometrium, RIF, CE and AS
- Though increasing evidence suggests the possible value of PRP treatment on the endometrium of infertile women, more carefully designed studies, especially RCTs, on larger scales are required

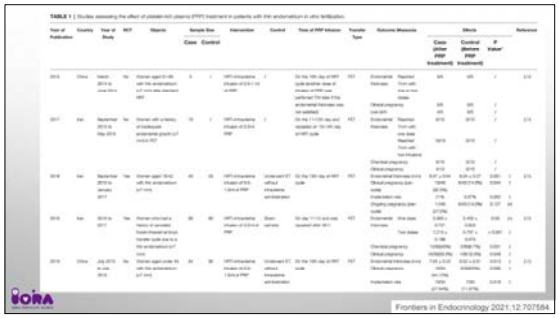

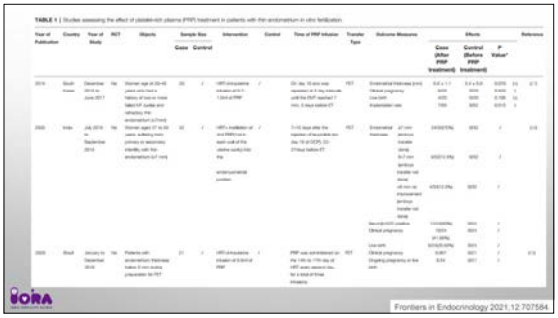


Can autologous platelet rich plasma expand endometrial thickness and improve pregnancy rate during frozen-thawed embryo transfer cycle? A randomized clinical trial
Maryam Eftekhar [a], Nosrat Neghab [a,*], Elham Naghshineh [b], Parisa Khani [a]
• Endometrial thickness increased significantly to 8.67 ± 0.64 in PRP group than in controls (p = 0.001)
• This increase was higher in women who conceived in PRP group (p = 0.031)
• The implantation rate and per-cycle clinical pregnancy rate were significantly higher in PRP group (p = 0.002 and 0.044, respectively (p = 0.002)
• PRP may be effective in improving the endometrial growth, and possibly pregnancy outcomes in women with a thin endometrium

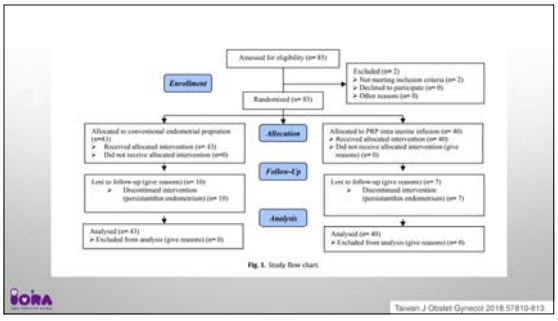
Assessed for eligibility (n= 85)
Enrollment
Excluded (n= 2)
Not meeting inclusion criteria (n= 2)
Declined to participate (n= 0)
Other reasons (n= 0)
Randomized (n= 83)
Allocation
Follow-Up
Analysis
Fig. 1. Study flow chart.

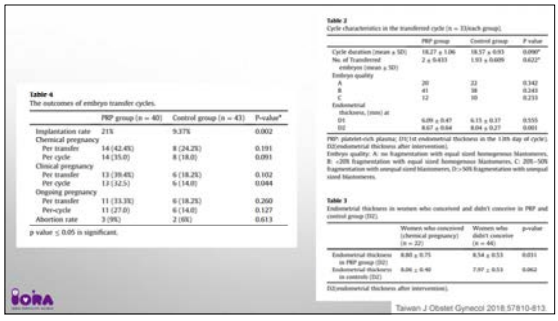

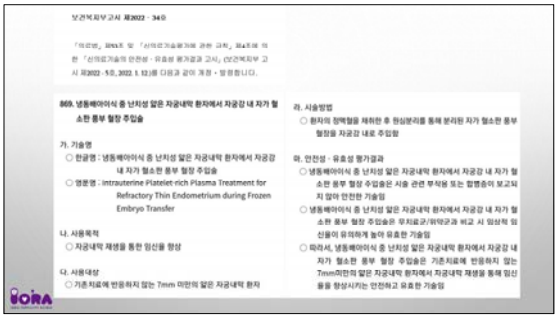

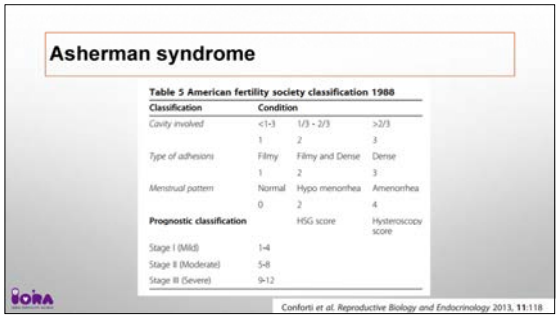
Asherman syndrome
Table 5 American fertility society classification 1988
Conforti et al. Reproductive Biology and Endocrinology 2013, 11:118

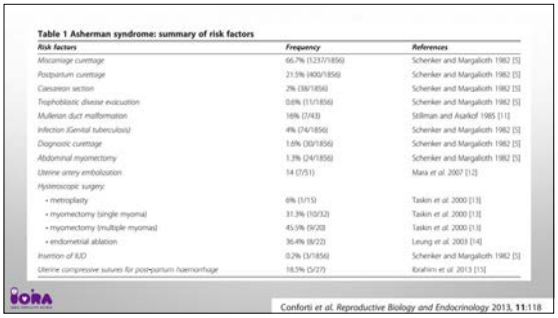

Table 1 Asherman syndrome: summary of risk factors

Risk factors	Frequency	References
Miscarriage curettage	66.7% (1237/1856)	Schenker and Margalioth 1982 [5]
Postpartum curettage	21.5% (400/1856)	Schenker and Margalioth 1982 [5]
Caesarean section	2% (38/1856)	Schenker and Margalioth 1982 [5]
Trophoblastic disease evacuation	0.6% (11/1856)	Schenker and Margalioth 1982 [5]
Mullerian duct malformation	16% (7/43)	Stillman and Asarkof 1985 [11]
Infection (Genital tuberculosis)	4% (74/1856)	Schenker and Margalioth 1982 [5]
Diagnostic curettage	1.6% (30/1856)	Schenker and Margalioth 1982 [5]
Abdominal myomectomy	1.3% (24/1856)	Schenker and Margalioth 1982 [5]
Uterine artery embolisation	14 (7/51)	Mara et al. 2007 [12]
Hysteroscopic surgery:		
• metroplasty	6% (1/15)	Taskin et al. 2000 [13]
• myomectomy (single myoma)	31.3% (10/32)	Taskin et al. 2000 [13]
• myomectomy (multiple myomas)	45.5% (9/20)	Taskin et al. 2000 [13]
• endometrial ablation	36.4% (8/22)	Leung et al. 2003 [14]
Insertion of IUD	0.2% (3/1856)	Schenker and Margalioth 1982 [5]
Uterine compressive sutures for postpartum haemorrhage	18.5% (5/27)	Ibrahim et al. 2013 [15]

Conforti et al. Reproductive Biology and Endocrinology 2013, 11:118

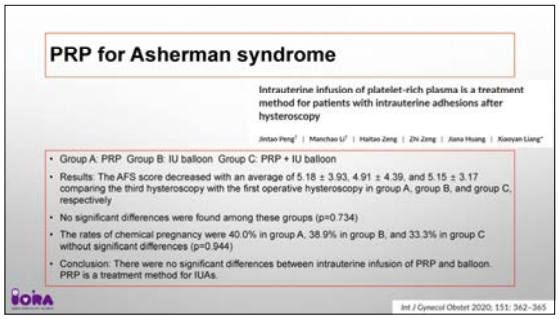

PRP for Asherman syndrome

Intrauterine infusion of platelet-rich plasma is a treatment method for patients with intrauterine adhesions after hysteroscopy

Jintao Peng[1] | Manchao Li[1] | Haitao Zeng | Zhi Zeng | Jiana Huang | Xiaoyan Liang*

- Group A: PRP Group B: IU balloon Group C: PRP + IU balloon
- Results: The AFS score decreased with an average of 5.18 ± 3.93, 4.91 ± 4.39, and 5.15 ± 3.17 comparing the third hysteroscopy with the first operative hysteroscopy in group A, group B, and group C, respectively
- No significant differences were found among these groups (p=0.734)
- The rates of chemical pregnancy were 40.0% in group A, 38.9% in group B, and 33.3% in group C without significant differences (p=0.944)
- Conclusion: There were no significant differences between intrauterine infusion of PRP and balloon. PRP is a treatment method for IUAs.

Int J Gynecol Obstet 2020; 151: 362–365

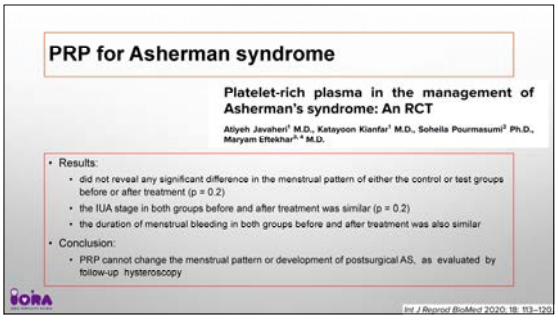

PRP for Asherman syndrome

Platelet-rich plasma in the management of Asherman's syndrome: An RCT

Atiyeh Javaheri[1] M.D., Katayoon Kianfar[1] M.D., Soheila Pourmasumi[2] Ph.D., Maryam Eftekhar[3,4] M.D.

- Results:
  - did not reveal any significant difference in the menstrual pattern of either the control or test groups before or after treatment (p = 0.2)
  - the IUA stage in both groups before and after treatment was similar (p = 0.2)
  - the duration of menstrual bleeding in both groups before and after treatment was also similar
- Conclusion:
  - PRP cannot change the menstrual pattern or development of postsurgical AS, as evaluated by follow-up hysteroscopy

Int J Reprod BioMed 2020; 18: 113–120

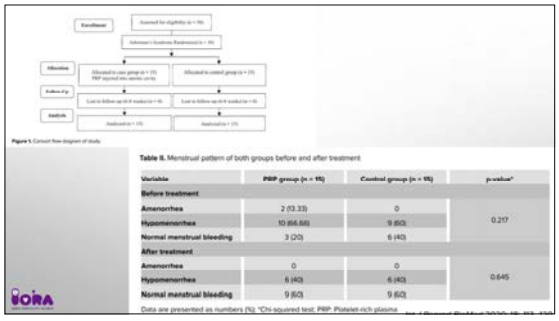

Figure 1. Consort flow diagram of study.

Table II. Menstrual pattern of both groups before and after treatment

Variable	PRP group (n = 15)	Control group (n = 15)	p-value*
Before treatment			
Amenorrhea	2 (13.33)	0	0.217
Hypomenorrhea	10 (66.66)	9 (60)	
Normal menstrual bleeding	3 (20)	6 (40)	
After treatment			
Amenorrhea	0	0	0.645
Hypomenorrhea	6 (40)	6 (40)	
Normal menstrual bleeding	9 (60)	9 (60)	

Data are presented as numbers (%). *Chi-squared test. PRP: Platelet-rich plasma

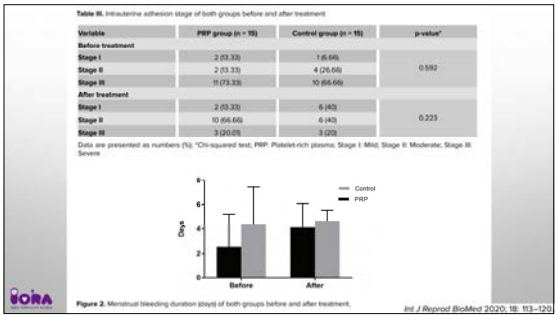

Table III. Intrauterine adhesion stage of both groups before and after treatment

Variable	PRP group (n = 15)	Control group (n = 15)	p-value*
Before treatment			
Stage I	2 (13.33)	1 (6.66)	0.592
Stage II	2 (13.33)	4 (26.66)	
Stage III	11 (73.33)	10 (66.66)	
After treatment			
Stage I	2 (13.33)	6 (40)	0.223
Stage II	10 (66.66)	6 (40)	
Stage III	3 (20.01)	3 (20)	

Data are presented as numbers (%). *Chi-squared test; PRP: Platelet-rich plasma; Stage I: Mild; Stage II: Moderate; Stage III: Severe

Figure 2. Menstrual bleeding duration (days) of both groups before and after treatment.

Int J Reprod BioMed 2020; 18: 113–120

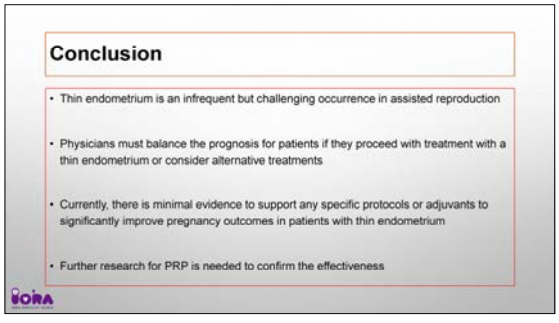

Conclusion

- Thin endometrium is an infrequent but challenging occurrence in assisted reproduction
- Physicians must balance the prognosis for patients if they proceed with treatment with a thin endometrium or consider alternative treatments
- Currently, there is minimal evidence to support any specific protocols or adjuvants to significantly improve pregnancy outcomes in patients with thin endometrium
- Further research for PRP is needed to confirm the effectiveness


THANK YOU FOR ATTENTION

Dev. Reprod. Vol 26, 2022 (Suppl. 1). pp 129

불응성 자궁내막 및 아셔만 증후군의 치료: II. 수술 치료 및 재발방지

권혁찬
미래와희망산부인과

불응성 자궁내막 및 아셔만 증후군의 치료
II. 수술 치료 및 재발방지

권 혁 찬
미래와희망산부인과

IUA Classification I

- American Fertility Society (1988)

Scoring/ Characteristics	Extent Cavity Involved	Type of Adhesions	Menstrual Pattern
1	<1/3	Filmy	-
2	1/3 ~2/3	Filmy~Dense	Hypomenorrhea
3	>2/3	Dense	-
4	-	-	Amenorrhea
Stage I (mild: 1~4) , Stage II (Moderate: 5~8), Stage III (Severe: 9~12)			

IUA Classification II

- European Society of Gynecological Endoscopy (ESGE) (1995,2017)

I	Thin or filmy adhesion, easily ruptured by hysteroscopic sheath alone and normal cornual area.
II	Singular dense adhesion that cannot be ruptured by the hysteroscopic sheath, but a uterine cavity connected to a separate space, and visualization of both tubal ostia.
IIa	Occluding adhesion only in the region of the internal cervical os with normal upper uterine cavity
III	Multiple dense adhesions connected to a separate space of the uterine cavity and unilateral obliteration of tubal ostia.
IV	Extensive dense adhesion with partial occlusion of the uterine cavity and tubal ostia
Va	Extensive endometrial scarring and firosis in combination with grade I/II , accompanied by amenorrhea or pronounced hypomenorrhea.
Vb	Extensive endometrial scarring and fibrosis in combination with grade III / IV, accompanied with amenorrhea.

Techniques using IUA Classification for Treatment

Approach	Sensitivity (%)	Specificity (%)
TVS	91~100	78.6~100
SHG	12.8~98	94~100
HSG	21.6~98.0	25.6~98.8
H/S	Gold standard	

HSG → PreOV/TVS → Dx/Tx H/S
SHG

Doroftei B et al. Diagnostics 2020;10:706
Lee et al. Int. J. Mol. Sci. 2021; 22:5175

Treatment Strategy of IUA

1. Treatments (D/C, H/S, hysterotomy)
2. Re-adhesion prevention (IUD, Uterine balloon stent, Foley's catheter, anti-adhesion barriers)
3. Restoring NL. EM. (ERT, ASC)
4. Post OP. assessment & repeat H/S

Hysteroscopic Tx for IUA

- The method of choice
- Outcome
  - NL mense: 75%–100%.
  - CPR : between 25 and 76%
  - LBR after preg : between 25 and 79.7%.
- Recurrence rate (ESGE)
  GI-GIIa: 21%–25%, GIII: 29.1%,
  GIV: 38.5%, and GIV 41.9%

Dreisler and Kjer. Int J Women's Health 2019:11:191–198.
Hanstede MMF et al. Fertil Steril. 2015; 104(6):1561–1568.

Readhesion Prevention & Restoring EM

- RCT of Hyaluronic acid gel and no Tx.
  - 32% Vs. 14%, P < 0.05 [1]
- RCT/Retrospective cohort study for mechanical barriers and Hyaluronic acid
  - Equally effective in mechanical barriers [2]
  - Significantly more effective than Hyaluronic acid [3]
- Estrogen alone and ancillary use with mechanical barriers
  - In CPR, 42~53% Vs. 51~100% [4,5,6,7]

1. Acunzo G et al. Hum Reprod. 2003;18(9):1918–1921.
2. Lin XN et al. Fertil Steril. 2015;104(1):235–240.
3. Lin XN et al. Eur J Obstet Gynecol Reprod Biol. 2013;170(2):512-6.
4. Chen L et al. J Minim Invasive Gynecol. 2017;24(2):299–304.
5. Dawood A et al. J Obstet Gynaecol Can. 2010;32(8):767–770.
6. Orhue AAE et al. Int J Gynaecol Obstet. 2003;82(1):49–56.
7. Zikopoulos KA et al. Reprod Biomed Online. 2004;8(6):720–725.

Second-look Hysteroscopy

- Retrospective cohort study of 151 pts. [1]
  - Second-look within 2 weeks to 2 months after primary adhesiolysis
  - Improve the cumulative PR (77% Vs. 56%) and LBR (77% vs 63%)
- A small observational study of 15 pts. [2]
  - Second-look after 2 weeks
  - Up to four H/S after primary surgery.
  - 46% (7/15) were either pregnant or had delivered

1. Xu W et al. Int J Surg. 2018;50:49–54.
2. Robinson Jk et al. Fertil Steril. 2008;90(2):409–414.

Personal Treatment Strategy

1. TVS/HSG
2. Diagnostic/operative H/S
3. Foley's catheter (8F, 2.5~3cc) (for minimal/HA) W/ E2VD 5mg IM
4. 7-10 days later, catheter removal and E2VD 5mg IM (weekly 3 times)
5. P4 WBL (100mg) & repeat H/S

Dev. Reprod. Vol 26, 2022 (Suppl. 1). pp 131

Intrauterine adhesion

조정현
사랑아이여성의원
(medicho@hotmail.com)

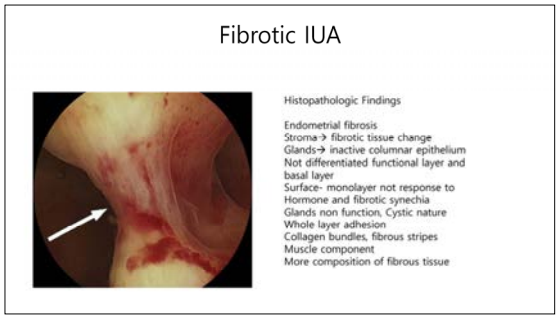

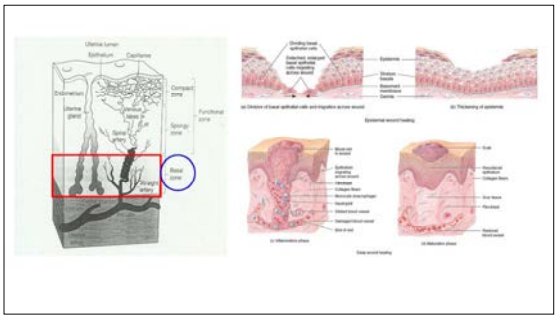

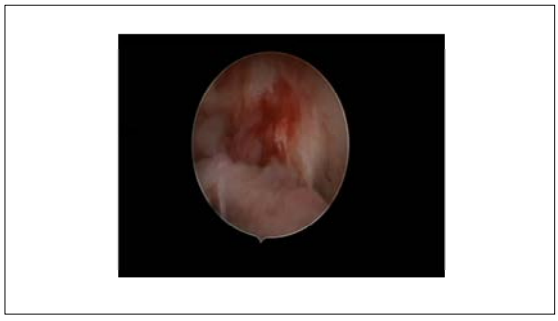

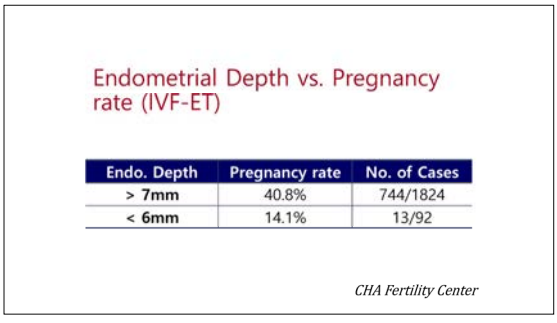

Endo. Depth	Pregnancy rate	No. of Cases
> 7mm	40.8%	744/1824
< 6mm	14.1%	13/92

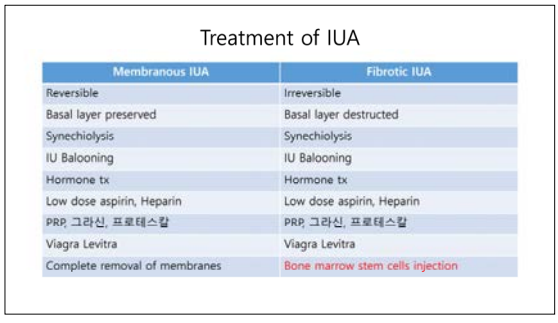

Membranous IUA	Fibrotic IUA
Reversible	Irreversible
Basal layer preserved	Basal layer destructed
Synechiolysis	Synechiolysis
IU Balooning	IU Balooning
Hormone tx	Hormone tx
Low dose aspirin, Heparin	Low dose aspirin, Heparin
PRP, 그라신, 프로테스칼	PRP, 그라신, 프로테스칼
Viagra Levitra	Viagra Levitra
Complete removal of membranes	Bone marrow stem cells injection

Autologous Bone Marrow Cells injections (BMI) into the uterine Wall in case of Thin endometrium

J.H. CHO M.D, Ph.D
CHA Medical University
Seoul Korea

Treatment of Leukemia Patients

Leukemia → Chemotherapy → Healthy Donor Bone marrow Transplantation → Endometrial Biopsy

Endometrial Biopsy : 4 patients
Donor derived endometrial cells
Epithelium : 0.2 - 48%
Stromal cell : 0.3 – 52%

H.S. Taylor
JAMA 292(10), 2004

BM Cells Injection : Where ?

Injection

Infusion

BM Cells Injection : How ?

	Injection	Infusion
Path	Transmurally(TM)	Transcervically(TC)
By	Needle	Catheter
Sites	Myometrium near E-M junction	Endometrial Cavity
Volome(cc)	3.5, 2.5, 1.0	0.2
When	Mid proliferative Estrogen priming 中 COH 中	Early proliferative phase COH 初期
Try	45	4
Pregnancy	15	2

BMI 施術數 : 患者數

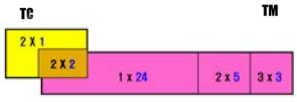

BM Cells Injection : When ?

- Early Follicular Phase : COH in IVF-ET
- Endometrial Estrogen Priming :
  Forzen-thawed ET

年度別 患者數

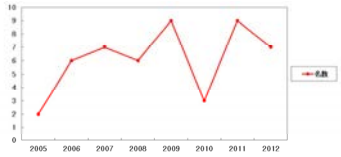

Pregnancy

- COH- IVF-ET FET OD-ET
- IVF-ET FET

	Pregnancy	Aborted	Delivered
IVF-ET	8	1	7
IVF-ET oocytes donation	1	1	0
Frozen-thawed ET	5	3	2
Natural pregnancy	2	1	1
Total	16	6	10

Pregnancy Delivery

No.	Date of BMI	uET	months	Type of pregnancy
2	2005.12.20	2006.8.21	32	IVF-ET
7	2006.8.1	2007.2.27	6	IVF-ET
8	2006.12.7	2007.1.3(I.NMP)	4	Natural pregnancy
9	2007.11.14	2010.4.8	28	Frozen embryo transfer
11	2007.9.10	2011.3.16	31	FET
12	2007.9.20	2007.10.5	1	IVF-ET
15	2008.5.2	2008.5.14	1	IVF-ET
24	2009.3.5	2009.8.24	4	IVF-ET
26	2009.11.5	2009.12.15	1	IVF-ET
32	2011.8.29	2011.10.4	2	IVF-ET

Pregnancy Aborted

No.	Date of BMI	uET	months	Type of pregnancy	
6	2007.5.8	2007.7.4	2	FET	46XX
10	2008. 1.11	2008.1.29	1	FET	IUP at 8weeks
14	2008.1.30	2008.2.6	1	IVF-ET with Donor	OD ,Progest. Allergy
23	2009.2.27	2009.5.14	2	Natural pregnancy	IUP at 8weeks 47XY+2
31	2011.5.19	2012.6.12	1	IVF-ET	IUP at 7weeks 47XX+22
35	2012.2.7	2012.2.20	1	FET	IUP at 8weeks 92XXXX

Duration:BMI-Pregnancy

Month	No. Patient	%
1	7	44%
2	3	19%
4	2	13%
6	1	6%
28	1	6%
31	1	6%
32	1	6%
Total	16	100%

BM injection and TET

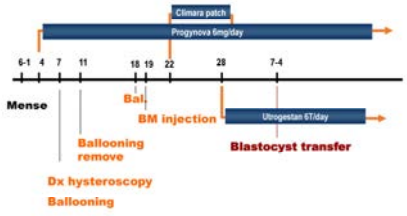

Conclusion Ⅰ

- Pretreatment procedures : hysteroscopy, fundal dome cuttings, IU Balooning
- Additive theraphy :
  estrogen priming : progynova, climara patch
  luteal support : progesterone in oil, suppository, gel
  Immunotherapy : IVIG, solondo(steroid)
  vasodilator : viagra, levitra
  clotting prevention : astrix, fragmin(heparin)
- BMI, 49 cases of 37 patients
- 16 patients were pregnant, 10 patients were delivered, 6 patients aborted
- BMI is one of the treatments in repeatedly failed case of thin endometrium

Patients profiles : Bone marrow cells

Patient	BMI Vol (ml)	Initial cell count(uL)	Product count(uL)	T.MNC	Injection Volume (ml)
1	50	9,670	5,690	5.7	0.2
3	65	11,380	11,000	11	0.2
4	40	12,390	11,940	11.9	1
6	50	9,960	6,370	6.4	2.5
6-1	60	15,660	5,520	5.5	3.5
8	50	9,160	8,770	8.8	0.2
8-1	50	17,030	8,430	8.4	2.6
10	50	23,990	28,520	28.5	3.5
12	50	18,160	12,580	12.6	3.5
13	50	10,730	9,720	9.7	3.5
14	50	17,310	16,900	16.9	3.5
15	55	16,210	4,512	4.5	4
16	50	10,870	12,930	12.9	3.5
18	45	7,590	3,430	3.4	4
19	50	26,210	6,170	6.2	3.5
20	40	9,390	7,270	7.2	3.5
20-1	50	19,170	10,900	10.9	3.5
21	50	24,030	11,700	11.7	3.5
22	40	13,860	7,110	7.1	3.5
23	50	12,160	9,870	9.9	3.5

Patient	BMI Vol (ml)	Initial cell count(uL)	Product count(uL)	T.MNC	Injection volume (ml)
2	70	13,420	15,360	15.3	3.5
25	50	14,760	3,550	3.6	3.5
27	48	22,180	11,650	11.6	3.5
27-1	48	21,010	7,670	7.7	3.5
28	50	35,600	25,580	25.6	3.5
29	50	42,190	12,530	12.5	3.5
29-1	60	13,390	9,360	9.4	3.5
29-2	60	22,950	11,650	11.7	3.5
30	60	54,030	25,540	25.5	3.5
31	30	4,540	2,160	2.1	3.5
31-1	60	4,440	6,000	6	3.5
31-2	50	6,590	3,590	3.6	3.5
31-3	60	5,800	3,460	3.5	3.5
32	60	11,350	24,550	24.5	3.5
33	60	13,130	8,190	8.2	3.5
34	60	34,960	20,140	20	3.5
35	50	36,230	33,310	33.3	3.5
36	40	16,980	5,820	5.8	3.5
37	50	8,810	1,580	1.6	3.5
Mean	**50**	**17,366**	**10,362**	**10.34**	**2.83**

Patients profiles I

Patient	Age	不妊期間 (年)	No. ART (他病院)	No. IVF-ET	No. FET
1	40	3	4	6	
2	31	4		4	2
3	40	5		7	2
4	31			1	2
5	33	3	7	2	1
6	35	5	2	10	7
7	44	11		2	2
8	36	8	4	1	1
9	38	3	1	2	1
10	34	6		2	1
11	40	6	3	2	5
12	35	4	4	1	1
13	25	2		4	5
14	46	6		3	1
15	42	4		2	1
16	41	6	11	7	1
17	30	3	4	1	1
18	27	6	3	4	1
19	34	7	1	1	2
20	30	4	1	1	

Patient	Age	不妊期間 (年)	No. ART (他病院)	No. IVF-ET	No. FET
21	34	6	6	5	5
22	40	6	1	2	1
23	43	2		7	
24	34	8	10	3	
25	31	4	4	2	2
26	38	1	1	2	1
27	32	1		2	6
28	27	2	3	5	1
29	40	4	5	5	4
30	40	4	6	1	
31	37	3	5	6	2
32	34	5	5	4	2
33	35	8	5	2	1
34	35	2	6	1	1
35	32	4		1	2
36	35	5	2	2	
37	37	7	3	3	4
Mean	**36**	**4.69**	**4.07**	**3.24**	**2.29**

Patients profiles II : eggs, endometrium

Patient	No. retrieved oocytes	No. transferred eggs	No. good embryos	BMI 前 maximum ED	BMI 前 FET ED	BMI 後 maximum ED	BMI 後 FET ED
1	42	21	10	7	6	7	
2	82	23	16				
3	63	32	12			8	
4	18	8	6				6
5	26	11	6			6	5
6	148	64	36	7	5	6	5
7	21	6	6	5	4	4	5
8	12	8	2	4	5		5
9	39	10	5	5	5	5	6
10	36	6	6	4	5	4	5
11	62	20	8	7	6	7	8
12	14	5	5	7	7	7	7
13	70	29	22	6	5	6	6
14	44	7	7	6	6	7	7
15	41	9	7	7	7	8	
16	22	15	10	6	6	5	5
17	9	3	1	6	6	6	5
18	19	11	5	6		7	
19	24	12	7	5	5	5	5
20	7	3	1	4	4	5	5

Patients profile II : eggs, endometrium

Patient	No. retrieved oocytes	No. transferred eggs	No. good embryos	BMI 前 maximum ED	BMI 前 FET ED	BMI 後 maximum ED	BMI 後 FET ED
21	164	31	16	7	7	6	6
22	5	5	1	4	6	5	6
23	63	21	12	9	8	7	7
24	17	9	6	11	8	8	8
25	62	10	9	11	10	8	6
26	10	7	3	4	5	5	6
27	69	20	16	3	7	7	7
28	32	14	11	8	7	6	6
29	58	17	10	4	5	6	6
30	8	4	2				
31	43	20	16	7	7	6	6
32	51	15	10	3	4	5	
33	52	10	10	4	4	3	4
34	3	3	3	4	4	7	7
35	16	6	1	4	4	5	5
36	17	6	4	5	5	6	6
37	55	25	15	7	7	5	5
Mean	**40.64**	**14.21**	**8.73**	**5.84**	**5.80**	**5.93**	**5.86**

감사합니다

조정현 사랑아이 여성의원 IVF Center

의학 심포지엄 Session 2

최신 치료법들의 임신 성적

Dev. Reprod. Vol 26, 2022 (Suppl. 1). pp 137

AI time-lapse

Mi Kyung Chung
Seoul Rachel Fertility Center
(mkchung2@gmail.com)

The usefulness of artificial intelligence (AI) -based approaches is making them increasingly popular in the medical field; their use is also increasing in the assisted reproductive technology (ART) field to improve *in vitro* fertilization (IVF) outcomes. Artificial intelligence (AI) technology combined with time-lapse not only aims to enhance embryo selection, but can also help the diagnostic accuracy of preimplantation genetic testing (PGT). In particular, it can reportedly offer advantages such as standardized embryo grading, clearer data entry, better patient experiences, greater efficiency in the laboratory, and automated quality control. However, AI, and machine learning are still developed in small and professional samples, their performance is variable, external verification remains insufficient, and the black box characteristics of AI models are inherently difficult to interpret; hence unintended bias can be introduced into the model during training. Although AI seems to offer good predictions, significant limitations, including a common lack of understanding. This can happen in the AI analysis of blastocyst images where we can see patterns we don't want. AI time-lapse may be a promising tool to solve long-standing challenges in reproductive medicine and achieve more objective and promising outcomes for healthy baby births. However, AI time-lapse has not yet fully established its role in the world of reproductive medicine; further, the use of AI time-lapse to improve outcomes has not yet been demonstrated in much papers. Identifying the directed use of this highly promising tool requires new methodologies and studies to identify the advantages and potential limitations of emerging technologies.

Key words: artificial intelligence (AI), time-lapse, IVF outcome, embryo selection

Dev. Reprod. Vol 26, 2022 (Suppl. 1). pp 138

ERA, CD138 등 자궁내막검사

김자연
감자와눈사람여성의원
(dr.jykim76@gmail.com)

Dev. Reprod. Vol 26, 2022 (Suppl. 1). pp 139

최신 프로토콜

박경의
디온여성의원

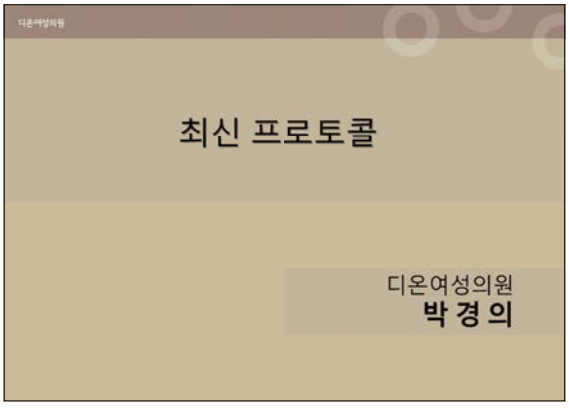

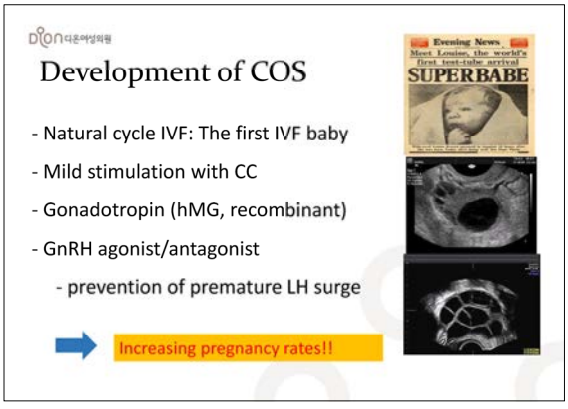

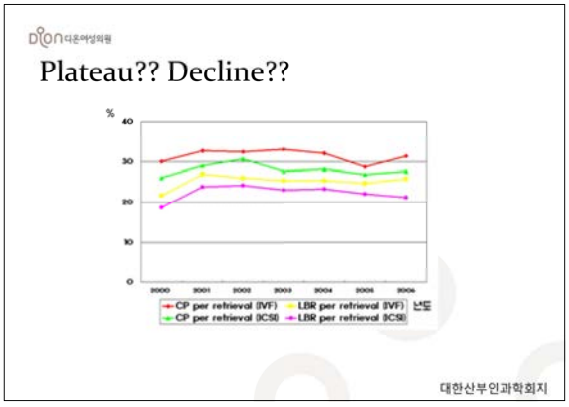

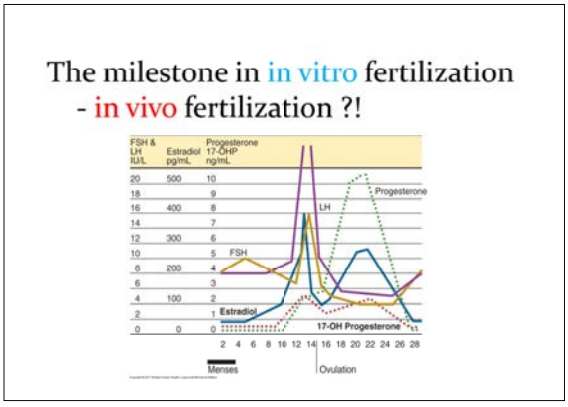

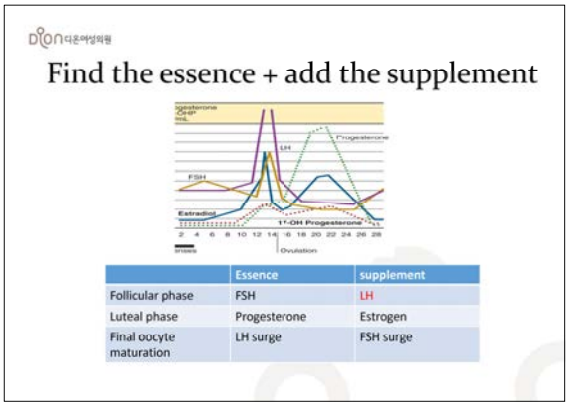

	Essence	supplement
Follicular phase	FSH	LH
Luteal phase	Progesterone	Estrogen
Final oocyte maturation	LH surge	FSH surge

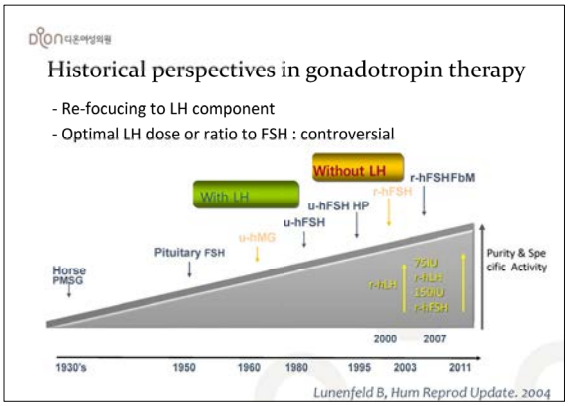

LH

- Background
  - LH-dose-dependent increase of follicular fluid E2, A, T
  - MI oocytes were obtained from follicles that had significantly lower E2 & higher T & A
  - Oocytes with multiple anomalies were recovered from follicles with significantly higher LH levels

Optimal levels of LH action achieves adequate maturation & maximal competence.

- Clinical studies
  - MERIT study (hp-hMG vs. rFSH)
    - Higher concentration of E2, A, T
    - More good-quality embryos
    - PR comparable

LH may be helpful for pts with low serum androgen

LH

- Low serum androgen condition
  - Old age (>35YO)
    - Serum A decline steeply with age
  - GnRHa long protocol
    - Even in antagonist cycle, beneficial in old age(>35YO)
  - Cycle after OC

Better oocyte maturation rate, fertilization rate, implantation rate, clinical pregnancy rate in several clinical studies

LH

- LH inhibits premature luteinization
  - LH lower P level on hCG day
  - LH enhances the conversion on pregnenolone into androgens
  - P increase at the end of stimulation was significantly related to dose of FSH but not of LH
  - Recent large cohort study showed that lowest risk of having high P at the end of stim is achieved when LH is administered in a ratio of 0.3-0.6 with respect to the dose of FSH.

Find the essence + add the supplement

	Essence	supplement
Follicular phase	FSH	LH
Luteal phase	Progesterone	Estrogen
Final oocyte maturation	LH surge	FSH surge

Triggering

- Mimicking endogenous LH surge to induce final oocyte maturation & resumption of meiosis

Immature oocyte

Mature oocyte

Traditional hCG(LH) trigger

- Prolonged half-life of hCG
  - Half-life of LH ~60min vs. half-life of hCG >24h
  - Sustained luteotropic activity & induce OHSS

LH

hCG

FSH surge

Most mammalian species spontaneous ovulation is preceded by surges of both FSH and LH.

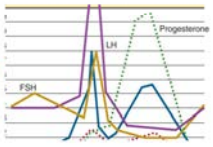

1. FSH induce LH receptor in luteinizing granulosa cell
   → optimizing the function of CL
2. FSH seems to promote oocyte nuclear maturation
   - Resumption of meiosis
   - Cumulus expansion
   - clinically more mature oocytes were retrieved
   (Humaidan et al., 2005, 2009, 2010; Oktay et al., 2010)

Introduction of GnRHa trigger

- GnRHa given IV can induce LH surge
  (Nakano et al., 1973)
- GnRHa trigger first used when GnRH ant protocol introduced
  (Gonen et al., 1990)

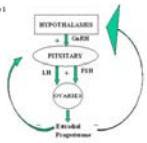

More physiologic LH + FSH surge

GnRHa trigger

- Leuprorelin (Lorelin) 0.5~ 1.0 mg
- Triptorelin (Decapeptyl) 0.2 mg
- Buserelin (Superfact) 0.5 mg

Humaidan et al., 2011

GnRHa trigger

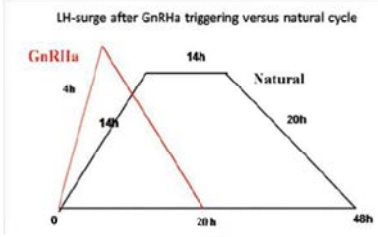

Humaidan et al., 2011

Advantage of GnRHa trigger (vs. hCG)

1. FSH surge
2. Prevent OHSS
   - lower luteotropic potency & duration
3. Decrease the post-trigger E2 exposure
   - Breast cancer pts

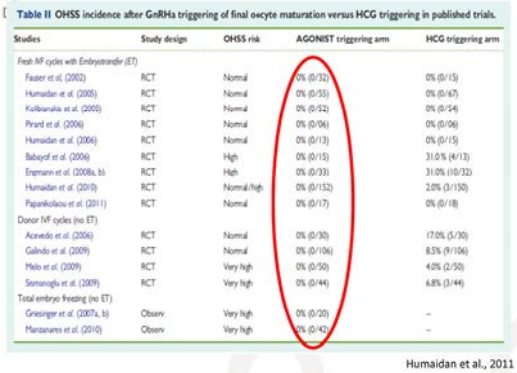

Table II OHSS incidence after GnRHa triggering of final oocyte maturation versus HCG triggering in published trials.

Studies	Study design	OHSS risk	AGONIST triggering arm	HCG triggering arm
Fresh IVF cycles with Embryotransfer (ET)				
Fauser et al. (2002)	RCT	Normal	0% (0/32)	0% (0/15)
Humaidan et al. (2005)	RCT	Normal	0% (0/55)	0% (0/67)
Kolibianakis et al. (2005)	RCT	Normal	0% (0/52)	0% (0/54)
Pirard et al. (2006)	RCT	Normal	0% (0/06)	0% (0/06)
Humaidan et al. (2006)	RCT	Normal	0% (0/13)	0% (0/15)
Babayof et al. (2006)	RCT	High	0% (0/15)	31.0 % (4/13)
Engmann et al. (2008a, b)	RCT	High	0% (0/33)	31.0% (10/32)
Humaidan et al. (2010)	RCT	Normal/high	0% (0/152)	2.0% (3/150)
Papanikolaou et al. (2011)	RCT	Normal	0% (0/17)	0% (0/18)
Donor IVF cycles (no ET)				
Acevedo et al. (2006)	RCT	Normal	0% (0/30)	17.0% (5/30)
Galindo et al. (2009)	RCT	Normal	0% (0/106)	8.5% (9/106)
Melo et al. (2009)	RCT	Very high	0% (0/50)	4.0% (2/50)
Stomanoglu et al. (2009)	RCT	Very high	0% (0/44)	6.8% (3/44)
Total embryo freezing (no ET)				
Griesinger et al. (2007a, b)	Observ	Very high	0% (0/20)	–
Manzanares et al. (2010)	Observ	Very high	0% (0/42)	–

Humaidan et al., 2011

Disadvantage of GnRHa trigger (vs. hCG)

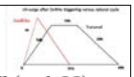

- Low E2 & P4 during luteal phase (Itskovitz et al., 1991)
- Extremely high early PL (Fause et al., 2002; Humaidan et al., 2005; Kolibianakis et al., 2005)
- Luteal phase insufficiency despite standard LPS

Luteal phase insufficiency

Modified LPS can rescue

- One bolus of hCG
- Repeated boluses of hCG
- Recombinant LH
- Intensive P + E2

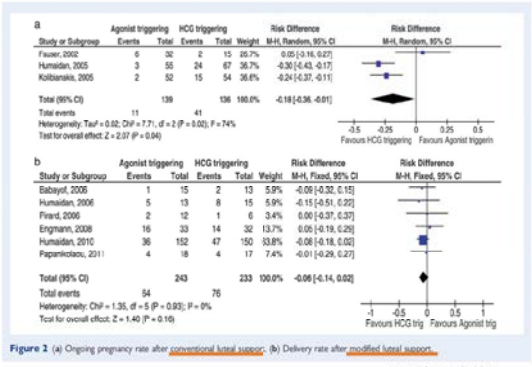

Figure 2 (a) Ongoing pregnancy rate after conventional luteal support; (b) Delivery rate after modified luteal support

Humaidan et al., 2011

Disadvantage of GnRHa trigger (vs. hCG)

- Suboptimal response to GnRHa trigger
- Low basal LH/FSH d/t long-term use of OC

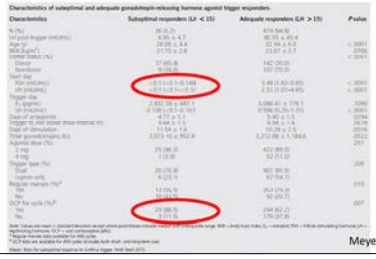

Meyer et al., 2015

Dual trigger

High responder

- GnRHa + reduced dosage of hCG
  : usually for reduction of OHSS
  : low dose hCG also make OHSS
  : vs. GnRHa trigger + intensive LPS vs. all freezing

Conflicting!

Normal or poor responder

- GnRHa + standard dosage of hCG
  : summation each advantage
  : oocyte maturation via FSH surge (GnRHa)
  + sufficient LPS (hCG)

Dual trigger for normal responder

Comparison of the standard and dual-trigger methods: outcomes of in vitro fertilization/intracytoplasmic sperm injection cycles.

Variable	Control group (hCG)	Study group (hCG + triptorelin)	*P* value
Implantation rate (%)	18.43 (106/575)	29.68 (160/539)	<.001
Clinical pregnancy rate per ET (%)	40.11 (75/187)	50.79 (97/191)	.047
Abortion rate (%)	18.67 (14/75)	16.49 (16/97)	NS
Live-birth rate per ET (%)	30.49 (57/187)	41.36 (79/191)	.042
Blastocyst progression rate (%)	55.6 (299/538)	52.9 (379/720)	NS
OHSS rate (%)	0.005 (1/187)	0 (0/191)	NS

Note: Values are expressed as percentage. ET = embryo transfer; hCG = human chorionic gonadotropin; OHSS = ovarian hyperstimulation syndrome.

Lin. Dual trigger improves live-birth rates. Fertil Steril 2013.

Lin et al., 2013

Dual trigger for normal responder

- Standard dose of hCG + GnRHa
- Overcome implantation defect from GnRH antagonist

Combined administration of gonadotropin-releasing hormone agonist with human chorionic gonadotropin for final oocyte maturation in GnRH antagonist cycles for in vitro fertilization.

Author information

Abstract

OBJECTIVE: To evaluate the effects of combined administration of gonadotropin-releasing hormone (GnRH) agonist with human chorionic gonadotropin (hCG)for final oocyte maturation in GnRH antagonist cycles for in vitro fertilization (IVF).

STUDY DESIGN: A total of 120 infertile women undergoing GnRH antagonist multiple-dose protocol for controlled ovarian stimulation were recruited and randomized into 2 groups: a study group (n=60) and a control group (n=60). For the study group, both GnRH agonist and recombinant hCG (rhCG) were injected concomitantly for final oocyte maturation when 1 or more follicles reached a mean diameter of 18 mm. For the control group, rhCG alone was administered for final oocyte maturation.

RESULTS: There were no significant differences in patient characteristics. The 2 groups were also similar with respect to the number of oocytes retrieved, fertilized oocytes and good-quality embryos. Embryo implantation rate (24.7% vs. 14.9%), clinical pregnancy rate per cycle (53.3% vs. 33.3%), and live birth rate (50.0% vs. 30.0%) were significantly higher in the study group than in the control group (p = 0.006, p = 0.027, and p = 0.025, respectively).

CONCLUSION: Combined administration of GnRH agonist with rhCG may be beneficial in improving endometrial receptivity and pregnancy rate in GnRH antagonist cycles for IVF.

Administration of single-dose GnRH agonist in the luteal phase in ICSI cycles: a meta-analysis

João Batista A Oliveira[1,2,3*], Ricardo Baruffi[2,3], Cláudia G Petersen[1,2,3], Ana L Mauri[2,3], Mario Cavagna[2], José G Franco Jr[1,2,3]

Implantation rate | Clinical PR | Ongoing PR

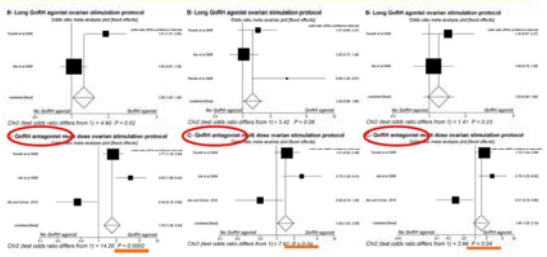

Oliveira et al., 2010

Dual trigger for prior low oocyte maturation rate

- > 25% immature oocyte in prior IVF cycle
- However, IVF outcomes remain poor, suggesting an underlying oocyte dysfunction.

Ovarian stimulation outcomes and endocrine profiles between the dual trigger and prior IVF cycle.

Variable	Prior cycle (n = 27)	Dual trigger (n = 27)	P value
Outcome of ovarian stimulation			
Total days of stimulation	10 (8–11)	10 (9–11)	NS
Total dose of gonadotropins (IU)	4,200 (2,575–6,000)	5,400 (3,300–6,750)	.02
Oocytes retrieved (n)	9 (4–14)	11 (5–16)	.02
Mature oocytes (n)	3 (1–5)	7 (4–9)	< .01
% of mature oocytes	38.5 (16.7–55.6)	75.0 (55.6–80.0)	< .01
Fertilization rate (%)	66.7 (40.0–100.0)	83.3 (72.4–93.8)	NS
Embryos transferred (n)	1 (0–2)	2 (2–3)	NS
Endocrine profile			
Peak E_2 (pg/mL)	1,490 (1,142–2,752)	1,661 (1,163–2,162)	NS
E_2 day after trigger (pg/mL)	2,032 (1,140–3,827)	1,904 (1,176–2,592)	.01
P, day after trigger (ng/mL)	2.6 (1.9–4.0)	4.0 (2.9–5.2)	< .01
U1, day after trigger (IU/L)	NA	54.2 (36.0–81.4)	NA
hCG, day after trigger (IU/L)	135 (96–190)	203 (128–297)	< .01

Note: NS = not significant; LH = luteinizing hormone; hCG = human chorionic gonadotropin; NA = not applicable.

Griffin. GnRH-aHCG trigger for low egg maturity. Fertil Steril 2014.

Griffin et al., 2014

Dual trigger for prior low oocyte maturation rate

- > 50% immature oocyte in prior IVF cycle

Table 2. In Vitro Fertilization and Pregnancy Outcomes.

	hCG Trigger (n = 81)	Dual Trigger (n = 81)	P Value
Total oocytes number	5.5 ± 2.7 (4.8-6.2), n = 81	7 ± 4.4 (6.0-8.0), n = 81	.02
MII (number)	2.4 ± 2.2 (2.0-2.9), n = 81	5.3 ± 3.6 (4.4-6.1), n = 81	<.001
MII rate (%)	43.6 ± 29 (37.4-49.8), n = 81	72.9 ± 26.4 (66.7-79.2), n = 81	<.001
Fertilized eggs	2.9 ± 2.1 (2.2-3.6), n = 40	4.8 ± 2.7 (4.0-5.6), n = 52	<.001
Fertilization rate (%)	79.6 ± 53 (62.4-96.8), n = 40	82.5 ± 32.8 (73.4-91.7), n = 52	.7
Transferred embryos	1.2 ± 0.8 (0.9-1.4), n = 40	1.3 ± 0.8 (1.1-1.6), n = 52	.5
Frozen embryos	0.8 ± 1.5 (0.3-1.3), n = 31	1.3 ± 1.6 (0.8-1.8), n = 47	.2
Implantation rate (%)	17.3 ± 31.4 (4.6 -30.0), n = 26	30.8 ± 39 (18.1-43.4), n = 39	.1
Clinical pregnancy rate (%)	26.9 ± 45.2 (8.6-45.2), n = 22	43.6 ± 50 (27.3-59.9), n = 26/59	.2
Ongoing pregnancy rate (%)	15.3 ± 36.7 (0.5-30.3), n = 2	31.6 ± 47.1 (16.1-47.1), n = 18/59	.1

Abbreviations: hCG, human chorionic gonadotropin; MII, metaphase II.

Fabris et al., 2017

Dual trigger for poor responder

- High rate of premature ovulation/luteinization
- Early triggering (15-16mm)
- Shortening duration btw trigger and OPU
  → may cause low oocyte maturation rate

How about DUAL trigger?

Dual trigger for poor responder

	Group A: 5000 IU HCG (n = 328)	Group B: 0.1 mg GnRHa + 5000 IU HCG (n = 386)	Group C: 10,000 IU HCG (n = 363)	Group D: 0.1 mg GnRHa + 10,000 IU HCG (n = 312)	P-value[a]	P-value[b]
Duration of HMG treatment (days)[a]	8.55 ± 2.40	8.53 ± 2.13	8.55 ± 2.42	8.60 ± 2.14	NS	NS
Total doses of gonadotrophins (IU)[a]	1562.42 ± 560.91	1559.65 ± 505.66	1547.31 ± 557.14	1601.44 ± 503.26	NS	NS
Oestradiol on trigger day (pg/ml)[a]	1066.26 ± 781.52	1094.48 ± 634.74	1070.51 ± 772.56	1140 ± 656.07	NS	NS
Progesterone on trigger day (ng/ml)[a]	0.40 ± 0.32	0.41 ± 0.36	0.40 ± 0.31	0.42 ± 0.39	NS	NS
Oestradiol on day after trigger (pg/ml)[a]	1178.74 ± 815.78	1265.54 ± 718.72	1191.88 ± 825.60	1285.70 ± 769.20	NS	NS
Progesterone on day after trigger (ng/ml)[a]	1.38 ± 0.71	1.82 ± 1.14	1.39 ± 0.70	1.89 ± 1.22	<0.001	<0.001
No. of oocytes retrieved[a]	2 (0–9)	3 (0–11)	2 (0–9)	3 (0–11)	<0.001	<0.001
No. of mature oocytes[a]	2 (0–8)	3 (0–10)	2 (0–8)	3 (0–9)	<0.001	<0.001
No. of top-quality embryos[a]	1 (0–5)	1 (0–7)	1 (0–5)	1 (0–6)	NS	NS
No. of viable embryos[a]	1 (0–6)	1 (0–8)	1 (0–6)	1 (0–7)	NS	NS
ICSI rate, n (%)[a]	106 (32.3)	116 (30.1)	118 (32.5)	97 (31.1)	NS	NS
Oocyte retrieval rate, n/n (%)[a]	784/1373 (57.1)	1119/1623 (68.9)	886/1532 (57.8)	936/1372 (68.2)	<0.001	<0.001
Mature oocyte rate, n/n (%)[a]	638/784 (81.4)	990/1119 (88.5)	717/886 (80.9)	820/936 (87.6)	<0.001	<0.001
Fertilization rate, n/n (%)[a]	552/737 (74.9)	781/1070 (73.0)	623/830 (75.1)	649/890 (72.9)	NS	NS
EPS, n (%)[a]	11 (3.4)	12 (3.1)	12 (3.3)	11 (3.5)	NS	NS

Zhang et al., 2017

Dual trigger for poor responder

Table 2 Comparison between hCG and dual-trigger protocols: Outcomes of ovarian stimulations

	Control group (hCG)	Study group (hCG + triptorelin)	*P* value
E_2 on trigger day (pg/ml)	775.29 ± 500.1	628.16 ± 503.4	NS
No. of oocytes Retrieved	3.40 ± 1.36	3.27 ± 1.53	NS
No. of MII oocytes Retrieved	2.85 ± 1.33	2.75 ± 1.42	NS
Fertilization rate (%)	58.63 ± 36.23	73.10 ± 71.80	0.015
No. of embryo transferred	1.67 ± 1.10	2.06 ± 1.11	NS

Table 3 Comparison between hCG and dual-trigger protocols: Outcomes of IVF-ICSI cycles

	Control group (hCG)	Study group (hCG + triptorelin)	*P* value
Cancellation of embryo transfer (%)	15.4 (20/130)	6.1 (18/297)	0.003
Implantation Rate (%)	10.58 ± 2.45	15.02 ± 1.74	NS
Biochemical pregnancy rate per cycle (%)	4.6 (6/130)	2.0 (6/297)	NS
Clinical pregnancy rate per cycle (%)	20.7 (27/130)	33.0 (92/297)	0.035
Live birth rate per cycle (%)	13.1 (17/130)	27.2 (76/297)	0.014
Abortion rate (%)	37.0 (10/27)	17.4 (16/92)	0.037
Twin pregnancy rate (%)	1.5 (2/130)	4.4 (13/297)	NS

Lin et al., 2019

Recent Meta-analysis

- Four RCT, 527 women
- Significantly **higher pregnancy rate** in dual trigger
- No differences in number of oocytes retrieved, fertilized oocytes, good-quality embryos or implantation rate

Study(year)	Study design	Country	Patients (n)	Cycles (n)	Age	BMI	Interventions	Outcome measures
Schachter 2008	RCT	Israel	105	97	33.7 ± 5.6	-	Triptorelin(0.2mg(SC)+hCG	①②④
			106	103	34.7 ± 4.7	-	hCG(5000IU)	
Decleer 2014	RCT	Belgium	61	61	30.0 ± 3.6	23.8 ± 4.6	Triptorelin(0.2mg(SC)+hCG	①②③④
			59	59	30.5 ± 4.1	30.0 ± 3.6	hCG(5000IU)	
Kim 2014	RCT	Korea	60	60	36.2 ± 3.7	21.7 ± 2.0	Cetrotide(0.1 mg(SC)+hCG	①②③④⑤⑥
			60	60	35.8 ± 3.8	21.4 ± 2.2	rhCG(250ug)	
Mahajan 2016	RCT	India	38	38	32.4 ± 4.5	25.8 ± 3.9	Injectide (1 mg(SC) +hCG	①②③④
			38	38	33.1 ± 4.1	24.2 ± 3.2	hCG(10000IU)	

-(The author did not give details of BMI, but the author declared in the exclusion criteria that patients with BMI <18 or >30 kg/m^2 were excluded.
Outcome measures: ① Number of oocytes retrieved ② Number of mature oocytes retrieved ③ Number of fertilized oocytes ④ Number of usable embryos on day3 ⑤ Implantation rate ⑥ pregnancy rate.

Ding et al., 2017

Recent Double-blinded RCT

- 155 normal responder

Table III Embryology outcome, calculated by intention to treat.

	hCG	Dual trigger	Mean difference, (95% CI)	*P*-value
Number of patients	78	77		
Oocytes (n)	11.1	13.4	2.4 (0.8–3.9)	0.002
Oocytes/n of follicles >10	77.8%	93.4%	16% (5.2–26.7%)	0.005
MII (n)	8.6	10.3	1.7 (0.4–3)	0.009
2PN (n)	6.3	7.8	1.6 (0.4–2.7)	0.007
Cleavage stage embryos (n)	5.6	7.0	1.3 (0.2–2.4)	0.02
Blastocyst (n)	2.9	3.9	1 (0.2–1.9)	0.01
Top-quality blastocyst (n)	1.4	2.4	0.9 (0.4–1.5)	0.001

MII, metaphase 2; 2PN, 2-pronuclear.

Haas et al.,HR, 2020

Table IV Pregnancy outcome, calculated by intention to treat.

	hCG	Dual trigger	Odds ratio	95% CI	*P*-value
Number of patients included in the analysis	75	74			
Clinical pregnancy rate (fresh transfers)	17/33 (52%)	12/23 (52%)	1.02	0.35–2.98	0.96
Total Implantation rate	28/114 (23%)	42/97 (43%)	2.74	1.32–4.29	0.003
TQE transferred/all embryos transferred	51/114 (45%)	63/97 (65%)	2.29	1.31–3.99	0.003
Clinical pregnancy rate per transfer	28/107 (24%)	42/91 (46%)	2.65	1.33–4.39	0.009
Clinical pregnancy rate per patient	28/75 (37)	42/74 (57%)	2.20	1.14–4.24	0.01
Live birth per transfer	24/107 (22%)	33/91 (36%)	1.98	1.05–3.67	0.03
Cumulative live birth per patient	24/75 (32%)	33/74 (45%)	1.67	0.87–3.32	0.11

Haas et al.,HR, 2020

Double trigger

- For empty follicle syndrome
- GnRHa 40h + standard hCG 34h prior to OPU
- GnRHa for FSH surge overcome impairment in granulosa function, oocyte meiotic maturation or cumulus expansion

Oocyte recovery via FSH surge

Beck-Fruchter et al., 2012

Double trigger

Gynecol Endocrinol. 2019 Feb 27:1-3. doi: 10.1080/09513590.2019.1576621. [Epub ahead of print]

Does double trigger (GnRH-agonist + hCG) improve outcome in poor responders undergoing IVF-ET cycle? A pilot study.

Haas J[1,2], Zilberberg E[1,2], Nahum R[1,2], Mor Sagon A[1,2], Hourvitz A[1,2], Gat I[1,2], Orvieto R[1,2,3].

Author information

Abstract

Many strategies are offered for the treatment of poor responders. However, no compelling advantage for one stimulation protocol over another has been hitherto established. In this study, we aimed to evaluate the role of different modes and timings of final follicular maturation trigger, on in vitro fertilization (IVF) cycle outcome of poor responder patients. n the present randomized controlled study, poor responder patients, according to the Bologna criteria, undergoing controlled ovarian hyperstimulation (COH) using the gonadotropin-releasing hormone (GnRH) antagonist protocol were randomly assigned to three different final follicular maturation trigger modes and timings: hCG 36 h before oocyte pick-up (OPU) (hCG-trigger); GnRH agonist (GnRHag) 36 h before (OPU) and hCG on day of OPU (GnRHag trigger); and GnRHag and hCG, 40 and 34 h prior to OPU, respectively (double trigger). Pregnancy rate, number of oocytes, and top quality embryos (TQEs). Thirty-three poor responder patients were recruited and randomized to the different study groups. While there were no in-between groups' differences in patients' demographics and stimulation variables, patients in the double trigger group had a significantly higher number of TQE (1.1 ± 0.9 vs. 0.3 ± 0.8 and 0.5 ± 0.7; $p < 0.02$) as compared to the hCG trigger and the GnRH-ag trigger groups, respectively, with an acceptable pregnancy rate. Double trigger offers an additional benefit to poor responder patients. Larger studies are required to support this new concept prior to its implementation to IVF practice.

Amphiregulin & epiregulin

- Higher level in GCs after double trigger
- Ligands of EGF receptors
- Important roles in cumulus expansion, oocytes maturation, and meiosis resumption

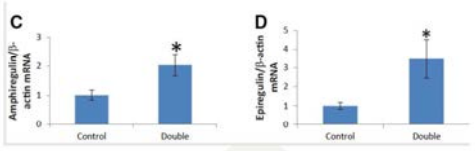

Haas et al., 2016

Dual trigger & double trigger

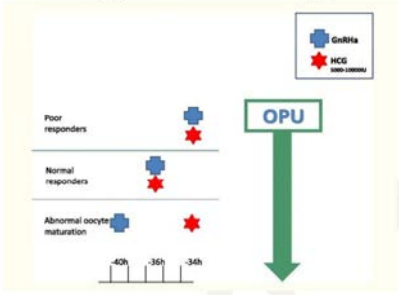

Orvieto, 2015

Is there any specific indication for

Dual trigger?

Good for all?

Dion's study

- Retrospective cohort study
- 235 infertile couples with 262 completed IVF/ICSI-ET cycles
- Btw January 2017 and September 2018

	< 35 yrs	≥ 35 yrs
Normal wt (BMI < 23 kg/m²)	Group 1	Group 3
Overweighted (BMI ≥ 23 kg/m²)	Group 2	Group 4

Table 1. Cycle outcomes in 4 groups.

	Group 1		Group 2		Group 3		Group 4	
	hCG-only (cycle=49)	dual trigger (cycle=28)	hCG-only (cycle=27)	dual trigger (cycle=23)	hCG-only (cycle=48)	dual trigger (cycle=48)	hCG-only (cycle=24)	dual trigger (cycle=21)
No. of oocyte retrieved	11.6±5.3	13.1±5.6	11.8±5.6	14.2±7.8	8.6±5.6	9.9±6.0	8.5±5.6	10.6±5.4
No. of Mature oocytes	8.2±4.6	8.9±4.1	9.2±5.1	9.9±5.9	6.4±4.9	7.5±4.7	6.2±4.9	8.3±4.0
Maturation rate (%)	70.8	70.9	74.6	70.3	76.6	78.8	70.1*	81.9*
Fertilization rate (%)	69.2	72.0	73.3	77.7	75.6	78.4	74.3	81.4
Good embryo rate (%)	55.8	57.3	48.3	54.1	58.9	61.1	59.4	61.7
Implantation rate (%)	37.3	47.5	39.3	28.0	22.8	15.2	25.0	39.5
Clinical pregnancy rate (%)	41.3	65.4	56.3	46.2	28.6	30.3	28.5**	52.9**

Note: Data are presented as mean ± SD, Student's t-test, * : $P < 0.05$, ** : $P < 0.05$

Group1 : young (<35 years), normal weighted (BMI < 23 kg/m2) women, Group2 : young, overweighted BMI ≥ 23 kg/m2) women, Group 3: old (≥ 35 years), normal weighted women, Group 4: old, overweighted women

There were no significant differences in other groups, even in overall.


Cost-effectiveness?
- 건강보험 고시
"배란유도(ovulation trigger) 또는 황체기 보강 목적으로 투여하는 leuprolide, triptorelin은 약값 전액을 환자가 부담토록 함."
652500031 데카펩틸주0.1밀리그램(트립토렐린아세트산염)_(0.105mg/1mL) 2.0000 1 1 52 3,455 전액본인

발표자 초록

Dev. Reprod. Vol 26, 2022 (Suppl. 1). pp 149

발생공학과 미니돼지모델의 현황 및 미래

김선욱

한국생명공학연구원 미래형동물자원센터

(sunuk@kribb.re.kr)

2016년 다보스포럼의 핵심키워드는 '4차 산업혁명'과 '인공지능'이었습니다. 수많은 분야에서 물밀듯이 쏟아지는 정보들을 빅데이터화하고, 이를 딥러닝하여 실질적인 분야에 활용하는 디지털경제 시대의 태동을 알린 것입니다. 바이오 분야도 다양한 연구 결과/정보를 표준화된 형식으로 디지털화하는 데이터 사이언스가 주목받기 시작하였고, 보다 실효적이고 재현성이 높은 데이터 확보를 위해 생명연구자원의 중요성이 크게 부각되었습니다. 이러한 측면에서 최근 10개의 국가전략자원이 선정되었는데, 이 중 4개가 동물자원이라는 것은 인간과의 다양한 측면에서의 연관성 및 유연관계가 중요했던 것으로 판단됩니다. 바이오의학 연구개발에서도 동물자원에 대한 활용도 제고를 위해 모델동물 클러스터 사업이 과기부를 중심으로 시작되었고, 공유/공통 등의 철학을 담아낼 수 있는 거점은행을 선정하여 본격적인 모델동물 실물자원 및 정보 확보를 추진하게 되었습니다. 본 센터는 현재 국가과학기술연구회 'BIG(Big Issue Group)' 사업과 과기부 모델동물클러스터 '미니돼지자원 거점은행' 사업을 수주/운용함으로써, 인간과 해부생리학적으로 매우 유사한 대표적 중대형 실험동물인 미니돼지로부터 첨단재생의학(인공혈액) 및 인간질환 관련 모델동물 실물자원・분석정보를 확보하기 시작하였습니다. 본 기회를 통해 생명(연) 미래형동물자원센터의 핵심인프라인 발생공학 기술 기반의 미니돼지 모델동물 개발/활용 현황 및 계획을 공유함으로써, 다양한 분야와의 융합을 도모하고, 미래발전 전략 구상을 함께 시작하고 싶은 바람입니다. 이를 통해 4차 산업을 선도하는 바이오강국 도약은 물론, 앞으로 다가올 수 있는 인류 공존 및 생존 문제 해결에 조금이나마 기여하고 공감될 수 있기를 희망합니다.

Key words: 생명연구자원, 미니돼지, 모델동물, 발생공학

Acknowledgement: Korea Research Institute of Bioscience and Biotechnology (KRIBB) Research Initiative Program (KGM4252122); the Ministry of Education, Science and Technology (MEST; No. 2021M3H9A1096895).

Dev. Reprod. Vol 26, 2022 (Suppl. 1). pp 150

The present of environmental DNA (minuteness of the aquatic ecosystem)

Ihn-Sil Kwak
Chonnam National University
(iskwak@jnu.ac.kr)

eDNA, or environmental genes have become one of the most widely used and commonly used familiar scientific terms. It has become a tool for drawing miniatures in that it can extract and express traces and fragments of living things contained in various media, water, soil, air, and soil that make up the earth. It is becoming a science and technology that makes it possible to draw through creative thinking for the purpose of use. Nevertheless, large and small problems and solutions are needed to be addressed.

The purpose of the study is to examine the research case of investigating the biodiversity of water bodies using the sea, estuary, river, and water, and analyzing the stomach contents of living things. eDNA is also used more frequently in ecology. However, the processing and analysis of the produced data is limited, and there are inconsistencies in the reliability of the analyzed and produced biotaxon identification data, the sample medium, and the improvement of quantification and analysis methods. Therefore, in order to secure the reliability and accuracy of biodiversity research using the environmental DNA of the domestic ecosystem, it is a process that actively utilizes the database accumulated through ecological taxonomy and undergoes verification procedures.

Research on environmental DNA is necessary. Environmental DNA research cannot be solved only by applying molecular biology techniques. Interdisciplinary research cooperation such as ecology-taxa identification-genetics-informatics is essential to secure the reliability of the produced data, and researchers dealing with various media can approach it together. It is an area in desperate need of an information-sharing platform that can be used to achieve this goal, and the speed of development will proceed rapidly. Moreover, the accumulated data are expected to grow as big data within a few years.

Key words: eDNA, biodiversity, water ecology

Dev. Reprod. Vol 26, 2022 (Suppl. 1). pp 151

Development of biomarkers and identification of signaling pathways related to reproductive toxicity of pesticides

Jeong-Won Bae, *Woo-Sung Kwon

Department of Animal Science and Biotechnology, Kyungpook National University

(wskwon@knu.ac.kr)

In 2017, the toxicity and harmful effects of pesticides have considering worldwide after the announcement existence of pesticides on the egg shell surface. Recently, another pesticide was detected in a product of a famous ice cream company. In addition, it has been reported that decreased population of honey bees due to misuse and abuse of pesticides. Although various toxic researches related to pesticides have been performed on various organs, the reproductive toxic study was not enough performed to now. To understand the toxic mechanism of reproduction, it is needed to study based on molecular levels with physiological monitoring. Therefore, the present study was designed to identify the molecular mechanism of male reproductive toxicity induced by pesticides. First, various concentrations of pesticides (fipronil and bifenthrin) were treated with mouse spermatozoa and induced capacitation. Then, sperm functions (sperm motility, motion kinematics, capacitation status, intracellular ATP level, and cell viability), fertilization, and embryo formation rate were evaluated. In addition, protein profiling to identify differentially expressed proteins (DEPs) after treatment of pesticides was performed by proteomic techniques. Finally, bioinformatics study was conducted to recognize related signaling pathways and establish new pathways. Almost physiological parameters were significantly suppressed in dose-dependent manners. Especially, fertilization and embryonic development rate were dramatically decreased in dose-dependent manners. Fourteen proteins were differentially expressed > 3-fold after treatment fipronil, and 9 proteins were differentially expressed > 3-fold after treatment of bifenthrin. It was confirmed that the DEPs were involved in various signaling pathways such as structure, motility, cell signaling, metabolism, oxidative stress, and so on. Moreover, new signaling pathways were established based on DEPs. It was shown that the interaction between DEPs and other proteins, as well as association with various cell processes and diseases related to reproduction. The present study was the first study to try to understand the male reproductive toxicity of pesticides based on molecular levels and those signaling pathways. Consequently, our results suggest that pesticides may be suppressed the male reproduction system, resulting in infertility. Therefore, we anticipate that the present study provides a new understanding of the reproductive toxicity of pesticides on male reproduction.

Key words: biomarker, signaling pathways, reproductive toxicity, pesticides

Dev. Reprod. Vol 26, 2022 (Suppl. 1). pp 152

해양오염 유해인자 영향평가 사례 연구

***정지현[1,2], 홍상희[1,2], 김문구[1,2], 임운혁[1,2], 심원준[1,2]**

[1]한국해양과학기술원 생태위해성연구부, [2]과학기술연합대학원대학교

(jungjh@kiost.ac.kr)

해양생태계는 다양한 물리, 화학 및 생물학적 과정에 의해 복잡하게 영향을 받고 있으며, 특히, 외부로부터 연안으로 유입된 유해화학물질은 해양 서식하는 생물에 대하여 예측 불가능한 형태로 압력을 주고 있다. 따라서 해양환경의 '질', 'Good Environmental Status(GES)'를 평가하는 것은 매우 복잡하고 전문적이며, 다학제적 접근이 필요한 분야로 알려져 있다. 이미, 2010, 2012년 Intergovernmental Council for the Exploration of the Sea(ICES, 2010, 2012)에서는 "Contaminants and Biological Effects Report"를 통하여 GES의 평가는 유해물질의 화학적 분석결과와 동시에 현장생물의 아치사 수준의 생리화학적 지표(biochemical monitoring)의 결과가 함께 제시될 것을 권고하고 있다. 최근의 연구결과들은 아치사 수준의 생리·화학적 지표가 생물의 군집변화와도 밀접한 연관성이 있음을 과학적으로 증명하고 있어, 검증되고 특이적인 생리화학적 지표를 활용한다면 유해화학물질로 인한 생태계 영향을 조기에, 보다 정밀하게 평가할 수 있을 것으로 생각된다.

먼저 본 연구에서는 생리화학적 기법을 이용하여 해양의 유해인자의 영향을 평가한 여러 사례 중 지난 2007년 발생한 국내 최대규모의 유류유출사고대응연구인 "유류오염 환경영향평가 및 환경복원 연구"를 첫 번째 사례로 소개하고자 한다. 본 연구는 단시간 고농도의 원유가 광범위한 지역으로 확산된 국내해양사고의 최악의 사고이며, 동시에 국내 최대·최장의 과학적 조사연구로서 유출사고로 인한 생태계 영향의 정도, 범위, 회복기간에 대한 다양한 모니터링 및 입증 연구를 담고 있다. 10년간의 장기연구를 통해 해양유출사고가 해양생태계에 미치는 영향은 매우 복합적이며, 다양한 생물의 서식지/서식형태에 따른 다양한 회복(복원)주기를 보여주고 있음을 확인할 수 있었다. 두 번째 연구사례는 3단계 총 8년간 수행된 해양환경유해물질의 평가 및 관리기술개발"연구에 대한 내용이다. 본 연구에서는 다매체내 유해화학물질의 거동과 신규오염물질 분석기법 확립등 오염평가에 대한 내용을 담고 있을 뿐 아니라, 연안 환경 중 유해물질의 영향을 평가할 수 있는 생리화학적 지표의 개발과 모니터링에 적용에 대한 결과를 담고 있다. 특히 유해물질에 특이적으로 반응하는 어패류생체지표의 남·동·서해안의 배경값을 설정하였고, 울산만/마산만/시화호 등을 포함한 특별관리해역에서 이를 비교·분석하여 우선관리 유해물질목록을 시범도출하였다. 또한, 본 연구에서는 어류의 생체지표분석결과를 Generalized Linear Model(GLM)에 적용한 Fish Biomarker Index를 산출하여 유해화학물질로 인한 영향의 정도를 조사해역별 비교분석할 수 있는 기반을 마련하였다.

육상으로부터 유입되는 다양한 오염원은 해양에 서식하는 생물에게 매우 심각한 압력요인이 되며, 이를 되돌리고 회복할 수 있는 골든타임은 제한적이다. 따라서 서식 생물이 받고 있는 육상기인의 환경적 압력을 보다 재현성 있고 민감한 기법을 이용하여 장기적으로 심화되지 않도록 정책적으로 잘 관리한다면, 건강한 해양생태계를 유지하고 관리하는 데 매우 유용하게 활용될 수 있을 것으로 생각된다. 비록 현재 연구현장과 국가 정책간에는 활용성 부분에 있어 많은 검토와 분야별 이익에 따른 큰 격차가 있으나, 해양생태계가 더 파괴되거나 복원되지 못하는 시점이 오기 전에 선진국의 사례를 참고하여 막대한 시간과 예산이 투입된 연구개발과제에서 발굴된 과학적 연구기법이나 결과를 관리주체가 현장에서 효율적으로 활용할 수 있도록 긴밀한 소통이 필요할 것으로 생각된다.

Key words: marine, ecosystem, protection, pollution, biomarker

Dev. Reprod. Vol 26, 2022 (Suppl. 1). pp 153

Drug-induced renal injury and regeneration in zebrafish model

강영선
고려대의대 안산병원 신장내과
(starch70@korea.ac.kr)

신장(콩팥, kidney)은 손상 후 재생(regeneration)이 어려운 장기로 알려져 있다. 신손상 후 회복이 안 되어 말기신부전으로 진행되면 신기능이 거의 없는 상태에서 평생동안 투석이나 이식과 같은 신대체요법을 받아야 한다. 다양한 약제의 개발과 고령인구의 증가로 약물에 의한 신독성은 점차 늘고 있지만 이에 대한 기전은 많이 밝혀져 있지 않다. 제브라피쉬는 다른 실험모델과 달리 신손상후 재생과정을 연구할 수 있는 좋은 모델로서 독성약물에 의한 신손상 모델을 확립하고, 재생과정의 기전을 연구하고 치료후보물질을 찾고자 연구하였다.

신손상을 유발하는 독성약제는 젠타마이신, 퓨로마이신 등을 사용하였으며, 성체 제브라피쉬복강내 주입 방식을 통하여 신손상을 유발하였다. 약제투여 후 1~3일에 신손상이 발생하고, 이후부터 7일까지 재생과정이 활발하게 일어나며, 14일쯤에는 재생과정이 거의 완료된다. 비스파틴(visfatin)은 림프구에서 처음 추출되어 pre-B cell colony-enhancing factor(PBEF)-1라고 명명되었으며, nuclear nicotinamide adenosine dinucleotide(NAD^+) salvage/recycling 경로에 관여하여 NAD^+-dependent enzymes 혹은 protein deacetylase sirtulin(SIRT)-1의 기능을 조절하는 nicotinamide phosphoribosyltransferase(nampt)라고도 불리고 있는데, 여러 장기에서 연구들이 보고되어 왔고, 에너지 대사와 관련하여 인슐린저항성 기전에 관여하는 아디포킨으로 알려져 있다. 저자들의 연구결과에서 nampt는 약물에 의한 신손상후 재생과정에서 발현이 증가하였고, 약물투여시 재생과정을 촉진하였는데, 신손상 후 재생과정의 기전에서 중요한 역할을 할 것이라 기대된다.

Key words: 급성신손상, 비스파틴, 신재생, 퓨로마이신, 제브라피쉬

Dev. Reprod. Vol 26, 2022 (Suppl. 1). pp 154

영장류 및 인간화 마우스를 이용한 조혈계 질병 기전 연구

Kyung-Rok Yu

Department of Agricultural Biotechnology and Research Institute of Agriculture and Life Sciences, Seoul National University

(cellyu@snu.ac.kr)

Given the unique self-renewal and differentiation properties of Hematopoietic stem and progenitor cells (HSPCs), a small number of genetically modified HSPCs could accomplish lifelong, corrective reconstitution of the entire hematopoietic system in patients with various hematologic disorders. We adapted CRISPR/Cas9 editing of rhesus macaque (RM) hematopoietic stem and progenitor cells (HSPCs) to create the engineered large animal model of a hematologic disease based on close phylogenetic/functional similarity of RM to human HSPCs. My talk will focus on my recent studies; 1. The impact of aging on hematopoiesis; To investigate the hematopoietic aging, we compared the clonal output of thousands of genetically barcoded HSPCs in aged vs young macaques after autologous transplantation. 2. Engineering HSPCs to enable immunotherapy for acute myeloid leukemia (AML); To avoid a non-tumor toxicity in myeloid cells, we proposed a novel approach to the treatment of AML, CD33 KO HSPC derived hematopoietic system resistant to anti-CD33 CAR-T cells while enabling specific targeting of AML. 3. Modeling clonal hematopoiesis (CH) in non-human primates; Recent population-based genomic studies of human blood cells have identified somatic mutations associated with clonal expansions commonly arising with aging. We identified natural CH mutations equivalent to humans in aged rhesus macaques through error-corrected ultra-deep sequencing with DNMT3A and TET2 mutation being the most frequent. Furthermore, we generated CH models in young macaques via CRISPR/Cas9-mediated gene editing at the top three CH genes, DNMT3A, TET2 and ASXL1, and confirmed significant expansion of multiple HSPC clones with heterozygous TET2 loss-of-function mutations. Our data provide insight into the translational hematology research for aging and cell therapy, which is relevant for designing transplantation and immunotherapy strategies.

Key words: hematopoietic stem and progenitor cells, CRISPR/Cas9, clonal hematopoiesis, CAR-T cells, disease model

Dev. Reprod. Vol 26, 2022 (Suppl. 1). pp 155

Convergent differentiation of multiciliated cells

Shinhyeok Chae[1], *Taejoon Kwon[1,2]

[1]Department of Biomedical Engineering, College of Information and Biotechnology, Ulsan National Institute of Science and Technology (UNIST)

[2]Center for Genomic Integrity, Institute for Basic Science

(shchae@unist.ac.kr)

Multiciliated cells (MCCs) are epithelial cells that play roles in controlling the flow of bodily fluid. While MCC exists in many different tissues, they have various functions in each tissue. In the airway, they protect the airway by clearing particles in the airway. Also, they control the cerebrospinal fluid in the ependymal tissue. In the oviduct, they transport eggs. In this context, we wonder how different organs have similar MCC structures although their origin is different, and which differences exist in each tissue origin. To understand the characteristics of MCC in multiple organs, we investigated 14 single-cell RNA sequencing (scRNA-seq) data from nasal epithelial cells, bronchial tubes, fallopian tubes, ependymal cells in the subventricular zone (SVZ) and spinal cord from both human and mouse tissues. By using Seurat and UMAP, we normalized and clustered the scRNA-seq dataset. After identifying multiciliated cells in each data based on well-known cilia-related genes as markers, we integrated those cells together, to analyze their difference. To control the cross-species data integration process, we utilized more than two independent datasets for each tissue, both in humans and mice, and confirmed that the multiciliated cells from the same tissue were more similar than others. In this study, we can find similar expression of common MCC genes and ciliopathies-related genes. It suggests that key functions of MCC are well conserved across the tissues and species. In addition, we analyzed differentially expressed genes (DEGs) of each tissue to see the difference depending on the tissue. We can identify the relationship of precursor cells of MCCs in each tissue.

Key words: scRNA-seq, multiciliated cell, airway, oviduct, ependyma, Integrated analysis

Dev. Reprod. Vol 26, 2022 (Suppl. 1). pp 156

Establishment of a male fertility prediction model with sperm RNA markers in pigs as a translational animal model

Won-Ki Pang, S Amjad, DY Ryu, EO Adegoke, MS Rahman, YJ Park, *MG Pang

Department of Animal Science & Technology and BET Research Institute,
Chung-Ang University
(wkpang@naver.com)

Male infertility is a major problem that can threaten the survival of humans and animals. The clinical acceptance of the current method to diagnose/prognose male fertility is unclear. To solve the male fertility crisis in the humans and animals, the prediction of sperm quality is the most important step. Sperm RNA is the potential marker for male fertility prediction. We hypothesized that the expression of functional genes related to fertilization will be the best target for male fertility prediction markers. To investigate optimum male fertility prediction marker, we compared target genes expression level and a wide range of field data acquired from artificial insemination of boar semen. Among the genes related to acrosomal vesicle exocytosis and sperm–oocyte fusion, equatorin (EQTN), zona pellucida sperm-binding protein 4 (ZP4), and sperm acrosome membrane-associated protein 3 exhibited high accuracy (70%, 90%, and 70%, respectively) as markers to evaluate male fertility. Combinations of EQTN-ZP4, ZP4-protein unc-13 homolog B, and ZP4-regulating synaptic membrane exocytosis protein 1 (RIMS1) showed the highest prediction value, and all these markers are involved in the acrosome reaction. The *EQTN-ZP4* model was efficient in clustering the high-fertility group and may be useful for selection of animal that has superior fertility in the livestock industry. Compared to the *EQTN-ZP4* model, the *ZP4-RIMS1* model was more efficient in clustering the low-fertility group and may be useful in the diagnosis of male infertility in humans and other animals. The appointed translational animal model and established biomarker combination can be widely used in various scientific fields such as biomedical science.

Key words: male fertility, multiple markers, pig model, prediction model, sperm RNA

Acknowledgement: His research was supported by the Basic Science Research Program through the National Research Foundation of Korea (NRF), funded by the Ministry of Education (NRF-2018R1A6A 1A03025159).

Dev. Reprod. Vol 26, 2022 (Suppl. 1). pp 157

Energy pathways involved in the maturation of the Pacific oyster, *Crassostrea gigas*

Su-jin Park[1], Soyeon Hwang[1], Yein Lee[1], *Youn Hee Choi[1,2]

[1]Department of Fisheries Biology, Pukyong National University

[2]Devision of Fisheries Life Sciences, Pukyong National University

(unichoi@pknu.ac.kr)

The Pacific oyster *Crassostrea gigas* is commercially-important aquaculture species worldwide. In marine bivalves like *C. gigas*, glycogen is used as energy storage for maturation and to provide energy for gametogenic development and maintenance. The stored glycogen is broken down into glucose when needed and used for energy production or blood sugar control. Additionally, it is known that growth factors inactivate glycogen synthase kinase 3 (GSK3) through phosphorylation, promote glycogen synthase (GS) activity, and regulate glucose synthesis and glycogen metabolism. Various signal transductions regulate GSK3 activity, and examples of phosphorylating enzymes capable of inducing such phosphorylation include protein kinase B (Akt). Therefore, this study was confirmed to investigate the relationship between GSK-3 and glycogenolysis/glycogenesis and compare the reproductive cycle of the *C. gigas* to the energy pathway.

Fifty oysters were randomly collected monthly for one year from the long-line culture system in Jaran Bay, Tongyeong, twenty of which were fixed in 4% paraformaldehyde for histological observation. To confirm changes in the GSK3 mRNA expression, gonads and adductor muscles were subjected to Reverse Transcription PCR (RT-PCR) and fluorescence in situ hybridization (FISH) methods, and the AKT/GSK3 signaling pathway in the gonads was analyzed using western-blot.

The expression of GSK3 mRNA levels in the female gonad was highest in October when spawning occurred after maturation, and the lowest expression was shown in July when spawning and spent. Similarly, in the male gonad, the expression of GSK3 mRNA levels was lowest in July. Also, in the adductor muscle, males and females showed the highest expression in April and low in July and October, when spawning and spent. This pattern was similar to the result confirming that GSK3 mRNA was detected in female and male gonad and adductor muscle by the FISH method. Furtherly observed that matured and spawned oysters from April to July exhibited higher AKT activities and lower GSK3 activities. In conclusion, GSK3 expression appears high at the time of ripe, inhibiting the synthesis of glycogen is used as energy for maturation, and glycogen synthesis occurs for energy storage during degeneration.

Key words: *Crassostrea gigas*, GSK3, energy, glycogen, maturation

Dev. Reprod. Vol 26, 2022 (Suppl. 1). pp 158

Effects of environmental stressors in antioxidant response of scallops

***Jin Ah Song**

Marine Bio-Resources Research Unit, Korea Institute of Ocean Science and Technology

(jinah@kiost.ac.kr)

Scallops are widely known around the world for aqua culturing as a species with an exceptionally high economic value. Specifically, the bay scallop *Argopecten irradians* is a commercially important species of shellfish in Korea and China, as well as the Atlantic Coast of the United States. The population of scallops inhabiting these areas is continuously decreasing due to global climate change. To manage healthy individuals, studying effects of various stressors of the marine environment on scallops is urgently needed, as studies on the endocrine physiology of this species are rare.

A. irradians inhabiting shallow waters is frequently exposed to an environment with rapidly changing salinity caused by sudden fluctuations in water temperature due to the movement of the water layer and the inflow of fresh water. In addition, the temperature of the sea surface has been increasing due to global warming caused by rapid industrialization. Some of impacts of global climate change include glaciers and ice sheets melting, and the salinity of seawater changing, which lead to changes in the environment of the marine ecosystem. This phenomenon not only transforms the one-dimensional ecosystem, but also increases frequency of harmful algal blooms, resulting in toxicity to filter-feeding organisms such as scallops. Industrialization has caused various organic and inorganic pollutants to be continuously discharged into the marine environment, which allows these chemicals to accumulate in marine organisms and to produce toxic reactions. Of these harmful pollutants, benzo[α]pyrene (BaP) is an endocrine disrupting substance. This study investigated variations in bay scallops when exposed to important ecological factors of the ocean such as changes in water temperature and salinity, BaP, and domoic acid (DA) (a toxic substance derived from algae), by using molecular endocrinology analysis techniques.

Key words: antioxidants, bay scallops, environmental stress, oxidative stress

Dev. Reprod. Vol 26, 2022 (Suppl. 1). pp 159

Zebrafish as a model system to investigate human liver diseases

Azra Memon[1], Siyeo Lee[2], *Tae-YoungChoi[1,2]

[1]Department of Pathology, Digestive Disease Research Institute,
Wonkwang University School of Medicine

[2]Department of Biomedical Science, Graduate School, Wonkwang University

The zebrafish (Danio rerio) is becoming a favorite vertebrate model organism in developmental biology. Zebrafish models are critical for advancing our understanding of human pathogenesis and are a popular model for liver diseases allowing researchers to identify therapeutic targets and test novel drugs. The larval transparency of the zebrafish is a great advantage for real-time imaging in hepatic studies.

Part I, Here we describe *epcam* mutants in zebrafish as a helpful model system to investigate Primary biliary cholangitis (PBC), formerly known as primary biliary cirrhosis. PBC is a disease that harms the liver's ability to function. In people with PBC, the bile ducts become injured, then inflamed, and eventually permanently damaged. our findings suggest that *epcam* positively regulates liver development and liver regeneration and plays a potential role in bile duct formation in regenerative response.

Part II. A large number of heritable and acquired diseases are related to the interruption of liver function. Zebrafish can be a valuable model system to investigate a rare inherited disorder Sjogren-Larsson syndrome (SLS). SLS is a rare autosomal recessive condition characterized by significant ichthyosis symptoms, mental retardation, and spasticity due to a defect of the fatty aldehyde dehydrogenase (FALDH), which is related to mutations in the Aldehyde Dehydrogenase 3 Family Member A2 (ALDH3A2) gene. FALDH, a key component of the detoxification pathway of aldehydes arising from lipid peroxidation and the enzymatic function of ALDH3A2 is well-known, but the disease model is necessary to investigate the molecular mechanisms of which fatty aldehyde or of which metabolic liver pathway mainly contributes to the pathogenesis of SLS ichthyosis symptoms.

Even though zebrafish have advanced our understanding of liver diseases as well as liver cancer and regeneration, the disease model is necessary to investigate the molecular mechanisms of inherited and acquired liver diseases as well as liver primary biliary cirrhosis.

Key words: zebrafish, liver diseases, EpCam, primary biliary cirrhosis (PBC), Sjogren-Larsson syndrome (SLS), FALDH, ALDH3A2

Dev. Reprod. Vol 26, 2022 (Suppl. 1). pp 160

Autophagic induction and dual functions of trehalose *via* PI3K/Akt and VPS34/mTOR pathways on porcine oocyte and cumulus cells

Lian Cai[1,2], *Sang-Hwan Hyun[1,2,3]

[1]College of Veterinary Medicine, Chungbuk National University

[2]Graduate School of Veterinary Biosecurity and Protection, Chungbuk National University

[3]Institute for Stem Cell & Regenerative Medicine (ISCRM), Chungbuk National University

(cailian005@nate.com)

Autophagy, an intracellular recycling system, is essential for the proper meiotic maturation of porcine oocytes. Trehalose, a non-reducing disaccharide, has been reported as a novel mammalian target of rapamycin (mTOR)-independent autophagy enhancer in various types of cells. Relevantly, our previous study has indicated that trehalose supplementation during *in vitro* maturation of porcine oocytes improves the developmental competence of parthenogenetic embryos, possibly via autophagic activation. However, the underlying mechanisms remain unclear. To do so, the aim of this study was to address this issue. Here, we found that trehalose indeed plays a role as an autophagy activator by autophagic flux assay, as well as verified by immunoblotting that it promotes phosphatidylinositol-3 kinase (PI3K)/protein kinase B (Akt) inhibition and vacuolar protein sorting 34 (VPS34)/mTOR activation not only in cumulus cells (CCs) but also in oocytes. However, interestingly, the effects and the mechanisms regulated by trehalose were different on them, respectively. In CCs, the autophagy was activated through the improvement of lysosomal function/autophagic clearance viability by upregulation of coordinated lysosomal expression and regulation genes via PI3K/Akt inhibition. Whereas in oocytes, autophagy was activated via induction of VPS34 which directly influences autophagosome formation, and the proper meiotic process was ensured via Akt inhibition and mTOR activation. Taken together, this study, for the first time, elucidates the autophagic and molecular modulation of trehalose during porcine oocyte maturation, thus laying the biological foundations for pharmacological application.

Key words: trehalose, PI3K/Akt, VPS34/mTOR, oocytes, cumulus cells

Acknowledgement: This work was supported by grants from the “NRF funded by the Korean Government (2017K1A4A3014959, 2020R1A2C2008276, 2022R1A4A1025557)” and “IPET in Food, Agriculture, Forestry and Fisheries (318016-5, 320005-4)”, Korea.

Dev. Reprod. Vol 26, 2022 (Suppl. 1). pp 161

Metabolic restructuring and cell fate conversion through controlling cellular organelles

***Man Ryul Lee**

Soon Chun Hyang Institute of Medi-Bio Science (SIMS)

(leeman@sch.ac.kr)

Even though there have been lots of researches and attention on transcriptome and epigenome, efficiency of cell transformation is still low and many parts of the mechanism of determining the fate of cells are not entirely known. The reason is that the transformation mechanism of cell fate occurring mainly on a nucleus and the changes of many cell organelle within cytoplasm are not sufficiently identical, and in particular that there are few researches or understanding about changes of mitochondrial metabolism and stress of endoplasmic reticulum. In the process of transformation of cell fate, the changes of transcriptome which changes within a nucleus are relatively dynamic, and it is known that morphological/ functional changes of cell organelle existing in cytoplasm also occur simultaneously. We gave it a new name of cytoplasmic reprogramming or cytoplasmic synchronization. It is urgently required to find the mechanism which is comprehensively moderated when the cell fate is transformed through the research on the changes of cell organelle and understanding about the control of cell stress when the cell fate is transformed.

Key words: reprogramming, metabolic shift, organelles, cell fate conversion

Acknowledgement: This study was supported by National Research Foundation of Korea (NRF-2020 R1A2C1012294).

Dev. Reprod. Vol 26, 2022 (Suppl. 1). pp 162

Single-cell lineage recording and tracing unravel epigenetic regulation of cell fate decisions

Ik Soo Kim

Department of Microbiology, Gachon University College of Medicine

(iksookim@gachon.ac.kr)

My lab's research goal is to understand how cells decide their fate to be specific cell types. This knowledge will foster us to utilize cell-fate decision mechanisms to modulate cell states in various biological systems involving development and disease. With recent technological advances in genomics and single-cell research, we are unraveling heterogeneous cell states in biological systems and demonstrating cell's origin (where each cell comes from) and cell's destination (where each cell progress into). Recently, we combined single-cell transcriptomics and genetic recording to characterize embryoid bodies (EBs), a heterogeneous mixture of three germ layers, differentiation. We mapped transcriptional states along a time course and model cell fate trajectories and branch points as cells progress to distinct germ layers. To validate this inferential model, we proposed an innovative inducible genetic recording technique that leverages recombination to generate cell-specific, timestamp barcodes in a narrow temporal window. We validated trajectory architecture and key branch points, including early specification of a primordial germ cell (PGC)-like lineage from preimplantation epiblast-like cells. We will further identify a temporally defined role of epigenetic regulation of cell fate decisions. To this end, we are developing new single cell technologies recording cell state in molecular level and tracing innate or acquired cell barcodes in developing cells. Our study provides a high-resolution lineage map for developmental or disease model systems, insights into epigenetic determinants of fate specification, and a strategy for lineage mapping of differentiation processes.

Key words: cell fate decision, single cell research, epigenetics, stem cell, embryo development

Dev. Reprod. Vol 26, 2022 (Suppl. 1). pp 163

Effect of nanoplastics on the behavioral and nutritional characteristics of aquatic organisms

채유은, 김다솜, 김도경, 김신웅, *안윤주

건국대학교 환경보건과학과

(yooeun.chae@kitox.re.kr)

Microplastic (<5 mm) pollution, a major threat to marine environments, is a source of growing concern and it is currently receiving considerable worldwide attention. Especially, nanoplastic (<100 μm) have recently been highlighted as harmful in several studies showing the degradation or fragmentation of microplastics into nanoplastics in the environment. The first study investigated the individual impact, and embryonic uptake of fluorescent nanoplastics on microalgae, daphnia, and two fish species through indirect and direct exposure in a freshwater ecosystem and the second study investigated the changes in certain important biochemical and nutritional indicators of whiteleg shrimp after nanoplastic exposure through food. Overall, our findings indicate that plastic pollution can directly interfere with behavioral and nutritional changes in aquatic organisms, thereby indirectly causing potential health implications for human consumers.

Key words: nanoplastic, food chain, aquatic organism, freshwater, whiteleg shrimp

Dev. Reprod. Vol 26, 2022 (Suppl. 1). pp 164

Chemokine regulates eye morphogenesis in *Xenopus*

Hosung Jung

Department of Anatomy and Brain Korea 21 PLUS Project for Medical Science,
Yonsei University College of Medicine
(hosungjung@yonsei.ac.kr)

Collective cell migration is a key mechanism underlying organogenesis, but extracellular signals that regulate this type of cell movement are largely unknown. During vertebrate eye morphogenesis, the continuous lateral migration of the neuroepithelial sheet from the ventral midline places the prospective ventral retina in its proper position. I will present evidence showing that chemokine signaling controls this process in *Xenopus*. A chemokine ligand presented as a dorsal high-to-ventral low gradient is required for lateral migration of ventral retinal progenitors, and its signaling components appear to be distinct from those of the conventional chemokine receptor-mediated signaling pathways.

Key words: chemokine, retina, sheet migration, *Xenopus* tropicalis

Dev. Reprod. Vol 26, 2022 (Suppl. 1). pp 165

Enhanced hepatic functionality in long-term cultured 3D spheroids of zebrafish liver cells

Young Jun Kim

Environmental Safety Group, KIST Europe Forschungsgesellschaft mbH, Germany

(youngjunkim@kist.re.kr)

During the last decades, extensive efforts have been made to develop *in vitro* platforms for mimicking fish liver, with the purpose of better understand the acute or progressive impacts of toxicants on the aquatic lower vertebrates. In particular, fish liver cell lines have emerged as a promising culture system for the *in vitro* platforms because it is possible to expand the numbers of *in vitro* assay and pass strict regulatory requirements for primary cell isolation. However, monolayer cell lines exhibit lower transcriptional and physiological responses upon exposure to toxic chemicals than freshly isolated primary cells. To overcome this challenge, we utilized a 3D spheroid-based *in vitro* platform in which the hepatocyte cells self-organized in a spheroid form via E-cadherin bonds, and finally showed augmented transcriptomic and phenotypic regulations of liver cells in comparison to the monolayer cells. We examined this organoid platform by using the zebrafish liver (ZFL) cell line as a model system. The ZFL cells spontaneously clustered into 3D spheroids with long-term viability by optimizing cell seeding density on a non-adherent substrate. Interestingly, 3D ZFL spheroids treated with 17β-estradiol (E2) and endocrine-disrupting chemicals were activated to synthesize a higher level of vitellogenin (Vtg) than the monolayer cells. Whole transcriptome-sequencing analysis also confirmed that 3D ZFL spheroids hold the increased transcriptional regulations of genes related to reproductive toxicological response and liver functions, such as urea cycle, estrogen receptors, and vitellogenin, compared to monolayer cells. These results could help engineering novel 3D *in vitro* platforms for screening harmful chemicals and understanding the underlying liver toxicity mechanisms in both molecular and cellular levels

Dev. Reprod. Vol 26, 2022 (Suppl. 1). pp 166

지속 가능한 미래 생물자원 확보를 위한 남극 어류 연구

***김진형**

극지연구소

(kimjh@kopri.re.kr)

남극반도를 둘러싼 남극해는 연평균 빙점(–1.9℃)에 이르는 차가운 해수온과 더불어, 고염분, UVR 등 극지 특이적 환경을 지닌다. 남극어류는 현재까지 123종이 보고되었으며, 이중 남극암치아목(Notothenioidei) 어류가 남극해 전체 어류 생물량의 약 90%를 차지한다. 이 어류들은 척박한 극지 환경에 적응해 살아남기 위해서 종 특이적인 적응기작을 통해서 진화해 왔다.

극지연구소는 2016년부터 남극 세종과학기지 및 장보고과학기지 연안에서 채집된 극지 어류를 유지 배양하기 위하여 과학기지 및 국내 극지연구소에 극지 해양생물 전용 아쿠아리움을 구축하였다. 현재 남극검정암치, 남극대리석무늬암치, 남극에메랄드암치 등 지금까지 10종의 남극 어류를 국내로 이송하여 장단기에 걸쳐 유지하였고, 다양한 사육조건 및 먹이 선호도를 조사하여 장기간 유지에 필요한 호조건을 찾고 있다. 이를 통해 극지 어류의 환경 적응기작을 이해하고, 극지방에서 일어나고 있는 급격한 환경변화에 따른 생물 및 생리반응을 이해하기 위한 다양한 실험을 수행하고 있다. 또한, 극지 어류만이 특이적으로 가지게 된 특성을 기반으로 유전자원의 활용 및 기능 유전자를 발굴하기 위한 연구를 수행하고 있다. 전 세계적으로 극지 어류의 생식 및 인공번식에 관해서는 거의 알려진 바가 없다. 따라서 만약 남극 어류의 인공 산란을 유도하여 인공번식을 한다면 지속가능한 많은 흥미로운 결과를 얻을 수 있을 것으로 기대한다.

Key words: 남극 어류, 남극암치아목, 극지, 적응기작, 인공번식

Dev. Reprod. Vol 26, 2022 (Suppl. 1). pp 167

Tumor-derived Dilp8/INSL3 induces cancer anorexia by regulating feeding neuropeptides via Lgr3/8 in the brain

Eunbyul Yeom

School of Life Sciences, Kyungpook National University

(yeb@knu.ac.kr)

In patients with advanced-stage cancer, cancer-associated anorexia affects treatment success and patient survival. However, the underlying mechanism is poorly understood. Here, we show that Dilp8, a Drosophila homologue of mammalian insulin-like 3 peptide (INSL3), is secreted from tumour tissues and induces anorexia through the Lgr3 receptor in the brain. Activated Dilp8-Lgr3 signalling upregulated anorexigenic nucleobinding 1 (NUCB1) and downregulated orexigenic short neuropeptide F (sNPF) and NPF expression in the brain. In the cancer condition, the protein expression of Lgr3 and NUCB1 was significantly upregulated in neurons expressing sNPF and NPF. INSL3 levels were increased in tumour-implanted mice and INSL3-treated mouse hypothalamic cells showed Nucb2 upregulation and Npy downregulation. Food consumption was significantly reduced in intracerebrospinal INSL3-injected mice. In patients with pancreatic cancer, higher serum INSL3 levels increased anorexia. These results indicate that tumour-derived Dilp8/INSL3 induces cancer anorexia by regulating feeding hormones through the Lgr3/Lgr8 receptor in Drosophila and mammals.

Key words: cancer anorexia, cachexia, cytokine, tumor-host interaction

Dev. Reprod. Vol 26, 2022 (Suppl. 1). pp 168

Cardiotoxicity evaluation of drugs using human PSC-derived cardiomyocytes

Sung-Hwan Moon

Department of Animal Biotechnology, Sangji University

(safe33msh@gmail.com)

The use of hERG assay in the assessment of cardiotoxicity for drugs has prevented new drug development even if the drug is effective as the assay overly predicted the risks that are not detected in clinical practice. Moreover, the lack of database for prescribing drugs to patients with inherited arrhythmia has caused the difficulty of relying on clinical results. To overcome the limitations of the hERG assay, the CiPA project using iPSC-CMs has been conducted mainly in the U.S., Japan, and Europe, while the project goals include the construction of a database of 28 drugs. The database of drug cardiotoxicity based on iPSC-CMs for inherited arrhythmia could also be used as indirect data in drug prescription for patients with an underlying disease. In the present study, normal and inherited arrhythmia (IA) iPSC-CMs were used in constructing the database of 28 drugs evaluated through the CiPA project. As a result, 1) the arrhythmia function of the IA iPSC-CMs has been verified in terms of electrophysiology; 2) the IA iPSC-CMs were shown to have relatively high sensitivity towards arrhythmia-induced cardiotoxicity compared to normal iPSC-CMs at low concentrations of the CiPA low-risk drugs, which was an interesting finding. While the results in this study were obtained from in vitro analyses of cell lines from patients with LQTS and BrS, the analytic system developed in this study is anticipated to reduce the number of extensive clinical studies in search of optimal drugs for patients with an underlying disease. Based on the findings, further studies should be conducted to establish the databases of *in vitro* assessment of cardiotoxicity using iPSC-CMs obtained from more varied patients regarding the underlying disease, race, gender, and age. This is predicted to lead to the development of a search platform to determine the optimal drug concentration for prescription, as well as the development of new drugs for underlying diseases.

Acknowledgement: This work was supported by the Korea National Institute of Health (2020-NG-019-02, 2020-NG-016-00) and Korea Health Technology R&D Project through the Korea Health Industry Development Institute (KHIDI), funded by the Ministry of Health & Welfare, Korea (grant number: H120C0184) and the Korean Fund for Regenerative Medicine (KFRM) grant funded by the Korea government (the Ministry of Science and ICT, the Ministry of Health & Welfare) (21A0403L1).

포스터 초록

Dev. Reprod. Vol 26, 2022 (Suppl. 1). pp 171

A-01

Computational fluid dynamics using microfluidic devices and concave chip for 3D-culture system

Yun-Gwi Park[1], Yeo-Jin Son[1], *Sung-Hwan Moon[2], *Soon-Jung Park[1]

[1]Stem Cell Research Institute, T&R Biofab Co. Ltd

[2]Department of Animal Biotechnology, Sangji University

(ygpark@tnrbiofab.com)

The human pluripotent stem cells (hPSCs) have extensively researched as a source of developmental biology, regenerative medicine and tissue engineering. In many cases, the cell was cultured 3-dimentionally (3D) to mimic *in vivo* environment. For 3D culturing, spheroids are formed by suspending small clumps of hPSCs but they are heterogeneous because this method lacks of the ability to control the cell number and varies in size and shape. Therefore, in this study, we evaluated a computational fluid dynamics application in an *in silico*-designed and spheroid-based flow integration 3D cell culture chip to illustrate cell culture, drug screening, cytokine delivery, and differentiation of cells in a platform that partially recapitulates the natural environment. As a results, single hPSCs were forced to aggregate and generate uniformly, and the size of spheroid was controlled using 3D cell culture chip of different diameters (approximately 200 μm). Also, 0.05 mL/h or less flow rates induced no physical stress in the 3D cell culture chip. Advanced cell culture technologies can be used to accelerate research and discovery or the preclinical and clinical development of cell and cell-free therapies for urgent medical needs.

Key words: human pluripotent stem cells, 3D-culture system, microfluidic, concave chip, computational dynamic

Acknowledgement: This research was supported by This research was supported by grants from the Korea HealthTechnology R&D Project through the Korea Health Industry Development Institute (KHIDI), funded by the Ministry of Health & Welfare (HI20C0184) and the Korean Fund for Regenerative Medicine(KFRM) grant funded the Ministry of Science and ICT, the Ministry of Health & Welfare (21A0403L1) by the Korea government.

Dev. Reprod. Vol 26, 2022 (Suppl. 1). pp 172

A-02

Neurotrophin-4 supplementation promotes trophectoderm lineage specification during porcine preimplantation embryonic development

Mirae Kim[1,2], *Sang-Hwan Hyun[1,2,3]

[1]Laboratory of Veterinary Embryology and Biotechnology (VETEMBIO), Veterinary Medical Center and College of Veterinary Medicine, Chungbuk National University

[2]Institute for Stem Cell & Regenerative Medicine (ISCRM), Chungbuk National University

[3]Graduate School of Veterinary Biosecurity and Protection, Chungbuk National University

Neurotrophins are associated with successful implantation and maintenance of pregnancy. The aim of this study was to investigate the effect of neurotrophin-4 (NT-4) on porcine preimplantation embryonic development *in vitro*. Zygotes were treated with different concentrations of NT-4 (0, 1, 10, and 100 ng/mL) during *in vitro* culture (IVC). There was no significant difference in the cleavage rate of all NT-4 supplemented groups compared to the control group at 2 days after parthenogenetic activation (PA), but the blastocyst (BL) formation rate was significantly ($p<0.05$) higher only in the 10 ng/mL NT-4-treated group than the control. To investigate the effect of NT-4 on transcriptomic patterns during IVC, the mRNA expression levels of apoptosis- and trophectoderm (TE) lineage-related genes were evaluated in the NT-4-treated (10 ng/mL) BLs. The mRNA expression level of anti-apoptotic *BCL2L1* ($p<0.05$) was significantly increased in the NT-4-treated BLs than in the control, while the mRNA expression level of pro-apoptotic *BAX* ($p<0.05$) and the ratio of *BAX/BCL2L1* ($p<0.01$) were significantly decreased compared to the control group. In addition, we confirmed that the *CDX2* ($p<0.05$), *PPAG3* ($p<0.01$), and *GATA3* ($p<0.05$) transcript levels, which are known TE-related genes, were significantly increased in the NT-4-treated BLs. Furthermore, we also immunostained and analyzed BLs with SOX2 and CDX2 to determine the effect of NT-4 on the first lineage specification in porcine preimplantation embryonic development. Our results showed that NT-4 supplementation during IVC significantly ($p<0.05$) increased the number of CDX2-expressing cells, while significantly ($p<0.01$) decreased the number of SOX2-expressing cells and the ICM/TE ratio (SOX2/CDX2 ratio) in the PA-derived BLs. Taken together, we suggest that NT-4 supplementation during porcine preimplantation embryonic development can promote TE lineage specification.

Key words: pig, *in vitro* culture of embryos, neurotrophin-4, preimplantation embryonic development

Acknowledgements: This work was supported by grants from the “NRF funded by the Korean Government (2017K1A4A3014959, and 2020R1A2C2008276)” and “IPET in Food, Agriculture, Forestry and Fisheries (318016-5, and 320005-4)”, Korea.

Dev. Reprod. Vol 26, 2022 (Suppl. 1). pp 173

A-03

Treatment of CCL2 during *in vitro* maturation of porcine oocytes increases the efficiency

Sohee Kim, *Sang-Hwan Hyun

Laboratory of Veterinary Embryology and Biotechnology (VETEMBIO), Veterinary Medical Center and College of Veterinary Medicine, Chungbuk National University

Chemokines play an important role in regulating the complex immune system at the maternal-fetal interface during pregnancy. Chemokine (C-C motif) ligand 2 (CCL2) is also a key periovulatory chemokine in the cumulus-oocyte complexes (COCs). In this study, we confirmed the effect of CCL2 on the porcine COCs during *in vitro* maturation (IVM) and the subsequent embryonic development after parthenogenetic activation (PA) when several concentrations of CCL2 were treated during IVM. pFF (porcine follicular fluid) was obtained from different follicle sizes to perform the ELISA method. The concentration of CCL2 in pFF was significantly higher as the size of the ovarian follicle increases. RT-PCR and qRT-PCR was also performed to identify the expression level of *CCL2* in porcine follicular cells (Oocytes, Cumulus cells (CCs), Granulosa cells (GCs)) before and after IVM. As a result, the *CCL2* mRNA was expressed in GCs before and after IVM. However, *CCL2* mRNA expression in oocytes and CCs appeared only after IVM. In the qRT-PCR results, the mRNA expression levels were significantly higher in the group that underwent IVM in all porcine follicular cells. During IVM, CCL2 was added to the maturation media (TCM199-PVA) at concentrations of 0 (control), 1, 10, and 100 ng/mL for each group. After IVM, the 100 ng/mL CCL2-treated group (91.6±3.6%) showed a significantly higher ($p<0.05$) metaphase II rate compared to the control (81.8±1.8%). All CCL2-treated groups showed a significant ($p<0.05$) increase of intracellular GSH levels compared with control. On the other hand, the intracellular ROS levels in all of CCL2-treated oocytes were significantly decreased ($p<0.05$). In order to investigate the effect of CCL2 treatment on porcine COCs during IVM, various genes were analyzed by qPCR targeting CCs and oocytes. In apoptosis-related genes, pro-apoptotic gene *Bax* levels were significantly decreased in all CCL2-treated CCs and oocytes groups. *CASP3* levels were significantly decreased in the 100 ng/mL treatment group compared to the control in CC and significantly decreased in all treatment groups compared to the control in oocytes. In antioxidant-related genes, the levels of *SOD1* and *SOD2* were significantly increased in the 100 ng/mL group compared to controls in CCs, and the level of *NRF2* was significantly increased in the 10 ng/mL group compared to the control in oocytes. The level of *NPR2*, a gene associated with oocyte meiosis resumption, was significantly decreased in 100 ng/mL treatment CCs group compared to controls. The level of *NPM2*, a maternal effect gene, was significantly increased in the oocytes group treated with 10 ng/mL compared to the control. In CCL2 signaling pathway-related genes, it was confirmed that the *ERK1* level was significantly increased in the 10 ng/mL treatment group compared

to the control in both CCs and oocytes. Upon evaluation of subsequent embryonic development after PA, compared with the control group, the cleavage rate was significantly (p<0.05) improved in the 100 ng/mL CCL2-treated group, and the blastocyst formation rate in the 10 ng/mL CCL2-treated group was significantly improved.

In conclusion, the results suggest that CCL2 supplementation at appropriate concentrations in IVM media improves porcine oocyte maturation and the subsequent embryonic potential of PA embryos.

Key words: CCL2, *in vitro* maturation, porcine oocyte

Acknowledgements : This work was supported by grants from the “NRF funded by the Korean Government (2017K1A4A3014959, 2020R1A2C2008276)” and “IPET in Food, Agriculture, Forestry and Fisheries (318016-5, 320005-4)”, Korea.

Dev. Reprod. Vol 26, 2022 (Suppl. 1). pp 175

A-04

Miltefosine adversely affects sperm functions by altering the PI3K/AKT signaling pathway

Eun-Ju Jung[1], Jae-Hwan Jo[2], Seung-Ik Jang[2], Woo-Jin Lee[1], Ju-Mi Hwang[1], Jeong-Won Bae[1], *Woo-Sung Kwon[1,2]

[1]Department of Animal Science and Biotechnology, Kyungpook National University

[2]Department of Animal Biotechnology, Kyungpook National University

(red0787@naver.com)

Miltefosine is a therapeutic agent for leishmaniasis that occurred by Leishmania type parasites. Miltefosine is also considered as an AKT inhibitor and utilized in antineoplastic activity including inhibition of AKT that plays an important role in the PI3K/AKT signaling pathway. In spermatozoa, AKT is known to control sperm functions such as sperm motility and acrosome reaction. However, how miltefosine affects PI3K/AKT signaling pathway-related proteins in sperm and its effects on sperm functions have not yet been studied. Therefore, the purpose of this study is to investigate the effect of miltefosine on the PI3K/AKT signaling pathway-related proteins in sperm and reproductive toxicity. Duroc semen was treated with various concentrations of miltefosine (0, 2.5, 5, 10, 20, 40, and 80 μM) and incubated to induce capacitation. Then, expression levels of PI3K/AKT signaling pathway-related proteins [AKT, phospho-AKT (Thr^{308} and Ser^{473}), PI3K, phospho-PI3K, PTEN, phospho-PTEN, and PDK1] and tyrosine-phosphorylated proteins were measured. In addition, sperm functions (sperm motility, motion kinematic parameters, and cell viability) were assessed. The results show that expression levels of PI3K/AKT signaling pathway-related proteins except for PI3K, PTEN, and PDK1 were increased in a dose dependent manner. The expression levels of tyrosine-phosphorylated proteins were decreased in a dose dependent manner. Sperm motility and motion kinematic parameters were decreased. There was no significant difference in cell viability. Taken together, these results suggest that miltefosine may induce alteration of PI3K/AKT signaling pathway and suppress the sperm functions. Therefore, we suggest that when taking miltefosine, special attention needs to be paid to reproductive toxicity.

Key words: miltefosine, PI3K/AKT signaling pathway-related proteins, sperm functions, capacitation

Acknowledgements: This work was supported by the National Research Foundation of Korea (NRF) grant funded by the Korea government (Ministry of Science and ICT) (NRF-2022R1F1A1066103).

Dev. Reprod. Vol 26, 2022 (Suppl. 1). pp 176

A-05

Differentiation of porcine embryonic stem like cells derived from aggregated blastomeres into three germ layers

Joohyeong Lee[1,2], Eunsong Lee[3], *Sang-Hwan Hyun[1,2,4]

[1]Veterinary Medical Center and College of Veterinary Medicine, Laboratory of Veterinary Embryology and Biotechnology (VETEMBIO), Chungbuk National University

[2]Institute of Stem Cell & Regenerative Medicine (ISCRM), Chungbuk National University

[3]College of Veterinary Medicine, Kangwon National University

[4]Graduate School of Veterinary Biosecurity and Protection, Chungbuk National University

Production of high-quality blastocysts via aggregation can be a method to improve porcine embryonic stem-like cells (pESLCs) efficiency. Here, we determined the optimal conditions for blastomere aggregation using phytohemagglutinin-L (PHA-L) and examined PHA-L efficiency by comparing it with Well of the Well (WOW), a general blastomere aggregation method. As a result, we confirmed that treatment with 15 μg/mL PHA-L for 144 h was effective for blastomere aggregation and embryonic development of three zona-free 2-cell stage embryos (TZ2Es) after parthenogenetic activation (PA). The TZ2Es cultured with PHA-L showed a significantly (p<0.05) higher blastomere aggregation rate than the WOW method (93.5±1.9% vs. 78.0±8.5%). In addition, our results demonstrated that TZ2Es aggregation through PHA-L improved the quality of PA-derived blastocysts and improved pESLCs seeding efficiency and quality of colonies. It was also observed that PHA-L-derived pESLC could remain undifferentiated and exhibit typical embryonic stem cell pluripotency markers. It was confirmed that POU5F1, SOX2, and NANOG genes were expressed through immunostaining in pESLCs derived from PHA-L, unlike feeder cells. Interestingly, pESLCs derived from PHA-L showed significantly higher NANOG expression than control (pESLCs from non-aggregated embryos). Finally, we demonstrated that PHA-L-derived pESLCs could contribute to the formation of normal pESLCs by confirming that they are capable of differentiation into endoderm, mesoderm and ectoderm after embryoid bodies (EB) formation. In conclusion, TZ2E aggregation through PHA-L improved the quality of PA-derived blastocysts, as well as pESLC seeding efficiency and quality of colonies. It was also demonstrated that PHA-L-derived pESLCs could remain undifferentiated and exhibit typical Embryonic stem cell pluripotency markers, EB-forming ability, and differentiation into cell lineages of three germ layers. This technique is expected to improve embryo quality and embryonic stem cell establishment efficiency and can be utilized for blastocyst complementation systems and the production of chimeric animals.

Key words: blastomere aggregation, phytohemagglutinin-L, embryonic stem-like cells, parthenogenesis, pig.

Acknowledgements: This work was supported by the National Research Foundation of Korea (NRF) grant funded by the Korea government (Ministry of Science and ICT: NRF-2021R1C1C2013954).

Dev. Reprod. Vol 26, 2022 (Suppl. 1). pp 177

A-06

Tetraconazole induces apoptosis and autophagy in mammary epithelial cells

SeonAe Jeong[1], Jisoo Song[1], Gwonhwa Song[2], *Whasun Lim[1]

[1]Department of Biological Sciences, Sungkyunkwan University

[2]Institute of Animal Molecular Biotechnology and Department of Biotechnology, Korea University

Pesticide has been used in the agricultural industry from the past to the present. Although it indicates toxicity, it has contributed to reduce agricultural labor by controlling fungi, pests, and plants. However, the residual pesticides affect people who are the ultimate consumers of the food chain. Bovine milk is a primary nutrient source, essential for growth, and a source capable of making a variety of dairy products. The mammary epithelial cell regulates the blood-milk barrier conjunction, which is important to creating a dairy product. In the present study, we investigated the effect of tetraconazole which is one of the fungicides in triazole group on mammary epithelial cells (MAC-T). First, we checked whether tetraconazole regulates cell viability of MAC-T. Results of cell viability analysis revealed that tetraconazole decreased the cell viability in a dose-dependent manner. In addition, we performed annexin/FITC, JC-1, and rhod-2 assays by flow cytometry analysis. Tetraconazole induced cell death with mitochondrial membrane potential and disruption of mitochondrial calcium levels in MAC-T cells. Also, it caused cell cycle arrest and inhibited the expression of proliferating cell nuclear antigen protein by immunofluorescence analysis. The results of western blot analysis showed an increase of cleaved caspase-3, BAX and cytochrome c proteins in tetraconazole-treated MAC-T cells as compared to control. Moreover, it regulated activation of protein kinases belonged to MAPK and PI3K pathways. Collectively, tetraconazole may affect the milk production via regulating bovine mammary epithelial cells.

Key words: tetraconazole, mammary gland, cell death, calcium homeostasis, signal transduction

Acknowledgements: This work was supported by the National Research Foundation of Korea (NRF) grant funded by the Korea government (MSIT) (No. 2021R1C1C1009807). Also, this research was supported by Basic Science Research Program through the National Research Foundation of Korea (NRF) funded by the Ministry of Education (No. NRF-2019R1A6A1A10073079).

Dev. Reprod. Vol 26, 2022 (Suppl. 1). pp 178

A-07

Pendimethalin exposure induces bovine mammary epithelial cell (MAC-T) death through excessive ROS production and alterations in the PI3K and MAPK signaling pathways

Hojun Lee[1], Garam An[1], Whasun Lim[2], *Gwonhwa Song[1]

[1]Institute of Animal Molecular Biotechnology and Department of Biotechnology, Korea University

[2]Department of Biological Sciences, Sungkyunkwan University

Pendimethalin (PDM) is one of the dinitroaniline class herbicides which is used to protect crops from annual grasses. Although PDM is approved in many countries, PDM has been established to be toxic to non-target organisms. There is relatively high possibility of PDM exposure to livestock. However, the effect of PDM on milk production system has not been reported yet. In this study, we investigated the toxicity of PDM in the mammary glands. We used one of the mammary gland cell lines, mammary epithelial cells (MAC-T) of cattle. We treated MAC-T cells with different dosage (0, 2.5, 5 and 10 μM) of PDM. We found that PDM reduced cell viability and proliferation, and induced cell cycle arrest in MAC-T cells. In addition, PDM caused cell apoptosis, triggered oxidative stress which is producing reactive oxygen species excessively and led the mitochondrial membrane potential (MMP) loss in MAC-T cells. Furthermore, PDM disrupted calcium homeostasis both in cytosol and mitochondria of MAC-T cells and activated the expression of protein which is related to endoplasmic reticulum (ER) stress. PDM also altered the PI3K and MAPK signaling pathway. Collectively, our finding suggests that PDM has adverse effect on MAC-T cells and may interrupt producing milk in cattle.

Key words: pendimethalin, MAC-T, apoptosis, ROS, ER stress, cell signaling pathway

Acknowledgements: This research was supported by the National Research Foundation of Korea (NRF) grant funded by the Korea government (MSIT) (grant number: 2021R1A2C2005841).

Dev. Reprod. Vol 26, 2022 (Suppl. 1). pp 179

A-08

Oxyfluorfen causes apoptosis through MAPK and AKT signaling in bovine mammary gland epithelial cells

Hyewon Jang[1], Jisoo Song[1], Jiyeon Ham[2], Gwonhwa Song[2], *Whasun Lim[2]

[1]Department of Biological Sciences, Sungkyunkwan University

[2]Institute of Animal Molecular Biotechnology and Department of Biotechnology, Korea University

Oxyfluorfen is a compound used as an insecticide that can cause chronic effects on invertebrates, fish, and mammals, causing serious damage to the ecosystem. As a result, it becomes impossible to preserve various creatures, so it is necessary to investigate the toxicity of animals. However, to date, the mechanisms that cause the toxic effects in mammals are not well known. Therefore, this study was conducted to find out the toxic effect using the bovine mammary epithelial cell (MAC-T) with high access to humans. First, through several experiments, changes in the function of MAC-T cells were evaluated when oxyfluorfen were treated at various concentrations (0, 1, 2, 5, and 10 ppm). The results showed a reduction of cell survival and 3D-spheroid formation, cell cycle progression, and mitochondrial membrane potential in oxyfluorfen-treated MAC-T. In addition, phosphorylation of signaling molecules involved in the MAPK pathway was reduced, and phosphorylation of AKT signaling molecules was increased. Also, it was confirmed that early apoptotic cells were increased in a dose-dependent manner, and the apoptosis was ultimately caused by increased expression of pro-apoptotic proteins and decreased expression of anti-apoptotic proteins. Therefore, this toxic effect of oxyfluorfen can lead to the death of bovine mammary gland epithelial cells, resulting in a decrease in milk production capacity, which can eventually cause damage to humans.

Key words: oxyfluorfen, bovine mammary epithelial cells, cell cycle arrest, TAK1, MAPK

Acknowledgements: This work was supported by the National Research Foundation of Korea (NRF) grant funded by the Korea government (MSIT) (No. 2021R1C1C1009807).

Dev. Reprod. Vol 26, 2022 (Suppl. 1). pp 180

A-09

Effect of 4-nonylphenol on sperm functions

Ju-Mi Hwang[1], Jae-Hwan Jo[2], Seung-Ik Jang[1], Eun-Ju Jung[1], Woo-Jin Lee[1], Jeong-Won Bae[1], *Woo-Sung Kwon[1,2]

[1]Department ot Animal Science and Biotechnology, Kyunpook National University
[2]Department ot Animal Biotechnology, Kyunpook National University
(jmhwang1001@gmail.com)

4-Nonylphenol is well-known endocrine-disrupting chemicals and derives from the degradation of nonylphenol ethoxylates. 4-Nonylphenol is used as a surfactant in various industries, which are extensively used in formulation of detergents, plastic food packaging, and textiles. However, the underlying mechanisms of male reproductive dysfunction have been not fully elucidated. The purpose of this study was to investigate the effects of 4-Nonylphenol on sperm functions and mechanisms. Firstly, spermatozoa treated with 4-nonylphenol (0, 10, 25, 50, 75, and 100 μM) was incubated for 60 mins. Then, various sperm functions (sperm motility and motion kinematics, capacitation status, intracellular ATP level, and cell viability) were evaluated. Finally, the expression levels of phosphor-PKA substrates and tyrosine phosphorylation proteins were analyzed. As a results, sperm motility and motion kinematics decreased in a dose-dependent manner during capacitation, and intracellular ATP levels were significantly increased in high concentrations of 4-nonylphenol. For this reason, the capacitated sperm may be promoted abnormally. Thus, PKA activity and tyrosine phosphorylation were also significantly altered. The physiological suppression of sperm function may depend on abnormal tyrosine phosphorylation via the alteration of PKA activity. Consequently, 4-nonylphenol induces male infertility via a negative effect on sperm quality, it is substantial to take caution with the continued use of 4-nonylphenol that disrupts male reproductive health.

Key words: 4-nonylphenol, spermatozoa, capacitation, sperm functions

Dev. Reprod. Vol 26, 2022 (Suppl. 1). pp 181

A-10

Effects of fibroblast growth factor 7 (FGF7) on *in vitro* growth and maturation of porcine oocytes

Haomiao Zheng[1,2], Sang-Hwan Hyun[1,2]

[1]Institute of Stem Cell & Regenerative Medicine (ISCRM), Chungbuk National University

[2]Laboratory of Veterinary Embryology and Biotechnology (VETEMBIO), Veterinary Medical Center and College of Veterinary Medicine, Chungbuk National University

Fibroblast growth factor-7 (FGF7), also known as keratinocyte growth factor (KGF), is a cytokine belonging to the fibroblast growth factor family. As its effect on the growth, maturation and subsequent development of porcine oocytes has not been clarified, the present study will aim to investigate this effect. For the purpose of this study, different concentrations of FGF-7 were added to the *in vitro* maturation (IVM) medium, followed by examination of oocyte size, nuclear maturation and associated GSH levels. Supplemental concentrations of FGF-7 (0, 1, 10 and 100 ng/mL) were provided in IVM medium. After 42 h of IVM, oocyte diameter were significantly increased ($p<0.05$) in all FGF-7-treated groups (1 ng/mL, 108.7±0.9 μm; 10 ng/mL, 109.4±0.3 μm; 100 ng/mL, 108.8±0.7 μm) compared to the control group (106.3±0.3 μm). In addition, the 10 ng/mL FGF-7-treated group showed a significant effect in promoting oocyte maturation by increasing the polar body extrusion rate, 83.9±1.8% (control), 89.9±2.1% (1 ng/mL), 92.6±3.4% (10 ng/mL), and 89.1±3.6% (100 ng/mL), respectively ($p<0.05$). Furthermore, intracellular GSH levels were significantly increased in the 1 ng/mL FGF-7-treated group ($p<0.05$). Although further studies on the cytoplasmic and developmental mechanisms of FGF-7 are needed, its supplementation during IVM not only increases intracellular GSH levels in porcine oocytes, but also affects oocyte diameter and polar body extrusion. In conclusion, the results of this study suggest that FGF-7 can be used as a supplement to IVM media to regulate oocyte maturation.

Key words: IVM, FGF7, KGF, porcine oocyte

Acknowledgement: This work was supported by grants from the “NRF funded by the Korean Government (2017K1A4A3014959, 2020R1A2C2008276, 2021R1C1C2013954, 2022R1A4A1025557)” and “IPET in Food, Agriculture, Forestry and Fisheries (318016-5, 320005-4, 819029-2)”, Korea.

Dev. Reprod. Vol 26, 2022 (Suppl. 1). pp 182

A-11

Characteristics of boar semen treated with Myo-inositol during its liquid preservation

Ali Jawad[1,2], Joohyeong Lee[1,2], Sang-Hwan Hyun[1,2]

[1]Institute for Stem Cell & Regenerative Medicine (ISCRM), Chungbuk National University

[2]Laboratory of Veterinary Embryology and Biotechnology (VETEMBIO), College of Veterinary Medicine, Chungbuk National University

The quality of boar semen during its liquid preservation at 17℃ decreased by oxidative stress. Therefore, antioxidant supplementation can improve the semen quality when it is stored for 7 days. Myo-inositol (Myo-Ins) is an antioxidant that plays a vital role in improving human sperm quality and the rate of fertilization. There is a paucity of studies about Myo-Ins supplementation and its antioxidative role on boar semen. We evaluated the role of Myo-Ins on the viability and acrosome integrity of boar spermatozoa on day 0, 1, 3, 5, and 7 during liquid preservation. Moreover, we also investigated the effect of Myo-ins on the concentration of lipid peroxidation compound malondialdehyde (MDA) in boar semen. The aim of the present study was to assess the effect of different concentrations of Myo-Ins (2, 4, 6, and 8 mg/mL) on boar sperm quality parameters (viability and acrosome integrity) and oxidative stress. The results showed that the viable sperm cells increased significantly (p<0.05) on day 1 (84.5%), 3 (88.0%), and 7 (81.6%) in the 2 mg/mL group compared to the control group on day 1 (80.8%), 3 (80.9%), and 7 (81.6%). The acrosome integrity depicted no significant (p>0.05) results in the treatment groups compared to the control group. However, 2 mg/mL group displayed a significant result (p<0.05) on day 7 (91.9%) compared to the control group (85.2%). Furthermore, MDA content was slightly lower in the treatment groups compared to the control group, but no significant result (p>0.05) was observed. In short, these results suggest that the proper supplementation of Myo-Ins (2 mg/mL) in boar semen extender may improve the boar semen viability, acrosome integrity, and MDA via its antioxidant mechanism during preservation at 17℃.

Key words: boar, semen, viability, acrosome integrity, malondialdehyde

Acknowledgement: This work was supported by grants from the “NRF funded by the Korean Government (2017K1A4A3014959, 2020R1A2C2008276, 2021R1C1C2013954, 2022R1A4A1025557)” and “IPET in Food, Agriculture, Forestry and Fisheries (318016-5, 320005-4, 819029-2)”, Korea.

Dev. Reprod. Vol 26, 2022 (Suppl. 1). pp 183

B-01

Growth performance of red-spotted grouper according to water temperature conditions

Byeong-Hoon Kim, Song-Hee Choi, Kang-Hee Im, Young-Don Lee, *Chi-Hoon Lee

Marine Science Institute, Jeju National University

(endand1011@naver.com)

Red-spotted grouper *Epinephelus akkara* belonging to the Serranidae family are subtropical species and mainly distributed in tropical and subtropical regions. For red-spotted grouper, the summer season, when the water temperature increases, is a period when body growth is promoted due to active food activities. However, the winter season when the water temperature decreases is a period when food activity and motility decrease and body growth also slows. Therefore, the change in water temperature acts as a very important factor in the red-spotted grouper farming. The aim of this study was to explore the optimum rearing temperature conditions for red-spotted grouper for commercial production. We reared fish under different water temperature conditions (23℃, 26℃, 29℃, and 32℃) for 6 weeks, and the growth performance according to each condition was investigated. And histological changes in liver, intestine, and gonad tissues were observed using histological method. In addition, the change in mRNA expression of corticotropin-releasing hormone (CRH), known as a factor responding to stress in the hypothalamus, was investigated. As a result, the 29℃ condition showed a faster increase in body wight than the 23℃ condition. In addition, the weight gain, growth rate, food supply, feed coefficient, feed efficiency, and condition factor were also advantageously observed under 29℃ condition. The hepatosomatic index (HSI) levels showed the lowest at 23℃ condition, and the diameter of hepatocytes was observed the largest at 26℃ and 29℃ conditions. The number of goblet cells in the intestinal villi was observed more at 29℃ condition than under other conditions. There was no significant difference in gonadosometic index (GSI) levels between all experimental groups, and histological observation of ovaries showed that perinucleolar stage (Pn) oocytes in all experimental groups. However, the diameter of oocytes in the 23℃ condition tended to be slightly larger than that of other groups. Finally, the expression of CRH mRNA in the brain was higher at 32℃ condition than in other conditions. In order to effectively improve the body growth of red-spotted grouper through our experiment, it is considered that the water temperature conditions in the range of 26℃ to 29℃ are suitable. Our study provides preliminary information on the basic rearing environment for red-spotted grouper farming, and it is thought that it can be used as a reference study to evaluate the suitability of water temperature conditions.

Key words: corticotropin-releasing hormone, growth performance, hepatosomatic index, red-spotted grouper, weight gain

Dev. Reprod. Vol 26, 2022 (Suppl. 1). pp 184

B-02

Reproductive potential and cycles in cultured Pacific bluefin tuna (*Thunnus orientalis*) of sea net cage in South Korea

Jin Woo Park, Jae-Hoon Kim, Seung Cheol Ji, *Jeong-Hyeon Cho

Jeju Fisheries Research Institute, National Institute of Fisheries Science

(pjw1446@korea.kr)

Pacific bluefin tuna (*Thunnus orientalis*, PBT) is one of the commercially important fish species with high market price, and research has been underway in South Korea for the development of effective aquaculture production technology for PBT. However, there have been difficulties in terms of producing fertilized eggs. In order to overcome this problem, it is necessary to understand the reproductive biology of the PBT, but in Korea, the rearing technology up to matured-size has not been carried out smoothly, resulting in few studies on reproductive biology of PBT. Therefore, in this study, in order to increase the aquaculture productivity of PBT, the reproductive cycle of cultured PBT in South Korea was investigated and their reproductive potential was investigated. For this study, PBT samples were obtained from 70 individuals (5～6 year old PBTs / male: 37, female: 33 / folk length: >150 cm, body weight: >70 kg) cultured for commercial purposes in sea net cages near Yokjido Island, Tongyeong. The research period was from April 2020 to March 2021, and environmental data such as water temperature and photoperiod were collected during the period. All gonads of the PBTs were weighed to calculate gonadosomatic index (GSI), and male and female maturity stages were classified through histological analysis of gonads. Male and female gonadal developmental stages were examined, and were presented and classified in percentages by month. In addition, changes in sex steroid hormone (male, testosterone and 11-ketotestosterone; female, testosterone and estradiol-17β) levels in the plasma of PBTs were evaluated by monthly. As a result, both male and female gonadal developmental stages were classified into four major stages (stages I to IV), and the period of appearance of PBTs with mature gonad was from May to August for males and from June to August for females. Also, as a result of the analysis of GSI and sex steroid hormones of male and female PBTs, both males and females showed a trend of an increase in these values from May, reaching a peak in June, and decreasing thereafter. The water temperature in June to August (the spawning season) was in the range of 22 to 24℃, and the photoperiod was 14 h light: 10 h dark. In comprehensive consideration of the study findings, reproductive potential of PBTs cultured in sea net cages in South Korea was confirmed, and during the study period, gonads that reached reproductive maturity were confirmed in July. This study is the first research investigating reproductive biology of PBT conducted in South Korea, and the findings are expected to be utilized as basic data for future PBT aquaculture research in the country.

Key words: Pacific bluefin tuna, aquaculture, sea net cages, reproductive cycle, gonadal development

Dev. Reprod. Vol 26, 2022 (Suppl. 1). pp 185

B-03

Genetic analysis for hierarchical dendrogram of *Charybdis* crab population

***Jong-Man Yoon**

Department of Aquatic Life Medicine, College of Ocean Science and Technology, Kunsan National University

Korean *Charybdis* crab (*Charybdis japonica*) is one of ecologically significant portunid crab species in the Yellow sea, belonging to the family Portunidae, and the order Decapoda. Genomic DNA (gDNA) set apart from two populations of Korean *Charybdis* crab was augmented by PCR experiments. With the aim of accomplishment, this author achieved clustering analyses of Korean Charybdis crab (*Charybdis japonica*) in the Yellow Sea of Korea. Two sample collections of crab muscle was gathered in disinfected cylinders, proximately positioned on cold ice, and retained at –79℃ until required. PCR inquiry was achieved the genomic DNAs from 22 individuals, consuming different five ONT-primers. The median within-group correspondence was rated via pairwise matching inquiry between the parties within a group. A PHD was generated renowned on SMs to take a cluster tree using Systat version 10. The five oligonucleotides primers (ONT-primers) were spent to yield the number of unique loci shared to each crab population (ULSECP) and number of loci shared by the two crab populations (LSTCP). 305 fragments (FRAGs) were identified in the Charybdis crab population A (CCPA), and 344 in the Charybdis crab population B (CCPB): 44 number of ULSECP (14.43%) in the CCPA and 110 (31.98%) in the CCPB. 44 number of LSTCP, with an average of 8.8 per primer, were detected in the two crab populations. The bandsharing (BS) value between entity's no. 01 and no. 10 was the lowest (0.371) between the two CCPs. The average bandsharing (ABS) values of individuals in the CCPA (0.575±0.014) were lesser than in those originated from the CCPB (0.705±0.011) (p<0.05). The polar hierarchical dendrogram (PHD) achieved by the five ONT-primers denotes three genetic clusters (GCs): cluster I (CHARYBCRAB 01, 04, 05, 06 and 08), cluster II (CHARYBCRAB 02, 03, 07, 09, 10 and 11) and cluster III (CHARYBCRAB 12, 13, 14, 15, 16, 17, 18, 19, 20, 21 and 22). The longest GD showing significant MDs between two *Charybdis* crab populations was observed in individuals CHARYBCRAB no. 06 and CHARYBCRAB no. 01 (0.632). In due course, individual no. 01 of the CCPA was most distantly related to CCPA no. 06 (GD=0.632).

Key words: BS value; *Charybdis japonica*, CCP, GCs, GD, ONT-primer, PHD, SM.

Dev. Reprod. Vol 26, 2022 (Suppl. 1). pp 186

B-04

멍게 유생의 꼬리 끝에서 발현하는 유전자

신은영, 송미리, *김길중

강릉원주대학교 해양생명과학과

(*gjkim@gwnu.ac.kr)

해양무척추동물 멍게(*Halocynthia roretzi*)는 척추동물 및 두삭동물(창고기)과 함께 척삭동물문(phylum Chordata)으로 분류된다. 멍게의 수정란은 규칙적인 난할과 비교적 빠른 배아발생 단계를 거쳐 수온 13도에서 약 36시간 후에 척삭동물의 기본형으로 추정되는 올챙이형 유생으로 부화한다. 유생의 꼬리 끝에는 원시생식세포 운명을 포함하는 내배엽가닥(endodermal strand) 구조가 위치하는 데, 이 구조의 특성화 및 발생 기능에 관하여 불명확한 것이 많다. 본 연구에서는 멍게 배아발생 과정에서 꼬리싹(tailbud) 배아의 꼬리 끝에서 특이적으로 발현하는 2종류의 유전자를 클로닝하고 발현 패턴을 조사하였다. RTK 신호전달 과정에서 신호전달 매개자로 기능하는 것으로 알려진 Nck1(non-catalytic region of tyrosine kinase adaptor protein 1)의 멍게 상동체 HrNck1의 전사체는 초기 꼬리싹 배아의 꼬리 끝 부위와 간충직 전구세포에서 발현하였다. 이 발현 패턴은 부화시기까지 지속되었다. 다양한 세포 기능과 관련된 GTP 결합단백질에 속하는 Arf6(ADP-ribosylation factor 6)의 멍게 상동체 HrArf6의 mRNA는 중기 꼬리싹 배아의 꼬리 끝에서 발현하였다. 이 유전자들의 단백질은 다양한 기능을 갖지만, 그중에서 actin cytoskeletal remodeling에 관여하는 것으로 알려져 있다. 따라서 세포골격 재배치를 통한 원시생식세포의 이동을 포함하여 멍게 유생의 변태 과정에서 이 유전자 산물들이 중요한 역할을 할 가능성이 시사된다. 앞으로 이 유전자들의 발생학적 기능을 보다 상세하게 연구하고자 한다.

Key words: *Halocynthia roretzi*, endodermal strand, Nck1, Arf6

Dev. Reprod. Vol 26, 2022 (Suppl. 1). pp 187

B-05

Transcriptomic changes in the HPG axis of eel (*Anguilla japonica*) in response to seawater and SPE injection

Seong Hee Mun, Jeong Hee Yoon, Ji Eun Ha, Noh Young Kim, Dong Woo Kim, *Joon Yeong Kwon

Department of Applied Biological Science, Sunmoon University

(jykwon@sunmoon.ac.kr)

Artificial sexual maturation of female eel is induced by repeatedly injecting SPE (salmon pituitary extract) after acclimatizing from freshwater to seawater. However, it is not fully understood what kind of biological changes are caused by these treatments in the body of eels.

In this study, wild female eels were accommodated under four different conditions: FW (freshwater without SPE treatment), SW (seawater without SPE treatment), FW+SPE (freshwater with weekly SPE injection), SW+SPE (seawater with weekly SPE injection) to investigate transcriptomic changes in the HPG (hypothalamus-pituitary-gonad) axis of eels induced by different salinity and SPE injections.

Based on KEGG analysis, salinity increased the expression of genes related to the 'environmental information processing' pathway in the brain, pituitary and gonad of eels. SPE injection increased the expression of genes related to 'signaling molecules and interaction' and 'endocrine system' pathways in the eel brain, and increased the expression of genes related to 'metabolism' and 'genetic information processing' pathways in the pituitary, and increased the expression of genes related to 'signal transduction' and 'cellular processes' pathways in gonad. These results indicate that SPE injection may up regulate genes in wider range of pathways than salinity change may do.

There were more SPE sensitive genes than the salinity sensitive genes in reproduction-related pathways (MAPK signaling pathway, Wnt signaling pathway, insulin signaling pathway, neuroactive ligand-receptor interaction, GnRH signaling pathway, oocyte meiosis, progesterone-mediated oocyte maturation, steroid hormone biosynthesis and steroid biosynthesis) in all tissues investigated in this study. Theses results support the idea that pituitary-derived factors play key roles in the reproduction of eels.

Key words: eel, salinity, SPE injection, sexual maturation, differentially expressed gene analysis

Acknowledgement: This research was supported by Basic Science Research Program through the National Research Foundation of Korea (NRF) funded by Ministry of Education (NRF-2020R1A2C1010475).

Dev. Reprod. Vol 26, 2022 (Suppl. 1). pp 188

B-06

Production of fertilized eggs from captive-reared broodstock and larval rearing of Korean pomfret, *Pampus argenteus*

In Joon Hwang[1], Jong Cheol Han[1], Yeon Min Jeong[2], *Hee Woong Kang[1]

[1]Aquaculture Industry Division, West Sea Fisheries Research Institute

[2]Gyeongsangnamdo Fisheries Resources Research Institute

(hwgang@korea.kr)

The present study describes the first trial on broodstock development, induced breeding, production of fertilized eggs and larval rearing of Korean pomfret, *Pampus argenteus* in Korea. Korean pomfrets were collected from Tongyeong, southern coastal waters of Korea. These fishes were stocked in 10 m^3 flow-through circular tank having water temperature controlling facility for broodstock management. Broodstocks were fed using defrosted squid, oyster and shrimp at a rate of 5% of body weight per day. In March 2022, the water temperature was 18℃ and we increased it at a rate of 1℃ per 10 days until it reached at 24℃. The fish spawned after 12 days of induction at a temperature 24±0.5℃. Fertilized eggs were collected and stocked in 1 m^3 tank for hatching. The diameter of egg and oil droplet were 1.41±0.09 mm and 0.53±0.05 mm, respectively. The eggs hatched out after 42～44 h of rearing at a temperature of 20±1℃. The overall fertilization and hatching rate was found to be 97.40±2.19% and 50.26±30.45%, respectively. Larval rearing was carried out using green water system by addition of chlorella. The newly hatched larvae was 4.36±0.63 mm in total length. The mouth and anus had not yet opened. The mouth opening was formed 48～50 h post hatch. At 21 days post hatching, total length was 6.73±0.59 mm. The present study is the first report of broodstock development, induced spawning and larval rearing of this species in Korea.

Key words: Korean pomfret, natural spawning, fertilized eggs, hatched larvae

Acknowledgement: This study was granted from NIFS (R2022005).

Dev. Reprod. Vol 26, 2022 (Suppl. 1). pp 189

B-07

Ethalfluralin induces developmental toxicity via oxidative stress in zebrafish models

Taeyeon Hong[1], Hahyun Park[2], Gwonhwa Song[2], *Whasun Lim[1]

[1]Department of Biological Sciences, Sungkyunkwan University

[2]Institute of Animal Molecular Biotechnology and Department of Biotechnology, Korea University

(taeyeon97@g.skku.edu)

Ethalfluralin is a herbicide belonging to the dinitroaniline family that inhibits weed growth without harming agricultural products. In addition, early exposure to pregnant women and children from herbicide causes serious damages. In previous study, ethalfluralin has been elucidated that it interferes implantation during early pregnancy in other vertebrate models. However, the effect of ethalfluralin exposure has not been reported in embryonic development of zebrafish. In this study, we investigated the effect of ethalfluralin on developmental toxicity using wild type and transgenic models of zebrafish. First of all, we observed a decrease in survival rates as a result of treatment based on LC_{50}. And zebrafish larvae appeared morphological changes including body length, yolk and heart edema by ethalfluralin. According to toxic effects of ethalfluralin, larvae showed apoptotic cell death using acridine orange and TUNEL staining assay. Specifically, ethalfluralin increased mRNA expression level of apoptosis related genes such as *tp53*, *casp3*, *casp8*, *casp9*, and *cyc1*. In addition, we evaluated the effects of ethalfluralin by using *flk1:eGFP* transgenic model and the results indicated disruption of vasculature in brain and intestine. Specifically, ethalfluralin decreased the mRNA expression of angiogenesis related genes. Moreover, it increased relative oxygen species (ROS) production and inflammation with an increase of inflammatory factors such as *cox2a*, *cox2b*, *cxcl-c1c*, *il8*, and *nf-κb*. Furthermore, mitochondrial respiration of larvae were measured through Seahorse assay, and ethalfluralin decreased ATP production compared to control due to mitochondrial dysfunction. Collectively, ethalfluralin may interfere development of zebrafish and ecosystem.

Key words: ethalfluralin, angiogenesis, apoptosis, oxidative stress, inflammation

Acknowledgement: This work was supported by the National Research Foundation of Korea (NRF) grant funded by the Korea government (MSIT) (No. 2021R1C1C1009807). Also, this research was supported by Basic Science Research Program through the National Research Foundation of Korea (NRF) funded by the Ministry of Education (No. NRF-2019R1A6A1A10073079).

Dev. Reprod. Vol 26, 2022 (Suppl. 1). pp 190

B-08

The herbicide fluridone induces developmental abnormalities in embryo-larval zebrafish through cardiac malformation

Hahyun Park[1], Taeyeon Hong[2], Whasun Lim[2], *Gwonhwa Song[1]

[1]Institute of Animal Molecular Biotechnology and Department of Biotechnology, Korea University

[2]Department of Biological Sciences, Sungkyunkwan University

(pa1301@korea.ac.kr)

Fluridone is a well-known herbicide that slowly diffuses throughout the entire water to disturb the growth of undesirable aquatic weed species by inhibiting carotenoid biosynthesis. Since unpredictable environmental pollution from herbicide exposure has been reported in the last few decades, assessing the harmfulness of herbicides is important for regulating their use properly. The aim of this study is to evaluate developmental toxicity of the herbicide fluridone using zebrafish embryos. Our study organizes a relevant concentration of fluridone on account of its sub-lethal toxic effects which shown by the LC_{50} value. After exposure to fluridone for 96 hours, zebrafish embryos revealed increasing lethality and various developmental malformations including heart and yolk sac edema, shortened body length, spinal curvature, and reduced eye size. Exposure to fluridone caused apoptotic cell death in the anterior region of developing larvae particularly within the brain. Then, we used transgenic zebrafish (*fli1a;eGFP* and *cmlc2;dsRed*) to identify toxic mechanism of fluridone affected cardiovascular development in early stage of zebrafish. Ectopic growth of sub-intestinal vessels (SIVs) is highly inhibited in response to fluridone, and complete development has not been achieved in the vessels of hindbrain region and dorsal aorta. The genetic expression of VEGF signaling molecules were highly decreased, in addition, structural genes involved in cardiovascular system altered by fluridone. In conclusion, fluridone exposure to non-targeted organisms hampered the developmental process during embryogenesis. As zebrafish known as useful vertebrate *in vivo* model to determine toxicological characteristics of herbicides, the results generally indicated whether direct or indirect exposure of fluridone to the communities in aquatic organisms and even humans can evoke the problems related to the survival.

Key words: fluridone, developmental toxicity, cardiovascular malformation, embryos, apoptosis

Acknowledgement: This research was supported by Basic Science Research Program through the National Research Foundation of Korea (NRF) funded by the Ministry of Education (No. NRF-2019 R1A6A1A10073079 & 2022R1I1A1A01056642).

Dev. Reprod. Vol 26, 2022 (Suppl. 1). pp 191

B-09

Thiobencarb impairs development of zebrafish embryos through oxidative stress, inflammation, and cardiovascular toxicity

Garam An[1], Junho Park[1], Whasun Lim[2], *Gwonhwa Song[1]

[1]Institute of Animal Molecular Biotechnology and Department of Biotechnology, Korea University

[2]Department of Biological Sciences, Sungkyunkwan University

Thiobencarb is a thiocarbamate herbicide which is widely applied to agricultural lands including rice cultivation fields. Because herbicides utilized in paddy fields have a high risk to expose to aquatic ecosystems via drainage systems, adverse impacts of thiobencarb to aquatic organisms have been investigated. For example, thiobencarb-exposed medaka (*Oryzias latipes*) embryos showed delayed hatching and several morphological abnormalities. However, molecular mechanisms underlying embryotoxicity of thiobencarb have not been clarified. Thus, present study aims to demonstrate its toxic mechanisms by using zebrafish (*Danio rerio*) which is a representative model to assess toxicity of environmental contaminants. Thiobencarb reduced survival rates and hatching rates of zebrafish embryos. In addition, zebrafish exposed to thiobencarb showed multiple deformities including pericardial edema, enlarged yolk sac and inward curvature of the spine. Analysis of mRNA expression following thiobencarb treatment showed that these developmental defects were mediated by apoptosis, elevated production of reactive oxygen species and inflammation. Moreover, thiobencarb perturbed development of cardiovascular system. Specifically, zebrafish exposed to thiobencarb showed lower heart rates and impaired cardiovascular structures. Taken together, our study firstly elucidated adverse effects of thiobencarb on developmental stage of zebrafish and provided information for further studies elucidating aquatic risk and its molecular mechanisms of thiobencarb on non-target species.

Key words: developmental toxicity, thiobencarb, zebrafish embryos, oxidative stress, cardiovascular toxicity

Acknowledgement: This research was supported by the National Research Foundation of Korea (NRF) grant funded by the Korea government (MSIT) (grant number: 2021R1A2C2005841).

Dev. Reprod. Vol 26, 2022 (Suppl. 1). pp 192

B-10

Gonadal structure, sex ratio and main spawning period of *Buccinum osagawai* (Neogastropoda: Buccinidae)

Hyeon Jin Kim[1], So Ryung Shin[1], Jung Jun Park[2], Jae Won Kim[3], *Jung Sick Lee[1]

[1]Department of Aqualife Medicine, Chonnam National University

[2]Aquaculture Research Division, National Institute of Fisheries Science

[3]Department of Aquaculture, Gangwon State University

(hjin9577@naver.com)

Research on reproduction of marine organisms provides the information necessary for understanding their basic biology, as well as management of biological resources and development of aquaculture technology. The Buccinidae occur worldwide in all seas from tropical oceans to the cold seas of the Arctic Ocean and the Southern Ocean from the intertidal to the bathypelagic zones. Among them, the genus *Buccinum* is mainly distributed in Japan and along the east coast of Korea, and mainly inhabits muddy sands at a depth of 200 to 500 m. Within the genus *Buccinum*, studies on *B. undatum* have included reproductive cycle and seasonal feeding activity (Martel et al., 1986), reproductive cycle and energetic cost of reproduction (Kideys et al., 1993), reproductive cycle and maternal effects on offspring size and number (Valentinsson, 2002), and growth and reproduction (Heude-Berthelin et al., 2011), while a number of studies on reproduction, including the reproductive cycle and size at sexual maturity (Ilano et al., 2003) of *B. isaotakii*, have been reported. In this study, the information about basic reproductive ecological data and management of biological resources of *B. osagawai* was conducted. Samples were collected from August 2018 to October 2019 with a drum-shaped net on the continental shelf at a depth of 150～250 m in Jumunjin, East Coast of Korea. Specimens were prepared for light microscopy and were stained with Mayer's hematoxylin-eosin (H-E) stain. Histological quantification of oocytes was performed by converting microscope images into JPEG files, then subjecting these to an image analyzer (i-solution, IMT Inc., U.S.A.). Gonadal development was categorized into the following six stages for both male and female according to the degree of dominance of each developmental stage of germ cells and the degree of germ cell spawning: inactive stage (In), early active stage (Ea), late active and mature stage (LM), ripe stage (R), spent and degenerative stage (SD). Sex ratio, and gonad index (GI) were used as biomarkers. The sex of *B. osagawai* is gonochorism and lacks external sexual dimorphism. Mature ovary and testis, was white yellow color and yellow color. The overall sex ratio (F:M) was 1:1.2 (n=537, F=246, M=291), with a high male ratio, but as the individual size increased, the female ratio was a tendency to increase. The gonad consisted of multiple gametogenic acini. The development pattern of oocyte was synchronous development type, in which dominant group of oocytes was identified within the same ovary. According to oogenesis, the size of oocyte and nucleus increased and the stainability in the cytoplasm of oocyte changes form

basophilic to eosinophilic. The size of ripe oocyte was 82.3 (±22.6)×125.5 (±22.0) μm. As the oocytes matured, the follicle cells changed from a simple squamous type to a stratified cuboidal and columnar type. The spermatocyte development pattern was group-synchronous development type, in which multiple stages of germ cell populations were simultaneously identified with the same spermatogenic acinus. The GI for both male and female showed the highest value in June and then decreased sharply, and after August, it was below 2.0. The main spawning season was from June to July, and the GI and stages of gonadal development did not show a pattern of seasonal changes. The main gonadal active season is May-July, and both male and female gonad development and maturation take place in a short period of time, and the recovery period after spawning is long.

Key words: *Buccinum osagawai*, gonad, sex ratio, main spawning period

Dev. Reprod. Vol 26, 2022 (Suppl. 1). pp 194

B-11

Spermatophore formation and transportation of the squid, *Todarodes pacificus* (Oogopsida: Ommastrephidae)

So Ryung Shin, Hyeon jin Kim, *Jung Sick Lee

Department of Aqualife Medicine, Chonnam National University

(srshin12@naver.com)

Cephalopod reproduction has a different reproductive strategy than external fertilization in marine animals. Cephalopods, including *Loligo pealii* (Austin et al., 1964), internal fertilization fish *Neoditrema ransonneti* (Lee et al., 2001), and crustaceans *Carcinus maenas* (Subramoniam, 1993) males form spermatophores, which are responsible for sperm storage and efficient delivery of sperm to females. In cephalopod, females have vary sperm storage organ according to mating type and species. *Loligo forbesi* (Lum-Kong, 1992) and *Sepia apama* (Naude et al., 2005) have seminal receptacles in the buccal area. In *Moroteuthis ingens*, males attach spermatangia directly to female skin (Hoving and Laptikhovsky, 2007). However, studies on the formation and transportation of spermatophore in squid *Todarodes pacificus* have not been conducted. In this study, after dissecting a sample of an adult (mantle length: 193.2 mm) squid *T. pacificus*, the location and morphology of the reproductive organs in the mantle cavity were described with a dissecting microscope. Samples were fixed in 2.5% glutaraldehyde (0.1 M phosphate buffer, pH 7.4). Specimens for light microscopy were produced using the paraffin sectioning method. In addition, H-E stain, Masson's trichrome stain and AB-PAS (pH 2.5) reaction were performed. As a result, the sperm formed from the testis of *T. pacificus* passed through the seminal vesicle and a spermatophore was formed in the spermatophoric gland. The formed spermatophore passed through the spermatophoric sac and penis was attached to the seminal receptacle of the female buccal area.

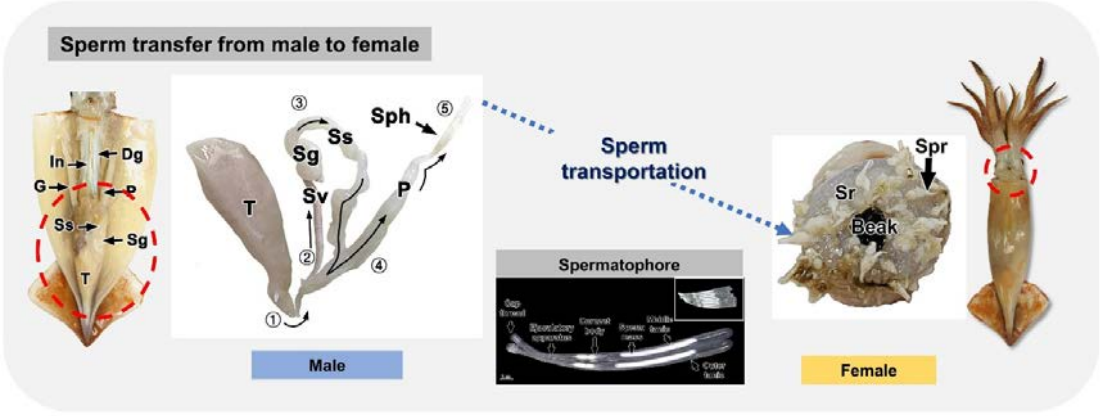

Key words: *Todarodes pacificus*, male, reproductive organ, spermatophore

Dev. Reprod. Vol 26, 2022 (Suppl. 1). pp 195

B-12

Prometryn induces failure of organogenesis in zebrafish (*Danio rerio*) via disruption of mitochondrial respiration and ROS production

Nayoung Min[1], Hahyun Park[2], Taeyeon Hong[1], Gwonhwa Song[2], *Whasun Lim[1]

[1]Department of Biological Sciences, Sungkyunkwan University

[2]Institute of Animal Molecular Biotechnology and Department of Biotechnology, Korea University

Herbicides have been used to control undesired weeds to improve the quality and productivity of agricultural products. Prometryn, 2-methylthio-4,6-bis(isopropylamino)-1,3,5-triazine, is one of triazine herbicide widely used to control weeds in celery, carrots, pigeon peas, peanuts, and cotton. However, prometryn threatens environment and human health due to continuous contamination, bioaccumulation, and damage to non-target organisms. In this study, zebrafish (*Danio rerio*), which is a non-target organism of prometryn, was used for the toxicity evaluation and several transgenic zebrafish models enabled visual confirmation of early development of zebrafish. Zebrafish embryos were exposed to 5, 10, and 20 mg/L prometryn for 96 h and loss of viability, shortened body length, yolk sac and heart edema, and abnormal heart rate were observed. Through fluorescence microscopy, deficiency of organ development, reactive oxygen species accumulation, and apoptotic cell death were monitored in zebrafish embryos by prometryn. Mitochondrial bioenergetics were also investigated to determine the effect of prometryn on the electron transport chain activity and metabolic alterations during embryogenesis of zebrafish. Prometryn interfered with the mitochondrial function, ultimately inhibiting energy metabolism and embryonic development. Collectively, our findings provide the developmental toxicity of prometryn in zebrafish during embryogenesis and emphasize the need to consider the toxic effects of prometryn on non-target sites and organisms.

Key words: prometryn, zebrafish, toxicity, developmental toxicity, oxidative stress, mitochondrial dysfunction

Acknowledgement: This work was supported by the National Research Foundation of Korea (NRF) grant funded by the Korea government (MSIT) (No. 2021R1C1C1009807). Also, this research was supported by Basic Science Research Program through the National Research Foundation of Korea (NRF) funded by the Ministry of Education (No. NRF-2019R1A6A1A10073079).

Dev. Reprod. Vol 26, 2022 (Suppl. 1). pp 196

B-13

Impermanent female-to-male sex change in the protogynous red-spotted grouper (*Epinephelus akaara*) by 17α-methyltestosterone treatment

Md Mofizur Rahman[1,2], Young Don Lee[3], *Hea Ja Baek[1]

[1]Department of Marine Biology, Pukyong National University

[2]Department of Fisheries and Marine Science, Noakhali Science and Technology University, Bangladesh

[3]Marine Science Research Institute, Jeju National University

(*hjbaek@pknu.ac.kr)

17α-methyltestosterone (MT) has been used to artificially induce male fate in many grouper species. In this study, the potentiality of MT-feeding to induce the gonadal sex change in red-spotted grouper (*Epinephelus akaara*) was investigated. 90-day-old red-spotted groupers (total length: 5.98±0.14 cm, body weight: 3.67±0.2 g) were fed MT-supplemented diets (10 mg and 40 mg MT/Kg diet) at the sex differentiation phase for 9 weeks and then, MT-feeding withdrawal; fed with a normal commercial diet until termination of the experiment (36 weeks). Gonadal histology and sex steroid (estradiol, E2; testosterone, T) levels were evaluated during the experimental period. MT-feeding induced to develop spermatogenic cyst-like structure, bypassing the formation of an ovarian cavity, and decreasing the plasma E2 levels in the MT-treated group. Over the long term, the sex-reversed testis was observed in the MT-fed group (40 mg MT/Kg diet) with numerous spermatozoa. A significant increase in plasma T levels and subsequent decrease in E2 levels were also observed. Plasma cortisol level was found higher during the gonad transformation phase and returned to the basal level after completion of sex change. Collectively, our results suggest that MT-feeding at a 40 mg/Kg diet can induce impermanent sex change from female to male in *E. akaara*, by increasing the plasma T levels.

Key words: red-spotted grouper, *Epinephelus akaara*, 17α-methyltestosterone, gonadal sex change

Acknowledgement: This research was supported by the Korean Ministry of Agriculture, Food and Rural Affairs (MAFRA), the Korean Ministry of Oceans and Fisheries (MOF), the Korean Rural Development Administration (RDA), and the Korea Forest Service (KFS) under the grant (No.: 213008-05-2-WT511).

Dev. Reprod. Vol 26, 2022 (Suppl. 1). pp 197

B-14

북방전복의 allatotropin 수용체와 리간드 반응성 연구

이상혁[1], 김미애[2], *손영창[1]

[1]강릉원주대학교 해양생명과학과, [2]강릉원주대학교 동해안생명과학연구원

(*ycsohn@gwnu.ac.kr)

Allatotropin(AT)은 곤충의 일주기 리듬, 소화효소 분비, 이온 수송, 장 수축 및 심박수를 조절하는 펩티드성 호르몬으로 알려져 있다. Allatotropin 수용체(ATR)는 GPCR rhodopsin 계열 subfamily에 속하며, orexin 수용체와 orthologue 관계로 추정되고, AT와 결합하여 세포 내 칼슘 이온을 증가시키는 신호전달경로가 알려져 있다.

본 연구는 해양무척추동물의 AT 및 ATR에 관한 기초적인 정보를 확보하기 위해 북방전복(*Haliotis discus hannai*)의 AT 전구체 및 ATR cDNA를 cloning하고, 분자계통수 분석을 진행하였다. 북방전복의 ATR은 연체동물의 ATR과 단일 clade를 형성하고, AT 전구체는 107개의 아미노산을 암호화하며, 그 중 13개의 아미노산으로 구성된 1개의 성숙형 펩티드를 동정하였다. ATR 발현벡터 및 serum response element(SRE) reporter를 형질도입한 HEK293세포를 이용하여 리간드 반응성을 조사한 결과, 북방전복의 AT 및 AT 2번째 아미노산인 페닐알라린 잔기를 D형으로 이성질체화시킨 AT-D2 모두 농도 의존적으로 ATR의 활성을 증가시켰다. 한편, 북방전복의 GnRH에 대한 SRE reporter 활성은 보이지 않았다. 전복의 조직(뇌신경절, 측족신경절, 생식소, 간췌장, 아가미, 장, 폐각근, 외투막)에서 ATR mRNA 발현을 조사한 결과, 뇌신경절 및 측족신경절, 폐각근에서 높은 발현을 보였다. 본 연구 결과를 종합하면, 북방전복의 ATR은 연체동물문 복족류의 ATR 그룹에 속하는 것으로 밝혀졌고, 북방전복의 AT 및 AT-D2는 북방전복의 ATR의 리간드로 추정된다. 본 연구는 향후 무척추동물의 AT 및 ATR에 대한 기초적인 자료로 사용될 수 있을 것으로 사료된다.

Key words: allatotropin, 북방전복, ATR

Dev. Reprod. Vol 26, 2022 (Suppl. 1). pp 198

B-15

Genetic analysis of cultivated *Takifugus obscurus* entities

***Jong-Man Yoon**

Department of Aquatic Life Medicine, College of Ocean Science and Technology,
Kunsan National University

The benthic river pufferfish (*Takifugus obscurus*) inhabit the floor regions, laying eggs under rock. They bear yellow stripes laterally with a dark-brown dorsal body and white belly. These pufferfish are rounded- and club-bodied with black spots detected on the pectoral and dorsal fins. This finfish represent a few of the finfish species, which are socioeconomically significant in many seashore regions. In an effort to upgrade river pufferfish aquaculture, this study elucidates the genetic distances and variations between untamed and cultivated river pufferfish populations. A cluster analysis of two cultivated river pufferfish populations was also performed. Genomic DNA (gDNA) examples segregated from *Takifugus obscurus* (cultivated river pufferfish population alpha, CRPPA) and cultivated river pufferfish population beta, CRPPB) gathered at Yesan of Korea, were PCR-enlarged continually. The amount of the acquired gDNA was quantified with the optical density (OD) proportion at 260 nm by a micro-spectrophotometer. The arithmetic mean of within-CRPP similarity was calculated by pairwise comparison between entities within a population. By means of similarity matrices to build a dendrogram, expedited by the PC-package program Systat version 10, a hierarchical CT was constructed. FRA size ranging from 50 to 800 bp. The complication of the banding forms were different spectacularly amid the ON-primers and entities. Most of all, the OPC-02 primer offered DNA précises with further FRAs than the other five ON-primers in the CRPPA population and OPC-16 from CRPPB. The band-sharing value (BSV) of similarity matrix (SM) between individuals numbered 13 and 08 in the cultured population was 0.253, which was the lowest recognized. The oligonucleotides primer (ON-primer) OPC-16 identified 22 unique loci shared within each population reproducing the cultivated river pufferfish population alpha. The OPC-16 primer detected 44 loci shared by the two populations. The average BS values of individuals in the population alpha between beta (0.544±0.007) were lower than in those derived from two cultivated populations (0.733±0.010 and 0.734±0.012, respectively) (p<0.05). The shortest genetic distance (GD) establishing a substantial molecular difference was create between the cultivated individuals #17 and #15 (GD=0.051).

Dev. Reprod. Vol 26, 2022 (Suppl. 1). pp 199

B-16

BP-3 and EHMC combination influence on estrogen levels and GVBD in maturing oocytes of Longchin goby (*Chasmichthys dolichognathus*)

Jinsung-Choi, Minseol-Kim, Jaehwan-Lee, *HeaJa Baek

Department of Marine Biology, Pukyong National University

(myers@pukyong.ac.kr)

2-hydroxy-4-methoxybenzophenone (oxybenzone, BP-3) and 2-ethyl-hexyl-4-methoxycinnamate (octinoxate, EHMC) are one of the major compounds of sunscreens. In our previous study, we exposed BP-3 (0.5, 5, 50 and 500 ng mL^{-1}) and/or EHMC (0.5, 5, 50 and 500 ng mL^{-1}) were examined in the maturing oocytes of longchin goby (*Chasmichthys dolichognathus*); showed a significant increase of estradiol (E2) level in the BP-3 5 ng mL^{-1}. Therefore, in this study, we investigated the effects of mixture (BP-3 and EHMC) on estrogen (E1 and E2) levels and GVBD using maturing oocytes of longchin goby. The oocytes with average diameters of 800 μm were incubated with different concentrations (BP-3 5 ng mL^{-1} with EHMC 0, 5, 50, and 500 ng mL^{-1}) for 24 h under 15℃ and 20℃ water temperature (WT). We analyzed estrogen levels using radioimmunoassay (RIA). GVBD was induced in BP-3 5 ng mL^{-1} with EHMC 50 ng mL^{-1} under WT 15℃ compared to control. There is no significant difference of E1 levels of all tested groups, but the E1 levels tended to increase in BP-3 5 ng mL^{-1} under WT 15℃ and 20℃ without a statistically significant difference. Significant increase of E2 level indicated in BP-3 5 ng mL^{-1} under WT 15℃ compare to control.

Key words: UV filter, BP-3, EHMC, GVBD, estrogen

Acknowledgement: This study was supported by Basic Science Research Program through the National Research Foundation of Korea (NRF) (2020R1I1A3072395136178206434010 3).

Dev. Reprod. Vol 26, 2022 (Suppl. 1). pp 200

B-17

붉바리(*Epinephelus akaara*) 자어의 성장과 등지느러미 발달

정희경[1], 부문수[2], 문영건[2], *이치훈[1], 이영돈[1]

[1]제주대학교 해양과학연구소, [2]어업회사법인 씨알 주식회사

(hiyi78@naver.com)

어류는 자어에서 치어로 발달하는 과정에 다양한 형태적 발달 과정을 갖는다. 바리과 어류의 경우, 자치어 시기 형태적 특징은 등지느러미 제2극과 배지느러미 극이 특이하게 신장되고 발달하면서 치어로 성장하는 변태과정을 겪는다. 이와 같은 종 특이적인 지느러미의 형태적 발달 특징은 바리과 어류의 종자 생산 과정에 있어 초기 자어의 사육 밀도 관리에 있어 중요한 사양관리 요소가 된다. 이 연구는 붉바리 종자의 변태과정에 대한 기초자료를 제공하기 위해 붉바리 자어의 성장과 등지느러미 발달에 대하여 조사하였다. 인공수정을 통해 얻은 붉바리 부화자어는 21.0～25.5℃에서 사육하였고, 로티퍼는 부화 5일부터 30일까지, 알테미아는 20일부터 60일까지 공급하였다. 미립자 사료는 13일부터 소량 공급하였으며, 20일부터 점차 공급량을 증가시켰다. 붉바리 자어의 성장과 지느러미 발달 과정을 조사하기 위해 부화 1일부터 72일까지 자어를 임의로 30마리 이상을 채집하여, 광학 현미경을 통해 외부형태 관찰 및 계측하였다. 부화 1일차 자어의 전장은 2.10±0.01 mm이었고, 부화 3일차 전장 2.39±0.01 mm로 성장하였으며, 이 시기에 등 안쪽에서 첨체형태의 것이 관찰되었다. 부화 6일차 자어의 전장은 2.62±0.01 mm이었고, 척추에서 극조의 뿌리 부분이 관찰되었다. 이후 부화 9일차 등지느러미 제2극과 배지느러미 극이 돌출하였다. 부화 10일차 자어의 전장은 3.0±0.2 mm이었고, 등지느러미 제2극은 0.2±0.01 mm이었다. 부화 13일차 자어의 등지느러미 제1극이 관찰되었으며, 등지느러미 제1극은 0.5±0.1 mm, 제2극은 1.0±0.1 mm이었고, 제2극 기저부위에 가시 같은 극(spine)이 6개 관찰되었다. 부화 17일차 자어의 꼬리지느러미의 기초적인 줄기가 발달하였고, 부화 19일차 전장은 5.7±0.1 mm이었고, 등지느러미 제2극은 1.9±0.1 mm로 신장되어 전장대비 44%를 차지하였으며, 미세한 톱니형태의 극(spine)이 10～12개로 증가하였고, 좌우대칭 형태로 발달하였으며, 제3극이 관찰되었다. 부화 23일차 뒷지느러미의 기초적인 줄기가 발달하였다. 부화 45일차 자어의 전장은 22.43±0.3 mm이었고, 지느러미 분화가 완료되어 등지느러미 극조는 10～12개, 연조는 15～16개로 분화되었으며, 꼬리지느러미 줄기는 16～17개, 뒷지느러미 줄기는 11개로 분화되어 변태 단계를 끝내고 성어와 유사한 지느러미 형태를 띄었다. 이 연구에서 붉바리 자어의 등지느러미 제2극은 10～12개의 미세한 톱니 모양의 극(spine)이 발달하였으며, 제2극의 길이는 전장 대비 최대 44%를 차지하였으나, 이후 성장하면서 비율이 감소하였고, 부화 후 45일경에 지느러미 분화가 완료되어 변태 단계가 종료되었다. 이러한 붉바리 자어의 성장과 지느러미 발달양상은 향후 붉바리 종자 생산에 있어 초기 사육 밀도 조절 등 사양관리 정보에 중요한 기초자료가 될 것으로 판단된다.

Key words: 붉바리, *Epinephelus akaara*, 성장, 변태, 등지느러미

Dev. Reprod. Vol 26, 2022 (Suppl. 1). pp 201

B-18

Differentiation and development of hepatopancreatic in red spotted grouper, *Epinephelus akaara*

Kang-Hee Im[1], Song-Hee Choi[1], Byeong-Hoon Kim[2], Moon-Soo Boo[1], Chi-Hoon Lee[2], *In-Kyu Yeo[1], *Young-Don Lee[2]

[1]Department of Marine Life Sciences, Jeju National University

[2]Marine Science Institute, Jeju National University

(imk0408@jejunu.ac.kr)

Understanding the developmental process of larvae's digestive system in aquaculture is a very basic factor in determining the initial food source selection and feeding timing. The liver is an accessory gland of the digestive tract and is a major organ that regulates various physiological functions such as bile production and secretion and homeostasis control through exocrine and endocrine functions. This study was conducted to provide basic information for understanding the hepatopancreatic differentiation and developmental processes of *Epinephelus akaara* larvae for developing aquaculture techniques. For this study, we investigated the hepatopancreatic differentiation and developmental processes from 1 to 30 day after hatching (dah) by artificial fertilization. For this, we performed sampling on 1, 3, 5, 7, 9, 10, 15, 20, 25, and 30 dah and investigated the hepatopancreas development process through the Haematoxylin & Eosin staining process. Larvae were reared at water temperature of 21.0～25.5℃. The feeding regime consisted of rotifers, Artemia, and commercial pellet feed. Larvae were fed with rotifer (*Brachionus rotundiformis*) from 5～30 dah. Newly hatched Artemia were provided from 20～25 dah and enriched Artemia from 26～60 dah. Commercial pellet feed was given starting at 13 dah. At 1 dah, the unabsorbed yolk has been observed and cannot confirm digestive system development. On the 3rd day of hatching, we observed that yolk was almost absorbed. A simple morphology of the digestive tract also has been observed, and pancreatic cells and hepatocytes began to come into view in the anterior part of the digestive tract. The yolk is no longer visible at 5 dah. And the liver morphology has watched for the first time. At the same time, we observed lipid granules in the hepatocytes. Pancreatic tissue was between the liver and the alimentary canal in larvae at 9 dah. It was also between the stomach and rectum. After that, we observed that the liver and pancreatic tissues were extant divided from each other until 30 days after hatching. Therefore, since we observed the liver and pancreatic tissues from 3 dah, it is thought that the liver and pancreatic tissues can influence digestion from this time. Liver and pancreatic tissues were observed respectively from 3 to 30 dah. Therefore, it is necessary to explore the process and timing of differentiation and development of liver and pancreatic tissue. Furthermore, the results of this study are looking forward to contributing to providing basic information in determining the exact feeding time and food source in the seedling production process.

Key words: *Epinephelus akaara*, hepatopancreas, liver, pancreas, development, differentiation

Dev. Reprod. Vol 26, 2022 (Suppl. 1). pp 202

B-19

Effect of dietary astaxanthin feed on colour change in red spotted grouper, *Epinephelus akaara*

Song-Hee Choi[1], Byeong-Hoon Kim[2], Kang-Hee Im[1], Chi-Hoon Lee[2], *In-Kyu Yeo[1], *Young-Don Lee[2]

[1]Department of Marine Life Sciences, Jeju National University

[2]Marine Science Institute, Jeju National University

(thdgml1126@naver.com)

Pigments of fish colour include melanin, guanine, uric acid, purin, pterin, and carotenoids. Most pigments are synthesized by themselves in the body and used for expression of body colour. However, carotenoids cannot be synthesized by themselves, so they can only be used as body pigments if they are absorbed through external sources of food. Fish coloration is one of the important factors for increasing the commercial value of red spotted grouper. For this reason, this study was carried out to enhance the value of commerciality by improving the colour of the cultured red spotted grouper using carotenoids. We investigated changes in body colour, histological changes in the intestines, and mRNA expression changes in carotenoid-related factors (*bco2*, *scarb1*, *xdh* mRNA) in the liver and intestines after astaxanthin were subsumed in the red spotted grouper. During the 4weeks experimental period, 1,000 ppm of astaxanthin was adsorbed in the feed and supplied to the experimental group, and general feed was supplied to the control group. As a result of performing HSL chromaticity analysis to compare and analyze body colour changes, the spots and of red saturation abdominal skin of the experimental group were higher than that of the control group. Although there was no difference between the experimental groups in the hepatosomatic index, the size of hepatocyte was observed significantly larger in the experimental group than in the control group ($p<0.05$). There was no difference between groups in the expression of *xdh* mRNA in the liver, and expression of *bco2* mRNA and *scarb1* mRNA in the intestine. Our research suggests that astaxanthin feeding in red spotted grouper can affect improving the red saturation of the body. In addition, it is thought that the size of the hepatocytes increased because astaxanthin was accumulated in the hepatocytes as a lipid. However, there was no change in the expression of carotenoid-related factors in the liver and intestines, and it is thought that research is needed to clarify the mechanism between astaxanthin and somatic coloration in the future.

Key words: astaxanthin, carotenoid, chromatophore, body colour, *Epinephelus akaara*

Dev. Reprod. Vol 26, 2022 (Suppl. 1). pp 203

B-20

Development of digestive tract in red spotted grouper, *Epinephelus akaara*

Moon-Soo Boo[1], Young-Gun Moon[1], Byeong-Hoon Kim[2], Hee-Kyung Jung[2], Song-Hee Choi[2], Kang-Hee Im[2], *Chi-Hoon Lee[2], Young-Don Lee[2]

[1]CR Co., Ltd., Korea

[2]Marine Science Institute, Jeju National University

(timorboo@hanmail.net)

The digestive tract of fish is an important organ for the digestion and absorption of nutrients. The information on development of digestive tract in larvae is basic data for improving the survival rate of larvae, such as the selection and supply timing of initial food source in the seed production. This study investigated the external shape change and developmental pattern of digestive tract in red spotted grouper according to growth stage. Larvae were reared at water temperature of 21.0～25.5℃. The feeding regime consisted of rotifers, Artemia, and commercial pellet feed. Larvae were fed with rotifer from 5～30 day after hatching (dah). The Artemia were provided from 20～60 dah. Commercial pellet feed was given starting at 13 dah. In order to investigate the external shape and digestive tract development of red spotted grouper, we performed sampling on 1 to 50 dah. The observation on external shape development of larvae was performed through an optic microscope and the developmental process of digestive tract was investigated by histological method through the Haematoxylin & Eosin staining. And the development of goblet cells was observed through Alcian Blue-Periodic Acid Schiff (AB-PAS) staining. At 1 dah, mouth and anus of larvae was closed. The digestive tract was observed in a straight line between ventral side and the yolk. At 3 dah, the yolk of larvae was almost absorbed and was surrounded by liver and some pancreatic tissue. The darkening of the eyes began and the lumen of the digestive tract gradually widened. At 4 dah, the mouth and anus of larvae were opened, rotifer intake was confirmed, and the intestine and rectum were separated. At 5 dah, the intestine of larvae began to rotate, the length of the intestine increased, and lumen was widened. The gastric lumen between the anterior intestine and esophagus was widened and distinguished. At 10 dah, the spines of dorsal fin and pelvic fin in larvae was elongated. The development of mucosal folds in the rectum was observed, and goblet cells were observed in the esophagus by PAS staining. At this time, the larvae have early digestive system such as esophagus, stomach, anterior intestine, midintestine, posterior intestine, and rectum, and the intestinal rotation was completed. At 13 dah, the teeth were observed in the mouth of the larvae, and as they grew, the size and number of teeth increased as the they grew. At 15 dah, the lumen of the stomach between the esophagus and anterior intestine gradually widened. At 20 dah, the development of mucosal folds in the stomach was observed. The number of goblet cells increased in the esophagus and the goblet

cells were observed all digestive organs. At 30 dah, the pyloric caeca was observed and the gastric mucosal folds were further development and the gastric gland was observed. At 40 dah, the sphincter was clearly development between the esophagus and stomach, and between the stomach and the anterior intestine. At 50 dah, the gastric lumen was enlarged, the gastric gland was further development. The mucosal folds were more densely distributed in all digestive organs, and a digestive system developed similar to those of adult fish. The information on digestive tract development according to the growth of larvae will contribute to the growth and survival rate of red spotted grouper larvae by systemizing the optimal feeding time during seed production of red spotted grouper.

Key words: red spotted grouper, *Epinephelus akaara*, digestive tract, gastric gland, goblet cell

Dev. Reprod. Vol 26, 2022 (Suppl. 1). pp 205

C-01

Increased activity of the Na^+-leak channel (NALCN) in arterial smooth muscle cells

Hye Ryeong Lee[1], Sang Woong Park[2]

[1]Department of Physiology, KU Open Innovation Center, Research Institute of Medical Science, Konkuk University School of Medicine

[2]Medical Services, Eulji University

Our previous study showed that oxidative stress induces Na^+ influx through non-selective cation channel in arterial smooth muscle cells. This oxidative stress-induced ion channel currents contributed to the increased arterial contraction. Here, we identified the oxidative stress-activated non-selective cation channel in normal and diabetic arterial smooth muscle cells. Microfluorometric intracellular sodium (Na^+) measurements, western blotting, organ chamber isometric contraction measurement, microarray and gene transfection techniques were used for this study. We screened H_2O_2-activated ion channels in arterial smooth muscle cells by microarray methods and found that NALCN ion channel mRNA level is increased by H_2O_2. In organ chamber experiments, H_2O_2 contracted arterial rings under normal condition. However, H_2O_2 failed to contract the arterial rings in low-Na^+ condition (NMDG-Cl bath). The activation of NALCN by H_2O_2 was confirmed in vitro analysis, in which H_2O_2 increased Na^+ influx in HEK293T cells that were transfected with NALCN channelosome genes. In contrast, activation of Na^+ influx by H_2O_2 in control HEK293T cells that were *NOT* transfected was minimal. In the pre-diabetic mice model that were fed with high glucose, NALCN levels in arterial tissue were increased. Furthermore, *in vitro* analysis showed that NALCN levels were higher in arterial smooth muscle cells cultured in high-glucose medium than in normal-glucose medium. Taken together, we conclude that NALCN is activated by H_2O_2 and its functional expression is also increased by oxidative stress as well as high glucose. This increased activity of NALCN by oxidative stress and high glucose may contribute to the pathogenesis of various cardiovascular dysfunctions such as diabetic vascular disorder.

Dev. Reprod. Vol 26, 2022 (Suppl. 1). pp 206

C-02

Autosumoylation of Ubc9 leads to restore a replicative lifespan defect by loss of Ulp2 SUMO protease

Dong Won Jeong, Seung Yeon Kim, *Hong-Yeoul Ryu

School of Life Sciences, BK21 FOUR KNU Creative BioResearch Group,
Kyungpook National University
(rhr4757@knu.ac.kr)

Post-translational protein modifications by the small ubiquitin-related modifier (SUMO) regulates numerous cellular pathways, including transcription, cell division, and genome maintenance. This modification is reversed by SUMO proteases, Ulp1 and Ulp2, in *Saccharomyces cerevisiae*. We previously found that *ulp2Δ* cells acquire mutations in genes encoding the SUMO-related enzymes Ubc9 or Uba2/Aos1 during laboratory evolution. Remarkably, despite the complete absence of the *ULP2* gene, these evolved cells exhibit an extended lifespan and do not present any obvious stress sensitivities. This is also accompanied by a reduction in polySUMO conjugate accumulation in most of the isolates. In addition, we identified several alterations in SUMO modification of proteins, and among them SUMO conjugation levels of Ubc9, a budding yeast E2 SUMO enzyme, show severe alterations during adpative evolution. SUMOylation of Ubc9 causes inactivation of Ubc9's enzymatic activity and functions as a cofactor for other active Ubc9. Ubc9's E2 activity is regulated through interactions between inactive SUMOylated and active Ubc9. Therefore, our results suggest that down-regulation of Ubc9 SUMOylation may be a crucial factor for restoration of a replicative lifespan defect caused by loss of Ulp2.

Key words: SUMO, Ubc9, Ulp2, replicative lifespan, autosumoylation

Dev. Reprod. Vol 26, 2022 (Suppl. 1). pp 207

C-03

Regulation of Chi3l1 expression in the uterus according to the estrogen

Byeongseok Kim, Giwan Lee, Semi Hwang, Siyoung Lee, Hyukjung Kim, Minju Kang, *Youngsok Choi

Department of Stem Cell and Regenerative Biotechnology, Konkuk University

(qufsksrlaqud@naver.com)

In the uterus, unlike other organs, dynamic modification occurs in response to ovarian hormones such as estrogen and progesterone. Chitinase-like proteins, CLPs, which belong to the glycoside hydrolase family 18 of proteins are expressed differently across the species due to mutations in the enzymatic active site of chitinase. Chitinase-3 like 1, Chi3l1, which is expressed in both humans and mice, is the most studied protein among CLPs and is known to play a role in host defense and immune regulation. Although many studies have been conducted in respect of pathology like asthma and cancer with Chi3l1, nothing has been revealed about the expression pattern of Chi3l1 in the physiology of the uterus and estrogen. In this study, according to microarray data, we confirmed that the Chi3l1 mRNA expression in the uterus was induced by 17β-estradiol treatment in the ovariectomized wild-type mice not in estrogen receptor alpha (ERa) knock-out mice. In addition, the expression of Chi3l1 mRNA was not promoted in the uterus-specific Era conditional knock-out mice with the injection of estradiol. In the uterus of mice, Chi3l1 mRNA and protein expression was significantly regulated during the estrous cycle. The expression was highest in the proestrus stage and gradually decreased until the diestrus stage. Moreover, Chi3l1 mRNA and protein expression was dramatically increased in the uterus of ovariectomized mice by administration of 17β-estradiol, especially 24 hours after. Progesterone could not induce the expression of Chi3l1 in the uterus. Like the informatics analysis, Chi3l1 was exclusively localized in the luminal and glandular epithelial cells of the uterus. Our study revealed that an increase in Chi3l1 mRNA and protein of uterine epithelial cells can be induced by estrogen. It is known that Chi3l1 also plays the role in epithelial-mesenchymal transition and angiogenesis. This represents a possibility that Chi3l1 has a crucial role in regulating the vigorous changes in the uterus with estrogen.

Key words: uterus, chitinase like protein, chitinase-3 like 1, estrogen, estrogen receptor alpha

Dev. Reprod. Vol 26, 2022 (Suppl. 1). pp 208

C-04

The regulation of TAZ expression by estrogen in mouse uterus

Semi Hwang, Byeongseok Kim, Siyoung Lee, Giwan Lee,
Hyeukjung Kim, *Youngsok Choi
Department of Stem Cell and Regenerative Biotechnology, Konkuk University
(tpal34567@naver.com)

The mouse uterus undergoes many morphological and functional changes. The dynamic modulation is precisely regulated by two steroid hormones, estrogen and progesterone, during the estrous cycle. TAZ known as a transcriptional coactivator, which shuttles between the cytoplasm and the nucleus under the Hippo signaling. Nuclear TAZ is involved in regulation of cell proliferation, organ overgrowth, survival to stress and dedifferentiation. However, the phosphorylation of TAZ at Ser89 leads destabilization of TAZ protein by sequestering into the cytoplasm resulting in proteasomal degradation. Recent studies indicated that estrogen is associated with regulation of TAZ activation via GPER (G protein-coupled estrogen receptor 1) by inhibiting TAZ phosphorylation. But the regulation of TAZ in mouse uterus remains unknown. In this study, we investigated TAZ expression and its regulation in mouse uterus. TAZ mRNA and protein did not show significant change during the estrous cycle. However, immunofluorescence analysis revealed that TAZ nuclear localization is significantly increase at the estrus stage. Interestingly, the phosphorylation of TAZ was changed according to the estrous stage, and it was lowest at the proestrus stage. And the expression level of TAZ mRNA and protein increased time-dependent by estrogen treatment. The expression level of TAZ mRNA was highest at 4 hours (4 h) and protein is significantly accumulated in 6h and 12h after estrogen treatment. Also, immunofluorescence staining showed that nuclear TAZ was significantly increased in 6h and 12h after estrogen treatment compared to control (oil). In conclusion, TAZ expression is regulated and activated by estrogen in mouse uterus, but further analysis is required to determine whether the TAZ expression is regulated by nuclear estrogen receptors ERα and ERβ, which are sequence-specific DNA-binding transcription factors or GPER, which is seven-transmembrane-domain receptor that mediates non-genomic estrogen related signaling. This research was supported by a grant from National Research Foundation of The Ministry of Science, ICT & Future Planning (2021R1A2C1011916).

Key words: TAZ, estrogen, mouse uterus

Dev. Reprod. Vol 26, 2022 (Suppl. 1). pp 209

C-05

Small molecule probe development for spermatogonial stem cells through fluorescent compound library screening

Seok-Man Kim[1], Yong-An Lee[2], Young-Tae Chang[3], *Buom-Yong Ryu[1]

[1]Department of Animal Science and Technology, Chung-Ang University

[2]Department of Stem Cell and Regenerative Biology, Genome Institute of Singapore, Singapore

[3]Department of Chemistry, Pohang University of Science and Technology

Throughout adult life, male fertility essentially depends on spermatogonial stem cells (SSCs) activity, including self-renewal and differentiation process for the continual generation of functional spermatozoa. Owing to SSCs existing in an extremely low population, the enrichment process is necessarily required for its downstream application. Antibodies for undifferentiated germ cell markers have conferred enrichment of SSCs. Yet, there has been an unmet demand for novel probe development for SSCs due to the absence of a unique validated marker that distinguishes functional SSCs from the undifferentiated germ cell population. To address this, we have performed a cell-based screening of small-molecule fluorescent compounds library on undifferentiated germline stem cell (GSC) lines. Our preliminary results have identified a candidate compound, RSC30, that confers selective staining with GSC lines over the non-GSC models, including mouse fibroblast and differentiated germ cells. In addition, the RSC30-dependent sorting significantly enhances SSCs enrichment from the whole GSC population in an in vitro germ cell clump forming assay without a prominent toxic feature. The further study aims to evaluate RSC30 as the SSC probe with spermatogonial transplantation and identify binding molecules. Our study may contribute a useful tool for SSCs research, especially in non-rodent species where appropriate cell-surface markers are not studied.

Key words: bio-imaging probe, RSC30, spermatogonial stem cell

Acknowledgement: This research was supported by the Bio & Medical Technology Development Program of the NRF funded by the Korean government (MSIP) (NRF-2018M3A9H1023139), Basic Science Research Program through the National Research Foundation of Korea (NRF) funded by the Ministry of Education (NRF-2018R01A6A1A03025159), and the National Research Foundation of Korea (NRF) grant funded by the Korea government (NRF2020R1A2C1009974).

Dev. Reprod. Vol 26, 2022 (Suppl. 1). pp 210

C-06

Low flow microfluidic chip system-based assay facilitates bisphenol-A treated GC-1 spermatogonial cells cytotoxicity evaluation

Seok-Man Kim[1], Seungjin Lee[2], Jinseop Ahn[1], Joong Yull Park[2], *Buom-Yong Ryu[1]

[1]Department of Animal Science and Technology, Chung-Ang University

[2]School of Mechanical Engineering, College of Engineering, Chung-Ang University

Cells naturally exist in three-dimensional (3D) microenvironments in living organisms with intricate cell-cell interactions and complex *in vivo* milieus supports. The microfluidic chip operates at extremely low flow speed, and these flow characteristics have the advantages in controlling the cell culture environment in the microfluidic chip versus conventional stationary mono-layered 2D culture cannot achieve. The purpose of this study is to observe the effect of endocrine disruptor bisphenol A (BPA) concentrations on the growth of GC-1 differentiated spermatogonia in a single microenvironment. The culture medium and the BPA solution (200 μM), each flow into the microfluidic channel through the two inlets, form a concentration gradient due to the characteristics of laminar flow. An osmotic pump was used to drive the microfluidic chip at a flow rate. The osmotic phenomenon in the osmotic pump produces an interstitial level flow without an external power source, and in our system, the flow rate was measured to be approximately 9.548×10^{-8} g/s. Twenty thousand GC-1 cells were seeded and cultured overnight and gradient flow of BPA : culture media were applied for 48 hrs. Cells were stained with LIVE/DEAD^{TM} Cell Imaging Kit and the whole chip was pictured with Nikon eclipse TE2000-U fluorescent microscope. We observed spatial gradient flow generates BPA concentration-dependent cytotoxicity on GC-1 cells. The results demonstrate the potential of the microfluidics platform for evaluating the cytotoxicity of single reagent with continuous flow.

Key words: microfluidics chip, GC-1 spermatogonial cell: cytotoxicity, bisphenol A

Acknowledgement: This research was supported by the Bio & Medical Technology Development Program of the NRF funded by the Korean government (MSIP) (NRF-2018M3A9H1023139), Basic Science Research Program through the National Research Foundation of Korea (NRF) funded by the Ministry of Education (NRF-2018R01A6A1A03025159), and the National Research Foundation of Korea (NRF) grant funded by the Korea government (NRF2020R1A2C1009974).

Dev. Reprod. Vol 26, 2022 (Suppl. 1). pp 211

C-07

Artificial skin manufacturing technology using 3D cell printing and skin therapeutic effect

Mi-jeong Kim[1], KyungMu Noh[1], *Sung-Hwan Moon[2,†], *SeokYun Jung[1,†]

[1]Stem Cell Research Institute, T&R Biofab Co., Ltd.

[2]Department of Animal Biotechnology, Sangji University

[†]These authors contributed to this work as corresponding authors

(kimmj@tnrbiofab.com)

Previous known artificial skin production methods are manual method and have limitations in productivity and uniformity. This has particular limitations in developing techniques to rapidly prepare therapeutically effective skin substitutes for extensive burns and surgeries requiring skin grafting. To overcome this, we used 3D bioprinting technology to create high productivity and uniform artificial skin and analyzed whether skin-derived extracellular matrix with fibroblasts and keratinocytes has a healing effect on skin wounds. The artificial skin production was possible within 5 minutes with 3D bioprinting technique, and the 3D cell-printed skin substitute showed rapid re-epithelialization and excellent tissue regeneration effect compared to the control group in a mouse wound model. These results are expected to help in the development of technologies that can quickly and easily provide customized skin replacement tissues to patients through 3D bioprinting technology.

Key words: artificial skin, dECM, 3D bioprinting, chimney wound model, mouse

Acknowledgement: This research was supported by the National Research Foundation of Korea grant funded (MSIT) (2022R1A2C1006622) and the Korean Fund for Regenerative Medicine (KFRM) grant funded the Ministry of Science and ICT, the Ministry of Health & Welfare (21A0403L1) by the Korea government.

Dev. Reprod. Vol 26, 2022 (Suppl. 1). pp 212

C-08

Microencapsulation-based large-scale cell culture platform in iPSC differentiation

김하은, 한정찬, 박서희, *Jiyou Han, *Jong Hyun Kim
Department of Biological Science, Hyupsung University

Research of neural differentiations using stem cells is a promising tool for new drug development cytotoxicity and cell therapeutic application. For this purpose, cell stability and mass production condition are necessary to control neural differentiation. In this present study, we established an optimal microfluidic chip system to generate a large-scale differentiation system of peripheral nerve cells. The optimal condition using an encapsulated-chip for 3D and directory differentiation of peripheral motor neurons showed three differences in the iPSC differentiation approach. Firstly, the microfluidic chip with alginate bead generated large-scale embryonic body (EB) formation and maintained single EB formation without aggregation of EBs during the differentiation process. We compared aggregation formation using two different fluorescence in conditions with/without alginate encapsulation and showed that the alginate encapsulation group prevented 100% aggregation of cell to cell and EB to EB. Secondly, a uniformed alginate bead size of 110±3 μm was induced uniform EB size as 50±5 μm, which led to an approximately 3-fold increase in the three germ layer marks such as SOX1 (ectoderm), BRACHYURY (mesoderm), SOX17 (endoderm) compared with non-uniform EB size. Finally, in induction condition with differentiation factors of peripheral motor neuron, alginate encapsulated cells highly upregulated genes expression of OLIG2 and NEUROG2 for motor neuron progenitor marks and HB9 and CHAT for mature motor neuron marks compared with non-encapsulated cells. Our results suggest that alginate bead-based encapsulation by using a microfluidic chip system combined with differentiation factors could be a powerful tool for deriving a high purity of desired cells and for producing large-scale cell culture from human pluripotent stem cells.

Acknowledgments: This research was supported by Basic Science Research Program through the National Foundation of Korea (NRF) funded by the Ministry of Education (NRF-2022R1F1A1062952, NRF-2022R1A2C2007696).

Dev. Reprod. Vol 26, 2022 (Suppl. 1). pp 213

C-09

Development of optimal protocol to induce capacitation on boar spermatozoa *in vitro*

Seung-Ik Jang[1], Jae-Hwan Jo[1], Eun-Ju Jeong[2], Woo-Jin Lee[2], Ju-Mi Hwang[2], Jeong-Won Bae[2], *Woo-Sung Kwon[1,2]

[1]Department of Animal Biotechnology, Kyungpook National University

[2]Department of Animal Science and Biotechnology, Kyungpook National University

(todwnl5787@naver.com)

In 1951, Colin Russell Austin and Min Chueh Chang have been identified “capacitation”. It is the special process of ejaculated spermatozoa in female reproductive tracts. The idea of capacitation came from in vivo phenomena, whereas the almost knowledge of capacitation are obtained from *in vitro* studies. Therefore, various trials have been performed to establish *in vitro* capacitation methods for applying various studies of reproduction. Although a series of studies have been conducted to develop optimal protocol to induce capacitation, almost studies focused on developing appropriate chemical compounds to induce capacitation for boar spermatozoa *in vitro*. Therefore, the purpose of this study is to develop the optimal incubation time to induce capacitation *in vitro*. Duroc semen were incubated during various time condition (60, 90 and 120 min) to induce capacitation. Then, sperm functions (sperm motility, motion kinematic parameters, and capacitation status) were evaluated. The results were showed that total sperm motility (MOT, %), rapid sperm motility (RPD, %), progressive sperm motility (PRG, %), curvilinear velocity (VCL, μm/s) and average path velocity (VAP, μm/s) were significantly decreased in time-dependent manners. However, capacitation status was not showed significant alteration. Taken together, these results were indicated that increase of incubation time more than 60 min suppress sperm motility and motion kinematic parameters. Therefore, we suggest that the 60 min may be the best incubation time to induce capacitation without negative effects of sperm motility and motion kinematics for boar spermatozoa *in vitro*.

Key words: boar, spermatozoa, capacitation, *in vitro*, sperm functions

Dev. Reprod. Vol 26, 2022 (Suppl. 1). pp 214

C-10

Deguelin suppresses sperm functions via the activating PI3K/AKT pathway during capacitation

Woo-Jin Lee[1], Jae-Hwan Jo[2], Seung-Ik Jang[2], Eun-Ju Jung[1], Ju-Mi Hwang[1], Jeong-Won Bae[1], *Woo-Sung Kwon[1,2]

[1]Department of Animal Science and Biotechnology, Kyungpook National University

[2]Department of Animal Biotechnology, Kyungpook National University

(wj9059lee@naver.com)

Deguelin is a natural flavonoid compound extracted from *Lonchocarpus*, *Derris*, or *Tephrosia*. It is also known as an AKT inhibitor, and several studies have been shown that Deguelin has the potential as a therapeutic agent for malignant tumors. However, risk of Deguelin on male fertility has not been fully explained yet. Therefore, the aim of the present investigation was to evaluate the effects of Deguelin on sperm functions during capacitation. Firstly, boar spermatozoa were incubated with various concentrations of Deguelin (0.1, 1, 10, 50, and 100 μM). Then, sperm motility, capacitation status, intracellular ATP level, and cell viability were evaluated. In addition, western blot was performed to investigate the effects of Deguelin on PI3K/AKT pathway and tyrosine phosphorylation. Our results revealed that Deguelin significantly decreased sperm motility and motion kinematics in a dose-dependent manner. Moreover, there was no significant difference in capacitation status, whereas acrosome reaction was decreased in the high concentrations (50 and 100 μM). Intracellular ATP level was significantly decreased in all treatment groups compared to the control group. However, there was no significant difference in cell viability. In addition, western blot results indicated that Deguelin diminished tyrosine phosphorylation. Unexpectedly, contrary to the previous studies that Deguelin inhibits AKT, our results significantly increased the expression of PI3K/AKT pathway-related proteins. Taken together, our data showed that Deguelin induces detrimental effects on sperm functions due to abnormal PI3K/AKT signaling activation. In conclusion, we provided the first evidence that Deguelin may act by differentially regulation of the PI3K/AKT pathway in spermatozoa. It is also suggested that the harmful effects of Deguelin should be considered when applying Deguelin to cancer treatment.

Key words: deguelin, PI3K/AKT, sperm functions, capacitation, male fertility

Acknowledgement: This work was supported by the National Research Foundation of Korea (NRF) grant funded by the Korea government (Ministry of Science and ICT) (NRF-2022R1F1A1066103).

Dev. Reprod. Vol 26, 2022 (Suppl. 1). pp 215

C-11

Oryzalin induces oxidative stress in porcine uterine luminal epithelial cells and trophectoderm cells leading to implantation failure

Jiyeon Ham[1], Whasun Lim[2], *Gwonhwa Song[1]

[1]Institute of Animal Molecular Biotechnology and Department of Biotechnology, Korea University

[2]Department of Biological Sciences, Sungkyunkwan University

(glorijy76@korea.ac.kr)

Oryzalin is one of dinitroaniline type pesticides to inhibit the growth of weeds via inhibition of microtubule synthesis. As studies about deleterious effect of dinitroaniline pesticides on development and reproductive system, we tried to demonstrate the toxic mechanisms of oryzalin on early pregnancy stage using porcine uterine epithelial cells (pLE) and trophectoderm (pTr) cells. pLE and pTr cells are adequate model for studying embryo development and implantation in molecular levels because of its similarity with humans. In our results, oryzalin inhibited the viability and proliferation of pLE and pTr cells, further affect to cell cycle progression. Additionally, oryzalin induced apoptotic cell death and impaired mitochondrial membrane polarity in pLE and pTr cells. Moreover, we confirmed that oryzalin significantly suppressed the ATP production and mitochondrial respiration using Seahorse XF analyzer. Furthermore, oxidative stress was also upregulated in oryzalin-treated pLE and pTr cells, and these effects were ameliorated by N-acetylcysteine, the ROS scavenger. In addition, the phosphorylation of ERK1/2, P38, AKT and P70S6K protein expression were stimulated by oryzalin treatment, but NAC reinstated the phosphorylation status into normal level in pLE and pTr cells. Finally, we verified the alleviation effect by NAC on suppressed migration and proliferation in oryzalin-treated pLE and pTr cells. Collectively, we elucidated the molecular mechanisms that oryzalin-induced oxidative stress impedes on proliferation and migration of pLE and pTr cells during early pregnancy.

Key words: oryzalin, oxidative stress, mitochondria, migration, early pregnancy

Acknowledgement: This research was supported by Basic Science Research Program through the National Research Foundation of Korea (NRF) funded by the Ministry of Education (grant number: 2022R1I1A1A01053162) and supported by the NRF grant funded by the Korea government (MSIT) (grant number: 2021R1A2C2005841).

Dev. Reprod. Vol 26, 2022 (Suppl. 1). pp 216

C-12

Biomarker in male fertility: Ras-related proteins

Jeong-Won Bae[1], Jae-Hwan Jo[2], Seung-Ik Jang[2], Eun-Ju Jung[1], Woo-Jin Lee[1], Ju-Mi Hwang[1], *Woo-Sung Kwon[1,2]

[1]Department of Animal Science and Biotechnology, Kyungpook National University
[2]Department of Animal Biotechnology, Kyungpook National University
(jwbae1822@gmail.com)

The development of efficient biomarkers for the prediction and diagnosis of male fertility is important to improve animal production and treatment of male infertility in humans. Ras-related proteins (Rab) are members of the Ras superfamily of monomeric G proteins associated with morphologic and motion kinematic functions in spermatozoa. Moreover, it has been reported that Rab2A, one of the Rab proteins can use male fertility-related biomarker. Therefore, the present study was designed to develop additional fertility-related biomarkers among various Rab proteins. First, expression levels of Rab proteins (Rab3A, Rab4, Rab5, Rab8A, Rab9, Rab11, Rab14, Rab25, Rab27A, and Rab34A) from 31 duroc boar spermatozoa were measured before and after capacitation, and then statistical analysis was performed to evaluate the correlation between expression level of Rab proteins and litter size. As a result, It was shown that Rab3A, Rab4, Rab5, Rab8A, Rab9, and Rab25 before capacitation as well as Rab3A, Rab4, Rab5, Rab8A, Rab9, and Rab14 after capacitation were negatively correlated with litter size. Moreover, increasing of litter size was observed in evaluation of the ability of the individual Rab protein to predict litter size depending on calculated cut-off values by ROC. Therefore, we suggest that the Rab proteins may be applied to use fertility-related biomarkers to select superior sires in the livestock industry. In addition, we anticipate that the Rab proteins will be applied to use prognosis and diagnosis of male infertility in humans.

Key words: Ras-related proteins, biomarkers, prediction, male fertility, pig

Dev. Reprod. Vol 26, 2022 (Suppl. 1). pp 217

C-13

The essential role of Wnt/β-catenin inhibition for establishing porcine embryonic stem cells from *in vitro*-derived blastocysts

Hyerin Choi, *Sang-Hwan Hyun

Laboratory of Veterinary Embryology and Biotechnology (VETEMBIO),
Veterinary Medical Center and College of Veterinary Medicine,
Chungbuk National University

Stable pig embryonic stem cells (pESCs) can be a promising tool for understanding human cell fate decisions during early development because pigs are more similar to humans in anatomy and physiology. We developed a simplified culture condition for deriving pESCs by using a minimum of small molecules in knockout serum replacement media. Blastocysts obtained *in vitro* on day 6 were seeded on the feeder cell layer with DMEM/F10 (1:1), DMEM/F12, and α-MEM medium to compare an efficiency of the pESCs establishment according to the type of the basal medium and small molecules. The small molecule conditions were (1) FGF2 (F), (2) FGF2 + IWR-1 (FI), and (3) FGF2 + IWR-1 + CHIR (FIC). All three basal media showed success attachment of the blastocysts to the feeder layer. However, the colony formation was observed only in DMEM/F10 and DMEM/F12 conditions. Both conditions showed negative results for the expression of SOX2 in the F group through immunostaining, while it was expressed homogeneously in the FI and FIC condition. We characterized the obtained pESCs under FI small molecule conditions in the DMEM/F12 which is most defined and simplified medium. Immunostaining data presented homogenous expression of pluropotency markers OCT4, SOX2, NANOG, and SSEA4 in FI condition. When the mRNA expression levels of naive and primed-relative genes were compared, it was found that the levels of FGFR1 and FGFR2, known as primed markers, as well as the core pluripotency markers, Oct4, Sox2, and Nanog transcripts, were significantly higher than those of pESCs in serum condition. Expression of ectoderm, mesoderm, and endoderm markers was confirmed in the result of verification of differentiation potential through embryoid bodies formation. Although further studies are required to adapt feeder-free condition, these findings demonstrate that an inhibition of Wnt/β-catenin pathway by IWR-1 supplementation are essential to establish pESCs from in vitro-derived blastocysts.

Key words: pig embryonic stem cells, FGF2, IWR-1

Acknowledgement: This work was supported by grants from the “NRF funded by the Korean Government (2017K1A4A3014959, 2020R1A2C2008276, 2022R1A4A1025557)” and “IPET in Food, Agriculture, Forestry and Fisheries (318016-5, 320005-4)”, Korea.

Dev. Reprod. Vol 26, 2022 (Suppl. 1). pp 218

C-14

Ahnak maintains pivotal functions of vertebrate urinary system

Tae-Yang Lim[1], Jong-Min Lee[1], Sang-Bin Oh[1], Seung-Jun Lee[1], Shujin Li[1], Adpaikar Anish Ashok[1], Yun Soo Bae[2], Han-Sung Jung[1]

[1]Division in Anatomy and Developmental Biology, Department of Oral Biology, Taste Research Center, Oral Science Research Center, BK21 Four Project, Yonsei University College of Dentistry

[2]Department of Life Sciences, Ewha Woman's University

Various renal abnormalities including hydronephrosis, polycystic and hydroureter had been reported and these symptoms are present in diseases such as DiGeorge syndrome, polycystic kidney disease, renal dysplasia and acute kidney failure. However, major target genes of various renal abnormalities are not elucidated yet. Ahnak plays a role in diverse processes as blood-brain barrier formation, cell structure, migration, cardiac calcium channel regulation, and tumor metastasis. Previous studies have reported that calcium imbalances cause various kidney diseases. Ahnak is expressed in intra-cellular locations such as plasma membrane, cytoplasm and nucleus. In this study, Ahnak localization was confirmed in developing ureteric bud and urothelium in mouse. Hydronephrosis, expanded Bowman's space, loss of urothelium and hydroureter were observed in Ahnak KO mouse. We confirmed that imbalance of calcium homeostasis was observed in Ahnak KO kidney. Moreover, smooth muscle in ureter has reduced peristalsis movement in Ahnak KO. These results indicated that Ahnak plays pivotal roles in kidney and ureter development to maintaining urinary system.

Key words: Ahnak, hydronephrosis, hydroureter, calcium homeostasis, muscle contraction.

Acknowledgements: This work was supported by the National Research Foundation of Korea (NRF) Grant funded by the Korea Government (MSIP) (NRF-2016R1A5A2008630, NRF-2021R1A2C1005506 and NRF-2022R1A2B5B03001627).

Dev. Reprod. Vol 26, 2022 (Suppl. 1). pp 219

C-15

Studies on cephalopod brain molecular atlas in *Octopus minor*

Chan-Jun Lee, Hae-Youn Lee, Yun-Sang Yu, *Sung-Jin Cho

School of Biological Sciences, College of Natural Sciences, ChungBuk National University
(jjjod1150@gmail.com)

Cephalopods (e.g. nautilus, cuttlefish, squid, octopus) belong to a class of the phylum Mollusca and have a high intelligence, complex atlas structures, and large brain. However, there are a few studies on cephalopod brain in Mollusca. *Octopus minor*, commonly called long arm octopus, is a highly valuable species of great commercial interest and excellent candidate for aquaculture diversification. In this study, we performed morphological and histological analysis to investigate the structure of *O. minor* adult brain. Then, we confirmed the compartments of central brain separated by commissural neuron using neuronal marker such as neurotransmitter receptor (*SerT*, *TH* and *vGluT*), proliferation marker (KI-67 and *BTG1*). We also analyzed transcriptome on the adult octopus brain to make anatomic definition based on gene expression classification. Finally, the up-regulated genes selected by Differentially Expressed Genes (DEGs) analysis were visualized by *in situ* hybridization to examine the expression of marker genes in central brain. This research is the first step for understanding the molecular atlas of cephalopod adult brain.

Key words: cephalopod, brain, differentially expressed genes, *in situ* hybridizaiton

Dev. Reprod. Vol 26, 2022 (Suppl. 1). pp 220

C-16

Dinitramine interferes with implantation during early pregnancy by mitochondrial malfunction and cell cycle arrest in porcine trophectoderm and luminal epithelial cells

Junho Park[1], Garam An[1], Whasun Lim[2], *Gwonhwa Song[1]

[1]Institute of Animal Molecular Biotechnology and Department of Biotechnology, Korea University

[2]Department of Biological Sciences, Sungkyunkwan University

As agricultural production increases, the role of herbicides is also becoming more important. However, several herbicides have been reported to be toxic to non-target species. One of dinitroaniline herbicides, dinitramine is used on crops to hinder the weed growth. The toxicity of dinitramine to aquatic organisms has been reported, but the toxicity to mammals, especially reproductive toxicity, has been rarely investigated. Therefore, we used pTr and pLE cells which are trophectoderm and endometrial luminal epithelial cells established at early pregnancy of pigs respectively to determine the toxicity of dinitramine to female reproductive systems. The survival rate of both cell types was reduced by dinitramine as it induced cell cycle arrest, notably at sub-G1 stage and suppressed DNA replication which trigger apoptosis. Also, dinitramine interrupted intracellular calcium homeostasis and produced reactive oxygen species (ROS) which induced oxidative stress in both cell types. These alterations caused the mitochondrial depolarization and disturbed oxidative phosphorylation. And MAPK pathways which are associated with apoptosis and cell survival, and gene expression levels related to pregnancy were changed by dinitramine. These effects reduced cell mobility and spheroid formation of both pTr and pLE cells. Thus, these results in the present study indicate dinitramine could interfere with implantation during early stages of pregnancy.

Key words: dinitramine, mitochondrial malfunction, cell cycle arrest, implantation failure

Acknowledgement: This research was supported by the National Research Foundation of Korea (NRF) grant funded by the Korea government (MSIT) (grant number: 2021R1A2C2005841).

Dev. Reprod. Vol 26, 2022 (Suppl. 1). pp 221

C-17

O-GlcNAcylation during tooth development

Elina Pokharel, Yam Prasad Aryal, Tae-Young Kim, Jae-Kwang Jung, Seo-Young An, Chang-Hyeon An, Youngkyun Lee, Do-Yeon Kim, Jung-Hong Ha, *Jae-Young Kim

School of Dentistry, IHBR, Kyungpook National University

(jykim91@knu.ac.kr)

Tooth development is regulated by reciprocal interactions between epithelium and mesenchyme through complex signaling regulations, and undergoes different stages; bud, cap and bell stages. However, the detailed fine tuning mechanisms underlying tooth morphogenesis is still unknown. To understand the detailed mechanisms in tooth development, we examined the O-GlcNAcylation, the posttranslational modification which regulates protein stability and activity through the addition or removal of a single sugar (GlcNAc) to the serine or threonine residue of the intracellular proteins, in tooth morphogenesis. For these signaling regulations, it is necessary to examine the O-GlcNAc transferase (OGT) which catalyzes the addition of the O-GlcNAc to the serine and threonine residues of proteins. Immunostainings against OGT, and O-GlcNAc showed tissue specific localizations in developing mice tooth germs at cap, secretory, birth and tooth root forming stages. To evaluate developmental function of the O-GlcNAcylation, we employed the *in-vitro* tooth germs cultivation method at E14.5 for 1 and 2 days with or without treatment of OGT inhibitor. In addition, to evaluate the level of mineralization and morphological changes, we performed renal capsule transplantation for 1 and 3 weeks, after 2 days of cultivation at E14.5. After inhibition of OGT, morphological and molecular alternations were examined using histology, 3-dimentional reconstruction, SEM, immunohistochemistry, RT-qPCR, and *in-situ* hybridization. Overall, inhibition of OGT showed the altered cellular physiology including proliferation, apoptosis, and epithelial rearrangements with significant changes of expression patterns of tooth development related signaling molecules such as β-catenin, Fgf4, and Shh. Moreover, OGT inhibited tooth germs showed the retarded second molar development. Based on our results, we suggest that O-GlcNAcylation would play important roles in mouse molar morphogenesis through protein modification for proper signaling regulations and cell physiology.

Key words: O-GlcNacylation, tooth development, OGT, signaling regulations

Dev. Reprod. Vol 26, 2022 (Suppl. 1). pp 222

C-18

Slit-Robo expression in the leech nervous system: insights into eyespot evolution

Keon-Hwi Jeong[1], Hee-Jin Kwak[2], *Sung-Jin Cho[1]

[1]School of Biological Sciences, College of Natural Sciences, ChungBuk National University

[2]Department of Ecology, Evolution and Behavior, Alexander Silberman Institute of Life Sciences, Faculty of Science, Hebrew University of Jerusalem, Israel

(ggasimamam@naver.com)

The nervous system is a major organ system in metazoans and the development of nerve system include evolutionarily conserved systems of ligands and receptors, such as the Slit/Robo system, that serve as guidance cues in patterning their respective nerve cords. The number of *slit* and *robo* gene paralogs varies across recent bilaterian genomes. Given the lack of data regarding Slit/Robo in the Lophotrochozoa compared to the Ecdysozoa and Deuterostomia, the present study aims to identify and characterize the expression of Slit/Robo orthologs in leech development. We found one *slit* (*Hau-slit*) and two *robo* genes (*Hau-robo1* and *Hau-robo2*) in the leech *Helobdella austinensis* genome, and that their transcripts are expressed dynamically in late stages of development. Our results were consistent with eyespot development in the Lophotrochozoa. Furthermore, based on comparison of the expression of *slit* and *robo* orthologs in another glossiphoniid leech, *Alboglossiphonia lata*, we provide a new insight into the molecular basis of evolutionary variation of eyespot development among leeches.

Key words: Slit, Robo, gene duplication, axon guidance, eyespot

Dev. Reprod. Vol 26, 2022 (Suppl. 1). pp 223

C-19

Interleukin-7 supplementation during *in vitro* culture of porcine parthenote embryos enhances embryonic development and blastocyst quality

Dongjin Oh[1,2], *Sang-Hwan Hyun[1,2]

[1]Laboratory of Veterinary Embryology and Biotechnology (VETEMBIO), Veterinary Medical Center and College of Veterinary Medicine, Chungbuk National University

[2]Institute for Stem Cell & Regenerative Medicine (ISCRM), Chungbuk National University

Interleukin-7 (IL-7) has been identified as a vital factor for cell development, proliferation, and survival. IL-7 also can play a significant role in porcine oocyte maturation, but its role in embryonic development has not yet been explored. Here, we found that IL-7 and its binding to IL-7Rα (IL-7R) were localized in porcine embryos. We also determine the effects of IL-7 supplementation on porcine embryos during *in vitro* culture (IVC) via analysis of embryonic development after parthenogenetic activation (PA), intracellular glutathione (GSH), and reactive oxygen species (ROS) levels in Day 2 embryos. As a result, the IL-7 and IL-7R proteins were located in the metaphase II state to the blastocyst stage. The cleavage rates were significantly higher ($p<0.05$) in 10- and 100 ng/mL IL-7-treated group (83.4% and 78.4%) than in the control group (63.4%). Day 7 after PA, only the 10 ng/mL IL-7 treated group showed significantly ($p<0.05$) higher blastocyst formation rates (71.3%) compared with the control group (51.9%). Furthermore, 1- and 10 ng/mL IL-7 treatment groups exhibited significantly ($p<0.05$) increased intracellular GSH levels in the control groups. The 10 ng/ml IL-7 treatment group displayed significantly ($p<0.05$) decreased intracellular ROS levels compared with the control group. Then, we examined the apoptosis rates of blastocysts by TUNEL assay. The 1- and 10 ng/mL IL-7 treatment groups (13.8% and 8.7%) displayed significantly ($p<0.05$) decreased apoptosis rates of blastocyst compared with the control group (19.2%). In Day 2 embryos, the mRNA expression of the proapoptotic gene *BAX* was significantly ($^{***}p<0.001$) reduced, and the anti-apoptotic gene *MCL1* level was significantly ($^{*}p<0.05$) increased in 10 ng/mL IL-7-treated embryos compared to control. Interestingly, the mRNA levels of maternal effect genes (MEG; *Filia* and *NPM2*) were significantly ($^{**}p<0.01$) decreased while zygotic genome activation (ZGA)-related genes (*DPPA2* and *EIF1A*) were significantly ($^{*}p<0.05$) increased in the IL-7-treated group compared to the control. The IL-7-treated blastocyst showed significantly ($^{*}p<0.05$ and $^{**}p<0.01$) increased mRNA expression of IL-7 signaling-related genes (*PIK3R1*, *AKT1*, and *ERK2*), and development-related genes (*OCT4* and *NANOG*) compared to control. Moreover, using immunostaining, we demonstrated that supplementation with IL-7 enhanced the expression of phosphorylated STAT5 (pSTAT5), the genuine inner cell mass (ICM) marker SOX2, and the ICM ratio, improving PA blastocyst quality. In conclusion, for the first time, we proved the localization of IL-7 and IL-7R in porcine preimplantation embryos *in vitro*. Furthermore, we suggest

that IL-7 supplementation enhances the embryonic development and ICM ratio by inducing the transcription of genes involved in the developmental competence during porcine PA embryo development *in vitro*.

Acknowledgment: This work was supported by grants from the “NRF funded by the Korean Government (2017K1A4A3014959, 2020R1A2C2008276, 2022R1A4A1025557)” and “IPET in Food, Agriculture, Forestry and Fisheries (318016-5, 320005-4)”, Korea.

Dev. Reprod. Vol 26, 2022 (Suppl. 1). pp 225

C-20

Fluroxypyr-1-methylheptyl ester-mediated ROS production and mitochondrial dysfunction trigger apoptosis through MAPK signaling in porcine trophectoderm and uterine luminal epithelial cells

Miji Kim[1], Garam An[1], Whasun Lim[2], *Gwonhwa Song[1]

[1]Institute of Animal Molecular Biotechnology and Department of Biotechnology, Korea University

[2]Department of Biological Sciences, Sungkyunkwan University

FPMH (Fluroxypyr-1-methylheptyl ester), a type of synthetic auxin herbicide that hinders plant growth, is widely used in agriculture. Various studies have been conducted on the toxicity of FPMH. However, the toxic effects of FPMH have not been reported for porcine implantation. This study provides a blueprint for the mechanisms of FPMH in the adverse effects on the pre-implantation stage using porcine trophectoderm cell (pTr) and porcine uterine endometrial cell (pLE). The results of this study demonstrate that FPMH can induce the oxidative stress via the production of reactive oxygen species (ROS) and disrupt the mitochondrial membrane potential. The effects of FPMH can also cause mitogen-activated protein kinase (MAPK) signaling to be phosphorylated. Activated MAPK signaling by FPMH forms crosstalk and elicits cell responses different from normal cells. Under this condition, the proliferation of pTr and pLE cells was decreased and the early and late stage of apoptosis was induced. In addition, FPMH-mediated cytotoxic effects can affect the ability of migration and adhesion between pTr and pLE cells through wound healing assay and 3D spheroid culture. Therefore, the results suggest that FPMH may interfere with the pre-implantation stage, and lead to implantation failure.

Key words: FPMH, implantation, apoptosis, ROS production, mitochondrial membrane potential

Acknowledgement: This research was supported by the National Research Foundation of Korea (NRF) grant funded by the Korea government (MSIT) (grant number: 2021R1A2C2005841).

Dev. Reprod. Vol 26, 2022 (Suppl. 1). pp 226

C-21

The brain regeneration of *P. excavatus*

Min-Young Choi[1], Seo-ji Lee[1], Yun-Sang Yu[1], Jung Kim[2], Hae-Youn Lee[1], Sangjune Kim[1], Soon Cheol Park[3], *Sung-Jin Cho[1]

[1]School of Biological Sciences, College of Natural Sciences, Chungbuk National University
[2]Department of Molecular and Cell Biology, University of California, USA
[3]Department of Life Science, Chung-Ang University
(c7m9y8@naver.com)

Regeneration is a biological process restoring lost or amputated body parts, exhibiting many differences in regenerative capacity among species. The earthworm, *P. excavatus*, is known as the highest evolutionary form capable of regenerating an anterior portion including a central nerve system (CNS), which is limited to specific animals. However, the molecular mechanisms of how *P. excavatus* regenerates the CNS, especially the brain, are still unclear. In this study, we investigate the morphology of the adult brain of *P. excavatus* and analyze the transcriptomic profile of the brain. We identify five candidate genes, which might function in the normal physiology of the brain. Importantly, we characterize the stages of the regeneration process. Furthermore, we establish transcriptome of the regenerating brain and identify 4 candidate genes associated with regeneration and confirm the spatiotemporal expression of candidates. In addition, we conducted behavioral test to assess the function of the regenerated brain. Our study would provide the groundwork for investigating mechanisms of CNS regeneration.

Key words: regeneration, *P. excavatus*, central nerve system, transcriptome, behavioral test

Dev. Reprod. Vol 26, 2022 (Suppl. 1). pp 227

C-22

Functional study of KDM1A and its non-histone target proteins in *Xenopus laevis*

Hongchan Lee, Seung Hwan Lee, Hyun-Shik Lee

School of Life Sciences, BK21 FOUR KNU Creative BioResearch Group,
Kyungpook National University

Lysine specific demethylase 1A (KDM1A or LSD1) is the first discovered enzyme that removes methyl group from the histone H3 protein, specifically both histone 3 lysine 4 and histone 3 lysine 9 mono-, di-methylation (H3K4me1/2, H3K9me1/2) and it is known to regulate both gene activation and suppression via modulating H3K4 and H3K9 methylation status. Even though LSD1 was first known to regulates histone methylation, it was revealed to modulates not only histone proteins but also non-histone protein methylation such as P53, SOX2 and FOXA1. In this study, we focused on the developmental role of *lsd1* and its non-histone target proteins using *Xenopus* embryos. Morpholino oligonucleotides (MO) mediated *lsd1* knockdown in *Xenopus* embryos induced bent axis which represents the defect of convergent extension movements. Moreover, *lsd1* morphants were rescued by injecting exogenous wild type dishevelled (*dsh*) implies *lsd1* is closely related to the Wnt signaling pathways. To investigate non-histone target protein of LSD1, we performed Mass Spec analysis following LSD1 immunoprecipitation and we found that some of candidates were physically interacted with the LSD1 indeed and its spatial expression overlaps with *lsd1*. Taken together, our results indicated the significance of this epigenetic regulators during embryonic development together with identification of its regulatory mechanism.

Dev. Reprod. Vol 26, 2022 (Suppl. 1). pp 228

C-23

북방전복(*Haliotis discus hannai*)의 B-type allatostatin 수용체 특성 및 리간드 반응성

박성우[1], 김미애[2], *손영창[1]

[1]강릉원주대학교 해양생명과학과, [2]강릉원주대학교 동해안생명과학연구원

(ycsohn@gwnu.ac.kr)

수컷 노랑초파리(*Drosophila melanogaster*)의 정액 속에서 최초로 동정된 성 펩티드(sex peptide, SP)는 성숙 암컷에게 전달되면 교미 거부, 산란량 증가와 같은 교미 후 반응이 유도된다. SP에 의해 활성화 되는 수용체는 성 펩티드 수용체(sex peptide receptor, SPR)라고 명명되었다. SPR은 다양한 무척추동물에 존재하며, SP 뿐만 아니라 근육억제펩티드(myoinhibitory peptide, MIP)와 반응하여 세포 내 cAMP를 증가시키는 신호전달경로가 알려져 있다.

MIP는 일부 곤충류의 경우 allatostatin-B(AST-B)로 알려져 있으며, N말단과 C말단 양쪽에 트립토판(tryptophan, W) 잔기가 보존되어 있는 WWamide 형태의 신경펩티드이다. MIP는 곤충류의 근육 수축 억제 및 수면 기능 조절, 곤충 앞가슴샘의 ecdysteroids의 생성을 억제하여 탈피를 제어한다. 갯지렁이(*Platynereis dumerilii*) 및 개불(*Urechis unicinctus*)과 같은 해양 환형동물의 부유 유생의 변태를 MIP가 유도하므로, 정착성 유생 발달에 관여하고 있다고 추정된다.

본 연구는 AST-B와 SPR에 관한 정보가 부족한 해양 무척추동물 중 북방전복(*Haliotis discus hannai*)의 *AST-B* 전구체 및 *SPR* cDNA를 cloning하고, 분자계통수 분석을 실시하였다. 북방전복의 *SPR*은 연체동물문 복족강의 *SPR*과 같은 clade에 속하고, 북방전복의 AST-B 성숙 펩티드 부위의 WWamide 모티브는 비교・조사한 모든 무척추동물의 AST-B WWamide 모티브 서열과 일치하였다. 또한, 성숙한 전복 암수 개체의 뇌신경절(cerebral ganglion, CG) 등 다양한 조직으로부터 total RNA를 추출하고, real-time polymerase chain reaction 분석 결과, *SPR*과 *AST-B* 전구체 유전자 모두 신경절에서 주로 발현됨을 알게 되었다. HEK293세포 및 북방전복의 SPR 발현 벡터를 이용한 transfection 실험을 통해 수용체・리간드 반응성을 확인하였다. 이상의 결과, 북방전복의 SPR은 AST-B의 특이적인 수용체로 추정되며, 본 연구는 향후 해양 무척추동물의 *AST-B*에 대한 기초자료로 활용될 수 있을 것으로 사료된다.

Key words: sex peptide receptor, myoinhibitory peptide, allatostatin-B, WWamide

Dev. Reprod. Vol 26, 2022 (Suppl. 1). pp 229

C-24

Facilitation of alveolar bone formation using an LPAR2 antagonist treatment

Tae-Young Kim[1], Jae-Kyung Park[2], Shijin Sung[1], Yam Prasad Aryal[1], Elina Pokharel[1], Sanjiv Neupane[3], So-Young Choi[4], Jung-Hong Ha[5], Jae-Kwang Jung[6], Hitoshi Yamamoto[7], Chang-Hyeon An[8], Jo-Young Suh[9], Wern-Joo Sohn[10], Youngkyun Lee[1], Il-Ho Jang[2], Derek D. Norman[11], Gabor J. Tigyi[11], *Seo-Young An[8], *Jae-Young Kim[1]

[1]Department of Biochemistry, Kyungpook National University
[2]Department of Oral Biochemistry and Molecular Biology, Institute of Translational Dental Sciences, Pusan National University School of Dentistry
[3]Department of Biochemistry and Cell Biology, Stony Brook University, Stony Brook, USA
[4]Department of Oral and Maxillofacial Surgery, Kyungpook National University
[5]Department of Conservative Dentistry, Kyungpook National University
[6]Department of Oral Medicine, Kyungpook National University
[7]Department of Histology and Developmental Biology, Tokyo Dental College, Japan
[8]Department of Oral and Maxillofacial Radiology, Kyungpook National University
[9]Department of Periodontology, School of Dentistry, IHBR, Kyungpook National University
[10]Pre-Major of Cosmetics and Pharmaceutics, Daegu Haany University
[11]Department of Physiology, University of Tennessee Health Science Center, USA
(syan@knu.ac.kr)

Tooth loss without periodontal disease would be caused by trauma, and most of these clinical cases are required to facilitate bone regeneration for transplantation of dental implant to restore masticatory function. However, it still remains to establish the efficient clinical treatment with its scientific background. In this study, we evaluated the osteogenic efficacy of an LPAR2 (lysophosphatidic acid receptor 2) antagonist, involved in various aspects of cell physiology, using *in vitro* and *in vivo* experimentations. *In vitro* cell cultivation results revealed that the LPAR2 antagonist treatment showed the increased positive reactions of osteogenic differentiation assays, ALP and ARS, in osteoblast rather than hPDLF. Moreover, LPAR2 antagonist treated osteoblast showed the increase expression levels of Runx2 and Tgf-β1. To confirm these *in vitro* experiment results in *in-vivo* system, LPAR2 antagonist was applied to the tooth loss without periodontal disease model after 5 and 10 days from the tooth extraction. The histomorphometry and micro-computed tomography results showed the facilitated bone formation in LPAR2 antagonist treatment group. These results were confirmed by immunohistochemistry using KI67, Osteocalcin (OCN), PERIOSTIN, and RUNX2. Particularly, altered localization of

PERIOSTIN positive cells suggest that AMC35 would affect cell type dependent manner as was examined in *in vitro* experiment. In addition, well maintained physiological balance between osteoclast and osteoblast was examined in LPAR2 antagonist treated group. Immunostainings against TGF-β1 and SMAD2/3 showed obvious stronger positive reactions in tooth loss lesion in AMC35 treated group compared with control. Overall, LPA signaling regulations by LPAR2 antagonist treatment on osteoblast in tooth loss lesion would facilitate bone formation with proper bone remodeling.

Key words: LPA signaling, trauma, TGF-β1, SMAD2/3, osteoblast

Dev. Reprod. Vol 26, 2022 (Suppl. 1). pp 231

C-25

Development of protocol to make organoids for 3D bioprinting research

Jihoon Kang[1,2], Shunske Mori[1], *Mototsugu Eiraku[1]

[1]Laboratory of Developmental Systems, Institute for Frontier Life and Medical Sciences, Kyoto University

[2]Korea Army Research Center for Future and Innovation

(sokay1412@gmail.com)

Parts of limb buds, branchial arch, and cardiac organoids' development starts with the formation of mesenchymal/epithelial complex tissues from PSCs. There are means for induction of an LB-like mesenchymal/epithelial complex tissues from murine pluripotent stem cells (PSCs) *in vitro*. Also LB-like tissues selectively differentiate into forlimb or hindlimb depending on a concentration of retinoic acid. Likewise by manipulating BMP or other signal lines, we can expect to get other appendages like branchial arch or cardiac –like tissues from PSCs and that can my used for research of 3Dbioprinting.

Key words: organoid, 3D bioprinting, limb bud, branchial arch

Dev. Reprod. Vol 26, 2022 (Suppl. 1). pp 232

C-26

Expression of luteinizing hormone (LH) subunit in rat stomach

Yu Jin Seo, Da Hea Mun, Na Young Kim, Jin Soo Park, *Sung-Ho Lee

Department of Biotechnology, Sangmyung University

(shlee@smu.ac.kr)

Luteinizing hormone (LH) is a hormone produced by gonadotrophs in the anterior pituitary gland, and LH production is regulated by GnRH from the hypothalamus. Interestingly, GnRH and LH were demonstrated that these also exist in some extrahypothalamus and extrapituitary regions, respectively. Since GnRH is expressed in rat stomach, we hypothesized and tested that LH is also expressed in the rat stomach. To verify our hypothesis, we examined the presence of LH subunits in adult rat (SD) stomach (divided into forestomach and glandular stomach) using RT-PCR and immunohistochemistry. The PCR revealed the presence of identical products for two LH subunits, Cgα and LH-β, in both part of stomach. The expected product sizes for rat Cgα and LH-β PCR were 232 bp and 259 bp, respectively. Immunohistochemistry results show that two subunits are localized in forestomach and glandular stomach. Both Cgα and LH-β positive signals were detected in the parietal cells, submucosal plexus and mucosa of esophagus-gastric junction. Squamous mucosa has Cgα positive signals, exclusively. In summary, our study demonstrated that the presence and localization of the LH subunits in rat stomach. Our results suggest that the stomach LH might be a auto- and/or paracrine factor, and ongoing studies will be helpful to understand the precise function of the stomach LH.

Key words: LH, stomach, Rat, IHC, PCR

Dev. Reprod. Vol 26, 2022 (Suppl. 1). pp 233

C-27

Cell spheroids as a versatile platform called SPHRINTER

Seokhwan Yun, Keunsun Ahn

Research Institute, SPHEBIO Co., Ltd.

Stem cells have been in the spotlight for the past 2 decades. However, apart from the achievements in the research field, there were no outstanding outcomes in therapeutic field. When stem cells are transplanted into pathogenic region, only about 0.8% of them survived in pathogenic condition. This low number indicate that the first step of stem cell therapy is failure.

When we used Spheroids, as an alternative of single cells, the engraftment rate of spheroid transplantation increased 12.5 times compared to single cell transplantation. However, we faced another problems. In conventional method of forming spheroids, we cannot control the spheroid diameter. Injection needle or nozzle were frequently jammed. Even if the transplantation were successful, 20% of animals were died within a day because of microembolic stroke.

Here we developed Spheroid producing machine called SPHRINTER as a versatile platform for cell therapy. Spheroids are capable of control the spheroid diameter and cell number within minimum error rate (<10%). These spheroids do not clog the injection needle or nozzle and do not induce microembolism.

We expected that SPHRINTER can be applicable to cell therapy, organoid research, alternative for *in vivo* testing, artificial organ, and exosome mass production. Further, we plan to apply it to bacterial cells, fungal cells, and plant cells.

Dev. Reprod. Vol 26, 2022 (Suppl. 1). pp 234

D-01

Production of a novel mouse model for Fabry disease

Dong-Won Seol[1], Jong Bin Choi[2], Jaemin Park[2],
***Yong-Mahn Han[2], *Gabbine Wee[1]**

[1]Preclinical Research Center, Daegu-Gyeongbuk Medical Innovation Foundation
[2]Department of Biological Sciences, KAIST

Patients of the Fabry disease (FD) don't produce enough an enzyme (blood chemical) called α -galactosidase A (α-GAL A). α-GAL A is the lysosomal enzyme and lysosomes function as the primary digestive tract of cells. Enzymes within lysosomes break down or digest particular compounds and intercellular structures. α-Gal A functions to break down complex sugar-lipid molecules called glycolipids, specifically, globotriaosylceramide (GL-3 or Gb3), its deacylated form Lyso-GL-3/Gb3 and related glycolipids, by removing the terminal galactose sugar from the end of these glycolipid molecules. The enzyme deficiency causes a continuous build-up of GL-3/Gb3 and related glycolipids in the body's cells, resulting in the cell abnormalities and organ dysfunction that particularly affect small blood vessels, the heart and kidneys. The GLA gene is located on the X-chromosome and therefor, FD is inherited as an X-linked disorder. Although the *Gla*$^{-/-}$ mice used as a lysosomal storage disease model seem to have a normal, complication- free life span. Recently, overexpression of thrombospondin-1 (TSP-1) secondary to Gb3 accumulation is primarily for the observed LSD-vascular endothelial cells (VECs) dysfunction. The aim of this study is to produce animal models similar to human FD. First of all, we produced the *Gla* knockout mouse by CRIPR/Cas9 system. *Gla*$^{-/-}$ was successfully produced and. Also, human TSP-1 overexpression mice was produced. Then, to generate double transgenic mouce (*Gla*$^{-/-}$ -hTSP-1, DB), crossbreeded Gla$^{-/-}$ and hTSP-1 mice. Generated DB mouse was not expressed *Gla* mRNA and abundantly expressed hTSP-1 gene. To check the human FD-like symptoms, various studies were conducted. In *Gla*$^{-/-}$ and DB mice, Left ventricular posterior wall was thicker and cardiac systolic ability was lower than normal aged mice. Interestingly, DB mice increased inflammation and fibrosis markers. Furthermore, DB mice were decreased number of sweat spots similar to the symptoms of hypohidrosis in human FD patients. These data suggest that DB mice is suitable for studying the pathogenesis of Fabry disease and for preclinical studies of candidate therapies.

Key words: Fabry disease, α-galactosidase A, globotriaosylceramied, double transgenic mice

Acknowledgement: This research was supported by the Korean Fund for Regenerative Medicine (KFRM) grant funded by the Korea government (the Ministry Science and ICT, the Ministry of Health & Welfare) (KFRM 21C0726L1).

Dev. Reprod. Vol 26, 2022 (Suppl. 1). pp 235

D-02

Ultrafine particles affect IgE-mediated mast cell and allergic responses

Minseong Kang[1,†], Seung Yeun Hyun[1,†], Jeong Won Park[1], *Hyuk Soon Kim[1,2]

[1]Department of Health Sciences, The Graduate School of Dong-A University

[2]Department of Biomedical Sciences, College of Natural Science, Dong-A University

[†]These authors have contributed equally to this work

(hskimxo@dau.ac.kr)

Acceleration of industrialization and urbanization is causing serious air pollution worldwide, which is well known to have detrimental effects on human health. The atmosphere contains a variety of ultrafine particles with different structures and properties. Ultrafine dust contains many substances that adversely affect health. In particular, ultrafine particles are very tiny and can be quickly absorbed into the body, so there are many studies reporting that ultrafine particles are related to the development of respiratory lesions in cancer, chronic obstructive pulmonary disease (COPD), and allergic diseases. However, there is still deficient research on clear immunological mechanisms in these allergic inflammatory diseases. Hence, we studied how ultrafine particles affect the function of mast cells, which are important immune cells for the initiation and activation of allergic reactions in the body. The ultrafine particles applied in the study were produced by making an ultrafine particle compound that mimics the composition of polluted air derived from exhaust gas in the atmosphere. And we introduced them into mast cell and animal diseases such as passive cutaneous anaphylaxis model to analyze their effects. It was confirmed that ultrafine particles further stimulated the degranulation response of IgE-mediated mast cells in a dose-dependent manner even under conditions that did not affect the cytotoxicity of mast cells themselves set in the *in vitro* experiment. Furthermore, ultrafine particles further increased the activity of mast cell degranulation reaction through calcium-mediated signaling pathway in mast cells by stimulation of ionomycin and thapsigargin. It was verified that the IgE-mediated FcεRI signaling mechanism, which is a representative signaling mechanism of mast cell, is further activated by ultrafine particles. In animal models of IgE-mediated passive cutaneous anaphylaxis disease and ultrafine particles exposed in lung tissue, it was confirmed that hypersensitivity reaction, mast cell infiltration, and mast cell degranulation were further exacerbated. We propose that ultrafine particles influence the activation and allergic response of IgE-mediated mast cells.

Key words: ultrafine particles (UFPs), allergy, mast cell, passive cutaneous anaphylaxis (PCA)

Dev. Reprod. Vol 26, 2022 (Suppl. 1). pp 236

D-03

6,8-Diprenylorobol induces cell death of endometriosis via mitochondria dysfunction and disrupting calcium homeostasis

Jisoo Song[1], Gwonhwa Song[2], *Whasun Lim[1]

[1]Department of Biological Sciences, Sungkyunkwan University

[2]Institute of Animal Molecular Biotechnology and Department of Biotechnology, Korea University

Endometriosis is known as benign chronic gynecological disorder indicating abnormal presence of endometrial-like tissue in other organs. Main symptoms of endometriosis are pelvic pain, infertility, intestinal pain, and reducing quality of life for reproductive aged women. Due to limitation of hormone therapy for management of endometriosis progression, development of novel therapeutic agents is required. 6,8-diprenylorobol extracted from the *Cudrania tricuspidata* has various physiological effects such as anti-cancer, anti-oxidant, anti-proliferative effects. However, the regulatory mechanisms of 6,8-diprenylorobol have not been confirmed yet in the progression of endometriosis. In this study, the inhibitory effect of 6,8-diprenylorobol was demonstrated on endometriosis like cell lines (VK2/E6E7 and End1/E6E7). Our result showed that 6,8-diprenylorobol inhibited the cell proliferation by cell cycle arrest and increased depolarization of mitochondrial membrane potential, production of ROS and disruption of calcium homeostasis in both VK2/E6E7 and End1/E6E7. Also, we confirmed the toxicity of 6,8-dirprenylorobol through the proliferation of primary normal uterine stromal cells and the result revealed that 6,8-diprenylorobol did not affect the proliferation of the primary normal cells. We also examined that the calcium inhibitors, 2-aninoethoxydiphenyl borate (2-APB) and ruthenium red (RUR) relieved the calcium accumulation in 6,8-diprenylorobol treated endometriosis cells. Moreover, 6,8-diprenylorobol decreased downstream of PI3K pathways whereas it activated reactive oxygen species-associated P38 MAPK pathway. In addition, the treatment of 6,8-diprenylorobol inhibited mitochondrial respiration leading to reduction of ATP levels on endometriosis-like cells. Therefore, we propose 6,8-diprenylorobol as novel treatment and adjuvant treatment for preventing human endometriosis progression.

Key word: Ca^{2+} homeostasis, mitochondria dysfunction, anti-proliferation, endometriosis, 6,8-diprenylorobol

Acknowledgement: This work was supported by the National Research Foundation of Korea (NRF) grant funded by the Korea government (MSIT) (No. 2021R1C1C1009807).

The 41st Annual Meeting of the Korean society of Developmental Biology

This work was supported by the Korean Federation of Science and Technology Societies(KOFST) grant funded by the Korean government.

제41회 한국발생생물학회 정기학술대회(2022년)

2022년 8월 16일 인쇄

2022년 8월 19일 발행

발행처 : (사)한국발생생물학회(www.ksdb1995.com)

발행인 : 류 범 용

편집인 : 박창범, 조성진, 문성환

인쇄처 : 거목문화사/거목인포 (TEL (02) 2277-3324 / FAX (02) 2277-3390)

㈜유비코리아
Universal Bio Korea

ThermoFisher SCIENTIFIC

- **Research total solution 제공**
- **학교, 제약회사, 연구소, 공공기간 협력 및 납품**

Authorized Representative | applied biosystems | invitrogen

PCR Machines (Thermal Cyclers)

SimpliAmp™ Thermal Cycler

▶ 본 제품은 질병 진단을 위해 특정 유전자(DNA)의 증폭에 사용하는 자동장치로서, 중합효소연쇄반응(PCR : Polymerase Chain Reaction) 원리를 이용하여 핵산을 증폭하여 질병의 진단에 사용하는 장비이다.

▶ Thermal block 부분이 서로 독립적인 3개의 Pertier block module로 이루어진 VeriFlex thermal block시스템입니다. 3가지의 annealing 온도를 설정하여 동시에 진행할 수 있습니다

본 제품은 의료기기이며, 사용시 주의사항과 사용방법을 잘 읽고 사용하십시오."

Real-Time PCR instruments

QuantStudio™ 5 Real-Time PCR System

▶터치스크린으로 간편 조작 가능

▶최적화된 프로토콜, 시약, 직관적인 소프트웨어를 사용해 다양한 어플리케이션에 적합

▶OptiFlex System을 활용하여 multiplexing 극대화 및 well 간 variation 최소화

▶클라우드 서비스 connect를 통해 언제 어디서나 데이터에 접근 가능

Genetic Analyzers

SeqStudio Genetic Analyzer

▶ 터치스크린으로 간편 조작 가능

▶ 카트리지 기반 통합시스템을 통해, 실험시간 최소화와 hands-on time으로 인한 오류 감소

▶ 동일 플레이트에서 Sanger Sequencing과 Fragment analysis (절편분석)이 가능

▶ 클라우드 기반 플랫폼 통해 원격으로 실시간 모니터링 및 분석

Next-Generation Sequencing instruments

SeqStudio™ Flex

▶ 4개 플레이트 용량, 연속 플레이트 로딩 및 긴급 검체 우선순위 재지정을 통해 가장 큰 중간 처리량 용량과 완벽한 일정 유연성을 제공

▶ 손쉬운 모세관 어레이 설치, 간소화된 원버튼 시동, 자동 보정 및 온보드 학습 센터

▶ 직관적인 소프트웨어와 간단한 검체 매핑, 플레이트 연결, 설정 실행을 위한 자세한 마법사를 갖춘 통합 터치스크린 컴퓨터.

▶ 음성 명령 및 다양한 연결 옵션과 같은 오늘날의 통신 기술을 통합하여 미래의 실험실 효율성을 개선

UBKorea

㈜유비코리아

☎ 033-731-0309 FAX 033-731-0308

✉ ubk0309@daum.net / ubk0309@naver.com

강원도 원주시 지정면 무릉로43 팬더프라자 2층 211, 212호

Lonza
Pharma & Biotech

HLA-Typed cells from Lonza

What is Human Leukocyte Antigen (HLA)?

The major histocompatibility complex (MHC) is a set of genes that code for cell surface proteins are essential for the immune system to recognize foreign molecules. The human MHC is called Human Leukocyte Antigen (HLA).

Key Advantages of HLA Information

- Donor/recipient matching for organ and bone marrow transplants, patient stratification for immune-oncology drug discovery
- Important for designing in vitro assays to identify on-and off-target cross-reactivities and assess risks of cytotoxicity
- Critical information for eg. preclinical cell therapy, cancer vaccine development and drug safety assessment studies

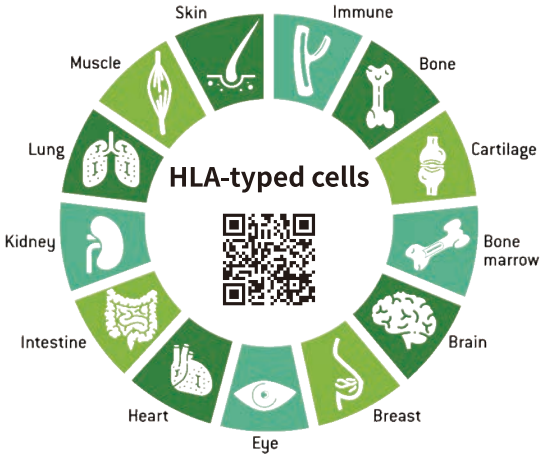

Characterization of HLA-Type

On chromosome 6 there are 6 different HLA genes:

- MHC class I: HLA-A, HLA-B and HLA-C - found in all nucleated cells in the body
- MHC class II: HLA-DR, HLA-DQ and HLA-DP - found in addition on certain immune cells

Lonza Leads Market with Large and HLA-Typed CD34+ Cell Lots for Efficient Humanized Mouse Model Development

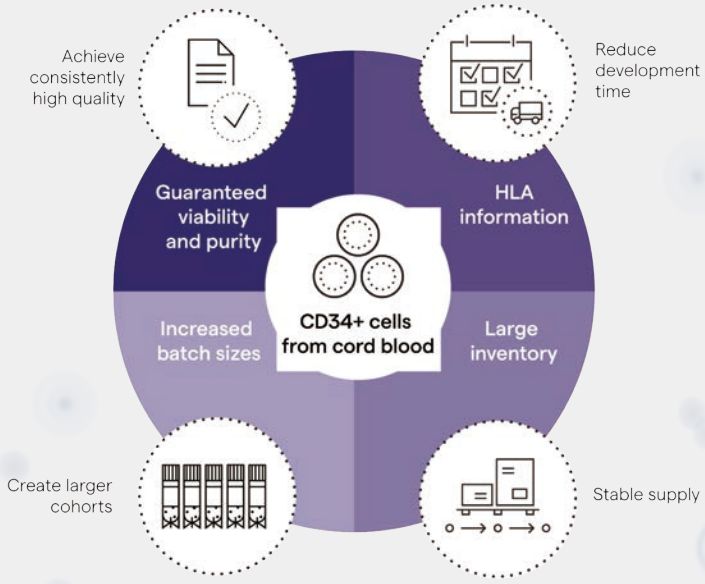

※ QR코드를 통해 상세한 제품 정보를 확인하실 수 있습니다.

YOUNG SCIENCES INC (주) 영사이언스 Tel. 032-624-4500 / Fax. 032-624-4505 / info@youngscience.com

CYTEK
TRANSCEND THE CONVENTIONAL

AURORA-CS

CYTEK AURORA Full Spectrum Cell Sorter

Aurora Full Spectrum analyzer의
최대 **5 laser 40 color analysis**를 그대로 **Aurora-CS**에 재현

Autofluorescence 제거 기능

최대 **6-way Multi Sorting** 가능

IMAGINE A CYTEK AURORA THAT CAN SORT

CYTEK Aurora Analyser

CYTEK Aurora-CS Cell Sorter

LK Bioscience 02-442-1218 lkcustomservice@gmail.com www.lkbio.co.kr

The Spheroid-based flow integration 3D Cell Culture Chip (3D 세포배양 칩)

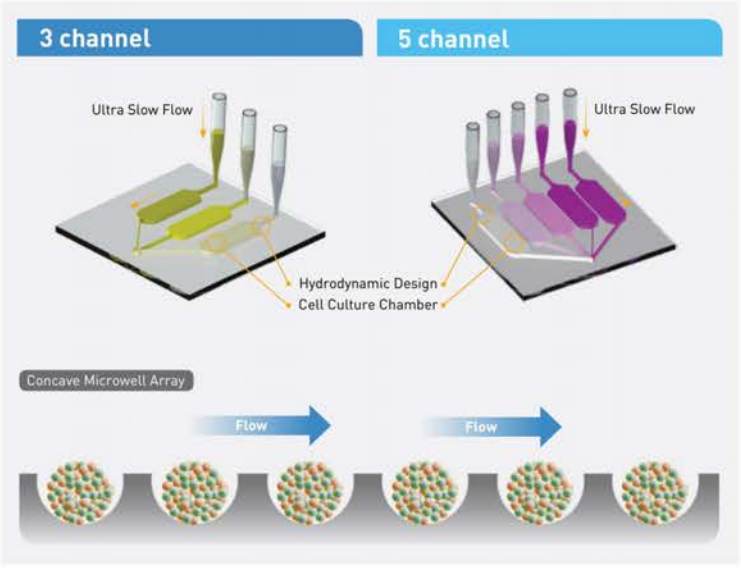

• Technology

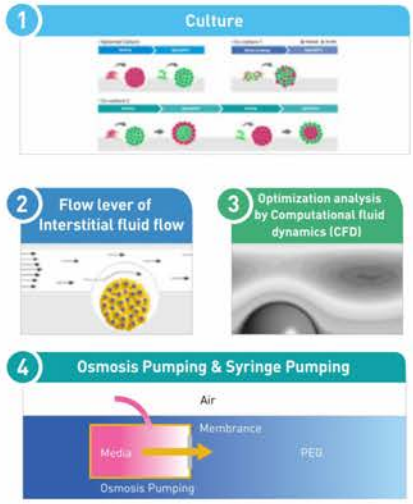

• Applications

- Multi Channel (3~5 ch.)
- 3D Spheroid Cell Culture
- Co & Tri Culture System
- Organoid
- Long-term Cell Culture
- High Throughput System
- Drug Screening
- Differentiation Efficiency

• Custom Fabrication Service

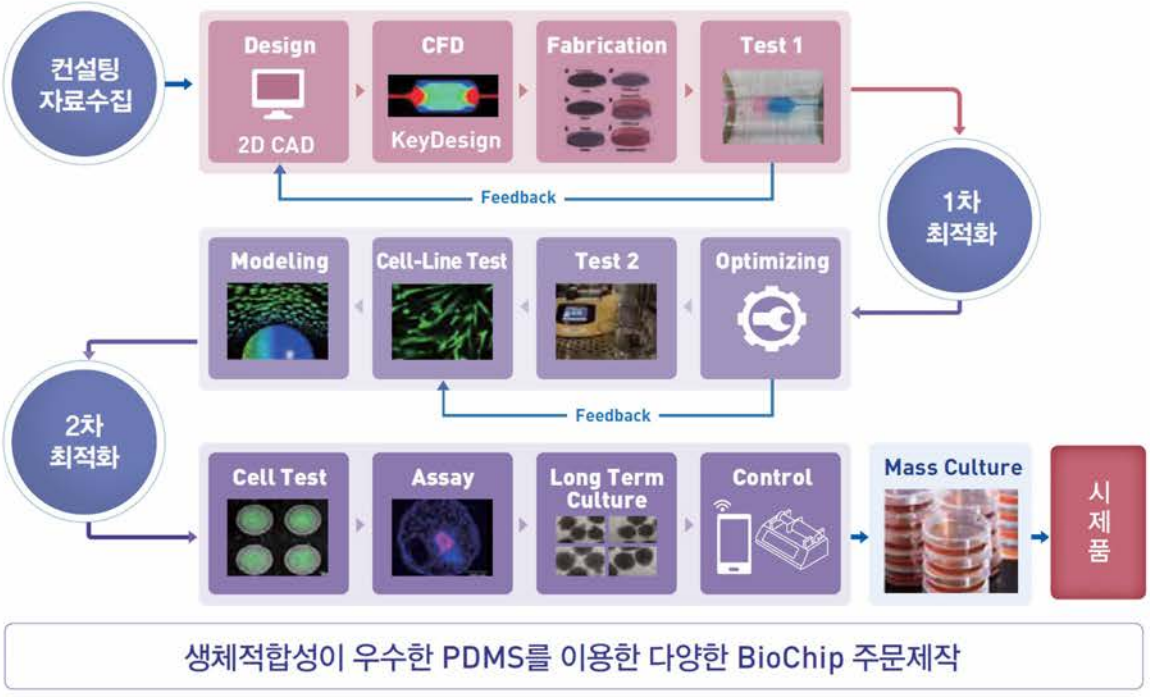

생체적합성이 우수한 PDMS를 이용한 다양한 BioChip 주문제작

에이비엠랩스 (ABMLabs) · 바이오 칩 & 기기/생체진단 전극 센서 전문기업

충남 아산시 탕정면 선문로 221번길 70, 선문대학교 산학협력관 411호
70, Sunmoon-ro 221beon-gil, Tangjeong-myeon, Asan-si, Chungnam, Korea
#411, University-Industry Foundation B/D, Sunmoon University
Tel. 041-534-3426, Email. abmlabs@naver.com, Web. www.abmlabs.kr

ABMLabs

임상용 심근세포 생산 및 특성 분석 완료

※ IRB 기관 승인 및 기증자 동의서 확보 및 체세포 은행 구축
※ mRNA 기반 Virus- / Vector-free 제품을 이용한 역분화 유도 시스템 활용
※ CMO 계약을 통한 GMP 시설에서 역분화줄기세포 10종 은행 구축
※ 임상용 역분화줄기세포 10종 유래 심근세포 생산 및 특성분석 완료

임상용 역분화 줄기세포 검증 및 심근세포 특성분석

역분화줄기세포 검증

• iPSC 특이 단백질 ≥ 90% 이상 발현 확인

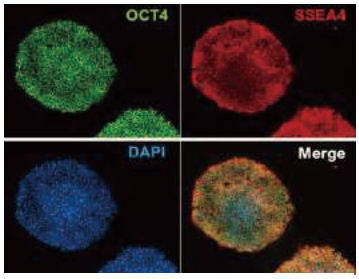

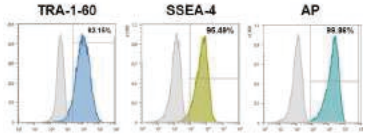

• iPSC 특이 유전자 발현 확인

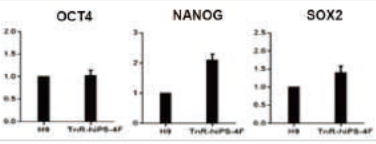

세포 유전적 안정성 검사

• 핵형 분석 46 XX 정상

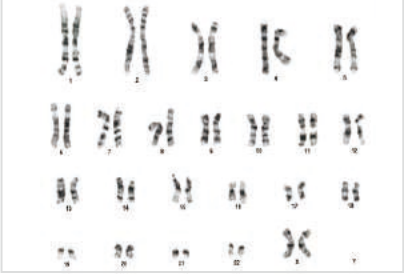

• 유전학적계통분석 : 체세포와 iPSC 100% 일치

Sample	Fibroblast	iPSC	Sample	Fibroblast	iPSC
Amelogenin	X	X	D21S11	31,32.2	31,32.2
D3S1358	15,16	15,16	D7S820	8,10	8,10
D1S1656	13,16	13,16	D5S818	9,11	9,11
D2S441	10,13	10,13	TPOX	8,9	8,9
D10S1248	14	14	D8S1179	13	13
D13S317	9,11	9,11	D12S391	21,23	21,23
pentaE	11,13	11,13	D19S433	14	14
D16S539	10,13	10,13	D6S1043	19	19
D18S51	16,18	16,18	D22S1045	12,15	12,15
D2S1338	17,19	17,19	DYSS391	-	-
CSF1PO	10,11	10,11	FGA	22,23	22,23
PentaD	11,12	11,12	DYS576	-	-
TH01	6,8	6,8	DYS570	-	-
Vwa	18,20	18,20			

심근세포특성 검증

• 심근세포 특이 단백질 ≥ 90% 이상 발현 확인

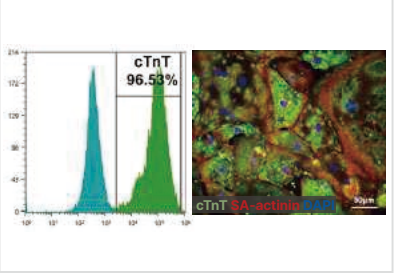

• 전기생리학적 분석 : 3가지 유형의 심근세포 모두 확인

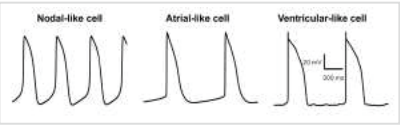

Cell type	Nodal-like	Atrial-like	Ventricular-like
Proportion (%)	7.7	26.9	65.4

임상 적용 가능한 심근세포응집체 제작 기술 개발

한국/일본 특허 등록 완료. PCT 출원(USA, Europe, China 등록 심사 중)

임상용 카테터에 적용 가능한 응집체 제작 기술 확보

• 1 응집체 ≒ 41±3 cells • 응집체 크기 ≒ 105±5 μm • 카테터 적용 가능성 검증

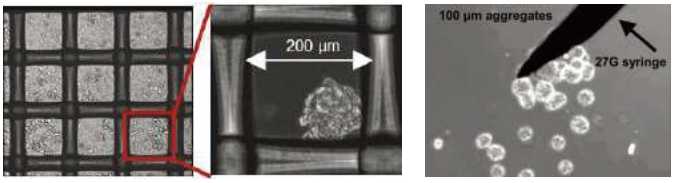

심근세포응집체[~100 μm]

1. 이식 직후 저산소 환경에서 생존율 향상
2. 장기간 동결 보관 가능(임상 즉시 사용)
3. 임상용 카테터 활용(규제 문제 극복)

전임상 시험(Rat 심근경색모델) – 심근세포 이식 8주 후 심장 조직 재생 확인

• 단일 심근세포 이식

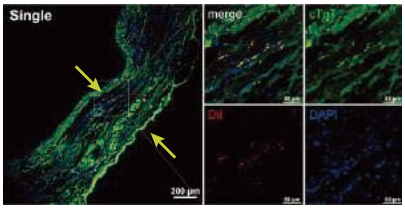

• 심근세포응집체 이식

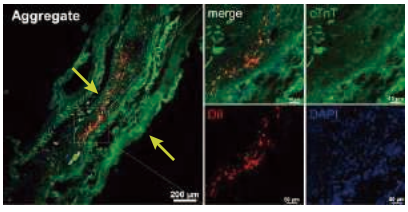

심장 기능 개선 확인(혈류 방출량 증가)

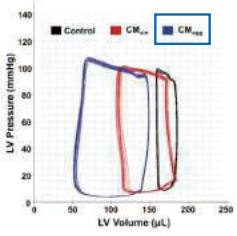

심근세포응집체 이식 실험군이 비응집 심근세포 이식 대조군에 비해 조직 재생 기능이 향상

[SCI 논문 발표] *Effect and application of "cryopreserved cardiac spheroids" for myocardial infarction therapy. 2022; Clinical Translational Medicine (IF 11.492).*

www.tnrbiofab.com sjpark@tnrbiofab.com T&R Biofab

BREXOGEN

Brexogen paves innovative cell free strategies for targeting incurable diseases via stem cell derived exosome

Technology

01 치료 효능·효율과 안전성. 대량생산, 품질관리 우수성

02 엑소좀 내 유효 성분 조절 기술 확립

03 다양한 질환에 적용 가능한 엑소좀 치료제 개발

세포치료제 한계 극복

BG-Platform 기술 확립

Pipeline 확장성

IPs & Pipelines

6건 용도 특허 출원, 2건 용도 특허 전용실시
- MI NASH, Renal Failure **용도 특허**
- **AD 용도** 등록 특허 전용실시권 이전

8건 출원 및 **등록**
- 줄기세포유래 엑소좀 생산 촉진 및 줄기세포능 **증가용 조성물**

1건 출원 및 **등록**
- 유도만능줄기세포 유래 중간엽 줄기세포 전구세포 및 그의 **제조방법**

Indication	MoA	2022				2023				2024			
		1Q	2Q	3Q	4Q	1Q	2Q	3Q	4Q	1Q	2Q	3Q	4Q
Atopic Dermatitis BRE-AD01	· Immune suppression · Skin regeneration	Pre-Clinical		IND		Clinical							
Myocadiac infarction BRE-MI01	· Cardiomyocyte regeneration · Angiogenesis · Anti-inflammation	Discovery				Pre-Clinical			IND	Clinical			
NASH BRE-NA01	· Liver cell regeneration · Suppression of lipogenesis · Anti-inflammation · Fibrosis suppression	Discovery					Pre-Clinical						
Renal Failure BRE-RF01	· Renal function improvement · Fibrosis suppression	Discovery					Discovery						

Therapeutic Exosome으로 열어갈 건강한 세상, 『 BREXOGEN 』이 준비하고 있습니다!

서울시 송파구 법원로8길 9, 3/9층 (문정동 청림타워) · 02-430-0401 · info@brexogen.com

Nikon

See More Than Before

Capture 2x More Data in a Single FOV

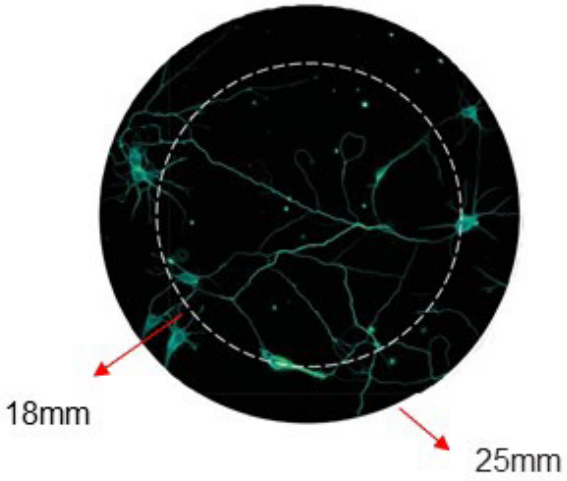

NANO INSTRUMENT

니콘 공식 특약점
엔아이 (N.I) Nano Instrument
TEL : 02-981-1144 H.P : 010-4786-8415
E-Mail : dhkim8415@gmail.com

Heathrow Scientific®
design | function | innovation

www.heathrowscientific.com

Tubes & Vials
Tube Racks & Storage

Sample Collection & Transport

Laboratory Equipment
Sample Handling
Cold Products & Storage
Slide Products & Accessories

Sealing & Labeling

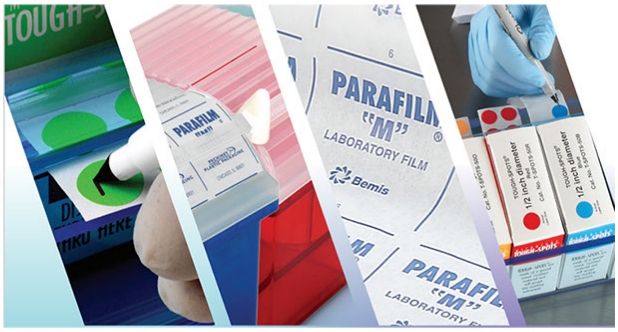

Everything you need for a well stocked laboratory or educational environment

GOLD PACIFIC
골드퍼시픽

㈜골드퍼시픽 강동지점
서울시 강동구 올림픽로 834 한강씨티라이프빌딩 2층
문의 ☎ 02-427-3669 ✉ curebio@curebio.co.kr

NEXEL

NEXEL'S CARDIAC SAFETY IS THE NEW PARADIGM

NeXST service

NeXST (Next Xight Screening Test)-(Cardiac Safety Evaluation Service)

NeXST는 보다 효율적인 신약개발이 가능하도록 hiPSC-CM을 이용하여 사람심장에 대한 위해성과 유해성을 예측·평가하는 넥셀의 심장 안전성 약리시험 서비스 입니다.
㈜넥셀은 HESI CiPA Working Group의 일원으로 ICH가이드라인 개정에 참여하고 있는 국내 유일의 기업입니다. 당사의 심장 안전성 약리시험 플랫폼은 다양한 표준시약들을 이용하여 정확한 결과의 도출을 검증하였으며, 자체 생산 iPSC 유래 심근세포인 Cardiosight® -S를 사용한 서비스를 제공하여 유연한 실험설계와 합리적인 비용을 제안합니다.

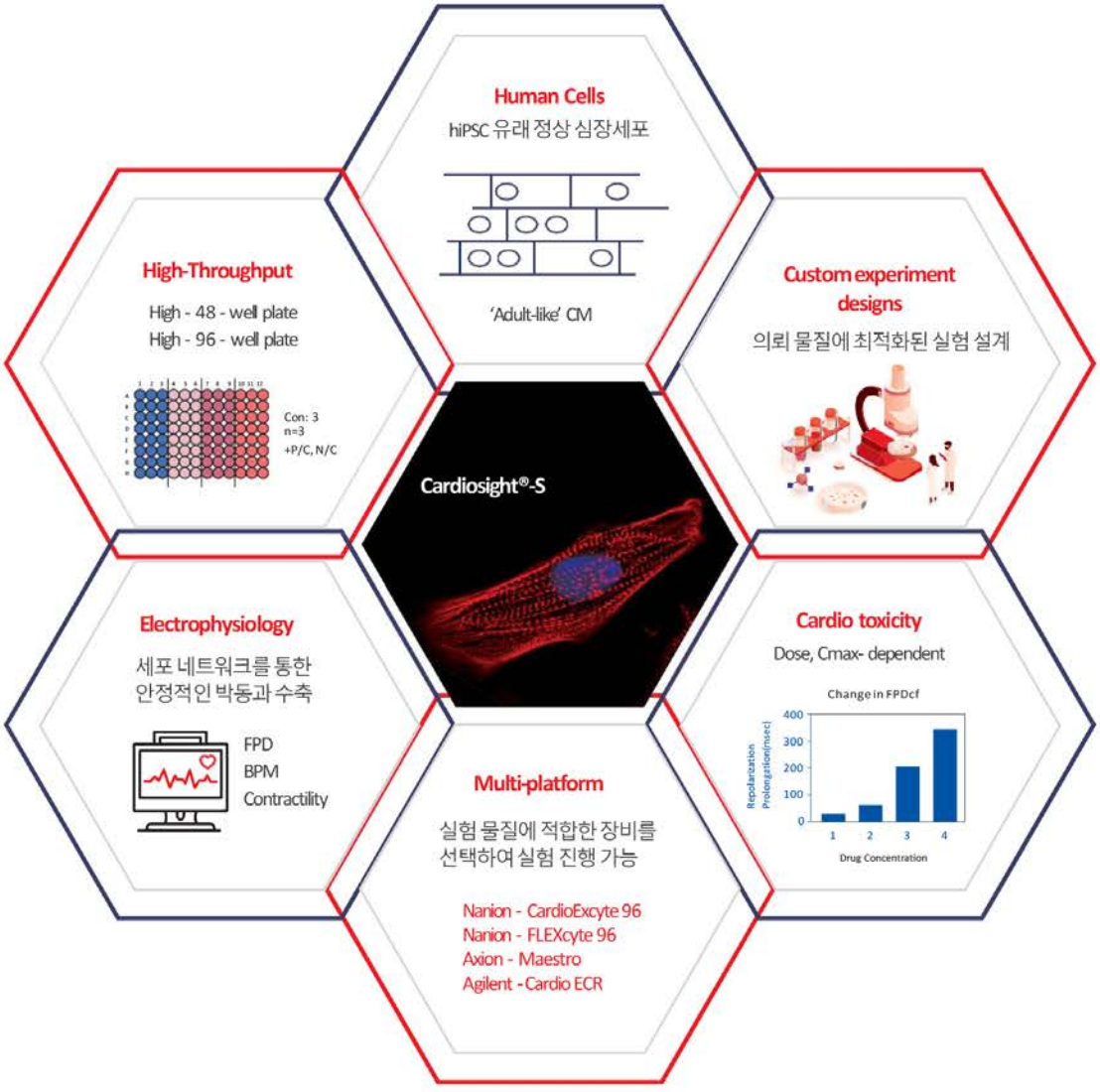

Please visit **www.nexel.co.kr** and get more information!

sales@nexel.co.kr 070-5118-2836

SONY
Sony Biotechnology Inc.

SH800S

Sorting Made Simple, Fully-Automated Cell Sorter

- 4-laser, 6 color
- Easy to Set up: Fully Automated System
- 3 Type Nozzle (70 um, 100 um, 130 um)
- 2 Way, 96 well Plate

제품 자세히 보기

CHAYON LABORATORIES, INC
자연과학(주)
02-3471-4100 | info@chayon.co.kr
chayon.kr

SPHEBIO

Spheroid Printer
[SPHRINTER]
[전용 자동화 생산장비]

㈜스페바이오
서울특별시 금천구
가산디지털2로 108
뉴티캐슬 305호

www.sphebio.com
02-6269-0826

회사소개

㈜ **스페바이오**는 2차원으로 배양되던 세포를 3차원 스페로이드로 정밀하게 배양할 수 있는 기초기술을 보유하고 있습니다. 생산된 스페로이드는 발생학, 세포치료제, 엑소좀 대량생산 등의 연구에 다양하게 활용될 수 있습니다.

스페로이드

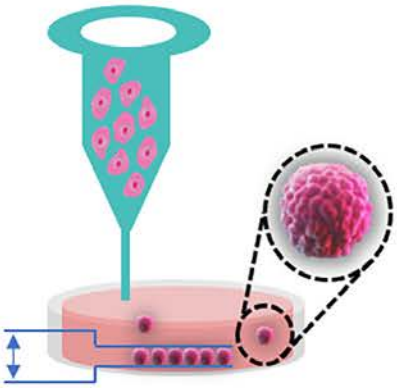

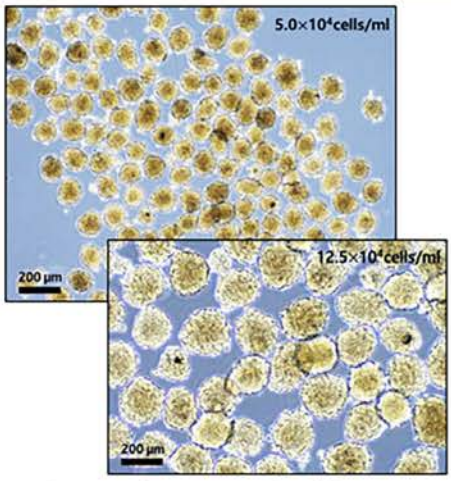

㈜ **스페바이오**에서 전용 자동화 장비로 생산되는 스페로이드는 세포수, 직경을 일정하게 제어조절할 수 있으며 대량생산이 가능합니다. 줄기세포, 섬유아세포 등 2D 세포배양접시로 배양 가능한 대부분의 세포에 적용 가능하며, 공배양도 가능합니다. 세포주 제공시 스페로이드 위탁생산 서비스를 제공합니다.

엑소좀

㈜ **스페바이오**의 엑소좀은 스페로이드의 배양액에서 분리합니다. 스페로이드에서 분리한 엑소좀은 배양조건에 따라 세포당 엑소좀 생산량이 약 100배 증가하는 가운데 엑소좀 마커와 형태를 원 상태 그대로 유지합니다. 세포주를 제공해 주시면, 엑소좀 위탁생산 서비스를 제공합니다.

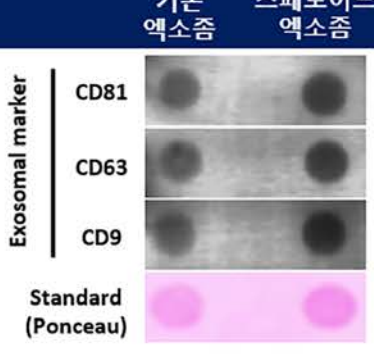

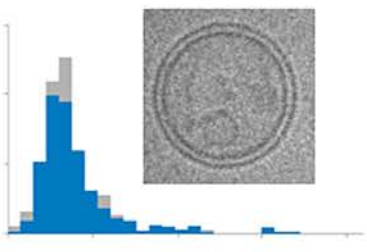

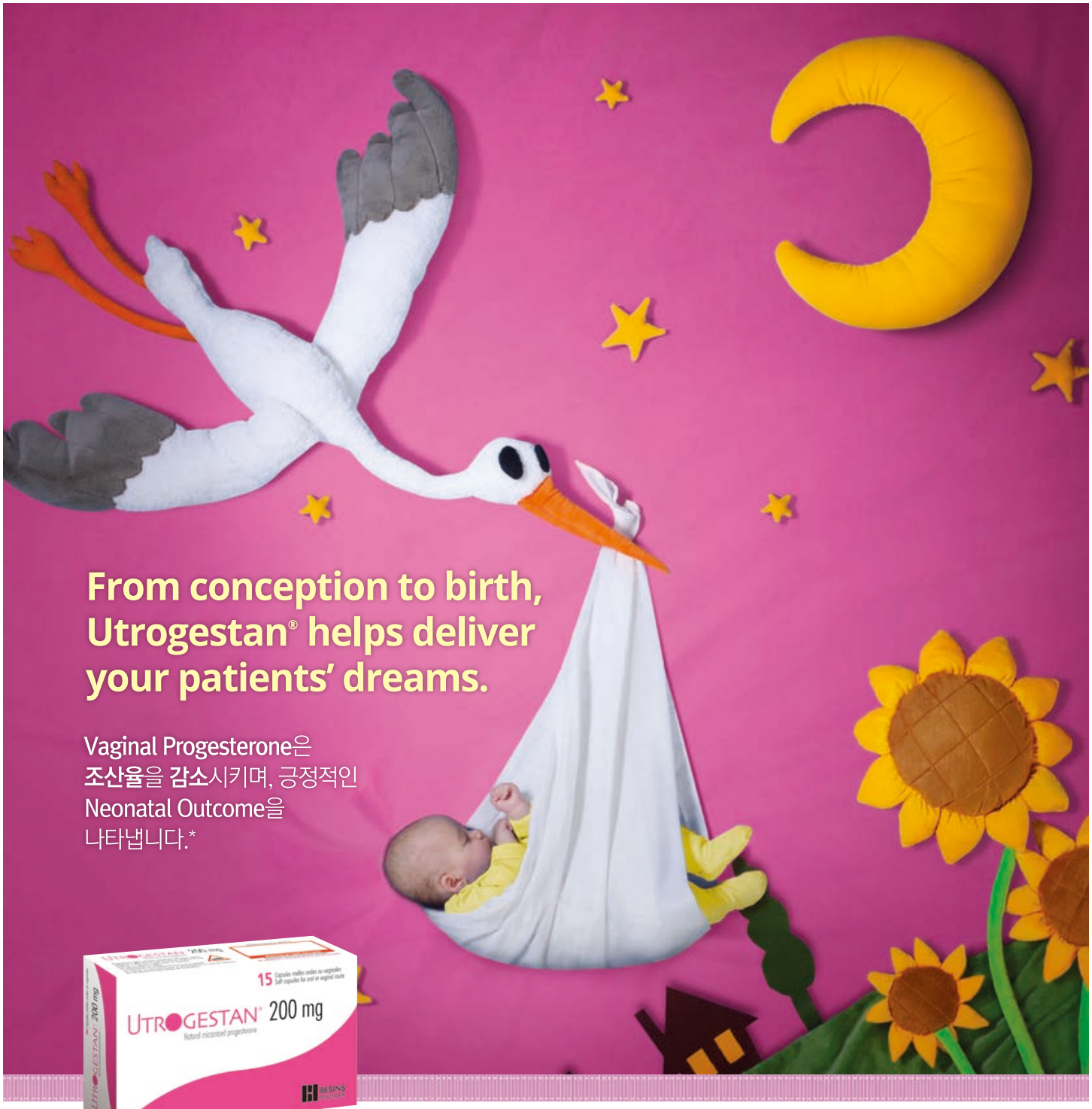

원료약품 및 그 분량 1 캡슐 중 주성분 : 프로게스테론(미분화)(별규)…200mg **성 상** 환색의 균질한 유상의 내용물이 충진된 환색 내지 유백색의 타원형 질좌제 **효능 · 효과** 프로게스테론 결핍으로 인한 불임 여성의 난모세포공여프로그램, 체외수정에서의 프로게스테론의 보충요법 **용법 · 용량** 투여 시에는 질 깊숙이 캡슐을 삽입합니다. 평균 용량은 1일 200mg이며 1회 용량이 200mg을 초과할 수 없습니다. 필요한 경우 삽입기를 사용하며, 환자의 반응에 따라 용량을 증가할 수 있습니다. 1. 난모세포공여시 - 월경주기 제 13일 및 제 14일에 100mg을 1일 1회 투여한 다음, 주기 제 15-20일까지 100mg을 1일 2회 투여합니다. 제 26일에 임신이 진단되면 아침, 저녁에 각각 100mg씩 또는 1회 200mg을 질 내 깊숙이 삽입합니다. 매주 용량을 1일 100mg씩 증가시켜 1일 최대 600mg, 1일 3회로 60일간 투여합니다. 2. 체외수정시 - hCG주사일로부터 최대 임신 12주까지 1일 600mg, 1일 3회 투여합니다. **사용상의 주의사항** 1. 경고 1) 의사는 혈전성 질환(혈전성정맥염, 뇌혈관 질환, 폐색증, 망막성 혈전증)의 조기 발현에 주의하고 이러한 질환이 일어나거나 의심이 되는 경우에는 즉시 투여를 중단합니다. (4. 일반적주의 참고) 2) 프로게스테론은 습관성 자연유산의 기왕력이 있는 여성의 유산 방지목적으로 사용되어 왔으나 이 목적으로 유효하다는 충분한 증거는 없습니다. 3) 임신중인 경우에는 임신 첫 3개월 동안만 질내투여로만 사용해야 합니다. 이 약은 절박성 미숙출산에 대한 치료제가 아닙니다. 예외적으로 프로게스테론(미분화)을 임신 4-9개월째 투여 시 간헐포성 간질환과 같은 간계통 질병 및 담즙분비 정지성 황달을 일으킬 수 있습니다. 2. 다음 환자에는 투여하지 마십시오. 1) 이 약의 구성성분에 대한 과민증 및 특이체질환자 2) 중증 간기능 장애 환자 3) 간종양, 담즙울체성 황달환자 4) 진단되지 않은 비정상적인 생식기 출혈환자 5) 기지 또는 의심되는 유방암 또는 생식기의 악성종양 6) 계류유산 또는 불완전유산환자 7) 혈전성 정맥염, 혈전색전증, 뇌혈관성 질환, 폐색전증 또는 그 병력이 있는 환자 8) 투반-존슨 증후군(Dubin-Johnson syndrome) 또는 로터 증후군(Rotor syndrome)환자 9) 저성선자극호르몬성 무월경 환자 3. 이상반응 1) 대두인지질로 인한 국소 자극이 발생할 수 있으나, 다양한 연구 결과,자극, 가려움증, 유성분비물 등의 국소 거부증상은 관찰되지 않았습니다. 2) 기면 및 현기증은 특히 에스트로겐 수치가 낮은 경우에 수반됩니다. 이러한 현상은 용량을 줄이거나 정상적인 에스트로겐 수치로 복귀하는 경우, 치료학적 유익성과는 무관하게 즉각적으로 사라집니다.3) 주기 성 너무 이른 시기, 특히 주기 15일째 전에 처치를 시작한 경우, 주기가 단축되거나 돌발성 출혈이 발생할 수 있습니다. 4) 일반적으로 황체활성억물을 사용하는 경우, 월경주기 변화, 무월경, 돌발성 출혈이 발생할 수 있습니다. 5) 경구투여 시 발생할 수 있는 일반적인 부작용, 특히 흡음 또는 현기증은 권장된 용량이 질내 투여된 임상시험 중에는 거의 관찰되지 않았습니다. 만약 이러한 증상이 나타나는 경우, 취침 전에 투여합니다. 6) 프로게스테론 질내투여를 다른 제형에서 다음의 이상반응이 관찰되었습니다. ①전신 : 부종, 경련, 통증, 복통, 회음부 통증 ②중추 및 말초신경계 : 현훈, 두통 ③소화기계 : 변비, 설사, 오심, 구토 ④근골격계 : 관절통 ⑤정신신경계 : 우울, 성욕감소, 긴장, 경련 ⑥여성생식기계 : 유방통, 음부 모닐리아증, 질분비물, 유방확대, 성교불쾌증 ⑦피부 및 연조직 : 음부 소양증 ⑧비뇨기계 : 야뇨증 4. 일반적 주의 1) 프로게스테론 요법을 시작하기 전에 파파니콜로 도말시험 및 유방 및 골반장기에 대한 신체검사를 실시합니다. 장기간 치료 시 6개월에 한 번씩 진단합니다. 2) 급작스런 출혈과 같은 불규칙한 질출혈의 경우에는 비기능적인 원인도 고려되어야 합니다. 진단되지 않은 질출혈의 경우에는 적절한 진단방법을 취하여야 하며, 요인이 확실시되기 전에는 본 제제를 처방하지 않습니다. 3) 프로게스테론은 체액저류를 유발하므로 이런 요소들로 인해 영향 받을 수 있는 상태(예를 들어, 간질, 편두통, 천식, 심장, 신질환)의 경우 신중한 관찰을 필요로 합니다. 4) 표본이 제출될 때 병리학자에게 프로게스테론 치료임을 알립니다. 5) 정신적 우울의 기왕력이 있는 환자는 주의 깊게 관찰하고, 심각한 정도 까지 우울이 재발하는 경우 약을 중단합니다. 6) 포도당 내성의 감소가 에스트로겐-프로게스틴 병용투여 환자 중에서 적은 수의 환자에서 관찰되었습니다. 이 감소의 기전은 알려져 있지 않습니다. 그러므로 당뇨환자 중에서 프로게스테론 치료를 받는 환자는 주의 깊게 관찰합니다. 7) 이 약은 다른 질내요법과 병용되어서는 안됩니다. 만약 다른 질내요법과 병용한다면 이 약 투여 전후로 적어도 6시간의 간격을 두고 사용합니다. 8) 에스트로겐 및 프로게스테론 투여 후 드물게 간의 양성 변화, 더욱 드물게 악성 변화가 나타나는 것이 보고되었으며, 드물게 이것에 의해 복강내 출혈이 야기되었습니다. 상복부의 통증, 간종대, 복강내출혈이 나타나는 경우에는 간종양에 대한 감별진단을 하며 경우에 따라 이 약의 사용을 중지합니다. 9) 혈전증 및 대사성 질환 등의 위험이 완벽하게 제어되지 않으므로 다음의 경우 복용 중단합니다. - 실명, 복시(증), 망막혈관손상 등과 같은 시각 이상 - 정맥혈전증 및 기타 각종 혈전증 - 중증 두통 10) 혈관정맥염 기왕력 환자는 치밀한 모니터링을 실시합니다. 11) 치료 도중 무월경증이 발생하는 경우, 임신 여부를 확인합니다. 12) 임신초기의 자연적인 유산은 대부분 유전적인 이상, 감염 또는 기계적인 이상에 의해 유발됩니다. 따라서 프로게스테론의 투여가 단지 사망한 태자의 배출만을 지연시킬 가능성이 있으므로 황체부전의 경우에만 제한적으로 투여합니다. 13) 권장 적응증에 사용될 경우 피임효과는 없습니다. 14) 이 약은 폐경 후 골다공증의 발생 또는 진행을 억제하는 데 있어서 에스트로겐을 대체하기에 적합하지 않습니다. 절박 또는 반복 유산의 방지나 치료에 적합하지 않으며 피임효과는 없습니다. 5. 상호작용 1) 간 효소 유도 약물들 (바르비탈계 약물, 카르바마제핀, 히단토인, 메프로바메이트, 페닐부타존 등)은 프로게스테론의 대사를 촉진시키므로 이 약의 효과를 감소시킬 수 있습니다. 2) 암피실린, 테트라사이클린, 글리세오물빈 등 항생물질의 병용은 장내 세균총의 변화를 가져와 이 약의 효과를 감소시킬 수 있습니다. 3) 이 약은 사이클로스포린 및 테오필린과 같은 약물의 약리적 및 동물학적 효능을 증가시킬 수 있습니다. 4) 과도한 흡연에 의하여 이 약의 생체이용율이 감소할 수 있으며 알콜 남용에 의하여 생체이용율이 증가할 수 있습니다. 6. 임부 및 수유부에 대한 투여 1) 이 약의 질내투여로 한정 수의 임상연구에서 프로게스테론 투여로 인해 태아 및 신생아의 기형관련성은 보고된 바 없습니다. 2) 황체호르몬의 사용과 선천성이상아 출산과의 인과관계는 아직 확립되어 있지 않습니다. 그러나 역학조사 결과에 의하면 심장, 사지 등의 선천성 이상아를 출산한 산모와 대조군 사이에는 임신초기 황체호르몬 및 황체 · 난포호르몬제 사용비율에 있어 유의성 있는 차이가 있다는 보고가 있습니다. 3) 이 약을 수유부에 투여 시 적은 양이 유즙으로 분비되는 것이 알려져 있으나 영아에 대한 영향은 알려져 있지 않습니다. 그러나 투여 후 증상이 나타나지 않으므로 예방목적으로 이 약을 수유부에 투여하지 않습니다. 7. 과량투여시의 처치 질투여에 대한 과량투여에 대한 보고는 없으나, 상기 이상반응은 과량투여의 징후일 수 있습니다. 과량투여의 경우에는 이 약을 중단하고 증상에 따라 치료합니다. **저장방법** 밀폐용기, 실온(1~30°C)보관 **포장단위** 15캡슐/PTP *Roberto Romero et al.(2018) American Journal of Obstetrics & Gynecology, 161-180

한화제약 서울특별시 성북구 화랑로32길 76
Tel (02) 959-3679 Fax (02) 6234-6020

BESINS HEALTHCARE

UTROGESTAN®
Natural micronized progesterone

피 한 방울로 15분 만에 끝나는 AI 건강검진 애니스캔

반려동물 사망원인 1위인 암부터 당뇨, 면역, 염증까지 -
이제 반려동물 정기검진은 애니스캔으로 빠르고 편리하게.

AniScan

주식회사 바이애틱
경기도 안양시 동안구 흥안대로 427번 길 16 평촌디지털엠파이어 305~306호
가맹점 문의 **1522-6125**
자세한 사항은 홈페이지를 참조해주시기 바랍니다
홈페이지 **biattic.com**

biattic
BETTER LIFE FOR HUMAN & ANIMAL

GONAL-f®
FOLLITROPIN ALFA

CONNECTING YOUR EXPERTISE TO TAILORED TREATMENTS

GONAL-f® : The world's most prescribed rFSH[1]
고날-에프 펜으로 전 세계에서 500만 명 이상의 아기가 태어났습니다.[7,*]

- 검증된 약효[2-5]와 잘 확립된 안전성 프로파일[6]
- 첨단의 유전자재조합기술[10,11]을 통해 제품의 구성요소가 일관성이 있고 신뢰할 수 있습니다.[8,9]
- Ready-to-use pre-filled pen 형태로 사용이 편리하고[10,11] 세밀한 용량 조절[12,13]이 가능합니다.

* 2019년 10월 기준. Estimated from Velthuis et al(2021) and Bosch et al(2019).

MERCK

REFERENCE **1.** Data on file. Market Data Analysis, Dec 2020. **2.** Anderson AN, et al., Hum Reprod., 2006 Dec 21:3217-27. **3.** Frydman R, et al., Hum Reprod. 2000 Mar;15(3):520-5. **4.** Bergh C, et al., Hum Reprod., 1997 Oct;12;10:2133-9. **5.** Schats R, et al., Human Reproduction, 2000 Aug;15;8:1691-7. **6.** Velthuis et al., Adv Ther (2020) 37:4831-4847. **7.** Manzi et al., Int. J. Mol. Sci. 2022;23:6762. **8.** Lisipi M et al., Reprod Biomed Online. 2006;13(2):179-193. **9.** Hugues et al., Reprod Biomed Online. 2005 Jun;10 Suppl 3:11-7. **10.** Longobardi et al., Expert Opinion on Drug Delivery, 2019 Sep;16(9):1003-1014. **11.** Buhler et al., Ther Clin Risk Manag. 2015 Jun 29;11:995-1001. **12.** Schertz et al., Expert Opinion on Drug Delivery, 2017;14:4, 473-81. **13.** Jeannerot et al., Expert Opin Drug Deliv. 2016 Sep;13(9):1221-9.

KR-GON-00056/Jul 2022